Universität Ulm

Institut für Analytische und Bioanalytische Chemie

Design and Synthesis of Submicron Polymer Particles for the Selective Capture of Proteases

- Dissertation -

zur Erlangung des Doktorgrades Dr. rer. nat.

der Fakultät für Naturwissenschaften der Universität Ulm

vorgelegt von

Bettina Pluhar

aus Wendlingen am Neckar

Ulm, 2016

Amtierender Dekan: Prof. Dr. Peter Dürre

1. Gutachter: Prof. Dr. Boris Mizaikoff

2. Gutachter: Apl. Prof. Dr. Ulrich Ziener

Tag der Promotion: 15.12.2016

In der Theorie ist praktisch alles möglich.

- Graf Fito

I. Table of contents

II. List of papers

Parts of this thesis have already been published within the following peer-reviewed research articles.

B. Pluhar, U. Ziener and B. Mizaikoff, “Surface Imprinting of Pepsin via Miniemulsion Polymerization”, *Journal of Materials Chemistry B*, 2013, *1*, 5489-5495. Reproduced with permission from the Royal Society of Chemistry.

B. Pluhar, U. Ziener and B. Mizaikoff, “Binding Performance of Pepsin Surface-imprinted Polymer Particles in Protein Mixtures”, *Journal of Materials Chemistry B*, 2015, *3*, 6248-6254. Reproduced with permission from the Royal Society of Chemistry.

B. Pluhar and B. Mizaikoff, “Advanced Evaluation Strategies for Protein-imprinted Polymer Nanobeads”, *Journal of Macromolecular Bioscience*, 2015, *15*, 1507–1511. Copyright Wiley-VCH Verlag GmbH & Co. KGaA. Reproduced with permission.

Journal of Macromolecular Bioscience cover (© Wiley-VCH 2015):

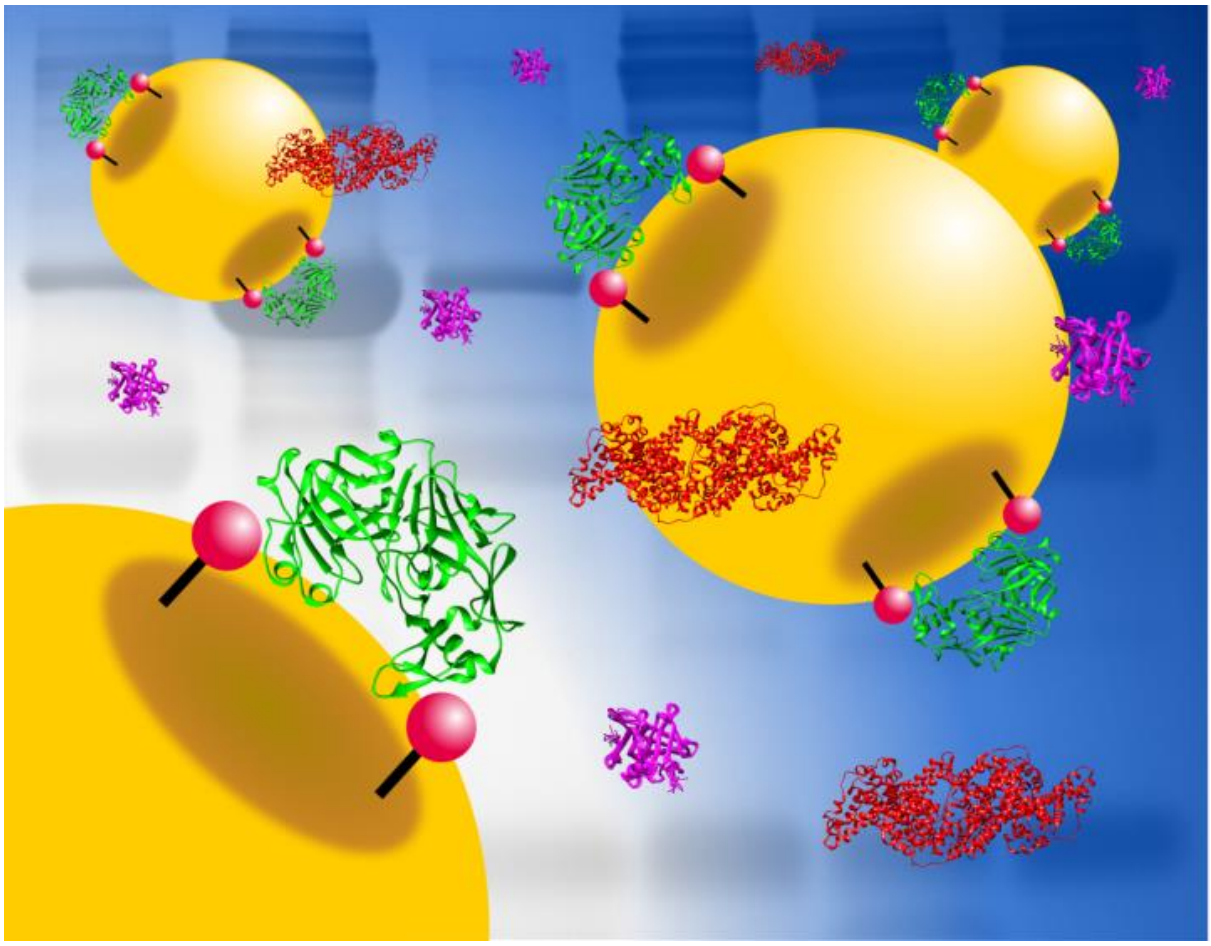

III. List of abbreviations

UV	ultraviolet
Vis	visible
MIP	molecularly imprinted polymer
NIP	non-imprinted polymer
APTMA	*N*-(3-acrylamidopropyl)trimethylammonium chloride
NPs	polymer nanoparticles
NIPAm	*N*-isopropylacrylamide
TBAm	*N*-(*tert*-butyl)acrylamide
BIS	*N,N'*-methylenebisacrylamide
LMK	Labor Dr. Merk & Kollegen GmbH
Atoll	Atoll GmbH
IABC	Institute of Analytical and Bioanalytical Chemistry
3D	three-dimensional
HPLC	high-performance liquid chromatography
SPE	solid phase extraction
AAc	acrylic acid
AAm	acrylamide
HMAm	*N*-(hydroxymethyl)acrylamide
MAA	methacrylic acid
EGDMA	ethylene glycol dimethacrylate
RNase A	ribonuclease A
MMA	methyl methacrylate
BSA	bovine serum albumin
SDS	sodium dodecyl sulfate
TM	target molecule
SDS-PAGE	sodium dodecyl sulfate-polyacrylamide gel electrophoresis
CD	circular dichroism
Pt-Ir	platinum-iridium
DLS	dynamic light scattering
PDI	polydispersity index
LDV	laser Doppler velocimetry
BET	Brunauer-Emmett-Teller

IUPAC	International Union of Pure and Applied Chemistry
TEM	transmission electron microscope
SEM	scanning electron microscope
Tris	tris(hydroxymethyl)aminomethane
HEMA	2-hydroxyethyl methacrylate
HCl	hydrochloric acid
NaOH	sodium hydroxide solution
NaCl	sodium chloride
AEMA	2-aminoethyl methacrylate hydrochloride
IBMA	isobutyl methacrylate
DMPAP	2,2-dimethoxy-2-phenylacetophenone
LG	β-lactoglobulin
GP	α1-acid glycoprotein
V-70	2,2-azobis(4-methoxy-2,4-dimethylvaleronitrile)
HD	n-hexadecane
KCl	potassium chloride
PABs	pepstatin immobilized agarose beads
CTAB	cetyltrimethylammonium bromide
MWCO	molecular weight cut-off
RT	room temperature
CB	citrate buffer solution
PB	phosphate buffer solution
IgG	immunoglobulin G
GUA	*N*-(3-methacrylamidopropyl)guanidinium chloride
APM	*N*-(3-aminopropyl)methacrylamide hydrochloride
HEAm	*N*-(2-hydroxyethyl)acrylamide
AIBN	azobisisobutyronitrile
^{1}H-NMR	proton nuclear magnetic resonance

IV. Abstract

Many different analytical methods for protein separation, detection and analysis used in disease therapy and diagnosis are based on the excellent recognition properties of antibodies. These enable the antibody to bind a specific protein, the antigen, with high affinity and selectivity. However, the production of antibodies is elaborately and costly. The design of biomimetic synthetic receptors capable of mimicking the molecular recognition properties of antibodies is of significant interest for research and the application of a cheaper and easier produced alternative to antibodies in analytical methods. The aim of this thesis is the design and synthesis of such a material capable of selectively binding pepsin, as well-characterized example protease, with high affinity. The selective binding of proteases is of great importance for the application in the purification process of pharmaceutical proteins, as proteases are frequently obtained as side product during their biotechnological production and may degrade these. Submicron polymer particles offer a large external surface area and thus a high number of accessible binding sites for proteins and may be applied in suspension assays. Two different approaches are pursued for the synthesis of such polymer particles in this thesis.

In the first part of the thesis, the concept of molecular imprinting is used. This enables the formation of specific recognition sites in synthetic polymers through the use of a template molecule and found promising applications in many fields such as in separation methods, pseudo-immunoassays and sensors. In comparison to the imprinting of small molecules, which is well-established nowadays, the imprinting of proteins is still challenging due to their molecular dimension, conformational flexibility, complexity and limited solubility in organic solvents. New synthesis strategies including bulk imprinting in water, surface and epitope imprinting have therefore been developed in recent years. Surface imprinting is promising, as the binding sites are thereby formed at the polymer surface and not within the polymer network as in bulk molecularly imprinted polymers and are therefore readily accessible for proteins as well. The miniemulsion polymerization enables the surface imprinting of submicron polymer particles in one step.

A synthesis strategy was developed for the preparation of pepsin surface imprinted submicron polymer particles via miniemulsion polymerization. Water was used as continuous phase, Lutensol AT 50 as non-ionic surfactant and ethylene glycol dimethacrylate as cross-linker in a molar ratio of 4 : 1 to the functional monomer. The type and amount of functional monomer, the pepsin template amount, pH value and type of extraction solution were varied. Furthermore, the influence of the surfactant was investigated. The miniemulsion polymerization was carried out and polymer suspensions containing spherical particles with a rough surface and a relatively broad size

distribution with diameters ranging from around 50 to 600 nm were obtained in the presence and absence of pepsin. The qualitative monitoring of the pepsin extraction using ultraviolet-visible (UV-Vis) spectrophotometry showed that most of pepsin was removed. The average hydrodynamic diameter of the particles was between 200 and 700 nm and the specific surface area between 26 and 50 $m^2 g^{-1}$ after the extraction. The pepsin binding capacity, affinity, selectivity and the imprinting efficiency were evaluated by performing single and competitive batch rebinding experiments with pepsin and different other proteins using UV-Vis spectrophotometry and sodium dodecyl sulfate-polyacrylamide gel electrophoresis. The results showed that higher pepsin binding capacities were obtained with positively charged than with neutral and negatively charged functional monomers due to ionic interactions with the in water (pH 5) negatively charged pepsin. The increase of the amount of positively charged monomer and thus the number of ionic interactions resulted in an increased pepsin binding capacity. The polymer particles with a high number of positively charged groups could almost bind the whole amount of pepsin and showed selectivity for pepsin against other proteins due to the extraordinary low isoelectric point of pepsin. The imprinting efficiency was investigated by comparing the pepsin binding capacity and selectivity of the molecularly imprinted polymers (MIPs) with those of corresponding non-imprinted polymers (NIPs). The result of the screening of different functional monomers showed that the highest effect from imprinting was obtained with *N*-(3-acrylamidopropyl)trimethylammonium chloride (APTMA) due to a combination of ionic and hydrophobic interactions. The imprinting effect was slightly increased by using twice the amount of the pepsin template. The pepsin binding capacity and selectivity for pepsin against some of the other proteins could generally be slightly increased due to the imprinting. The greatest increase of the selectivity was obtained with a combination of APTMA and the hydrophobic monomer isobutyl methacrylate. Since the selectivity is the primary goal of MIPs, the most successful result of using the molecular imprinting was obtained with those two functional monomers. The MIP prepared without any surfactant showed the highest selectivity for pepsin in a competitive rebinding experiment, which comes closest to the real situation in the final application. This bound most of pepsin and none of the other proteins. This indicates that the imprinting without surfactant was successful. However, this could not be fully proven, since the corresponding NIP was a bulk polymer and thus did not represent a suitable reference material. Maximum binding capacities and dissociation constants were obtained by fitting the Langmuir equation to binding isotherms. The maximum binding capacities of the MIPs were between 3.4 and 25.3 mg m^{-2} and significantly higher than those of the NIPs, thereby indicating that the MIPs had significantly more binding sites. The dissociation constants of the MIPs were between 4.71 and 39.95 µM and comparable with those of other protein imprinted polymer particles. However, the dissociation constants of the NIPs were lower. This may be explained by difficulties concerning the evaluation of

the data of the MIPs or indicates that the affinity could not be increased due to the imprinting. The equilibrium binding between pepsin and two MIP-NIP pairs was observed after just 1 min of incubation. The binding of pepsin was exceptionally fast due to the high mass transfer rate of pepsin from the solution to the binding sites, which were located at the surface of the submicron polymer particles and thus readily accessible for pepsin. On the other hand, the pepsin binding to the MIP prepared in absence of a surfactant was much slower possibly as a result of the formation of more selective interactions.

In the second part of the thesis, the concept of rational design is used. The type and ratio of different functional monomers are thereby selected according to the chemical composition of the surface of the target protein and varied to obtain the highest possible number of interactions between the resulting polymer particles and the target protein. The polymer particles with different composition are subsequently screened for the one with the highest affinity to the target protein. A low degree of cross-linking is used to enable the polymer chains considerable flexibility that gives the randomly distributed functional groups the possibility to align towards complementary functional groups of the protein. Polymer particles with high affinity and selectivity for melittin, lysozyme, immunoglobulin G and fibrinogen have already been prepared with this concept. A precipitation polymerization with a low monomer concentration and a low amount of surfactant enables the preparation of polymer nanoparticles (NPs) from water-soluble monomers in water.
A synthesis strategy using this concept was developed for the preparation of NPs with high affinity to pepsin. The precipitation polymerization was carried out with monomers with different functional groups, *N*-isopropylacrylamide (NIPAm), *N*-(*tert*-butyl)acrylamide (TBAm) and the cross-linker *N,N'*-methylenebisacrylamide (BIS). NPs with an average hydrodynamic diameter between 90 and 180 nm were obtained after dialysis, which was carried out in order to remove the surfactant, unreacted monomer and oligomers. The binding affinity of the different NPs to pepsin was evaluated with an incubation study in solution using UV-Vis-spectrophotometry and an incubation study in microtiter wells using an EnzChek® protease assay, which enabled a fast screening and the direct detection of bound pepsin. The highest content of pepsin was bound to the NPs prepared with different positively charged monomers mainly due to ionic interactions with the in citric buffer solution (pH 5) negatively charged pepsin. The increase of the amount of positively charged monomers resulted in an increase of the affinity of the NPs to pepsin due to the high number of acidic amino acid residues on the surface of pepsin. This was in agreement with the results obtained in the first part of the thesis. APTMA, which can form ionic and hydrophobic interactions with pepsin and turned out to be the most suitable monomer for imprinting pepsin, was also the most suitable positively charged monomer for binding pepsin to the NPs. The highest affinity to pepsin showed the NPs synthesized from 20 mol-% of APTMA, 40 mol-% of TBAm, 38 mol-% of NIPAm and 2 mol-% of BIS. A study of the

binding kinetic showed that the binding equilibrium has already been reached after 1 minute. The adsorption of pepsin to the NPs was very fast due to the good availability of the binding sites for pepsin due to the small size and flexibility of the lowly cross-linked NPs. Significantly more pepsin was bound to the NPs with the highest affinity to pepsin than to one of the MIPs with the highest affinity to pepsin and to commercially available beads for pepsin purification under the same binding conditions. This may be a result of the smaller size and thus larger surface area of the NPs, the combination of ionic and hydrophobic interactions and the fact that acrylamide based micro- and nanogels are possibly more compatible to proteins.

The described approaches provide a fundamental step towards the development of a synthetic receptor material for the selective binding of pepsin and a protease scavenger material and assay for the purification of pharmaceutical proteins.

V. Zusammenfassung

Viele verschiedene analytische Methoden zur Trennung, Detektion und Analyse von Proteinen, die zur Therapie und Diagnose von Krankheiten eingesetzt werden, beruhen auf den exzellenten Erkennungseigenschaften von Antikörpern. Diese ermöglichen es den Antikörpern ein spezifisches Protein, das Antigen, mit hoher Affinität und Selektivität zu binden. Die Herstellung von Antikörpern ist jedoch aufwendig und kostspielig. Das Design von biomimetischen synthetischen Rezeptoren mit der Fähigkeit die molekularen Erkennungseigenschaften von Antikörpern nachzuahmen ist von großem Interesse für die Forschung und für den Einsatz als einfachere und günstigere Alternative zu Antikörpern in analytischen Methoden. Das Ziel dieser Doktorarbeit ist das Design und die Synthese eines solchen Materials, das fähig ist Pepsin, als Beispiel einer gut charakterisierten Protease, mit hoher Affinität selektiv zu binden. Die selektive Bindung von Proteasen ist von großer Bedeutung für die Anwendung im Aufreinigungsprozess von pharmazeutischen Proteinen, da Proteasen häufig als Nebenprodukt während deren biotechnologischer Herstellung erhalten werden und diese wiederum abbauen können. Polymerpartikel im Submikrometerbereich bieten eine große äußere Oberfläche und somit eine hohe Anzahl an für Proteine erreichbare Bindungsstellen und können in Suspensionsassays zum Einsatz kommen. In der vorliegenden Doktorarbeit werden zwei verschiedene Ansätze um solche Polymerpartikel herzustellen verfolgt.

Im ersten Teil dieser Arbeit wird das Konzept des Molekularen Prägens verwendet, das durch die Verwendung eines Templatmoleküls die Bildung von spezifischen Erkennungsstellen in synthetischen Polymeren ermöglicht und vielversprechende Anwendungen in vielen Bereichen wie in Trennmethoden, Pseudo-Immunoassays und Sensoren gefunden hat. Im Vergleich zum Prägen von kleinen Molekülen, das inzwischen etabliert ist, stellt das Prägen von Proteinen aufgrund der molekularen Dimension, flexiblen Konformation, Komplexität und limitierten Löslichkeit von Proteinen in organischen Lösungsmitteln noch eine Herausforderung dar. Neue Synthesestrategien darunter das Bulk-Prägen in Wasser, das Oberflächen- und Epitop-Prägen wurden dafür in den letzten Jahren entwickelt. Das Oberflächenprägen ist vielversprechend, da hierbei die Bindungsstellen an der Polymeroberfläche und nicht innerhalb des Polymernetzwerkes wie in Bulk-molekular geprägten Polymeren gebildet werden und daher auch für Proteine gut zugänglich sind. Die Miniemulsionspolymerisation ermöglicht das Oberflächenprägen von Submikrometer-Polymerpartikeln in einem Schritt.

Eine Synthesestrategie wurde für die Herstellung von Pepsin oberflächengeprägten Submikrometer-Polymerpartikeln mittels Miniemulsionspolymerisation entwickelt. Wasser wurde dabei als kontinuierliche Phase, Lutensol AT 50 als nichtionisches Tensid und Ethylenglykoldimethacrylat als

Vernetzer in einem molaren Verhältnis zum funktionellen Monomer von 4 : 1 verwendet. Die Art und Menge des funktionellen Monomers, die Menge an Pepsintemplat, der pH-Wert und die Art des Extraktionsmittels wurden variiert. Des Weiteren wurde der Einfluss des Tensids untersucht. Die Miniemulsionspolymerisation wurde durchgeführt und Polymersuspensionen, die runde Partikel mit einer rauen Oberfläche und einer relativ breiten Größenverteilung mit Durchmessern von ungefähr 50 bis 600 nm enthielten, wurden in der Gegenwart und Abwesenheit von Pepsin erhalten. Die qualitative Kontrolle der Pepsinextraktion mittels Ultraviolet-visible-(UV-Vis-) Spektrophotometrie zeigte, dass Pepsin weitgehend entfernt wurde. Der hydrodynamische durchschnittliche Partikeldurchmesser war nach der Extraktion zwischen 200 und 700 nm und die spezifische Oberfläche zwischen 26 und 50 $m^2 g^{-1}$. Die Pepsinbindungskapazität, Affinität, Selektivität und die Prägeeffizienz wurden evaluiert, indem Einzel- und kompetitive Batch-Wiederanbindungsversuche mit Pepsin und verschiedenen anderen Proteinen unter Verwendung der UV-Vis-Spektrophotometrie und der Natriumdodecylsulfat-Polyacrylamidgelelektrophorese durchgeführt wurden. Die Ergebnisse zeigten, dass mit positiv geladenen funktionellen Monomeren durch ionische Wechselwirkungen mit dem in Wasser (pH 5) negativ geladenen Pepsin höhere Pepsinbindungskapazitäten als mit neutralen und negativ geladenen erreicht wurden. Die Steigerung der Menge an positiv geladenem Monomer und somit der Anzahl an ionischen Wechselwirkungen führte zu einer Erhöhung der Pepsinbindungskapazität. Die Polymerpartikel mit einer hohen Anzahl an positiv geladenen Gruppen konnten fast die gesamte Menge an Pepsin binden und zeigten aufgrund des außergewöhnlich niedrigen isoelektrischen Punkts von Pepsin eine Selektivität für Pepsin gegenüber anderen Proteinen. Die Prägeeffizienz wurde mittels Vergleich der Pepsinbindungskapazität und Selektivität zwischen den molekular geprägten Polymeren (MIPs) und dazugehörigen nicht geprägten Polymeren (NIPs) untersucht. Das Ergebnis des Screenings verschiedener funktioneller Monomere zeigte, dass der höchste Prägeeffekt mit *N*-3-Acrylamidopropyltrimethylammoniumchlorid (APTMA) aufgrund einer Kombination von ionischen und hydrophoben Wechselwirkungen erhalten wurde. Der Prägeeffekt wurde durch den Einsatz der doppelten Menge an Pepsintemplat leicht erhöht. Die Pepsinbindungskapazität und Selektivität für Pepsin gegenüber ein paar der anderen Proteine konnten generell durch das Prägen leicht erhöht werden. Die höchste Steigerung der Selektivität wurde mit einer Kombination aus APTMA und des hydrophoben Monomers Isobutylmethacrylat erhalten. Da die Selektivität das primäre Ziel von MIPs ist, wurde mit diesen beiden funktionellen Monomeren das erfolgreichste Ergebnis mittels Molekularem Prägen erzielt. Das MIP, das ohne Tensid hergestellt wurde, zeigte die höchste Selektivität für Pepsin in einem kompetitiven Wiederbindungsexperiment, das dem realen Zustand in der finalen Anwendung am nächsten kommt. Es band fast die gesamte Menge an Pepsin, während keines der anderen Proteine gebunden wurde. Dies deutet darauf hin, dass das Prägen ohne Tensid

erfolgreich war. Jedoch konnte dies nicht vollständig bewiesen werden, da das dazugehörige NIP ein Bulk-Polymer war und somit kein geeignetes Vergleichsmaterial darstellte. Maximale Bindungskapazitäten und Dissoziationskonstanten wurden durch Fitten der Langmuir-Gleichung an Bindungsisothermen erhalten. Die maximalen Bindungskapazitäten der MIPs waren zwischen 3.4 und 25.3 mg m^{-2} und deutlich höher als die der NIPs, was darauf schließen lässt, dass die MIPs deutlich mehr Bindungsstellen besaßen. Die Dissoziationskonstanten der MIPs waren zwischen 4.71 und 39.95 µM und vergleichbar mit denen anderer Protein geprägter Polymerpartikel. Jedoch waren die Dissoziationskonstanten der NIPs niedriger, was zeigt, dass die NIPs eine höhere Affinität für Pepsin hatten. Dies kann dadurch erklärt werden, dass Schwierigkeiten bei der Evaluierung der Daten der MIPs auftraten, oder deutet an, dass durch das Prägen die Affinität nicht erhöht werden konnte. Das Bindungsgleichgewicht zwischen Pepsin und zwei MIP-NIP-Paaren war bereits nach einer Inkubationszeit von 1 Minute zu beobachten. Die Bindung des Pepsins war aufgrund des hohen Stoffübergangs des Pepsins aus der Lösung zu den Bindungsstellen, die sich auf der Oberfläche der Submikrometer-Polymerpartikel befanden und somit für Pepsin gut erreichbar waren, außergewöhnlich schnell. Dahingegen war die Pepsinbindung an die Polymerpartikel, die in Abwesenheit eines Tensids hergestellt wurden, möglicherweise aufgrund der Bildung von mehr selektiven Wechselwirkungen viel langsamer.

Im zweiten Teil dieser Arbeit wird das Konzept des Rationalen Designs verwendet. Dabei werden die Art und das Verhältnis verschiedener funktioneller Monomere gemäß der chemischen Zusammensetzung der Oberfläche des Zielproteins ausgewählt und variiert, um eine möglichst hohe Anzahl an Wechselwirkungen zwischen den resultierenden Polymerpartikeln und dem Zielprotein zu erhalten. Die Polymerpartikel mit unterschiedlicher Zusammensetzung werden anschließend einem Screening unterzogen, um diejenigen mit der höchsten Affinität für das Zielprotein zu ermitteln. Ein niedriger Vernetzungsgrad wird verwendet um den Polymerketten eine gewisse Flexibilität zu verleihen. Diese Flexibilität soll den zufällig verteilten funktionellen Gruppen die Möglichkeit geben sich gegenüber komplementären funktionellen Gruppen des Proteins auszurichten. Mit diesem Konzept wurden bereits Polymerpartikel mit hoher Affinität und Selektivität für Melittin, Lysozym, Immunglobulin G und Fibrinogen hergestellt. Eine Fällungspolymerisation mit niedriger Monomerkonzentration und einer geringen Menge an Tensid ermöglicht die Herstellung von polymeren Nanopartikeln (NPs) aus wasserlöslichen Monomeren in Wasser.

Eine Synthesestrategie wurde für die Herstellung von Polymer-NPs mit hoher Affinität für Pepsin mit diesem Konzept entwickelt. Die Fällungspolymerisation wurde mit Monomeren mit unterschiedlichen funktionellen Gruppen, *N*-Isopropylacrylamid (NIPAm), *N*-*tert*-Butylacrylamid (TBAm) und dem Vernetzer *N,N'*-Methylenbisacrylamid (BIS) durchgeführt. NPs mit einem hydrodynamischen durchschnittlichen Durchmesser zwischen 90 und 180 nm wurden nach einer

Dialyse erhalten, die durchgeführt wurde um das Tensid, nicht umgesetztes Monomer und Oligomere zu entfernen. Die Bindungsaffinität der unterschiedlichen NPs zu Pepsin wurde mit einer Inkubationsstudie in Lösung mit Hilfe der UV-Vis-Spektrophotometrie und einer Inkubationsstudie in Mikrotiterplattenvertiefungen, die ein schnelles Screening und die direkte Detektion von gebundenem Pepsin ermöglichte, mit Hilfe eines EnzChek® Protease-Assays evaluiert. Der höchste Gehalt an Pepsin wurde an die NPs gebunden, die mit verschiedenen positiv geladenen Monomeren hergestellt wurden und somit ionische Wechselwirkungen mit dem in Zitronensäurepufferlösung (pH 5) negativ geladenen Pepsin ausbilden konnten. Die Steigerung der Menge an positiv geladenem Monomer führte aufgrund der hohen Anzahl an sauren Aminosäureresten auf der Pepsinoberfläche zu einer Erhöhung der Affinität der NPs zu Pepsin. Dies stimmte mit den im ersten Teil der Arbeit erhaltenen Ergebnissen überein. APTMA, das mit Pepsin ionische und hydrophobe Wechselwirkungen ausbilden kann und sich als geeignetstes Monomer für das Prägen von Pepsin herausstellte, war auch das geeignetste positiv geladene Monomer um Pepsin an die NPs zu binden. Die höchste Affinität zu Pepsin zeigten die NPs, die aus 20 mol-% an APTMA, 40 mol-% an TBAm, 38 mol-% an NIPAm und 2 mol-% an BIS hergestellt worden waren. Eine Studie der Bindungskinetik zeigte, dass das Bindungsgleichgewicht schon nach 1 Minute erreicht wurde. Die Adsorption von Pepsin an die NPs war durch die gute Erreichbarkeit der Bindungsstellen für Pepsin aufgrund der kleinen Größe und Flexibilität der leicht vernetzten NPs sehr schnell. Deutlich mehr Pepsin wurde unter gleichen Bedingungen an die NPs mit der höchsten Affinität für Pepsin als an eines der MIPs mit der höchsten Affinität zu Pepsin und als an kommerziell erhältliche Partikel für die Aufreinigung von Pepsin gebunden. Dies dürfte auf die kleinere Größe und damit verbundene größere Oberfläche der NPs, die Kombination aus ionischen und hydrophoben Wechselwirkungen und die Tatsache, dass Acrylamid-basierte Mikro- und Nanogele möglicherweise kompatibler zu Proteinen sind, zurückzuführen sein.

Die beschriebenen Ansätze bieten einen grundlegenden ersten Schritt in Richtung der Entwicklung eines synthetischen Rezeptormaterials für die selektive Bindung von Pepsin und eines Protease-Scavenger Materials und Assays für die Aufreinigung pharmazeutischer Proteine.

1. Introduction

1.1 Background of the thesis

Proteases are frequently obtained as side product in cell culture solutions during the production of pharmaceutical proteins from microorganisms. They constitute a group of enzymes that catalyzes the cleavage of peptide bonds in other proteins by hydrolysis. Hence, they may also degrade biotechnologically produced pharmaceutical proteins like antibodies and thereby reduce the yield, even if they are only present in trace amounts. This influences the formulation, stability and quality of the final protein products.[1] Consequently, they have to be either deactivated or removed from the desired pharmaceutical proteins. Deactivation is usually achieved by adding different inhibitor molecules that bind to the active site of different proteases and thus inhibit their activity. The inhibitor molecules have to be removed due to their toxicity and other interfering effects afterwards. The removal of the inhibitor molecules and the proteases is usually done by multiple purification steps, which is an expensive and time-consuming procedure in the downstream processing.[2,3]

A more rapid and sensitive method to remove unwanted proteases and to concurrently achieve a better yield of biopharmaceutical products would be the use of a synthetic scavenger material. This material is supposed to selectively bind different proteases, while the desired pharmaceutical proteins pass through unaffectedly. An advantage of the scavenger material over inhibitors is that it may easily be separated from the cell culture solution after binding. A synthetic receptor has the advantage over natural receptors such as antibodies that it will not be digested by the proteases and that its preparation is easier and cheaper. The fundamental development of such a scavenger material has been initiated by the company Labor Dr. Merk & Kollegen GmbH (LMK) in collaboration with the company Atoll GmbH (Atoll) and the Institute of Analytical and Bioanalytical Chemistry (IABC) at the University of Ulm.[2] An accompanying protease assay, which allows selective and sensitive identification and determination of different proteases, is additionally planned to be developed for monitoring the effective protease elimination by the scavenger material within this research project.

The distribution of the tasks within this research project was as follows. While LMK should provide protease containing fermentation solutions as test material and deal with the identification of the occurring proteases, Atoll should support the search for suitable biomimetic ligands with a screening method[4] and provide cartridges for the final scavenger material (Figure 1.1).[2] The task of the IABC was the development of the protease scavenger material and assay based on the molecular imprinting technique, which is a successfully applied technique for the creation of tailor-made

synthetic receptors for various target molecules enabling their selective binding with high affinity. Pepsin was selected as first exemplary protease for the use as template molecule in the molecular imprinting process, as it is a well-characterized protease available in sufficient quantity and purity at an affordable price and the occurring proteases have not yet been identified at the initial period of the project. Two different strategies were pursued for imprinting pepsin, which might be adapted to other proteases in the future or might result in affinity matrices exhibiting group selectivity for several proteases. One strategy was the inhibitor-assisted synthesis of pepsin surface imprinted core-shell microbeads.

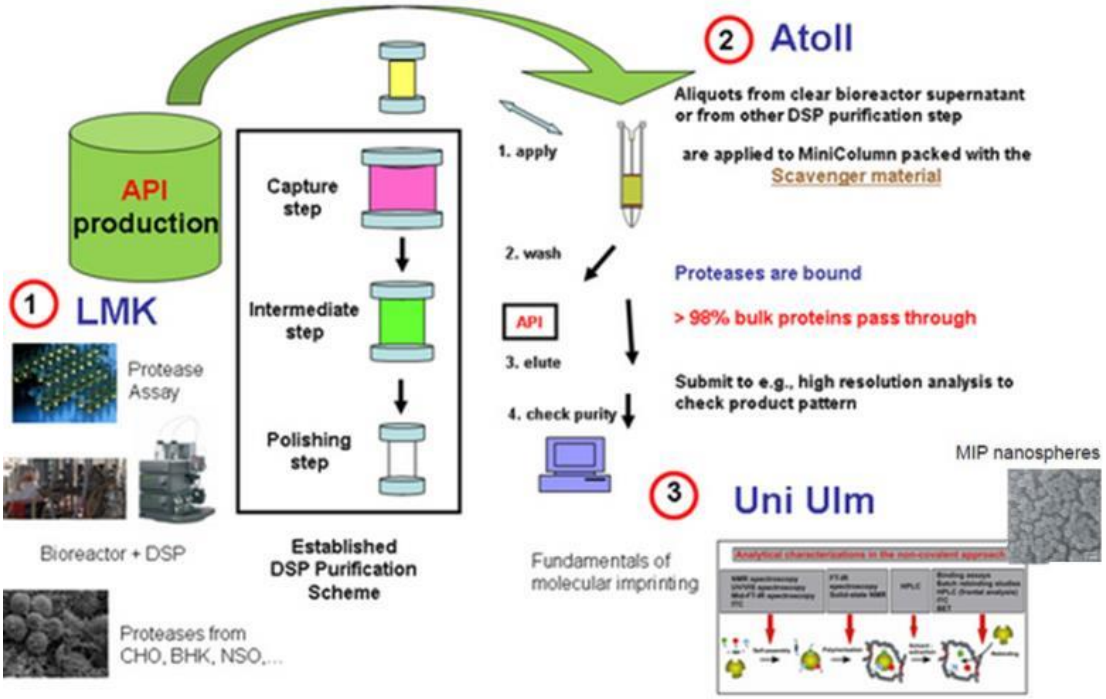

Figure 1.1 Scheme of the research project description for the development of a protease scavenger and assay.[2]

The other strategy was the synthesis of pepsin surface imprinted submicron polymer particles via miniemulsion polymerization. Polymer particles in the submicrometer range offer a large surface area associated with high binding capacities and remain in a liquid for the use in suspension.[5] This strategy is pursued within this thesis and described in chapter 2. Chapter 3 addresses the synthesis of polymer nanoparticles with high affinity to pepsin via precipitation polymerization by designing the composition of the nanoparticles based on the protein amino acid residue composition. This shall provide a complementary approach to the imprinting approach.

1.2 Background on proteins and proteases

1.2.1 Proteins

Proteins are biological macromolecules that have different structures and several functions in living organisms.[6] They are divided into globular and fibrous proteins, which provide structural support for cells and tissues such as keratins and collagens having a fibrous or filamentary structure. Globular proteins are spherical, have a more compact structure and many different functions: Enzymes catalyze metabolic reactions, hormones transmit messages to regulate biological processes and transport proteins move different molecules across membranes such as hemoglobin that transports oxygen in the blood circulation. Antibodies, also called immunoglobulins, recognize and specifically bind to bacteria, viruses or other foreign harmful large molecules, summarized under the term antigens, with very high affinity and tag them for attack by other parts of the immune system for preventing infections.

Proteins consist of hundreds or thousands of amino acid residues from 23 different amino acids that are linked together by peptide bonds in one or more polypeptide chains and have molecular weights higher than 10 kDa. A peptide is referred to as a chain out of two up to many thousands of amino acid residues. Polypeptides generally have molecular weights below 10 kDa.[6] All 20 of the common amino acids in proteins except glycine contain an amine and a carboxyl group and different side chains at the first carbon atom, thus also known as 2- or α-amino acids, and are L-stereoisomers. These can be classified into the groups of acidic, basic, polar neutral and hydrophobic amino acids according to their polarity and tendency to interact with water via the functional groups of their side chains.

Proteins are characterized by their amino acid residue sequence and folded into a unique three-dimensional (3D) structure, which is decisive for their function and described by four levels.[6] The primary structure refers to the covalent bonds including peptide and disulfide bonds, which bind the amino acid residues in a specific sequence inside a polypeptide chain. The secondary structure includes different regularly repeating local structures stabilized by hydrogen bonds such as α-helices, β-sheets, β-turns and irregular parts referred to as random coils. The tertiary structure summarizes all aspects of the 3D folding of a single polypeptide chain and is stabilized by non-covalent interactions such as hydrogen bonds, salt bridges and hydrophobic interactions and by disulfide bonds between different parts of the polypeptide chain. The spatial arrangement of different polypeptide chains in one protein is called quaternary structure.

The native conformation is the structure, into which a protein naturally folds. The protein stability describes the effort of a protein to maintain its native conformation. Small changes of the environment of proteins such as the temperature, pH value or the presence of organic solvents or

surfactants can result in a change of the conformation by affecting mainly non-covalent interactions in the protein and thus influence the function of the protein.[6] When the function is totally lost, the conformational change is called denaturation, which does not necessarily have to result in a total unfolding of the protein. Renaturation is the process, when the protein regains its native conformation due to changing the environment to its physiological conditions.

Proteins are of an amphoteric nature, since they contain carboxyl as well as amine groups coming from the side chains of acidic and basic amino acids. These amino acid residues can exist in a protonated or deprotonated form and can thus be neutral, negatively or positively charged resulting in a different net charge of the whole protein. The pH value, at which they contain the same number of positively and negatively charged side groups resulting in a neutral net charge, is called isoelectric point (*pI*).[6] At a pH value below the isoelectric point they carry a positive net charge and at a pH value above the isoelectric point they have a negative net charge. Different proteins have different isoelectric points, since they contain a different number of acidic and basic amino acid residues. At the isoelectric point, proteins have a minimum solubility in aqueous solutions and do not migrate in an electric field.[6]

1.2.2 Proteases

Proteases are enzymes forming a subgroup of the hydrolases and catalyze the cleavage of peptide bonds in other proteins by hydrolysis.[7] They can be found in plants, animals and microorganisms such as bacteria, viruses and fungi and play an important role in the regulation of physiological processes in living organisms such as digestion, growth, differentiation, immunological defense and wound healing. Proteases have several applications in the detergent, food, leather and pharmaceutical industry as well as in the structural elucidation of proteins in research.

Proteases are subdivided into two major groups depending on their site of action. Exopeptidases cleave peptide bonds from the amino (N-) or carboxyl (C-) terminus, whereas endopeptidases cleave internal peptide bonds of the protein substrates. Exopeptidases are further classified into aminopeptidases and carboxypeptidases based on their site of action at the N- or C-terminus. Endopeptidases are further classified into serine, aspartic, cysteine proteases and metalloproteases according to the type of functional group present in their active site.[7] Trypsin is an example for a serine, pepsin for an aspartic, papain for a cysteine protease and thermolysin for a metalloprotease. Alternatively, they can be classified based on the pH value of their optimal activity into acidic, neutral or alkaline proteases. They also differ in their specificity. Whereas some proteases have a broad range of substrates, others are highly specific and only cleave substrates with a certain sequence. There are several inhibitors that can bind to the active site of proteases and thus inhibit their activity. Most inhibitors are specific for one group of proteases such as pepstatin A that inhibits aspartic proteases[8]. A few can also inhibit proteases of different groups.

Aspartic proteases contain two aspartic amino acid residues in their active site that are responsible for their catalytic activity. One aspartic acid residue is protonated and the other one is deprotonated. A water molecule is bound by both aspartic amino acid residues and is thus activated for the nucleophilic attack on the carbonyl carbon of a substrate peptide bond.[9,10] Most aspartic proteases show maximal activity in an acidic environment, have isoelectric points between 3 and 4.5 and molecular weights between 30 and 45 kDa.[7]

1.2.3 Pepsin

Pepsin, mainly pepsin A, is the primary digestive protease in the gastric juice of vertebrates[7,11], where it catalyzes the degradation of food proteins. Its zymogen pepsinogen, an inactive precursor form, has to be activated by hydrochloric acid before that splitting of 44 amino acid residues, which block the access of the catalytic site.[12,13] Pepsin is a well-characterized[14] aspartic protease with the E.C. number 3.4.23.1 and cleaves internal peptide bonds between hydrophobic and preferably aromatic amino acids[15] of various substrates such as casein, several albumins and globulins and gelatin[16]. Pepsin has several applications such as the digestion of antibodies, the preparation of collagen for cosmeceutical purpose, the assessment of digestibility of proteins in food chemistry and subculture of viable mammary epithelial cells.[17]

Pepsin consists of 327 amino acid residues within a single polypeptide chain with two domains and has a molecular weight of 35 kDa.[18,19] Its isoelectric point between 2.2 and 3.0[20] is very low, as it contains 43 acidic and only 4 basic amino acid residues. Its secondary structure is mainly composed of β-sheets and contains only few α-helices.[21,22] Pepsin has three disulfide bridges and one phosphoseryl and one histidyl residue.[18] Pepsin has its maximum activity at a pH value of 2 comparable to the pH value in the stomach. It still has approximately 70% of its maximum catalytic activity between pH 3.5 and 4.5 and approximately 40% at pH 5. This is shown by an activity study determined by digestion of radioiodinated serum albumin.[23] Pepsin has no activity at pH values between 5.5 and 6, but is stable within this range, since it shows maximum activity after restoration of the pH value to 2. At pH 7, it has approximately 70% of the maximum activity after restoration of the pH value to 2. Above pH 8, it is irreversibly inactivated[23] and denatured.[24,25] A typical inhibitor of pepsin is pepstatin A[26,27] like of other aspartic proteases. Pepstatin is a low molecular weight compound that binds reversibly to pepsin with a dissociation constant of 97 pM[28] by the formation of hydrogen bonds and van der Waals interactions[26]. The statyl residue of pepstatin is considered to be responsible for the inhibition of pepsin, as it is an analogue of the transition state.[8] Pepstatin inhibition is highest at pH values between 1.5 and 3.8, but less effective at higher pH values.[29]

1.3 Adsorption of proteins on polymer particles

The adsorption of proteins on polymer particles has significant importance in biomedical applications such as drug delivery, biosensors, solid phase immunoassays and immobilized enzymes. For this reason, protein adsorption on polymer particles has been studied for a long time, but the exact mechanism of protein adsorption on polymer particles has not yet been elucidated due to the complexity of proteins.[30] In general, proteins adsorb on almost every surface with only a few exceptions causing non-specific adsorption. Protein adsorption occurs in a reversible and irreversible adsorption accompanied with a conformational change of the protein up to unfolding and denaturation.

The interaction forces between proteins and polymer particles are mainly hydrophobic interactions, ionic interactions, hydrogen bonds (Figure 1.2) as well as other electrostatic interactions.

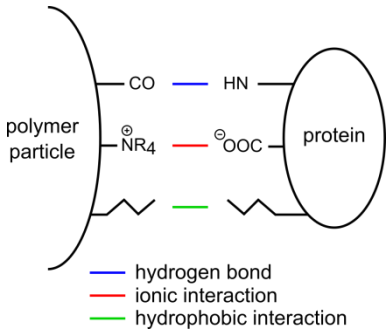

Figure 1.2 Scheme of the main interactions between a polymer particle and protein.

Generally, proteins adsorb stronger on a hydrophobic than on a hydrophilic surface, since hydrophobic interactions play a major role in the protein adsorption out of an aqueous environment being strongest at a pH value around the isoelectric point of the proteins.[30] Whereas ionic interactions, hydrogen bonds and other electrostatic interactions are based on energetic forces, hydrophobic interactions are based on entropic forces. The driving force behind hydrophobic interactions is the displacement of ordered water molecules from an area between two hydrophobic interfaces, which tend to aggregate resulting in a higher number of free water molecules in solution.[6] Ionic interactions are formed through the attraction of oppositely charged ions on the polymer particles and proteins and are strongest at a pH value below or above the isoelectric point of the proteins. Hydrogen bonds are frequently formed between oxygen and nitrogen atoms acting as hydrogen acceptor or donor.[30] Ionic interactions and hydrogen bonds are less effective in protein adsorption, since proteins are usually adsorbed out of an aqueous solution and water greatly weakens these interactions through competition for their attractions. Van der Waals interactions have an effect only over small distances, when water has been excluded, and are negligible, when the other interactions exist.

2. Pepsin surface imprinted submicron polymer particles

2.1 Motivation and scope

Several analytical techniques for protein detection, separation and analysis are based on the excellent recognition properties of biomacromolecules such as antibodies and enzymes for special target molecules. However, the production of biomacromolecules is complex and costly, they are only suited for single use due to their labile nature and natural receptors are not available for all target molecules. Molecularly imprinted polymers (MIPs) represent a good synthetic alternative[31], since they can mimic the recognition properties of biomacromolecules and their preparation is easier, faster and cheaper.[32] Furthermore they are stable over time, reusable and their synthesis is adaptable to various target molecules. The most widely used non-covalent imprinting approach[33,34] allows a straightforward preparation and easy and mild template extraction. In addition to that, the formation of non-covalent interactions enables fast rebinding.[35,36]

Surface imprinting is a promising approach for imprinting proteins, as the binding sites are predominantly formed at the polymer surface and are easily accessible even for large target molecules such as proteins.[37,38] This enables an easier template removal and an increased mass transfer and thus improved rebinding kinetics overcoming the diffusion limitation of proteins. The material surface can either be located on thin films or on polymer or silica particles. Surface imprinting of submicron particles is favorable due to their high surface-to-volume ratio providing a high external surface area and thus a large number of binding sites on the surface.[5,39] This results in an improved mass transfer without loss of the binding capacity.

The miniemulsion polymerization offers several advantages for the synthesis of protein surface imprinted submicron polymer particles. This enables a one-step preparation without the need of support particles compared with the grafting approach, where a polymer layer is grafted on core particles in the presence of a template molecule.[40] The miniemulsion polymerization is carried out in monomer droplets surrounded by water without monomer diffusion through the continuous water phase.[41,42] Hence, the protein template can be dissolved in water and assembled at the monomer-water interface for the formation of the pre-polymerization complex, which is preserved during the polymerization. Another advantage of using miniemulsion polymerization is that an incomplete coverage of the surface by the surfactant is sufficient for the stabilization of the miniemulsion compared with emulsion and microemulsion polymerization enabling free space for protein adsorption at the droplet surface.[41,42] Furthermore, the copolymerization of two monomers with different polarities may be carried out in a miniemulsified system in one step, where one monomer is dissolved in the continuous phase and copolymerized with the other dispersed

monomer at the droplet surface.[43–45]

In this part of the thesis, a synthesis strategy for the creation of pepsin surface imprinted submicron polymer particles via miniemulsion polymerization for the selective capture of pepsin is developed after a preliminary study of the stability of the conformation of pepsin under different conditions using circular dichroism spectroscopy. The influence of different parameters such as the type and amount of functional monomer, pH value, presence of surfactant and the type of extraction solution on the imprinting efficiency is investigated. The imprinting efficiency is evaluated by performing batch rebinding experiments with different initial pepsin concentrations, incubation solutions with different pH values, different competing proteins and during different time intervals. These are analyzed by ultraviolet-visible spectrophotometry and sodium dodecyl sulfate-polyacrylamide gel electrophoresis.

2.2 Molecular imprinting

2.2.1 State of the art

The effect of the presence of an additive molecule during the preparation of silica particles on their selective binding behavior was recognized by M. V. Polyakov for the first time 1931.[46] F. H. Dickey reported on a very similar phenomenon, when he used an orange dye as template molecule during a polymerization 1949.[47] He compared his finding with the mechanism that L. Pauling had proposed for the formation of antibodies 1940, in which an antigen directs the assembly of its own recognition site.[48] After this, the early era of molecular imprinting in silica began and was applied to organic polymers by the groups of G. Wulff[49] and I. M. Klotz[50] independently in 1972. After the pioneering work in the covalent imprinting concept mainly by G. Wulff et al[51,52], K. Mosbach introduced the non-covalent imprinting approach in the 1980's[53,54], which is the most widely used approach nowadays[33,34]. The semi-covalent imprinting approach was developed by B. Sellergren and L. Andersson 1990.[55] Later in 1993, MIPs were applied in a competitive binding assay with a performance comparable to an antibody.[56]

After intensive efforts were made to promote the molecular imprinting technique by the groups of G. Wulff and K. Mosbach, it became a steadily growing field in research apparent throughout the increase in the number of annual publications.[57,58] The technique was applied to a wide variety of target molecules such as propranolol[59,60], cholesterol[61,62], caffeine[63,64] and 17β-estradiol[65,66] as a result of its straightforwardness and versatility and is summarized in many review articles[57,67–70] and books[35,36]. MIPs found promising applications in many fields like in high-performance liquid chromatography (HPLC)[71–75], solid phase extraction (SPE)[76–79], antibody-mimicking pseudo-immunoassays[56,79–82], sensing devices[82–85], enzyme-mimicking catalysis[86–89] and drug delivery[90–93]. Molecularly imprinted SPE cartridges (SupelMIP SPE from Sigma-Aldrich and AffiniMIP SPE from Polyintell) are already commercially available, but further progress still has to be made towards commercial impact.[94] Since the potential of molecular imprinting is far from exhausted yet, it is continuously being developed.[95] The trend in molecular imprinting goes to using rational design[96–99] and new imprinting strategies including surface imprinting[40,64,100,101], nanoparticle synthesis[5,61,102,103] and larger template molecules like peptides[104,105] and proteins[37,106–108].

The first work on molecular imprinting of amino acid derivatives[54] and proteins[109] was reported by the research group of K. Mosbach 1985. The amino acid derivative phenylalanine ethyl ester was imprinted with acrylic acid (AAc) in acetonitrile.[54] The glycoprotein transferrin and glucose oxidase were imprinted with organic silanes on silica particles in water.[109] Only 10 years later, an increasing number of publications within the field of protein imprinting followed.[110] In comparison to the imprinting of small molecules, which is well-established, the imprinting of proteins is still in its initial

phase recognizable by a lower number of publications. The research is mainly focused on the proof of concept using mostly well defined, relatively stable and inexpensive model proteins such as albumin, hemoglobin and lysozyme.[110] This is, because the imprinting of proteins remains significantly more challenging due to their molecular dimension, conformational flexibility, complexity and limited solubility in organic solvents. New synthesis strategies including bulk imprinting in water, surface and epitope imprinting were therefore developed for protein imprinting during recent years and are summarized in a few review articles.[37,38,58,108,111,112]

An example for bulk imprinting in water is the imprinting of hemoglobin, cytochrome C and transferrin with acrylamide (AAm) resulting in a gel.[113] Hemoglobin imprinted hydrogel beads were obtained with AAm, *N*-(hydroxymethyl)acrylamide (HMAm) and *N,N'*-methylenebisacrylamide (BIS) in a water-in-oil Pickering emulsion.[107] An example for utilizing precipitation polymerization with water-soluble functional monomers in water is the imprinting of melittin, a peptide with 26 amino acids, using ionic and hydrophobic interactions.[104] Nanogels with a high affinity to melittin were thereby obtained. Another example is the imprinting of trypsin with AAm, a vinyl containing derivative of a trypsin inhibitor, and BIS enabling selective binding and competitive inhibition of trypsin.[106] Nanoparticles with a high binding affinity and selectivity for atrial natriuretic peptide were obtained by using epitope imprinting with a short sequence of this peptide and methacrylic acid (MAA) and *N*-isopropylacrylamide (NIPAm) as functional monomers, which were polymerized in water by precipitation polymerization.[114]

Papain and trypsin surface imprinted core-shell microbeads were obtained by forming nanofilms out of poly-3-aminophenylboronic acid in the presence of the template protein on the surface of polystyrene microbeads.[115] Lysozyme surface imprinted nanoparticles were obtained by grafting of a polymer shell around silica core particles in the presence of the template protein.[116] An imprinting factor of around 2 and selective rebinding were reported. A 9 amino acid residue containing sequence of the green fluorescent protein was imprinted using inverse microemulsion polymerization, in which the disperse phase was hydrophilic and the continuous phase hydrophobic. The peptide was coupled with fatty acid chains in order to orient the template peptide at the oil-water interface.[117] The peptide was subsequently recognized by the MIP with high affinity and selectivity through the formation of multiple weak hydrogen bonds.

The miniemulsion polymerization was used for the imprinting of the chiral amino acid derivative L-boc-phenylalanine anilid by D. Vaihinger et al 2002 for the first time.[105] The monomer droplets contained MAA as functional monomer and ethylene glycol dimethacrylate (EGDMA) as cross-linker and the template molecule. MAA and EGDMA were polymerized with the help of a hydrophobic initiator in order to prevent homopolymerization of MAA in the water phase. Polymer particles with a hydrodynamic diameter of around 200 nm and imprinting factors between 2 and 4 depending on

the initial concentration of the anilid were obtained with a molar ratio between MAA and EGDMA of 1 : 4. The L-imprinted MIP was selective for the L-enantiomer, as this bound 2 to 10 times more of the L- than of the D-enantiomer depending on the initial concentration of the anilid. In another approach L-lysine imprinted polymer nanoparticles were prepared for antibody recognition by a two-phase miniemulsion polymerization and showed selectivity for immunoglobulin G due to its high content of L-lysine at the C-terminus of its Fc region.[118]

The first work on protein surface imprinting via miniemulsion polymerization was reported by C. J. Tan and Y. W. Tong 2007, who successfully applied this method for imprinting the protein ribonuclease A (RNase A) with methyl methacrylate (MMA) as functional monomer and EGDMA as cross-linker.[119] Polymer particles with an average diameter of around 40 nm, which was determined from scanning electron microscope images, were thereby obtained. An imprinting factor between 2 and 10 depending on the initial RNase A concentration was reported. Selectivity for RNase A against bovine serum albumin (BSA) was demonstrated by a single and competitive batch rebinding experiment. The same synthesis protocol was applied for imprinting BSA and lysozyme, but no imprinting effect with BSA and only a modest imprinting effect with lysozyme were obtained.[120] Tan et al explained this by the fact, that a certain degree of interaction between the template protein and the surfactant is necessary to maintain the protein at the droplet surface. This interaction should not be too strong, because this can otherwise cause a significant change of the protein conformation. This is based on studies on the interactions between the template proteins and the surfactant using circular dichroism spectroscopy. BSA was successfully imprinted with another imprinting approach using core-shell miniemulsion polymerization reported by the same research group.[121] BSA was therefore covalently immobilized on polymer particles containing nano-sized magnetite before the polymerization of a shell from MMA and EGDMA. The template BSA was removed by base hydrolysis afterwards. The same approach was transferred to the imprinting of RNase A and lysozyme.[122] Both MIPs showed selectivity for their respective target protein in a single selectivity study, but only the lysozyme imprinted polymer particles showed selectivity for their target protein in a competitive selectivity study. This is attributable to the highly complex behavior of competitive selectivity studies. Although using miniemulsion polymerization for the preparation of protein surface imprinted submicron polymer particles provides several advantages, these are the only publications in this area so far.

Pepsin as a well-characterized protease and one of the most digestive enzymes[7,11] has only twice been used as target protein for the preparation of MIPs until now. In one approach, pepsin was imprinted onto a gold coated glass chip by means of poly-L-lysine.[123] The chip was therefore dipped into a solution containing a titanium fluoro complex, boric acid, poly-L-lysine and pepsin. After the reaction between the titanium fluoro complex and boric acid, a thin film of titanium oxide was

deposited on the chip. The obtained film had a high affinity to pepsin represented by the binding dissociation constant of 1.37 µM. The selectivity was investigated by single batch rebinding experiments using surface plasmon resonance spectroscopy. About 2 times more pepsin compared to albumin and around 10 times more pepsin compared to lactalbumin and chymotrypsin were bound to the thin film. In the other approach, pepsin was immobilized on glass beads before the copolymerization of NIPAm, *N*-(*tert*-butyl)acrylamide (TBAm), AAc and BIS in water.[124] High-affinity submicron polymer particles were eluted at high temperature and collected after the elution of low-affinity submicron polymer particles, unreacted monomer, oligomers and other impurities. A very low dissociation constant of 17 pM was obtained by surface plasmon resonance spectroscopic measurements after the immobilization of pepsin onto a gold sensor surface and incubation with the particles. The same experiment was carried out with immobilized trypsin and α-amylase, whereby around 3 times more pepsin was bound to the particles. A non-imprinted polymer (NIP) could not be prepared under the same conditions as the MIP and was thus not available for comparison with the MIP.

An alternative approach for the imprinting of pepsin using surface imprinting and miniemulsion polymerization is presented within this thesis.

2.2.2 Principle of molecular imprinting

Molecular recognition is the fundamental principle of many biological processes and occurs during the binding between a biological receptor and its ligand, e. g. between an enzyme and its substrate or an antibody and its antigen, based on their steric and functional complementary.[125] These fit exactly into each other due to their complementary shape according to the lock- and key-principle. The ligand binds with high affinity and selectivity to its receptor due to complementary functionalities situated on opposite positions. A stable complex between the ligand and its receptor is achieved through the formation of multi-site non-covalent interactions such as hydrogen bonds, ionic and hydrophobic interactions.

MIPs mimic the molecular recognition behavior of biological receptors and are thus also referred to as artificial receptors[36] or antibody mimics[56]. MIPs are prepared by the copolymerization of one or several functional monomers with a cross-linker in the presence of a template molecule, which is mostly the same as the target molecule or a derivative of it, as illustrated in Figure 2.1.

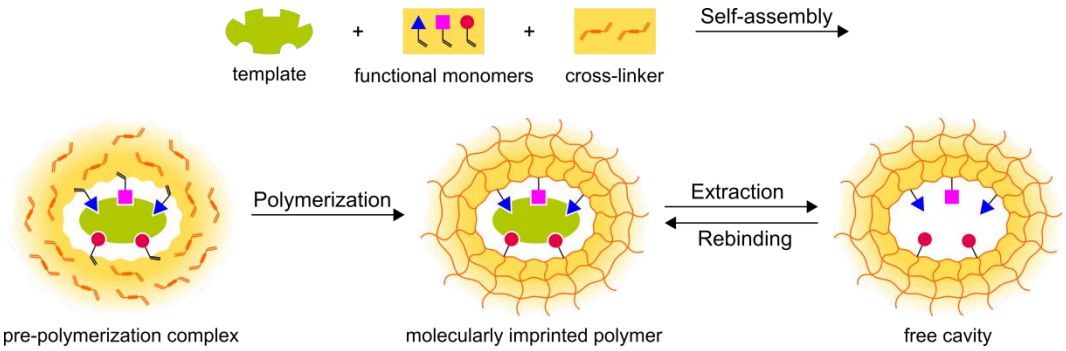

Figure 2.1 Principle of the molecular imprinting (bulk imprinting).

Prior to the polymerization, the functional monomers align their functional groups towards complementary functional groups of the template molecule resulting in the formation of a pre-polymerization complex, which can either be of covalent[51] or non-covalent[53] nature (see chapter 2.2.3). The steric arrangement of the functional groups is chemically fixed by the copolymerization of the functional monomers with the cross-linker resulting in a stable polymer matrix with selective binding sites. After the imprinting process the template molecule is extracted leaving imprinted cavities complementary in size and shape to the template molecule with selective binding sites complementary in functionality to the template molecule, which are accessible for rebinding the target molecule with high affinity and selectivity.[67–70]

2.2.3 Imprinting approaches

The preparation of MIPs can be categorized into different approaches dependent on the type of interaction between the functional monomers and the template molecule during the imprinting and rebinding. The two most common approaches are the non-covalent and the covalent imprinting. A combination of these two approaches is the semi-covalent imprinting. These approaches are described in the following subchapters.

2.2.3.1 Non-covalent imprinting

During non-covalent imprinting, the pre-polymerization complex[96,126] as well as the rebinding of the target molecule is achieved by the formation of non-covalent interactions such as hydrogen bonds, ionic interactions, π-π-stacking, van der Waals interactions and hydrophobic interactions between the functional monomers and the template molecule.[53,54] The molecular recognition between non-covalently imprinted polymers and their target molecules thus strongly resembles the molecular recognition between biomolecules.[51,52] Because of the comparatively weak binding strengths of non-covalent interactions, multiple interactions are utilized for a strong binding.[126,127] The functional monomers are therefore usually used in molar excess compared to the amount of template molecule in order to shift the binding equilibrium to the side of the pre-polymerization complex, whose presence is essential for a successful imprinting.[36,54] But this can result in the formation of non-selective binding sites coming from randomly incorporated, excess functional monomers and thus in binding site heterogeneity.[128,129] The lower stability of the pre-polymerization complex, which is dependent on the polymerization conditions such as the solvent, type and amount of functional monomer and temperature, and the connected lower selectivity are the main disadvantages of the non-covalent imprinting. The main advantages of this approach are the straightforward preparation and easy, mild template extraction. In addition to that, a large number of functional monomers are available and a wide variety of template molecules is possible. The formation of non-covalent interactions furthermore enables fast rebinding kinetics.[35,36]

2.2.3.2 Covalent imprinting

During covalent imprinting, the functional monomer is covalently bound to the template molecule before the polymerization. The covalent bond between the template molecule and the obtained polymer has to be chemically cleaved, before the target molecule can be rebound to the created functionality in the cavity by reestablishing the covalent bond again.[67] This approach is more complex, because an additional synthesis step is required and the template removal is often difficult. Harsh conditions are therefore sometimes needed, which can affect the binding sites.[36] The number of possible template molecules and functional monomers is limited, since the template molecule must be able to be reversibly covalently bound to the functional monomer. The strong

binding strength of the covalent bond in the imprinted cavities results in slow binding kinetics during the rebinding[130], but also in a stable pre-polymerization compound, which is hardly affected by the free radical polymerization enabling successful imprinting.[36] The functional monomer is used in a stoichiometric ratio to the template molecule. This favors the formation of homogeneous binding sites[129] and results in a high binding selectivity, which is the main advantage of this approach[35,130].

2.2.3.3 Semi-covalent imprinting

The semi-covalent imprinting is a combination of the covalent and the non-covalent imprinting approaches.[55] The template molecule is thereby covalently bound to the functional monomer before the polymerization like at the covalent imprinting. After the removal of the template molecule by chemical cleavage of the covalent bond, the target molecule is rebound by non-covalent interactions.[131] This approach combines the advantages of the formation of a stable and stoichiometric pre-polymerization compound and the fast non-covalent rebinding. This enables high selectivity and fast rebinding to homogeneous binding sites, but is complex.[57]

2.2.4 Imprinting strategies

There are different imprinting strategies such as bulk, surface and epitope imprinting. Whereas bulk imprinting is rather used for small molecules, surface imprinting is rather used for proteins. Epitope imprinting is a strategy for protein imprinting only. These strategies are explained in the following.

2.2.4.1 Bulk imprinting

During bulk imprinting, the template molecule is imprinted in a 3D cavity within a polymer network. This is illustrated in the scheme of Figure 2.1 in chapter 2.2.2. This strategy is most commonly used for imprinting small molecules, since it is comparably easy and straightforward. This is obtained by bulk polymerization in the presence of an organic solvent used as pore-forming agent called porogen.[36] A porous, highly cross-linked bulk polymer is thereby obtained, which has to be crushed and ground afterwards, so that the entrapped template molecule can be extracted and that the binding sites in the pores are accessible for rebinding.[77,132] The grinding results in particles with a broad size distribution and an irregular shape, which is a drawback for many applications like in chromatography.[36,132] An alternative to overcome the drawbacks of bulk MIPs is the preparation of porous MIP microparticles, which have a spherical shape and can be directly applied as stationary phase in HPLC[133] or as sorbent in SPE[134] without a grinding and sieving procedure. These are prepared by suspension[134,135], precipitation[63,133] and a multi-step swelling polymerization[59,136] in the presence of a porogen. MIP particles with a diameter below 1 µm easily remain in solution or suspension and have favorable binding properties for the use in ligand binding assays.[133,137] Imprinted spherical submicron polymer particles are prepared by precipitation[133,137], core-shell-emulsion[62,64], microemulsion[117] and miniemulsion polymerization[138,139].

Since the conventional bulk imprinting is performed in organic solvents, it is adjusted to aqueous solutions for protein imprinting resulting in hydrogels and sol-gels. Imprinted hydrogels[140] and sol-gels[141] with a high degree of cross-linking result in a poor protein mass transfer, since most of the binding sites are located within the dense polymer network. Polymer hydrogels are therefore prepared with a low degree of cross-linking to facilitate protein transfer, but this results in a lower stability and thus a lower recognition efficiency.[113,142] An additional disadvantage is the requirement of grinding to expose the binding sites, which may greatly diminish the selectivity for proteins, as larger binding sites are rather destroyed by the mechanical process of grinding.[37,38] Bulk imprinting is therefore performed in monomer droplets by inverse-phase suspension polymerization[143] and Pickering emulsion polymerization[107] resulting in gel beads. Protein imprinted micro- and nanogels[104,106,144] are prepared by precipitation polymerization under high dilution. However, environmental changes as during template extraction can result in pore collapse and permanent loss of function of these gels.[37,38]

2.2.4.2 Surface imprinting

During surface imprinting, the template molecule is imprinted onto a surface of a material, whereby the binding site orientation and local solvation state can be controlled.[40,101] This is a promising strategy especially for imprinting proteins, as the binding sites are situated at the material surface and not within the polymer network as in bulk MIPs and therefore are easily accessible even for large target molecules like proteins.[37,38] An approach for surface imprinting is grafting of a thin material layer on a surface of a planar film or of particles (Figure 2.2). The template molecule is therefore adsorbed on the surface by covalent[145,146] or non-covalent bonds[147,148] before the monomer addition or is added with the functional monomers at the same time[148–151]. After the formation of the thin layer, the template molecule is extracted leaving a surface imprinted film or surface imprinted particles.

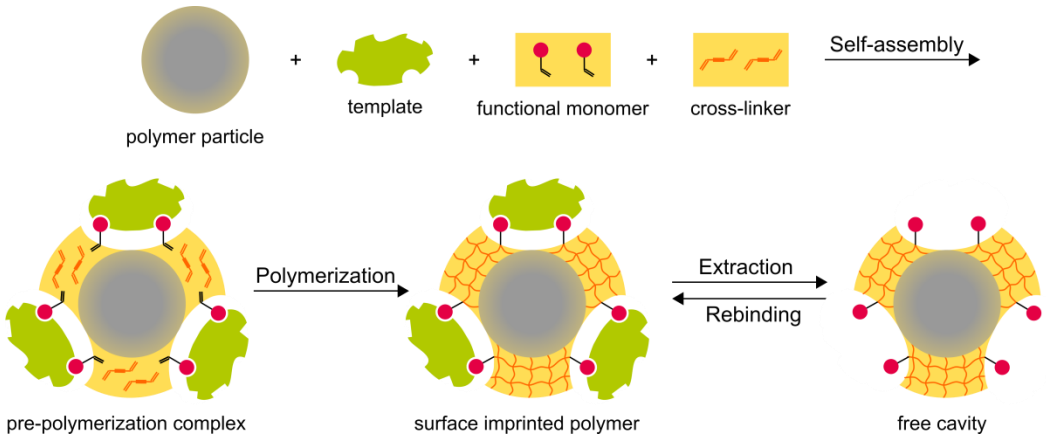

Figure 2.2 Principle of the surface imprinting on a preformed particle by the grafting approach.

Thin films[101] are obtained by grafting a polymer layer[152], by plasma[153], electrochemical[148] or liquid phase deposition[123] or chemisorption[154] on planar support substrates out of mica[153], gold[123], glass[145] or on an electrode[154] or a microtiter plate[152]. Polymer[151], silica[146] or hybrid[155] core-shell microparticles are obtained by grafting a thin layer of polymer on preformed polymer[150,151] or silica particles[146,149] used as core.

By further decreasing the size of the particles, the total available external surface area and thus the number of accessible binding sites on the particle surface is increased. This is obtained by the preparation of surface imprinted submicron particles due to their high surface-to-volume ratio and results in enhanced rebinding kinetics without loss of the binding capacity.[5,39,156] Surface imprinted submicron silica particles are prepared in the same way as silica microparticles, but with silica core particles in the nano-size range.[116] Surface imprinted submicron polymer and hybrid particles are prepared by core-shell miniemulsion polymerization[121] and precipitation polymerization using submicron silica support beads[157,158].

The direct surface imprinting of submicron polymer particles enables a one-step preparation without the need of support particles (Figure 2.3).[40,159]

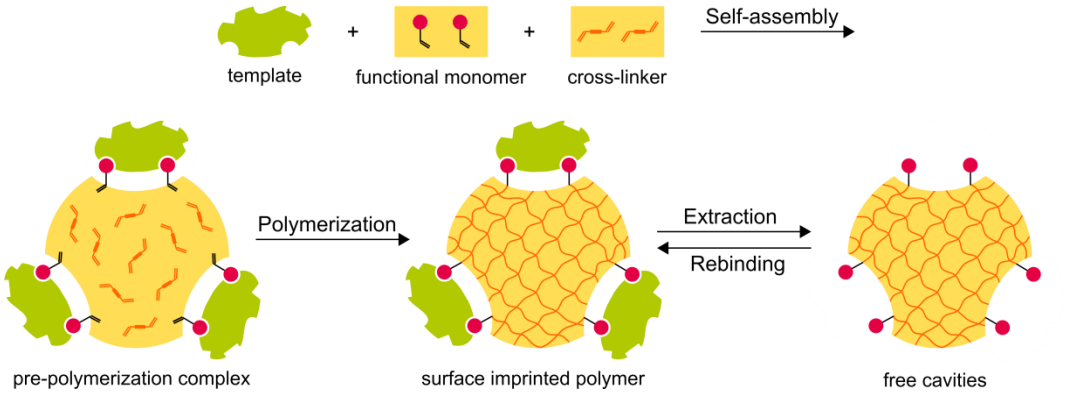

Figure 2.3 Principle of the direct surface imprinting without core particles.

This is done by inverse microemulsion[117] and miniemulsion polymerization[120]. The template molecule is therefore assembled at an oil-water interface for the formation of a pre-polymerization complex at the phase boundary. This assembly may be supported by a derivatization of the template protein[117] or an interaction of the template protein with a surfactant[120]. The complex is preserved during the polymerization, since this takes place in the monomer droplets.

The advantage of readily accessible imprinted binding sites results in an easier template removal and improved rebinding kinetics overcoming the diffusion limitation of proteins.[37,38] This usually outweighs the possibility of obtaining reduced selectivity and binding site heterogeneity, since only a part of the molecule is imprinted and recognized.

2.2.4.3 Epitope imprinting

During epitope imprinting, only a short peptide, which has the same amino acid residue sequence as an exposed, small fragment of the whole protein, is used as template molecule during imprinting. After the imprinting, this fragment of the whole protein is recognized.[37,38] The word epitope is borrowed from immunology. The epitope is a short exposed domain of an antigen, which is recognized by the paratop of the corresponding antibody. Small peptides are cheaper, less sensitive to their environment and soluble in organic solvents. This enables the use of organic solvents, which do not interfere with hydrogen bonds and ionic interactions, and of more conventional imprinting approaches such as bulk imprinting.[160] Epitope imprinting is also carried out using precipitation polymerization[114] and used for film formation[145,161].

A strong interaction between this small part of the protein and the MIP can be more selective than relying on numerous weak interactions all over the protein molecule due to minimized non-selective binding. A disadvantage of this strategy is that a suitable peptide has to be synthesized first.

2.2.5 Preparation conditions

There are many different parameters such as the type and amount of the functional monomer, cross-linker and solvent, the type of initiation[162,163], polymerization temperature[164,165] and the way of template extraction[166] during the preparation of MIPs that affect the final polymer properties and imprinting efficiency. A short overview on these parameters is described in the following.

2.2.5.1 Functional monomer

The choice of the functional monomer is crucial, since it is responsible for the creation of the selective binding sites. It is selected on the basis of the type and strength of its interaction with the template molecule.[36] Frequently used functional monomers for the non-covalent imprinting are MAA[105,114], AAm[107,117], NIPAm[104,124], HMAm[107] and 3-aminophenylboronic acid[100,150], which can form different non-covalent interactions. Different silanes[116,146] are used, if the imprinting is carried out in a sol-gel system. Vinylboronic acids, diols and amines are mostly used for the covalent imprinting.[67]

2.2.5.2 Cross-linker

The selection of a suitable cross-linker and its content is also important, as it preserves the steric orientation of the functional groups and imparts mechanical stability to the imprinted cavities and the whole polymer.[67] This additionally controls the polymer morphology and porosity[167,168]. EGDMA, divinylbenzene and BIS are commonly used cross-linkers.[35] Usually a relatively high content of cross-linker is used that the cavities retain their shape yielding in increased selectivity and to ensure high rigidity of porous polymers.[67] A typical molar ratio between the functional monomer and cross-linker is between 1 : 3[167,169] and 1 : 5[168,170] for the non-covalent imprinting.

2.2.5.3 Solvent

The type and volume of solvent plays an important role, because it has a significant influence on the polymer morphology as well as the porosity[171,172] in combination with the cross-linker. Besides this, the solvent affects the strength of the interaction between the functional groups of the polymer and the template molecule[171,172] and the stability of the pre-polymerization complex during the non-covalent imprinting and thus the imprinting efficiency. Non-polar, aprotic solvents such as toluene or chloroform are preferably used, if the template molecule and the functional monomer interact by hydrogen bonds and other electrostatic interactions, as they do not interfere with these like polar, protic solvents such as water or methanol. These solvents can be used for imprinting small organic molecules and peptides, whereas aqueous solutions have to be used for protein imprinting. Since the shape of the imprinted cavities is affected by swelling changing the steric position of the functional groups to the target molecule and thus the ability of the selective binding, best rebinding

performance is obtained in the same solvent as used during the imprinting.[170,172]

2.2.5.4 Polymerization reaction and initiation

The free radical polymerization is the most commonly applied type of polymerization reaction for the preparation of MIPs, because it is straightforward and a broad range of vinyl monomers and cross-linkers is commercially available. Other types of polymerization reactions such as polycondensation[173] or living radical polymerization[174] are used much rarer. The radical polymerization is usually thermally initiated. Using photochemical initiation through ultraviolet (UV) irradiation or redox initiation allows the preparation of MIPs at low temperatures. This is favorable for the stability of the pre-polymerization complex during non-covalent imprinting and the imprinting of proteins and can result in a higher selectivity.[163] Popular radical initiators are azobisisobutyronitrile, 2,2'-azobis-2,4-dimethylvaleronitrile and ammonium persulfate used alone or in combination with *N,N,N',N'*-tetramethylenediamine.

2.2.5.5 Template extraction

Typical extraction methods are the continuous extraction in a Soxhlet apparatus and the discontinuous immersion in organic solvents or aqueous solutions.[166] Proteins are usually extracted by repeated centrifugation and redispersion.[119,123,166] The extraction solvent or solution has to be a good solvent for the template molecule and to be able to break the strong interactions with the imprinted binding sites. Typical solutions for protein extraction are pure water, solutions of high salt[151] and of acetic acid[119] containing sodium dodecyl sulfate (SDS)[143]. The complete removal of the template molecule is important, since residual template molecules can result in template molecule bleeding during rebinding and thus to falsified results and to decreased performance of the MIP due to blocking of the imprinted sites.[110] However, the complete removal of the template molecule is hard to obtain even under harsh conditions such as high temperatures, extreme pH values or ultrasound application for a long time.[166] It has been reported that between 50 and 95% of the original protein template molecule could be removed depending on the type of protein and polymer using an extraction solution containing acidic acid and SDS.[110,142] However, the use of such harsh conditions may result in damage or collapse of the imprinted cavities and thus decrease the imprinting efficiency.[166] A second problem is the subsequent removal of the extraction agents, since remaining SDS molecules can result in increased non-selective protein binding and in combination with acetic acid in protein precipitation.[110]

2.2.6 Challenges of protein imprinting

Proteins differ a lot in their properties compared with small molecules including their solubility, molecular dimension, complexity and conformational flexibility.[37,38] These properties cause different challenges when imprinting proteins and are described in more detail in the following.

2.2.6.1 Solubility

The poor solubility of most proteins in organic solvents limits the choice of solvent and functional monomers to mainly aqueous solutions and water-soluble monomers such as different acrylamides. The use of water as solvent is challenging, since it can compete for hydrogen bonds between the template molecule and the functional monomers and reduces the strengths of hydrogen bonds and ionic interactions. Since the conventional bulk imprinting is performed in organic solvents, it is adjusted to aqueous solutions for protein imprinting (see chapter 2.2.4.1).

2.2.6.2 Molecular dimension

The large size of proteins hinders them from both reaching and leaving the imprinted cavities. This can result in a poor mass transfer and a permanent entrapment of the proteins inside the imprinted cavities and thus in unfavorable recognition properties.[37,38] This is particularly disadvantageous for highly cross-linked, dense bulk MIPs. Hence, other imprinting strategies are developed such as surface and epitope imprinting (see chapters 2.2.4.2 and 2.2.4.3).[37,38]

2.2.6.3 Complexity

The complex surface of proteins including different physicochemical properties such as charge, hydrophilicity and hydrophobicity provides numerous potential recognition sites and functional groups for several interactions. This increases the probability of non-selective interactions and of a poor selectivity, because similar regions are present on other proteins as well.

2.2.6.4 Conformational flexibility

The conformation of proteins is sensitive to the surrounding conditions such as temperature, pH value and ionic strength, the presence of a surfactant, functional monomer and cross-linker. Non-physiological conditions often employed during the polymerization may result in a change of the conformation, in denaturation or even aggregation of the proteins.[37,38] When the template protein changes its conformation during the polymerization, the wrong conformation may be imprinted and the protein existing in the native conformation used for rebinding may not fit into the imprinted cavities. Hence, the conformational flexibility can also affect the selectivity. The polymerization has therefore to be performed in a physiological solution under mild reaction conditions close to the conditions that are subsequently used for rebinding (compare chapter 2.2.5).

2.2.7 Protein imprinting in aqueous environment

Hydrophobic interactions caused by the exclusion of water are frequently used for imprinting in an aqueous system.[111] Hydrophobic residues are rather situated in the core of proteins, but there are a few hydrophobic patches on the surface, which can be bound to the polymer by hydrophobic interactions.[37] However, there are only a few examples of protein imprinting solely based on hydrophobic interactions[119], because they are less selective and can also cause a change of the protein conformation.[111] Since most of the amino acid residues on the protein surface are polar, the formation of hydrogen bonds and ionic interactions is suitable.[37] Hydrogen bonds are used in non-covalent imprinting due to their directional properties resulting in highly selective MIPs, but water as solvent can compete for the formation of hydrogen bonds. This effect can be reduced by the formation of a combination of different non-covalent interactions resulting in an overall strong interaction. Hence, there are many successful imprinting protocols using hydrogen bonds in combination with hydrophobic interactions.[105,111,147] Despite the fact that ionic interactions are non-directional, there are several protein imprinted polymers that are based on cooperative multiple ionic interactions[143] or on a combination of ionic and hydrophobic interactions[104,124]. There are also imprinting protocols using a combination of hydrogen bonds, ionic and hydrophobic interactions.[114,151] However, the formation of multiple interactions can result in increased non-selective interactions and the large size and complexity of proteins can result in binding site heterogeneity.[37,38]

2.2.8 Evaluation of the imprinting efficiency

The imprinting efficiency is evaluated by the analysis of several different binding characteristics as the imprinting factor, binding affinity and selectivity. These are determined by chromatographic evaluation, for which the MIP particles are packed into a column, or by batch rebinding experiments, which are usually used for the evaluation of submicron MIP particles. The evaluation methods of the imprinting efficiency are described in the following.

2.2.8.1 Batch rebinding experiment, binding capacity and affinity

In a batch rebinding experiment, a certain amount of MIP particles is incubated with a solution of a defined initial concentration of the target molecule under continuous shaking at controlled temperature, often room temperature (Figure 2.4).[35,175] The incubation time is usually between 15 minutes and 24 hours and mostly adjusted, so that the binding equilibrium is reached.

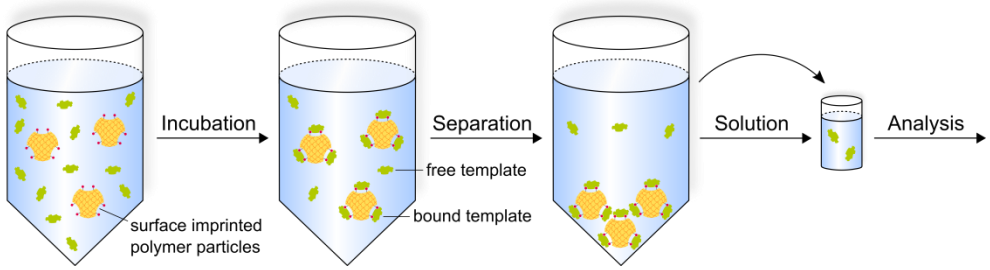

Figure 2.4 Scheme of a batch rebinding experiment.

The solution is separated from the MIP particles by centrifugation or filtration after the incubation. The concentration of free target molecule remaining in the solution is determined by UV-Vis (ultraviolet-visible) or fluorescence spectroscopy or scintillation detection. The amount of bound target molecule is assumed to be the difference between the initial and the final free target molecule concentration.

The amount of bound target molecule per amount of polymer is called binding capacity as described in equation (2-1).[36] The binding capacity is often related to the specific surface area of the polymer.[36]

$$Q = \frac{m_b}{m_p} \qquad \textbf{(2-1)}$$

Q: binding capacity
m_b: mass of bound
m_p: mass of polymer

The binding equilibrium between a MIP, the target molecule (TM) and the MIP-TM association can be written as in equation (2-2).[35]

$$MIP + TM \rightleftharpoons MIP{-}TM \quad \textbf{(2-2)}$$

MIP: molecularly imprinted polymer
TM: target molecule
MIP-TM: MIP-TM association

The binding affinity describes the strength of the interaction between the MIP and the target molecule and is directly related to the association and inversely to the dissociation constant as in equation (2-3).

$$K_a = \frac{1}{K_d} = \frac{c(MIP-TM)}{c(MIP)c(TM)} \quad \textbf{(2-3)}$$

K_a: association constant
K_d: dissociation constant
c: equilibrium concentration

The higher the association or the lower the dissociation constant is, the more the binding equilibrium is on the side of the MIP-TM association and the higher is the affinity of the MIP to the target molecule. MIPs usually reach dissociation constants from the mili- to the nanomolar range.[58] The dissociation constants of antibodies are generally from the micro- to the picomolar range. The dissociation constant is obtained from the analysis of binding isotherms (see chapter 2.2.8.3).

2.2.8.2 Contribution of non-selective binding and imprinting factor

The determination of the contribution of non-selective binding to the total binding of a MIP is an important part in the evaluation of the imprinting efficiency. The contribution of non-selective binding is obtained from a batch rebinding experiment with the target molecule and a NIP, which is prepared and treated in the same way as the MIP, but in absence of the template molecule[36] resulting in a random distribution of the functional groups in the polymer. The binding capacity of the NIP is either directly compared with the binding capacity of the MIP or an imprinting factor is determined. The imprinting factor was introduced to normalize the total binding by the non-selective binding leaving a value for the binding that can be attributed solely to the imprinting effect.[175] The imprinting factor is the ratio of the binding capacity of the MIP and the NIP[151,176] as described in equation (2-4).

$$IF = \frac{Q_{MIP}}{Q_{NIP}} \quad \textbf{(2-4)}$$

IF: imprinting factor
Q_{MIP}: binding capacity of MIP
Q_{NIP}: binding capacity of NIP

A high imprinting factor points out that the imprinting is successful. However, the comparison between the binding capacity of a MIP and its corresponding NIP does not completely proof the success of the imprinting process, since the existence of a template molecule would most likely change the morphology of the polymer network and affect the distribution of the functional groups.[170] The change of the morphology can result in a change of the specific surface area that can affect the binding capacity. For this reason selectivity studies are used to further proof the selective binding of the MIP (see chapter 2.2.8.5).

2.2.8.3 Binding isotherms

Since the imprinting factor can change with different initial target molecule concentrations, the measurement and comparison of binding isotherms of the MIP and NIP is therefore recommended as an extended evaluation method.[177] An experimental binding isotherm is obtained by plotting the free target molecule concentration versus the amount of bound target molecule after a batch rebinding experiments with different initial target molecule concentrations. The first conclusions can be drawn from the curve progression of the binding isotherms. For further analysis of the binding properties such as the apparent dissociation constant and the maximum binding capacity, the data is fitted to a specific binding model.

The Langmuir isotherm[178] is a widely used homogeneous binding model for characterizing the binding properties of MIPs[35]. The Langmuir model is based on the assumptions, that all binding sites are equal, there are no interactions between the bound molecules on adjacent sites and that only a monolayer can be bound. This is typically observed for the binding behavior of enzymes and monoclonal antibodies. The Langmuir equation can be written like in the following equation (2-5).

$$Q = \frac{Q_{max} K_a c}{1 + K_a c} = \frac{Q_{max} c}{K_d + c} \qquad \textbf{(2-5)}$$

Q: binding capacity
Q_{max}: maximum binding capacity
c: equilibrium concentration
K_a: association constant
K_d: dissociation constant

The Langmuir isotherm has a hyperbolic curve progression like the example curve in Figure 2.5.

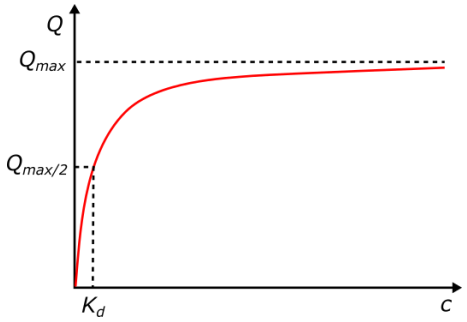

Figure 2.5 Schematic diagram of a Langmuir isotherm with the maximum binding capacity (Q_{max}), half of the maximum binding capacity ($Q_{max/2}$) and the dissociation constant (K_d).

The dissociation constant is equal to the target molecule concentration, at which half of the binding sites are saturated. The maximum binding capacity is reached, when all binding sites of the adsorbent are saturated. The apparent dissociation constant and maximum binding capacity can be calculated from equation (2-5) after fitting it to the measuring points.

The Freundlich isotherm[179] is a heterogeneous binding model and used for the characterization of the binding properties of MIPs that have different types of binding sites with different binding affinities[180] coming from randomly oriented functional groups due to an excess use of functional monomer in the non-covalent imprinting, different cross-linking degrees around the binding sites or collapsing of binding sites after template removal.[181] The Freundlich model takes different binding sites, interactions between the bound molecules on adjacent sites and the formation of multilayers into account. The Freundlich equation is as follows in equation (2-6).

$$Q = Kc^m \tag{2-6}$$

Q: binding capacity
K: Freundlich constant
c: equilibrium concentration
m: heterogeneity index

The Freundlich constant is a measure of the binding capacity and the average association constant, but the individual contribution of each parameter cannot be extracted directly unless experimental data or additional assumptions are made.[181,182] The heterogeneity index varies from 0 to 1, whereas 1 corresponds to a homogeneous material. The lower the heterogeneity index is, the higher is the heterogeneity and the broader is the distribution of the association constants and thus of the binding affinity. The Freundlich isotherm has a curve progression like the example curve in Figure 2.6.

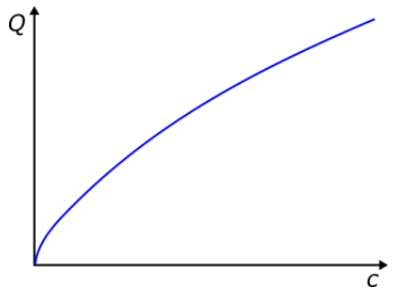

Figure 2.6 Schematic diagram of a Freundlich isotherm.

The Langmuir-Freundlich isotherm is another binding model for describing the binding behavior of MIPs.[183] It is a combination of the two above described binding isotherms and thus a heterogeneous binding model with a saturation limit, but can also only behave like the Langmuir or the Freundlich isotherm. It has the following equation (2-7).

$$Q = \frac{Q_{max} K c^m}{1 + K c^m} \tag{2-7}$$

Q: binding capacity
K: constant
c: equilibrium concentration
m: heterogeneity index

The constant K is related to the mean association constant $\overline{K_a}$ with equation (2-8).

$$\overline{K_a} = K^{1/m} \quad \textbf{(2-8)}$$

$\overline{K_a}$: mean association constant
K: constant
m: heterogeneity index

The heterogeneity index varies from 0 to 1. When *m* is equal to 1, the adsorbent is homogeneous and equation (2-7) reduces to the Langmuir equation (2-5). When *K* or *c* approaches zero, equation (2-7) reduces to the Freundlich equation (2-6). The lower the heterogeneity index is, the higher is the heterogeneity and the broader is the distribution of the association constants. The curve progression of the Langmuir-Freundlich isotherm follows the Freundlich isotherm at low concentrations and the Langmuir isotherm at high concentrations.

2.2.8.4 Binding kinetics

The binding kinetic is investigated by performing batch rebinding experiments with the same initial target molecule concentration during different time intervals. The amount of bound target molecule is plotted versus the time of incubation. The obtained graph enables the determination of the time, at which the binding equilibrium is reached (Figure 2.7).

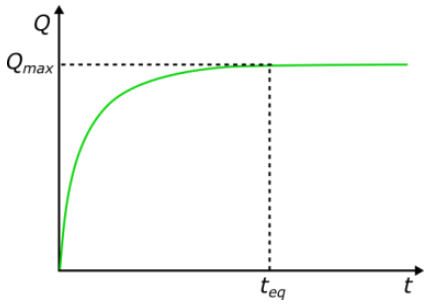

Figure 2.7 Schematic diagram of a binding kinetic with the time of the binding equilibrium (t_{eq}) and the maximum binding capacity (Q_{max}).

The binding process includes the transport within the incubation solution to the adsorbent, the diffusion through the liquid film on the adsorbent surface, the diffusion to the binding sites and the final binding process. The first two steps are faster due to shaking during the rebinding experiment compared to the last two steps, which determine the rate of the binding process.[184] These are influenced by different factors such as the morphology of the polymer, the size of the target molecule and the type of binding. The mass transfer of the target molecule to the binding sites of the MIP is expected to be faster for surface imprinted polymers than for bulk MIPs, where the target molecule has to diffuse in the pores to reach the binding sites. The formation of non-covalent bonds may be faster than the formation of covalent bonds. The binding process of large molecules like proteins may be slower due to their molecular size.

2.2.8.5 Selectivity study and binding selectivity

A selectivity study includes one or more batch rebinding experiments with the target molecule and other compounds under the same conditions. The other compounds mostly are structural analogues of the target molecule[36] and other proteins, when the target molecule is a protein.[119,146,151] In single selectivity studies, the proteins are separately incubated with the MIP.[106,107,119] Their content in the remaining solution is usually analyzed by UV-Vis spectrophotometry[100,107,150] or by staining methods such as the Bradford[146] or the bicinchoninic acid protein assay[106]. In competitive selectivity studies, the target protein and the other proteins are incubated with the MIP in the same solution and compete for the binding sites of the MIP (Figure 2.8).[119,146,151,159] This is more complex, since it requires the separation of the proteins before their analysis by sodium dodecyl sulfate-polyacrylamide gel electrophoresis (SDS-PAGE)[146,151] or size exclusion chromatography[119] and protein-protein interactions should be avoided[122].

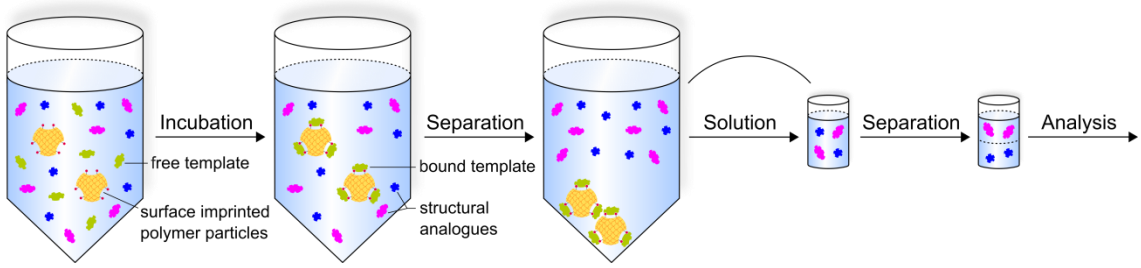

Figure 2.8 Scheme of a competitive selectivity study.

The binding selectivity refers to the relative strength of the interactions between the MIP and the target molecule compared to the relative strength of the interactions between the MIP and other compounds and describes the ability of the MIP to differentiate between the target molecule and the other compounds. A high selectivity is obtained, when the MIP binds only or at least predominantly the target molecule instead of the other compounds.[36] The selective binding of the target molecule comes from the positioning of the functional groups of the MIP towards complementary functional groups of the target molecule and the formation of a cavity that is complementary to the shape of the target molecule as a result of the imprinting process.[175] The binding of the other compounds is regarded as non-selective. The selectivity relies on relative, but not on absolute binding values. This can be quantified by the selectivity ratio, which is described in equation (2-9)[175], and indicates how many times better the MIP binds the target molecule than the other compound.

$$SF = \frac{Q_{TM}}{Q_A} \qquad \textbf{(2-9)}$$

SF: selectivity factor
Q_{TM}: binding capacity of the target molecule
Q_A: binding capacity of a structural analogue

2.3 Miniemulsion polymerization

The miniemulsion polymerization is a method for the preparation of polymer particles in the size range of 30-500 nm with a particularly narrow size distribution.[41] The polymerization is thereby carried out in monomer droplets of a miniemulsion, which is a system of two immiscible liquid phases, whereas one phase is dispersed in the other continuous phase.[41,42] The dispersed phase usually contains the monomer, an initiator and a hydrophobic agent. The continuous phase is a solvent and contains a surfactant. The miniemulsion is obtained by shearing a pre-emulsion of these two phases through the application of ultrasound creating a maximum interface and is stabilized by a surfactant against coalescence and a hydrophobic agent against Ostwald ripening. Small monomer droplets with a narrow size distribution are thereby obtained (Figure 2.9). The polymerization is initiated and carried out in each monomer droplet without diffusion of the monomer through the continuous phase.[41,42] The droplets can be regarded as locally separate reactors. The obtained polymer particles have the same size and size distribution as the monomer droplets. Hence, small polymer particles with a narrow size distribution are obtained depending on the type and amount of surfactant, monomer, hydrophobic agent, continuous phase and shear rate.

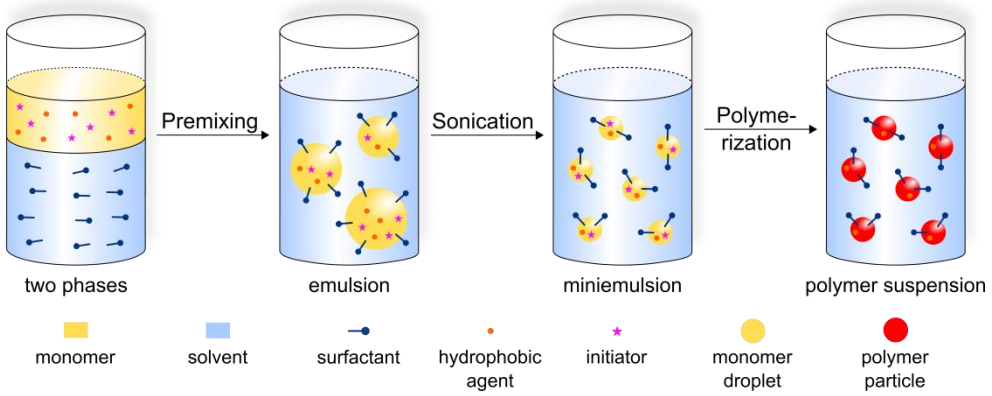

Figure 2.9 Principle of the miniemulsion polymerization.

The reduction of the droplet size is caused by the mechanism of cavitation. The ultrasonic waves produce a negative pressure, whereby small steam bubbles and cavities emerge. These collapse during the subsequent overpressure and thereby disrupt the droplets. The polydispersity is still high in the beginning of the homogenization. Since the new interface is slowly stabilized by the surfactant, fusion and fission processes occur resulting in a decrease of the polydispersity, until the miniemulsion reaches a steady state. Coalescence is the process, where two or more droplets merge to form a single droplet after collision.[41] This is prevented by the adsorption of an ionic or non-ionic surfactant at the interface resulting in a repulsion of the droplets due to ionic or steric interactions. An example for an anionic surfactant is SDS and Lutensol AT 50 for a non-ionic surfactant. Lutensol AT 50 contains 50 units of a poly(ethylene glycol) chain, which is etherified with a linear,

saturated C_{16} or C_{18} fatty alcohol. The stability efficiency of non-ionic surfactants is slightly lower than of ionic surfactants resulting in larger droplets.[185] The coverage of the interface with surfactant is usually incomplete and a relatively low amount of surfactant is sufficient for the stabilization of the miniemulsion.[41,42] This is in contrast to the emulsion and microemulsion polymerization as well as that a miniemulsion is additionally stabilized against Ostwald ripening. This describes the diffusion of liquid from smaller to larger droplets due to the higher surface curvature of the smaller droplets resulting in an increase of the overall droplet size. The diffusion is suppressed by the addition of a low amount of a hydrophobic agent such as hexadecane or a perfluorinated alkane, which is highly insoluble in the continuous phase and thus builds up an osmotic pressure that counteracts the Laplace pressure.[41,42]

A direct miniemulsion contains a hydrophobic monomer that is usually dispersed in water. A wide variety of hydrophobic monomers such as styrene and different acrylates can be polymerized.[41,42] The initiator can be either oil- or water-soluble. The polymerization of more hydrophilic monomers such as AAc or MAA is possible with an oil-soluble initiator to avoid secondary nucleation in the water phase.[45,105] Hydrophilic monomers such as 2-hydroxyethyl acrylate, AAm or AAc can be dispersed in an organic solvent such as cyclohexane and be polymerized by an inverse miniemulsion polymerization.[186] Two monomers of different polarities can be copolymerized in a miniemulsified system.[43–45] The monomer, which is insoluble in the continuous phase, forms the disperse phase and the other monomer is dissolved in the continuous phase. The dissolved monomer is polymerized at the droplet surface through the initiation in the droplets or at the droplet surface after diffusion from the continuous phase to the droplet surface.

The miniemulsion polymerization is used for the preparation of pepsin surface imprinted submicron polymer particles in the following part of this thesis.

2.4 Analytical methods

2.4.1.1 Circular dichroism spectroscopy

Circular dichroism spectroscopy is a method for the structure elucidation of small organic molecules and biomacromolecules and the investigation of charge-transfer-, metal d→d-transitions. This is based on the property of optically active substances to absorb right and left circularly polarized light to a different extent, which is referred to as circular dichroism (CD).[187,188] Circularly polarized light is obtained by superposition of two linearly polarized light waves of the same amplitude that oscillate perpendicular to each other. This results in a helical rotation of the electric field vector about its axis of propagation either clockwise or counter-clockwise and is referred to as right or left circularly polarized light (Figure 2.10).

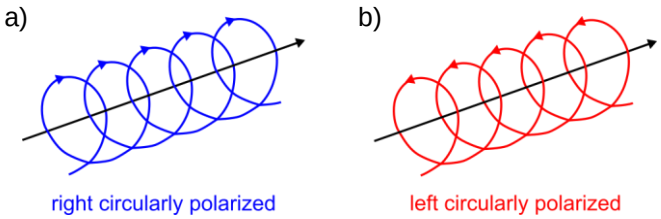

Figure 2.10 Scheme of right (a) and left (b) circularly polarized light.

The difference in absorption of right versus left circularly polarized light is measured as a function of the wavelength resulting in a spectrum that is characteristic for each substance.[187,189] The absorbance difference obeys the Beer-Lambert law as in equation (2-10).

$$\Delta A = A_L - A_R = (\varepsilon_L - \varepsilon_R)dc \qquad \textbf{(2-10)}$$

A: absorbance
$_L$: index for left circularly polarized light
$_R$: index for right circularly polarized light
ε: molar decadic extinction coefficient
d: optical path length
c: concentration of the substance

The difference in absorption of right and left circularly polarized light is usually reported in terms of the ellipticity.[187,189] This is an angle in the ellipse that results from the recombination of the attenuated right and left circularly polarized light having different amplitudes. The ellipticity is numerically related to the difference in absorbance by the following equation (2-11).

$$\Theta = 32980\Delta A \qquad \textbf{(2-11)}$$

Θ: ellipticity
A: absorbance

The instrument for measuring a CD spectrum is a very sensitive CD spectropolarimeter consisting of a high intensity light source such as a xenon arc lamp, a monochromator and a linear polarizer. A modulator with a high frequency electrical alternating field alternately converts the linearly polarized light into a right and left circularly polarized light beam, so that a synchronously operated photomultiplier can alternately detect the intensity of both light beams.

The CD spectroscopy is a valuable tool for showing changes in the conformation of mainly proteins, but also of peptides and nucleic acids.[187–189] It enables the investigation, how the secondary and partially the tertiary structure of proteins change as a function of several environmental conditions such as the temperature, pH value, type and amount of buffer, presence of a solvent and other molecules. It indicates, whether the protein is present in its native conformation, is denatured or if it interacts with a ligand or another protein resulting in a change of its CD spectrum, which depends on both the conformation of the protein and its concentration. CD bands are in the same wavelength range as usual absorption bands.

The secondary structure of proteins is investigated in the wavelength range of 160-250 nm. Here are the n→π*- and π→π*-transitions of the peptide bond, which contains a stereo center and is optically active. Each type of secondary structure such as an α-helix, β-sheet and a random coil shows a characteristic CD spectrum as visible in Figure 2.11.[187–189]

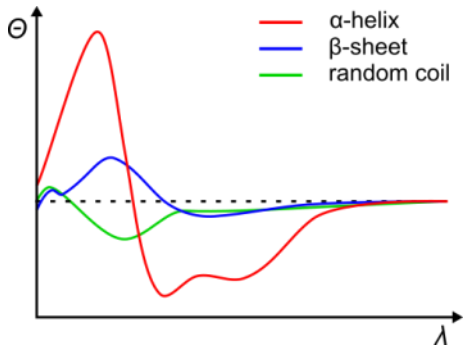

Figure 2.11 Schematic CD spectra of peptides containing α-helices, β-sheets or random coils. [187] This figure was adapted and minimally altered with permission of Springer.

The positive signal is obtained by absorption of right circularly polarized light and the negative signal by absorption of left circularly polarized light. The absence of a signal means absence of circular dichroism. The content of each type of secondary structure of a protein can be estimated by comparing the obtained spectrum with spectra of the corresponding pure forms.

The wavelength range between 250 and 300 nm provides information on the tertiary structure of proteins, but does not show any particular three-dimensional structure.[187–189] Here are π→π*-transitions of the aromatic amino acid residues and n→σ*-transitions of disulfide bonds making it possible to study the nature of the surrounding environment of phenylalanine, tyrosine and tryptophan residues and disulfide bonds.

2.4.1.2 Du Noüy ring method

The du Noüy ring method is a method for measuring the surface tension between a liquid and a gas as well as the interfacial tension between two liquids.[190] The interfacial tension is defined as the reversible force that is required to increase the interface by one area unit under isothermal and isobar conditions. A scheme of a du Noüy ring tensiometer is shown in Figure 2.12.

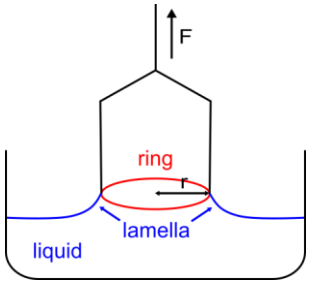

Figure 2.12 Scheme of a du Noüy ring tensiometer.

The tensiometer contains a ring made of a platinum-iridium (Pt-Ir) alloy with a defined circumference. The ring is hung up horizontally and connected to a force transducer, usually a digital balance. Then it is immersed into the liquid and as soon as it is completely wetted, it is slowly lifted out of the liquid and a lamella of the liquid is formed between the ring and the surface of the liquid.[190] A force has to be exerted to pull the hydrostatic weight of the lamella and to counteract the surface tension. The maximum force required to pull the ring from the surface of the liquid arises shortly before the liquid lamella breaks away and is measured by the force transducer. This is proportional to the surface tension and two times the circumference of the ring, because the lamella hangs at the inside and the outside of the ring, as in the following equation (2-12).

$$\sigma = \frac{F_{max}}{2(2\pi r)} f \qquad \textbf{(2-12)}$$

σ: surface tension
F_{max}: maximum force
r: radius of the ring
f: correction factor

The influence of the lamella is taken into account by the correction factor at absolute measurements.

The same experiment can be carried out for measuring the interfacial tension between two immiscible liquids. The ring is therefore immersed into the lower liquid and pulled from this liquid to the upper one in order to measure the maximum force required to pull the ring from the interface.

2.4.1.3 Dynamic light scattering

Dynamic light scattering (DLS) is a method for the determination of the hydrodynamic diameter and size distribution of particles such as polymers, proteins or colloids in a liquid. The hydrodynamic diameter is the diameter of a hypothetical hard sphere that has the same diffusion coefficient like the particle being measured. In practice, this particle may not necessarily be spherical, is dynamic tumbling and surrounded by a solvation shell.[191] The diameter is determined by analyzing the particle movement in a liquid through measuring the intensity changes of scattered light with time.

A sample containing particles dispersed in a liquid is illuminated with a laser beam (Figure 2.13).

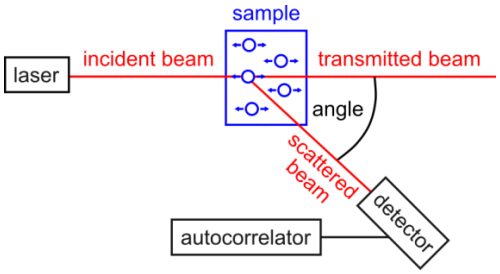

Figure 2.13 Scheme of a dynamic light scattering instrument.

Some light is scattered in all directions by the particles and can interfere with one another either constructively or destructively. The particles in the liquid are randomly moving due to Brownian motion depending on their size, the temperature and viscosity of the liquid.[191] The distance between the particles in the liquid is thus constantly changing with time resulting in a fluctuation of the intensity of the scattered light. This is detected by a photomultiplier at a fixed angle in dependence on the time.[192]

The fluctuation pattern is converted into an intensity autocorrelation function by the autocorrelator. The intensity of the scattered light at one point in time is thereby correlated to the intensity of the scattered light at a time later. The correlation is therefore reducing with time until reaching zero.[191]

The rate of the decay of the correlation function of small particles is high, since they move faster causing faster fluctuations of the scattered light intensity over time. Larger particles move slower and cause fewer changes of the scattered light intensity per time unit resulting in a lower rate of decay of the correlation function. This is illustrated in Figure 2.14.

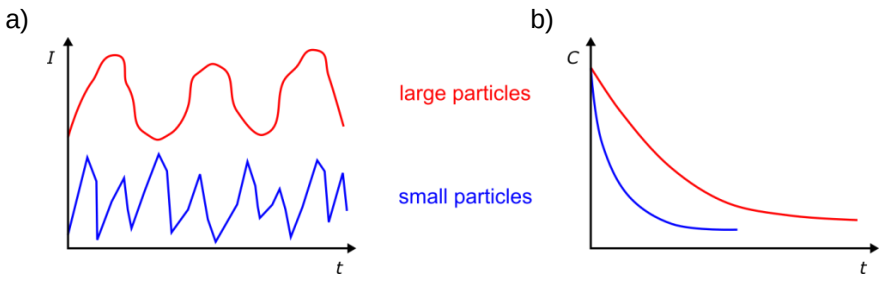

Figure 2.14 Schematic diagrams of intensity fluctuations[193] (a) and exponential correlation functions[191] (b) per time of large and small particles.

The correlation function follows a single exponential decay for monodisperse, round particles, which do not interact with each other, and has the following equation (2-13).[193]

$$g(t) = e^{(-q^2 D t)} \quad \textbf{(2-13)}$$

g: correlation function
q: scattering vector
D: diffusion coefficient
t: time

The diffusion coefficient is obtained by fitting an exponential function to the correlation curve. If the sample is polydisperse, the autocorrelation function is a sum of the exponential decays corresponding to each size class.[191] Another method of analyzing the data is the cumulant analysis. The correlation function therefore has the following general equation (2-14).

$$\ln g(t) = a + bt + ct^2 + \cdots \quad \textbf{(2-14)}$$

g: correlation function
a: coefficient
b: z-average diffusion coefficient
c: polydispersity index

The diffusion coefficient is obtained by fitting a polynomial function to the logarithm of the correlation curve.[191]

The hydrodynamic radius of the particles is calculated from the diffusion coefficient knowing the temperature and viscosity of the surrounding liquid by using the Stokes-Einstein equation (2-15).[192]

$$R_H = \frac{k_B T}{6\pi\eta D} \quad \textbf{(2-15)}$$

R_H: hydrodynamic radius
k_B: Boltzmann's constant
T: temperature
η: viscosity of the liquid
D: diffusion coefficient

The analysis of the exponential correlation function results in one hydrodynamic radius for a monodisperse sample and in an intensity size distribution for a polydisperse sample. The hydrodynamic radius obtained from the cumulant analysis is called z-average and is a mean value.[191] This is the primary and most stable parameter in dynamic light scattering, but only reliable up to a polydispersity index (PDI) of 0.5. The PDI is a dimensionless constant and used to get an idea about the width of the particle size distribution. Samples with a PDI below 0.1 have a reasonably narrow size distribution, whereas samples with a PDI over 0.5 have a broad size distribution.[191] Very dilute samples are used in order to prevent interactions between the particles and multiple scattering, which have a strong influence on the particle mobility.[192]

2.4.1.4 Laser Doppler electrophoresis

Laser Doppler electrophoresis is a combination of an electrophoresis and laser Doppler velocimetry (LDV). It is used to determine the zeta potential of particles in colloidal systems via the electrophoretic mobility, which is the velocity of charged particles in an electric field.[191] The zeta potential is the electrokinetic potential at the slipping plane between the movable and the stationary part of an electrochemical double layer (see Figure 2.15).[194]

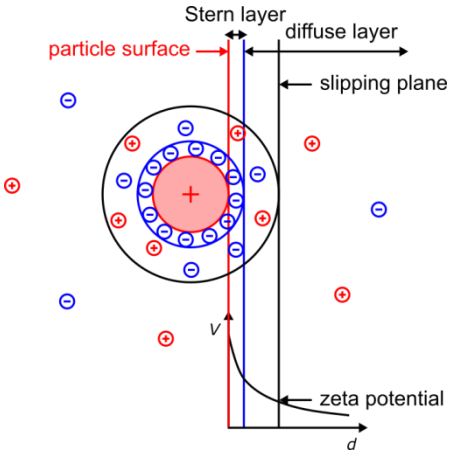

Figure 2.15 Scheme of the electrochemical double layer around a positively charged particle and of a diagram of the electrokinetic potential (*V*) versus the distance (*d*) between the particle surface and the bulk solution.

An electrochemical double layer around a particle is formed, when a charged particle is suspended in an ion containing liquid. Then an increased concentration of oppositely charged ions is attracted to the surface of the charged particle.[194] The liquid layer surrounding the particle consists of an inner region, where the ions are close and strongly bound to the surface forming a rigid layer called Stern layer, and an outer region, where the ions are further away from the surface and loosely bound forming a diffuse layer. The slipping plane is a boundary within the diffuse layer. All the ions within the slipping plane move with the particle in the liquid.

An electric field is applied across the liquid during an electrophoresis and the particles move towards the electrode of opposite charge against viscous forces acting on them. The velocity of the particles is thereby determined by LDV.[191] The moving particles are illuminated with laser light and the scattered light is detected. The Doppler frequency shift of the scattered light caused by the moving particles is proportional to their velocity.

The zeta potential is calculated from the electrophoretic mobility by the Henry equation (2-16) knowing the viscosity and dielectric constant of the dispersion medium.[194]

$$\zeta = \frac{3\eta U_e}{2\varepsilon f} \quad \textbf{(2-16)}$$

ζ: zeta potential
η: viscosity of the medium
U_e: electrophoretic mobility
ε: dielectric constant of the medium
f: Henry's function

The Henry's function describes the ratio between the radius of the particles and the Debye length used as a measure of the electrochemical double layer thickness. There are two approximations for the Henry's function. The Smoluchowski approximation is valid for larger particles ($d > 0.2$ µm) dispersed in an aqueous medium with a moderate electrolyte concentration ($c > 10^{-3}$ M). In this case Henry's function is 1.5. It becomes 1.0 for small particles dispersed in a non-aqueous medium with a low dielectric constant according to the Hückel approximation.[191]

The zeta potential depends on the type of boundary and the concentration and type of electrolyte in the medium[194] and is mainly affected by the pH value.[191] The calculation of the zeta potential contains some inaccuracies due to the use of the viscosity and dielectric constant of the inner of the medium instead of these constants of the double layer and can thus only be considered relatively. The magnitude of the zeta potential gives information about the charge structure of dispersed particles and interfaces.[194] This is often used to indicate the potential stability of colloidal systems. Particles with zeta potentials higher than 30 mV or lower than -30 mV are generally considered as stable, since they will tend to repel each other instead of aggregating.[191] The construction of the measuring device is similar to the DLS instrument besides that it contains an electrophoresis cell with a U-pipe capillary instead of a conventional cuvette and electrodes at either end, to which a potential is applied.

2.4.1.5 BET nitrogen adsorption method

The Brunauer-Emmett-Teller (BET) nitrogen gas adsorption method is used for the determination of the specific surface area and pore size distribution of solid materials. Nitrogen is used due to its high purity and strong interactions with most solids at low temperatures. It is adsorbed to the material by physisorption at low temperatures and the change of the gas pressure due to the adsorption process is measured and analyzed.[193]

The surface area is determined by using the BET adsorption model.[195] This is an extension of the Langmuir model (see chapter 2.2.8.3) and additionally takes the multilayer adsorption without saturation of the sorbent into account.[193] The BET model is based on the assumptions, that all binding sites are equal, that there are no interactions between the bound molecules on adjacent sites, that infinite layers can be adsorbed and that all layers above the first have liquid-like properties.[195] This is typical for the binding behavior of gases.[196] The linear form of the BET equation is shown in the following equation (2-17).[197]

$$\frac{p}{V(p_0 - p)} = \frac{C - 1}{V_{mono} C}\left(\frac{p}{p_0}\right) + \frac{1}{V_{mono} C} \qquad \textbf{(2-17)}$$

p: equilibrium vapor pressure of nitrogen
p_0: saturation vapor pressure of nitrogen
V: volume of adsorbed nitrogen
V_{mono}: volume of complete nitrogen monolayer
C: constant

The BET isotherm is obtained by measuring the equilibrium vapor pressure relative to the saturation pressure of nitrogen in dependency of the known, step-wise released volume of nitrogen in and out of a degassed, weighted and evacuated solid sample, which is cooled to 77 K with liquid nitrogen for adsorption and heated for desorption measurements.[193] The volume of adsorbed nitrogen per unit mass of adsorbent is subsequently plotted versus the relative pressure resulting in a sigmoidal curve progression like the example curve in Figure 2.16. This type of isotherm is also called type II isotherm according to the classification of the International Union of Pure and Applied Chemistry (IUPAC).[198]

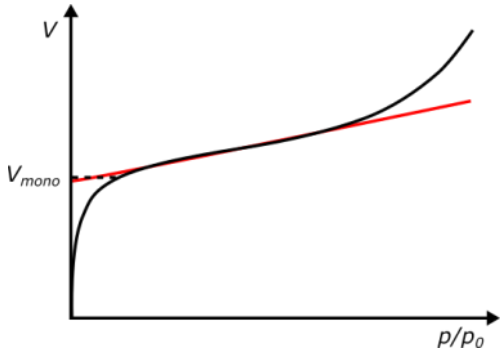

Figure 2.16 Schematic diagram of a BET isotherm with the volume of a complete nitrogen monolayer (V_{mono}) and a linear regression (BET-plot, red) for the analysis of the specific surface area.

At low pressures the isotherm is concave towards the x-axis and resembles the progression of the Langmuir isotherm. This is the region of the adsorption of the first layer, i. e. monolayer formation.[197] At higher pressures the isotherm is convex towards the x-axis. The intermediate region between the relative pressures of approximately 0.05 and 0.35 is closely linear and represents the beginning multilayer adsorption. The volume of adsorbed nitrogen at the beginning of this region (V_{mono} in Figure 2.16) corresponds to the volume required for completely covering the surface of the adsorbent with one monolayer of nitrogen.[199] This volume is used for the determination of the specific surface area and is determined by linear regression to the closely linear region of the adsorption isotherm. The nitrogen volume of the monolayer is determined from the slope and intercept of the so-called BET plot according to the linear form of the BET equation (2-17). The surface area is obtained by multiplication of the number of nitrogen molecules of a complete monolayer, which is assumed to be closest packed, with the average area occupied by each nitrogen molecule. The molecular cross-sectional area of 0.162 nm^2 of nitrogen at 77 K is therefore used. The number of nitrogen molecules is calculated from the measured monolayer volume, the Avogadro's number and the molar volume of nitrogen of 22.41 L mol^{-1}.[200] The specific surface area is obtained by normalizing the surface area with the mass of the adsorbent. The whole equation (2-18) for the calculation of the specific surface area is as follows.

$$A_s = \frac{V_{mono} N_A a_m}{M_v m} \qquad \textbf{(2-18)}$$

A_s: specific surface area of the adsorbent
V_{mono}: volume of a nitrogen monolayer
N_A: Avogadro's number
a_m: molecular cross-sectional area of nitrogen
M_v: molar volume of nitrogen
m: mass of adsorbent

The BET method can also be applied to a type IV isotherm according to the IUPAC classification.[198] This has the same progression like the type II isotherm (see Figure 2.16) besides that there is a hysteresis loop between the adsorption and desorption curve at higher pressures. This indicates the existence of mesopores (d = 2-50 nm) due to capillary condensation of nitrogen within these pores. In contrast to this, the adsorption and desorption curve of the type II isotherm have the same progression.

2.4.1.6 Electron microscopy

Electron microscopy is a method for the investigation of the morphology, structure, size and size distribution of small objects such as polymers, metals, crystals, biomacromolecules, cells and microorganisms. It is based on the interaction between an electron beam and an object resulting in an image of the object.[201] Electron microscopes have a higher resolving power (up to 0.02 nm) compared with light microscopes and thus higher magnifications (up to 1000000 times) are possible. This enables imaging of smaller objects and of finer details down to the nm size range. The resolving power designates the closest possible spacing of two points, so that these are just distinguishable. This decreases with decreasing wavelength as shown by the equation of Abbé (2-19) derived from the diffraction theory.

$$\delta = \frac{1.22\lambda}{A} \qquad \textbf{(2-19)}$$

δ: spacing of two points
λ: wavelength
A: numerical aperture

The higher resolving power of electron microscopes is obtained by the use of electrons instead of light as radiation source, since the wavelength of electrons is more than 50000 times smaller than of visible light.[202] The wavelength of electrons is dependent on their velocity according to the following equation (2-20), which is derived from the de Broglie equation.

$$\lambda = \frac{h}{m_e v} \qquad \textbf{(2-20)}$$

λ: wavelength
h: Planck's constant
m_e: electron mass
v: velocity

The wavelength of electrons can thus be decreased by increasing their velocity resulting in increased resolving power. This is realized by the implementation of an acceleration voltage in an electron microscope, which is between 40-200 kV in a standard transmission electron microscope (TEM) and between 0.2-35 kV in a scanning electron microscope (SEM).[202]

The basic components of an electron microscope are the electron source, electromagnetic lenses for the deflection of the electron beam, a detector and a screen.[202] These components are assembled into a vertical column. High vacuum is used in all optical paths in order to avoid scattering of the electrons by gas molecules. The image contrast comes from elastic and inelastic scattering processes of the electrons at the atoms of the object.

At the transmission electron microscopy, a beam of electrons is transmitted through a thin object. An objective aperture stops all electrons that are mainly elastically scattered by the object and only

transmitted electrons can travel further down to the detector (Figure 2.17). A magnified two-dimensional image of the object and its internal structure is thereby obtained.[203]

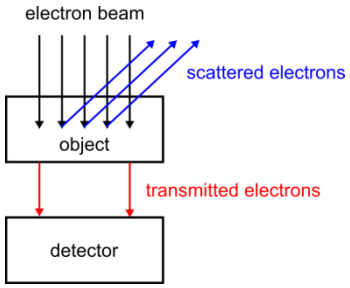

Figure 2.17 Principle of the transmission electron microscopy.

The most common imaging mode is the bright field imaging. Here regions of the object having a high electron density appear dark, because most of the electrons are scattered. The regions with a low electron density are of a different grey scale and the regions with no object appear bright, since all electrons are transmitted.[203] The object is placed as thin film on an electron transparent support grid, so that the electrons can pass through. The object may be coated with a thin layer of a conducting material such as carbon to prevent any surface charge build-up. Organic macromolecules are stained with heavy metals such as osmium to get a better contrast, since they have low electron densities.

At the scanning electron microscopy, a finely focused electron beam is scanned point by point over the object surface and a magnified three-dimensional image of its external morphology and topography is obtained.[203] Here the electron beam interacts with the object surface and thereby emits secondary and back-scattered electrons, which are detected and responsible for the image (Figure 2.18).

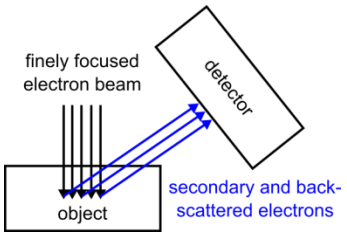

Figure 2.18 Principle of the scanning electron microscopy.

A SEM contains similar components like a TEM plus an additional scanning unit and another imaging system. The different brightness levels of the obtained image arise from the different number of secondary and back-scattered electrons emitted by each point of the object surface. The number of back-scattered electrons increases with increasing atomic number. The object can be placed in the form of a bulk on an object holder, since only the surface is imaged. Non-conductive materials require coating with conductive materials such as palladium, carbon or osmium to prevent the accumulation of static electric fields at the object surface.

2.4.1.7 UV-Vis spectrophotometry

UV-Vis spectrophotometry is a method for the quantitative determination of organic compounds, biomacromolecules and transition metals and is furthermore applied for the determination of enzyme kinetics, the analysis of water and as detector for the HPLC.[204] This method is based on the absorption of light in the ultraviolet (UV) and visible (Vis) range of the electromagnetic spectrum (100-780 nm). The radiation intensity is thereby measured as a function of the wavelength resulting in a spectrum that is characteristic for each substance.

Radiation of this wavelength range causes the excitation of valence electrons in molecules from the ground state to an excited state of higher energy. Vibration and rotation transitions are also excited resulting in spectra with broad bands. The energy is subsequently released by non-radiative transitions.[204] Four types of electronic transitions in organic molecules and biomacromolecules can be excited by the absorption of UV-Vis radiation. These are the transitions from bonding σ- and π-orbitals and non-bonding n-orbitals to anti-bonding σ*- and π*-orbitals referred to as σ→σ*, n→σ*, n→π* and π→π* according to the molecular orbital theory (see Figure 2.19).

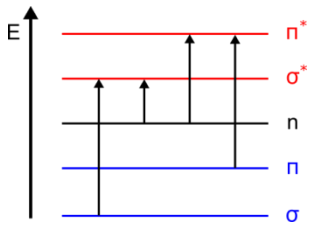

Figure 2.19 Scheme of the electronic transitions in organic molecules after absorption of UV-Vis light.

The most commonly used transitions are the n→π*- and π→π*-transitions, since they are excited by light with a wavelength higher than 200 nm that is experimentally easily accessible. These transitions occur in molecules with free electron pairs or in unsaturated molecules. Molecules with a conjugated π-electron system are excited by light with a higher wavelength (bathochromic shift) and usually show a higher absorption.[204] Proteins have several chromophoric groups that absorb light in the UV range. The peptide bonds absorb light with two absorption maxima at approximately 190 and 220 nm, whereas the first one is used for protein detection due to a higher molar extinction coefficient. The absorption of the aromatic amino acid residues is also used for the detection of proteins. The absorption bands of the tryptophan, phenylalanine and tyrosine residues overlay. This results in an absorption maximum between 260 and 280 nm dependent on their ratio in the protein.[187] The absorption maxima can shift depending on the molecular environment such as the pH value, temperature and type of solvent.

The absorption of light results in an attenuation of the light intensity at its way through a solution of the absorbing substance proportional to the path length of the light and the concentration of the substance (Figure 2.20). This is determined by measuring the intensity of a light beam before and after passing through a solution containing the absorbing substance.

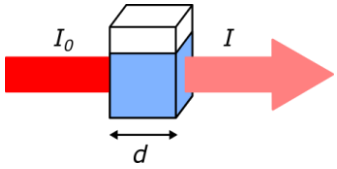

Figure 2.20 Scheme of the attenuation of the incident light intensity I_0 at its way through a solution of an absorbing substance with the optical path length *d* resulting in the transmitted light intensity *I*.

The fraction of the intensity of the transmitted and incident radiation is referred to as transmittance.[204] The absorbance is calculated from the transmittance by the following equation (2-21) in order to get a linear relationship of the already above described proportionality.

$$A = -\log T = -\log \frac{I}{I_0} \qquad \textbf{(2-21)}$$

A: absorbance
T: transmittance
I: intensity of the transmitted light
I_0: intensity of the incident light

The linear relationship between the absorbance, optical path length, the molar decadic extinction coefficient and concentration of the absorbing substance is called Beer-Lambert law. This is the basic equation (2-22) for the determination of the concentration of substances by the UV-Vis spectrophotometry and as follows.

$$A = \varepsilon_\lambda d c \qquad \textbf{(2-22)}$$

A: absorbance
ε: molar decadic extinction coefficient
$_\lambda$: index for wavelength
d: optical path length
c: concentration of the substance

The law is valid, if the absorbing molecules are homogeneously distributed and their concentration is low in order to avoid interactions between them. Since the law only considers absorption, scattering due to particulates in the solution and light emission of the sample has to be avoided.[204] The incident radiation has to be monochromatic, since the molar decadic extinction coefficient is dependent on the wavelength. The extinction coefficient is a characteristic constant for each substance under defined conditions such as the type of solvent, pH value and temperature and can be determined by calibration with standard solutions of known concentrations of the substance.

The instrument for measuring the transmittance in the UV-Vis range in dependence on the wavelength is a UV-Vis spectrophotometer.[204] A scheme of a single-beam UV-Vis spectrophotometer is shown in Figure 2.21.

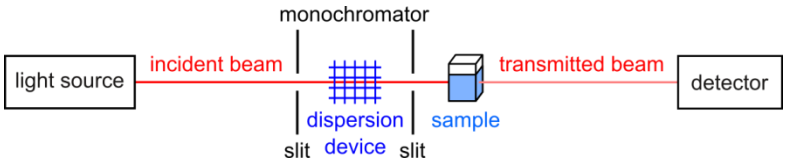

Figure 2.21 Scheme of a single-beam UV-Vis spectrophotometer.

The light source consists of a deuterium arc and a tungsten-halogen lamp in order to achieve a continuous emission spectrum of all wavelengths in the UV and Vis range. Polychromatic light is focused on the entrance slit and broken down into its individual wavelengths by a dispersion device, mostly a grating. Then light of one selected wavelength is passed through the exit slit. These three elements constitute the monochromator.[205] The monochromatic light is passed through a cuvette containing the sample, which consists of a material that transmits UV-Vis light such as quartz. The transmitted light reaches the detector, usually a photomultiplier, and is converted into an electrical signal. The incident light is determined with a blank, which is usually the pure solvent placed in the same cuvette in order to eliminate interferences of the solvent and the cuvette. In a single-beam spectrophotometer the blank and sample are measured consecutively. In a dual-beam spectrophotometer, the blank and sample are measured in parallel.

The measurement of a spectrum is relatively slow with a conventional spectrophotometer, because the monochromator has to be rotated to let light of different wavelengths through.[205] This is faster with a diode array spectrophotometer, where polychromatic light is passed through the sample, focused through an entrance slit and broken down into its individual wavelengths by a dispersion device.[205] Afterwards the light of different wavelengths is simultaneously converted into electric signals by a series of photodiodes positioned in an array.

2.4.1.8 Sodium dodecyl sulfate-polyacrylamide gel electrophoresis

The sodium dodecyl sulfate-polyacrylamide gel electrophoresis (SDS-PAGE) is a method for the separation of proteins and based on the migration of unfolded overall negatively charged proteins through a cross-linked polymer gel in an electrical field, whereas their migration rate is primarily depending on their size.[206]

The proteins are mixed with a Laemmli buffer[207] containing an excess of SDS and heated to 95 °C before the electrophoresis. This results in a breakup of the secondary and tertiary structure and thus a linearization of the proteins.[206] The bound SDS masks the intrinsic charge of the proteins and gives them an overall negative charge. A similar charge-to-mass ratio for all proteins is obtained, since SDS binds at a consistent rate of about one SDS molecule per two amino acid residues. As a result, the migration rate of the long, rod-like shaped SDS-protein associations primarily depends on the protein size. A reducing agent such as dithiothreitol or 2-mercaptoethanol is optionally added for reducing disulfide linkages resulting in a further breakup of the tertiary and quaternary structure of the proteins.

Subsequently, the proteins are loaded into pockets of a cross-linked polyacrylamide gel. These gels are chemically inert, stable and transparent and have different mesh sizes dependent on the content of acrylamide and *N,N'*-methylenebisacrylamide. The gels are located between two buffer chambers in a vertical position. The electrophoresis is started by the application of an electrical field across the buffer chambers. This forces the negatively charged proteins to migrate through the gel toward the positive electrode.

Commonly a discontinuous electrophoresis is used to prevent aggregation of the proteins when entering the gel for obtaining sharper bands.[206] At a discontinuous electrophoresis, a stacking gel with large meshes on top of the resolving gel serves for the pre-separation and concentration of the proteins. The buffer contains ions with high (leading ion) and low electrophoretic mobility (trailing ion). Proteins have an intermediate mobility causing them to stack between the two ions forming a tight band for an improved resolution. A typical buffer system is an SDS containing tris(hydroxymethyl)aminomethane (Tris)-chloride/Tris-glycine-system.[207]

After passing slowly from the stacking to the resolving gel, the proteins migrate with different rates depending on their size due to the sieving effect from the small meshes of the resolving gel. Smaller proteins migrate faster than larger proteins, since they fit better through the meshes and are less retarded.[206] This enables the separation of proteins of different molecular weights. After completion of the gel electrophoresis, the proteins are stained with a dye such as Coomassie Blue or with silver.

2.5 Experimental

2.5.1 Chemicals

Methacrylic acid (MAA, ≥ 99%), 2-hydroxyethyl methacrylate (HEMA, 99%), ethanol (99.5%, denatured 1% MEK), hydrochloric acid (HCl, 1 M), sodium hydroxide solution (NaOH, ~ 32% and 1 M), sodium chloride (NaCl, ≥ 99.5%), glycerol (87%), dipotassium hydrogen phosphate, phosphoric acid (65%) and albumin fraction V from bovine serum (BSA) were purchased from Merck KGaA. 2-Aminoethyl methacrylate hydrochloride (AEMA, 90%), *N*-(3-acrylamidopropyl)trimethylammonium chloride (APTMA, 75 wt.-% in water), isobutyl methacrylate (IBMA, 97%), ethylene glycol dimethacrylate (EGDMA, 98%), 2,2-dimethoxy-2-phenylacetophenone (DMPAP, 99%), sodium citrate tribasic dihydrate (≥ 99.0%), sodium dodecyl sulfate (SDS, 99+%), 2-mercaptoethanol (99%), glycine (≥ 99%), pepsin from porcine gastric mucosa (pepsin 1, ≥ 250 U mg^{-1} solid and pepsin 2, 3200-4500 U mg^{-1} protein), thermolysin from geobacillus stearothermophilus (type X, 30-175 U mg^{-1} protein), trypsin from bovine pancreas (≥ 10000 U mg^{-1} protein), hemoglobin human, lysozyme from chicken egg white (≥ 90 %, ≥ 40000 U mg^{-1} protein), β-lactoglobulin from bovine milk (LG, ≥ 90%), α1-acid glycoprotein from bovine plasma (GP, 99%) and pepstatin A (≥ 100000 U mg^{-1}) were purchased from Sigma-Aldrich. 2,2-Azobis(4-methoxy-2,4-dimethylvaleronitrile) (V-70, 95%) was purchased from Wako Chemicals GmbH. n-Hexadecane (HD, 99%), bromophenol blue and tris(hydroxymethyl)aminomethane (Tris, 99%) were purchased from Alfa Aesar GmbH & Co. KG. Potassium chloride (KCl, ≥ 99.5%) was purchased from Carl Roth GmbH & Co. KG. Lutensol AT 50 (powder) was obtained from BASF SE, which is a poly(ethylene oxide)hexadecyl ether with an ethylene oxide block length of about 50 units. Pepstatin immobilized agarose beads (PAB, 50% aqueous slurry, 4% agarose) were purchased from Thermo Fisher Scientific Inc. Aluminum sulfate tetra hydrate was purchased from VWR Chemicals. Coomassie Brilliant blue G-250 and cetyltrimethylammonium bromide (CTAB) were purchased from AppliChem GmbH. Argon gas (99.996%) was purchased from MTI Industriegase AG.

MAA, HEMA and EGDMA were distilled under reduced pressure using a P6Z-101 two-stage rotary vane pump (from Ilmvac GmbH) and stored at -20 °C before use. Water was always double-demineralized and then purified using a Milli-Q academic filter station (from Merck Millipore). The other chemicals were used as received.

2.5.2 Instrumentation and materials

An analytical scale balance (from Sartorius AG) was used for weighing the chemicals. Eppendorf Research pipettes (from Eppendorf AG) were used for volume measurements. The magnetic stirrer MR Hei-Standard (from Heidolph Instruments), the sonifier W450 Digital with a ½" tip (from Branson) and a UV lamp (366 nm from UVP) were used for the preparation of the solutions for the CD spectroscopic measurements and of the polymer particles. The pH meter Portamess (from Knick GmbH & Co. KG) was used for adjusting the pH values of the buffer solutions. The Vortex Genie 2 (from Scientific Industries Inc.) and the Aquasonic 150D Ultrasonic Cleaner (from VWR International) were used during the washing procedure. A Heraeus Megafuge 16 centrifuge (from Thermo Scientific) with Nalgene® round bottom tubes (from Thermo Scientific) and reaction vessels (from Eppendorf AG and Brand GmbH & Co. KG) were used for the washing procedure and rebinding experiments. A Heraeus vacuum oven (from Thermo Scientific) was used for drying the polymer particles and gravimetric analysis. The Advanced Digital shaker (from VWR International) was used for the incubation during the batch rebinding experiments. A Specord S 600 (from Analytik Jena AG) with a 10 mm semi-micro quartz cuvette (from Hellma Analytics) was used for the UV-Vis absorbance measurements during the washing procedure, and when syringe filters with an average pore diameter of 0.1 µm (polyethersulfone, Acrodisc from Pall GmbH) were used for the rebinding experiments. A Nanodrop 2000C (from Thermo Scientific) with 10 mm UV microcuvettes (from Brand GmbH & Co. KG) was used for the UV-Vis absorbance measurements, when centrifugal filters with a molecular weight cut-off (MWCO) of 100 and 300 kDa (modified polyethersulfone, Nanosep from Pall GmbH) were used for the rebinding experiments. Other instruments are mentioned in the respective subchapter.

2.5.3 Circular dichroism spectroscopic measurements

Different pepsin solutions of a concentration of 1 mg mL^{-1} were prepared for the measurements. Pepsin 1 and 2 were dissolved in pure water. Pepsin 1 was dissolved in 10 and 0.1 mM HCl, in 100 and 0.01 µM NaOH and in a citrate buffer solution (25 mM, pH 4). CTAB (5 mM), SDS (5 mM) and Lutensol AT 50 (1.2 wt.-%), respectively, were dissolved in an aqueous solution of pepsin 2. A part of the aqueous solution of pepsin 2 was sonicated with amplitude of 60% for 120 s at 0 °C. Another part was irradiated with a UV lamp (366 nm) at room temperature (RT) for 20 h. A third part was incubated under stirring for 20 h. The measurements were performed with a J-810 spectropolarimeter (from Jasco GmbH), which was calibrated with an ammonium d-10-camphor sulfonate solution. Argon was purged through the sample chamber before and during the measurements. The scanning mode was continuous and the scanning speed 50 nm min^{-1}. The sensitivity was 100 mdeg and the band width was 1 nm. The far-UV CD spectra (190 and 240 nm) of the pepsin 1 and 2 solutions were recorded in a 1 and 2 mm cuvette and the near-UV CD spectra (240-320 nm) of all solutions in a 10 mm cuvette. 5 measurements were performed and averaged. Blank solutions were measured in the same way and subtracted. An external thermostat was used to heat the aqueous solution of pepsin 1 during the measurements.

2.5.4 Surface tension measurements

Different solutions were prepared for the measurements. Pepsin 2 (1 mg mL^{-1}), CTAB (5 mM), Lutensol AT 50 (1.2 wt.-%) and APTMA (2.5 wt.-%), respectively, were dissolved in water. Pepsin 2 (1 mg mL^{-1}) and APTMA (2.5 wt.-%) were dissolved in water. The measurements were performed with a DCAT 21 tensiometer (from DataPhysics Instruments GmbH). The Pt-Ir-ring (RG11) was cleaned by rinsing with water and annealing before the measurements. The measurement was started after 10 to 60 min of equilibration at 20 °C. The geometric average and standard deviation of at least 20 pull- and push-cycles were determined.

2.5.5 Preparation of the polymer particles

2.5.5.1 Different functional monomers

The MIPs 1-4 were prepared by miniemulsion polymerization as follows. The disperse phase was obtained by mixing EGDMA and MAA (MIP 1) or HEMA (MIP 2), HD (75 mg) and DMPAP (51 mg). Pepsin 1 (75 mg) was dissolved in a solution of Lutensol AT 50 (180 mg) in water (15 g), which was purged with Argon for around 10 min before the surfactant addition. When AEMA (MIP 3) or APTMA (MIP 4) were used as functional monomers, these were dissolved in the water phase instead of the disperse phase. The total amount of cross-linker and monomer was 1.8 g and the molar ratio between cross-linker and monomer was 4 : 1. The maximum solid content was 12 wt.-%. A pre-emulsion was prepared by stirring the mixture for 1 h. A miniemulsion was obtained by ultrasonication of the pre-emulsion with amplitude of 60% at 0 °C in order to prevent polymerization for 120 s. The polymerization was initiated by irradiation with a UV lamp (366 nm) at RT and carried out under stirring at 750 rpm for 20 h. When AEMA was used as monomer, the amount of all components was multiplied by 1.33, V-70 (24 mg) was used instead of DMPAP as initiator and the polymerization was initiated at 30 °C. The NIPs were prepared in the same way as the corresponding MIPs, but without pepsin.

2.5.5.2 Different other parameters

The same protocol with APTMA as functional monomer was used for the preparation of MIP and NIP 5-10 as before, except that the double amount of pepsin 2 (200 mg) was used and that the amount of all components was multiplied by 1.33. The total amount of EGDMA and APTMA was 2.4 g. Water was replaced by a citrate buffer solution (25 mM, pH 4) and a phosphate buffer solution (25 mM, pH 7) for the preparation of MIP and NIP 6 and 7. MIP and NIP 8 were prepared without Lutensol AT 50. Half of the amount of substance of APTMA was replaced by IBMA for the preparation of MIP and NIP 9. The amount of APTMA was reduced to one tenth for the preparation of MIP and NIP 10. The total amount of EGDMA and APTMA was thus 2.2 g, the molar ratio between EGDMA and APTMA was 40 : 1 and the maximum solid content was 11 wt.-%.

2.5.5.3 Polymer particles of different sizes

The polymer particles for the study of the influence of the surface area on the binding capacity were prepared in the same way as NIP 5. The particles were subsequently centrifuged at 5000 rpm for 5 min. The supernatant was separated from the precipitate, which was resuspended in water using a vortex for 2 h. The amount of water was adjusted to obtain the same solid content as in the supernatant, which was determined to 1.7 wt.-% by gravimetric analysis.

2.5.6 Characterization of the polymer particles

2.5.6.1 Gravimetric analysis and conversion

The solid content of an aliquot of the polymer suspensions was determined gravimetrically with a moisture analyzer (MA150 from Sartorius AG). The conversion of the polymerization was calculated from the solid content by the following equation (2-23).

$$X = \frac{C_a m_s - m_{psi}}{m_m} = \frac{m_p}{m_m} \quad \textbf{(2-23)}$$

X: conversion
C_a: solid content of an aliquot
m_s: mass of the polymer suspension
m_{psi}: mass of pepsin, surfactant and initiator
m_m: mass of monomer
m_p: mass of polymer

2.5.6.2 Dynamic light scattering

The average hydrodynamic particle diameter (z-average) and polydispersity index (PDI) were determined by dynamic light scattering (DLS) with a Zetasizer Nano ZS (from Malvern Instruments Ltd.). The scattering angle was 173° and the wavelength of the laser 633 nm. The polymer suspensions were diluted to a solid content of 0.01 wt.-% in water before the measurements. Three measurements were performed at 25 °C. The results were averaged and the standard deviation was determined.

2.5.6.3 Zeta potential measurements

The electrophoretic mobility was measured by laser Doppler electrophoresis with a Zetasizer NanoZS (from Malvern Instruments Ltd.). The polymer suspensions were diluted to a solid content of 0.01 wt.-% in a KCl solution (1 mM) before the measurements. The zeta potential was determined by using the Smoluchowski equation. Three measurements were performed at 25 °C. The results were averaged and the standard deviation was determined.

2.5.6.4 Transmission electron microscopy

Transmission electron microscope (TEM) images were recorded with an EM10 microscope (from Carl Zeiss AG) operating at a voltage of 80 kV and magnifications of 1000, 4000 and 16000 times. The polymer suspensions were therefore diluted to a solid content of 0.1 wt.-% and placed on a 400-mesh copper grid, which was coated with Formvar and exposed to oxygen plasma. The samples were dried at RT. The polymer particles made with APTMA were coated with carbon. Additionally, the average particle diameters and particle size distributions were determined from the TEM images recorded with a magnification of 1000 times by determining the diameters of 1000 particles of different sizes by hand with the ImageJ software. An error of 10% was assumed.

2.5.6.5 Scanning electron microscopy

Scanning electron microscope (SEM) images were recorded with an S-5200 microscope (from Hitachi) operating at an acceleration voltage of 30 kV and a magnification of 200000 times. The polymer suspensions were therefore diluted to a solid content of 0.1 wt.-% and placed on a silicon wafer, dried and coated with platinum.

2.5.6.6 Nitrogen adsorption measurements

The specific surface areas of the polymer particles were determined by nitrogen adsorption measurements using a QuadraSorb SI (from Quantachrome GmbH & Co. KG) and the Brunauer-Emmett-Teller (BET) isotherm. The polymer particles were dried under reduced pressure ($p \sim 200$ mbar) at 40 °C before the measurements. Two measurements were performed. The results were averaged and the spread was calculated.

2.5.7 Washing of the polymer particles and extraction of pepsin

2.5.7.1 Different functional monomers

The polymer particles were centrifuged at 13000 rpm for 1 h and the supernatant was discarded. The precipitate was redispersed in around 50 mL of the respective extraction solution using a vortex for at least 40 min. This was repeated at least 5 times in water, in ethanol and in water, respectively. Water was used to remove pepsin and the surfactant. Ethanol was used to remove unreacted monomer, cross-linker and hydrophobic agent. Water was used to replace ethanol. UV-Vis spectra of the supernatants were measured between 190 and 400 nm. This procedure was done until the absorbance between 180 and 360 nm was significantly reduced and no absorbance at 277 nm was detected anymore. The NIPs were treated in the same way as the MIPs. After all, a last centrifugation step was performed and the polymer particles were dried under reduced pressure ($p \sim 200$ mbar) at 40 °C.

2.5.7.2 Different other parameters

At least 10 centrifugation/redispersion cycles were performed. Water was used to remove pepsin, the surfactant, unreacted monomer and hydrophobic agent. The centrifugation was done at 13000 rpm for 20 min up to 1 h. The redispersion in around 50 mL of water was done by using a sonication bath for 20 min and a vortex for 40 min. UV-Vis spectra of the supernatants were measured between 190 and 400 nm. This procedure was done until the absorbance between 180 and 360 nm was significantly reduced and no absorbance at 277 nm was detected anymore. The NIPs were treated in the same way as the MIPs. After the last centrifugation step, the particles were redispersed in around 15 mL of pure water. Then the solid content of 2 aliquots of the washed polymer suspensions was determined by gravimetric analysis and averaged. Afterwards pure water was added to adjust the solid content to 2 wt.-%.

2.5.7.3 Different extraction solutions

The same procedure was carried out as described above, but with other extraction solutions. A half of MIP and NIP 5 were washed with 0.1 M HCl, a third of MIP and NIP 10 were washed with concentrated NaOH solution and another third were washed with a 1 M NaCl solution. The extraction solutions were finally replaced by water.

2.5.8 Batch rebinding of pepsin

Batch rebinding experiments with the polymer particles and pepsin were performed as follows. The polymer particles were mixed and incubated with a pepsin solution under shaking at 280 rpm and at RT for 20 h. The reaction vessels were therefore placed lengthwise on the shaker to reduce the tendency of the polymer particles to sediment. The polymer particles were subsequently removed from the solution by centrifugation and filtration. The concentration of pepsin remaining in the solution was determined by measuring the absorbance at 277 nm with a UV-Vis spectrophotometer. Three measurements were performed per sample and averaged. The polymer particles were incubated in water without pepsin and treated in the same way as the samples containing pepsin for the blank measurements. Calibration solutions of different pepsin concentrations were treated in the same way as the samples containing pepsin. It was confirmed that pepsin adsorption to the filter was negligible. All experiments were performed in duplicates. The surface-normalized binding capacities of the polymer particles were determined according to the following equation (2-24). The average and spread of the results of the 2 samples were calculated.

$$Q_s = \frac{(\beta_{in} - \beta_{free})V}{m_p A_s} = \frac{m_b}{A_p} \quad \textbf{(2-24)}$$

Q_s: surface-normalized binding capacity
β_{in}: initial pepsin mass concentration
β_{free}: free pepsin mass concentration
V: volume of solution
m_p: mass of polymer particles
A_s: specific surface area of polymer particles
m_b: mass of bound protein
A_p: surface area of polymer particles

Imprinting factors were determined according to equation (2-4) in chapter 2.2.8.2.

2.5.8.1 Different functional monomers

20 mg of the dried polymer particles (MIP and NIP 1-4) were resuspended in 1 mL of a solution of pepsin 1 (0.8 mg mL^{-1}) and incubated under agitation with a vortex. The larger polymer particles were removed from the solution by centrifugation at 5500 rpm for 10 min. The smaller polymer particles in the supernatant were subsequently removed from the solution by filtration through a syringe filter (0.1 µm).

2.5.8.2 Different other parameters

The polymer particles of the MIPs and NIPs 5-10 were used in suspension (2 wt.-%). 1 mL of the suspensions of the MIPs and NIPs 5-9 were mixed with 1 mL of a solution of pepsin 2 (1.6 mg mL^{-1}) and incubated under shaking. A vortex was used for mixing and the incubation in the case of MIP and NIP 9. 250 µL of the suspensions of MIP and NIP 10 and of the pepsin solution were used. The polymer particles of the MIPs and NIPs 5-9 were removed from the solution by centrifugation at 5500 rpm for 10 min and subsequent filtration of the supernatant through a syringe filter (0.1 µm). The polymer particles of MIP and NIP 10 were removed from the solution by centrifugation at 3000 rpm for 5 min in centrifugal filters (100 kDa).

2.5.8.3 Different extraction solutions

Batch rebinding experiments with MIP and NIP 11 and pepsin were performed as with MIP and NIP 5. Batch rebinding experiments with MIP and NIP 12 and 13 and pepsin were performed as with MIP and NIP 10, only that 200 µL of the polymer suspensions and of the pepsin solution were used.

2.5.8.4 Comparison with pepstatin immobilized agarose beads

The solid content of an aliquot of the suspension of the PABs was determined by gravimetric analysis. Another aliquot of the suspension of the PABs was subsequently diluted with water to a solid content of 2 wt.-%. 200 µL of the suspension of the PABs and MIP and NIP 5 (2 wt.-%), respectively, were mixed with 200 µL of a solution of pepsin 2 (1.6 mg mL^{-1}) and incubated under shaking. The polymer particles were removed from the solution by centrifugation at 3000 rpm for 15 min in centrifugal filters (300 kDa). The content of bound pepsin was determined according to the following equation (2-25).

$$B = \left[\frac{(\beta_{in} - \beta_{free})V}{m_{in}}\right]100 = \left[\frac{m_b}{m_{in}}\right]100 \qquad \textbf{(2-25)}$$

B: content of bound protein
β_{in}: initial protein mass concentration
β_{free}: free protein mass concentration
V: volume of solution
m_{in}: mass of initial protein
m_b: mass of bound protein

The average and spread of the results of the 2 samples were calculated. This equation (2-25) was also used for the determination of the content of pepsin bound to all MIPs and NIPs, which is described in chapter 2.6.9.4.

2.5.8.5 Polymer particles of different sizes

200 µL of the suspension of the polymer particles of the supernatant and of the redispersed precipitated polymer particles (1.36 wt.-%), respectively, were mixed with 200 µL of a solution of pepsin 2 (1.36 mg mL^{-1}) and incubated under shaking. The polymer particles were removed from the solution by centrifugation at 3000 rpm for 15 min in centrifugal filters (300 kDa). The mass-based binding capacity was determined according to the following equation (2-26) additionally to the surface-normalized binding capacity. The average and spread of the results of the 2 samples were calculated.

$$Q = \frac{(\beta_{in} - \beta_{free})V}{m_p} = \frac{m_b}{m_p} \quad \textbf{(2-26)}$$

Q: binding capacity
β_{in}: initial protein mass concentration
β_{free}: free protein mass concentration
V: volume of solution
m_p: mass of polymer particles
m_b: mass of bound protein

2.5.9 Batch rebinding of different pepsin concentrations

Batch rebinding experiments with the polymer particles and pepsin solutions of different initial concentrations ranging from 0.2 to 2.4 mg mL^{-1} were performed as described in chapter 2.5.8.

2.5.9.1 Different functional monomers

20 mg of the dried polymer particles (MIP and NIP 1-4) were resuspended in 1 mL of each pepsin 1 solution of the concentration of 0.2, 0.4, 0.6, 0.8 and 1.0 mg mL^{-1} and incubated under agitation with a vortex. The polymer particles were removed from the solution by centrifugation at 5500 rpm for 10 min and subsequent filtration of the supernatant through a syringe filter (0.1 µm).

2.5.9.2 Different other parameters

1 mL of the suspensions of the MIPs and NIPs 6 and 9 and MIP 8 (2 wt.-%) were mixed with 1 mL of each solution of pepsin 2 (0.4, 0.8, 1.2, 1.6, 2.4, 4.8 mg mL^{-1}) and incubated under shaking. A vortex was used for mixing and the incubation in the case of MIP and NIP 9 and pepsin 2 solutions (0.6, 0.8, 1.2, 1.6, 2.0, 2.4 mg mL^{-1}). 250 µL of the suspensions of MIP and NIP 5 and of the pepsin 2 solutions (0.8, 1.2, 1.6, 2.4, 2.8 and 3.2 mg mL^{-1}) were used. The polymer particles of the MIPs and NIPs 6-9 were removed from the solution by centrifugation at 5500 rpm for 10 min and subsequent filtration of the supernatant through a syringe filter (0.1 µm). The polymer particles of MIP and NIP 5 were removed from the solution by centrifugation at 3000 rpm for 5 min in centrifugal filters (100 kDa).

2.5.10 Batch rebinding of pepsin during different time intervals

Batch rebinding experiments with the polymer particles and pepsin solutions with different incubation times from 1 min up to 20 h were performed as in chapter 2.5.8. 1 mL of the suspensions of MIP and NIP 6 and MIP 8 (2 wt.-%) were mixed with 1 mL of a solution of pepsin 2 (1.6 mg mL^{-1}) and incubated under shaking for 1 and 5 min, 2, 6, 10 and 20 h. 250 µL of the suspensions of MIP and NIP 5 (2 wt.-%) were mixed with 250 µL of a solution of pepsin 2 (1.6 mg mL^{-1}) and incubated under shaking for 1 and 5 min, 1, 2, 6, 10 and 20 h. The polymer particles of MIP and NIP 6 and MIP 8 were removed from the solution by centrifugation at 5500 rpm for 10 min and subsequent filtration of the supernatant through a syringe filter (0.1 µm). The polymer particles of MIP and NIP 5 were removed from the solution by centrifugation at 3000 rpm for 5 min in centrifugal filters (100 kDa).

2.5.11 Batch rebinding of pepsin at different pH values

Batch rebinding experiments with the polymer particles and pepsin buffer solutions of different pH values were performed as described in chapter 2.5.8. A citrate buffer solution (50 mM) was prepared and adjusted to the pH values of 2 and 4. A phosphate buffer solution (50 mM) was prepared and adjusted to the pH value of 7. Pepsin 2 was dissolved in the buffer solutions with an initial concentration of 1.6 mg mL^{-1}. 1 mL of the suspensions of MIP and NIP 6 and MIP 8 (2 wt.-%) were mixed with 1 mL of each pepsin solution and incubated under shaking. The polymer particles of MIP and NIP 6 and MIP 8 were removed from the solution by centrifugation at 5500 rpm for 10 min and subsequent filtration of the supernatant through a syringe filter (0.1 µm).

2.5.12 Single batch rebinding of different proteins

Batch rebinding experiments with the polymer particles and thermolysin, trypsin, lysozyme and hemoglobin were performed separately as described in chapter 2.5.8. The same amount of substance of each protein as of pepsin was used. The thermolysin solutions were filtrated before use with a syringe filter (0.1 µm). The initial thermolysin concentration was adjusted so that the thermolysin concentration after filtration was the same as the pepsin concentration. The surface-normalized binding capacities were divided by the molecular weight of the respective protein. The relative selectivity factors were determined according to the following equation (2-23).

$$RSF = \frac{SF_{MIP}}{SF_{NIP}} \quad \textbf{(2-27)}$$

RSF: relative selectivity factor
SF_{MIP}: selectivity factor of MIP
SF_{NIP}: selectivity factor of NIP

The selectivity factors were determined by using equation (2-9) described in chapter 2.2.8.5.

2.5.12.1 Different other parameters

1 mL of the suspensions of the MIPs and NIPs 5-9 were mixed with 1 mL of a thermolysin, trypsin, hemoglobin and lysozyme solution (45.7 nmol mL^{-1}) separately and incubated under shaking. A vortex was used for mixing and the incubation in the case of MIP and NIP 9. 200 µL of the suspensions of MIP and NIP 9 and MIP 8 and of the thermolysin solution were used. 200 µL of the suspensions of MIP and NIP 10 and of all protein solutions were used. The polymer particles of the MIPs and NIPs 5-9 were removed from the solution by centrifugation at 5500 rpm for 10 min and subsequent filtration of the supernatant through a syringe filter (0.1 µm). The polymer particles of MIP and NIP 9 and MIP 8 were removed from the solution by centrifugation at 3000 rpm for 15 min in centrifugal filters (300 kDa) after the incubation with the thermolysin solution. The polymer particles of MIP and NIP 10 were removed from the solution by centrifugation at 3000 rpm for 15 min in centrifugal filters (100 kDa). Centrifugal filters with a MWCO of 300 kDa were used after the incubation with the hemoglobin solution.

2.5.12.2 Different extraction solutions

Batch rebinding experiments with MIP and NIP 11 and the different proteins were performed as with MIP and NIP 5. Batch rebinding experiments with MIP and NIP 12 and 13 and the different proteins were performed as with MIP and NIP 10.

2.5.13 Single batch rebinding of pepsin and α1-acid glycoprotein

Batch rebinding experiments with the polymer particles and pepsin and α1-acid glycoprotein were performed separately as described in chapter 2.5.8. The same amount of substance of α1-acid glycoprotein was used as of pepsin. The surface-normalized binding capacities were divided by the molecular weight of the respective protein.

200 µL of the suspensions of the MIPs and NIPs 5, 6 and 11 were separately mixed with 200 µL of a solution of pepsin 2 and an α1-acid glycoprotein solution (45.7 nmol mL^{-1}) and incubated under shaking. The polymer particles were removed from the solution by centrifugation at 3000 rpm for 15 min in centrifugal filters (300 kDa).

2.5.14 Competitive batch rebinding of different proteins

Competitive batch rebinding experiments with the MIPs and NIPs 5-13 and a mixture of pepsin, BSA and LG were performed as follows. A Laemmli sample buffer solution was prepared by dissolving Tris (1.51 g), SDS (3 g), glycerol (20 mL), bromophenol blue (20 mg) and 2-mercaptoethanol (10 mL) in water and filling the volume to 50 mL with water. The pH value was adjusted to 6.8 with HCl. The solution was stored at 4 °C. A running buffer solution was prepared by dissolving Tris (30.3 g), glycine (141.89 g), SDS (10 g) in water and filling the volume to 1 L with water. The pH value of this solution was 8.8. The solution was stored at RT and diluted to 1 tenth with water before use. A staining solution was prepared by dissolving aluminum sulfate tetra hydrate (50 g) in water first. Then ethanol (100 mL), Coomassie Brilliant Blue G-250 (0.2 g) and phosphoric acid (20 mL) were added and the solution was filled to 1 L with water. A distaining solution was prepared by mixing ethanol (100 mL), phosphoric acid (20 mL) and water and filling the mixture to 1 L with water.

90 µL of the polymer suspensions (2 wt.-%) were mixed with 90 µL of a solution containing pepsin 2, BSA and LG at a respective concentration of 45.7 nmol mL^{-1}. The mixture was incubated under shaking at RT for 20 h. The polymer particles including the bound proteins were subsequently removed by centrifugation at 13000 rpm for 10 min with a Heraeus Pico 17 centrifuge (from Thermo Electron Corporation). 18 µL of the supernatants were mixed with 6 µL of the Laemmli sample buffer solution. The mixture was heated at 95 °C for 5 min with a HLC thermoblock TH21 (from BioTech). Then 16 µL of each mixture and 6 µL of a PageRuler prestained protein ladder (10 to 170 kDa from Thermo Fisher Scientific) were loaded onto an Any kD Mini-PROTEAN® TGX precast gel (from Bio-Rad Laboratories). The electrophoresis was performed in a Mini-PROTEAN Tetra cell (from Bio-Rad Laboratories) containing the running buffer solution under stirring at 250 rpm at 20 mA per gel. The gel was subsequently washed with excess amount of water (5 changes) and stained with the staining solution under gently shaking with a Duomax 1030 (from Heidolph Instruments) for 2 h or overnight. When the staining was performed overnight, the gel was distained by gently shaking in the distaining solution for 1 h after washing with water (2 changes). An image of the gel was recorded with an imaging system (Molecular Imager Gel Doc™ XR^+ from Bio-Rad Laboratories). The same experiments were carried out with pepsin, which was pre-incubated with pepstatin under shaking at RT for 1 h. The molar ratio between pepsin and pepstatin was 1 : 2. Reference samples containing the protein mixture and the pure proteins, respectively, but no polymer particles and control samples containing the polymer particles, but no proteins were prepared in the same way. The same experiments were carried out with MIP and NIP 9 and pepsin 2, BSA and LG solutions with a concentration of 45.7 nmol mL^{-1} separately. The content of proteins bound to the MIPs and NIPs was determined by comparing the density of the sample bands with the density of the reference bands on the gels using the program ImageJ. An error of 10% of bound protein was assumed.

2.6 Results and discussion

2.6.1 Study on the conformational stability of pepsin

The effect of different temperatures, pH values, the presence of buffer salts and surfactants, the incubation time and exposure to ultrasound and UV light on the conformation of pepsin was investigated using circular dichroism (CD) spectroscopy. Changing the temperature, pH value and the salt content of a protein solution may result in a change of its conformation by affecting mainly non-covalent interactions inside the protein.[6] High energy of UV light and high shear forces of ultrasound may alter the conformation of proteins. Surfactants can adsorb on proteins and thus cause unfolding or even denaturation of the proteins.[208] This study was done in order to find the conditions, which can be used for surface imprinting of pepsin via miniemulsion polymerization without significantly changing its conformation. A conformational change of the template protein during the polymerization may result in the imprinting of the wrong conformation. This can negatively affect the selectivity of the resulting MIP.[37,38] Far-UV (190-240 nm) and near-UV (240-320 nm) CD spectra provide information on the secondary and tertiary structure of pepsin.

Two different pepsin formulations were used for this study. Their far- and near-UV CD spectra are compared in Figure 2.22.

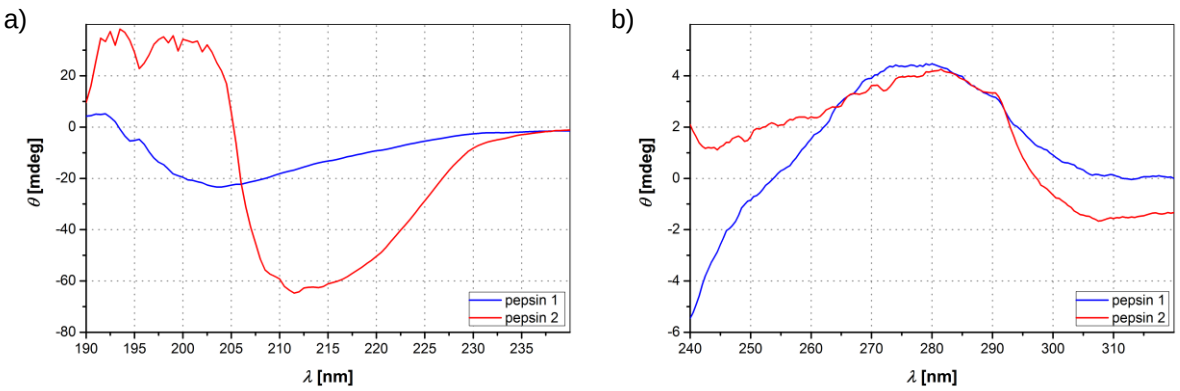

Figure 2.22 Far-UV (a) and near-UV (b) CD spectra of pepsin 1 and 2. All spectra represent the average of 5 measurements.

The far-UV CD spectrum of pepsin 2 had a broad single minimum between 205 and 245 nm. The comparison with reference CD spectra of proteins with various types of secondary structure[188,209,210] shows that this shape is typical for a highly β-sheet rich protein. A similar shape of the far-UV CD spectrum of pepsin is reported in literature.[25,211] The minimum of the CD spectrum of pepsin 1 was shifted towards shorter wavelengths (192-230 nm) due to a lower content of secondary structure of pepsin 1 and maybe also due to an increase of disordered structures[188,212]. The ellipticity was lower due to the use of a cuvette with a smaller path length. The near-UV CD spectra of pepsin 1 and 2 were slightly different. Hence, the aromatic amino acid residues and disulfide bonds in the tertiary

structure of the different pepsins have different environments. The shape of the near-UV CD spectrum of pepsin 2 is comparable to a spectrum of pepsin, which is reported in literature.[25,211,212]

The change of the far-UV CD spectrum of pepsin depending on the temperature, which was varied between 25 and 90 °C, is shown in Figure 2.23.

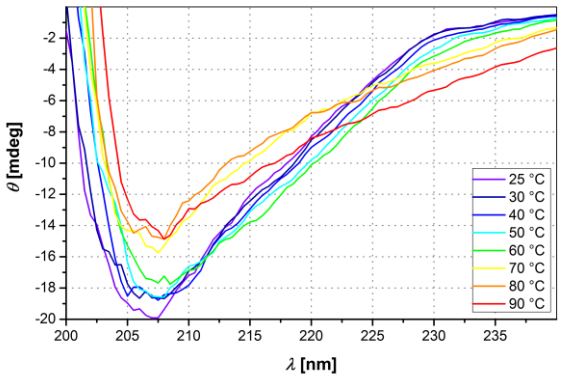

Figure 2.23 Far-UV CD spectrum of pepsin depending on the temperature. All spectra represent the average of 5 measurements.

The ellipticity of the minimum of the CD spectrum of pepsin slightly increased with increasing temperature. This shows that the content of secondary structure in pepsin decreased with increasing temperature. Whereas there was only a small change of the CD spectrum between 25 and 60 °C and between 70 and 90 °C, there was a larger change between 60 and 70 °C. This means that the secondary structure of pepsin is relatively stable up to 60 °C. Pepsin aggregates in the form of white flakes were observed after heating to 90 °C. Hence, the polymerization during the imprinting process shall preferably be carried out below 60 °C and in any case below 90 °C.

The influence of different pH values and a citrate buffer solution (CB) on the far- and near-UV CD spectrum of pepsin is shown in Figure 2.24.

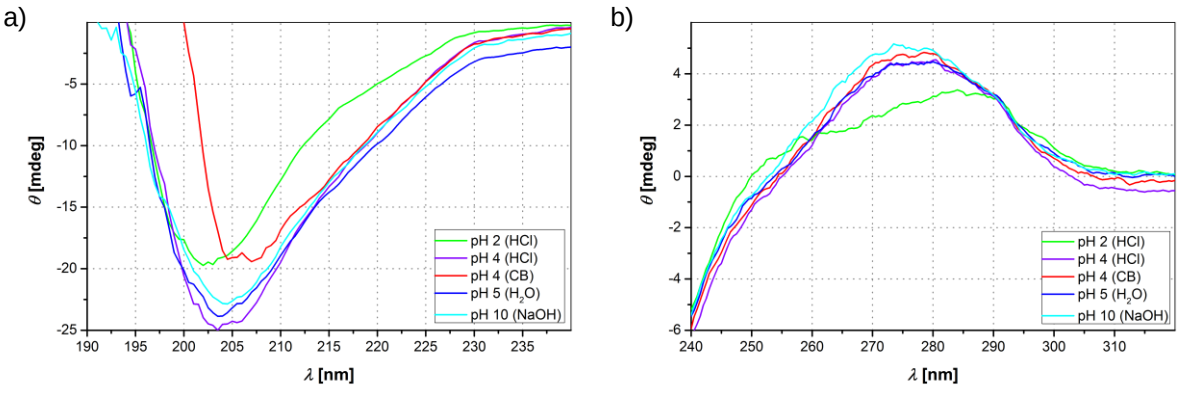

Figure 2.24 Far-UV (a) and near-UV (b) CD spectra of pepsin dissolved in pure water (H_2O, pH 5), water containing hydrochloric acid (HCl, pH 2 and 4) and sodium hydroxide (NaOH, pH 10) and in a citrate buffer solution (CB, pH 4). All spectra represent the average of 5 measurements.

The far-UV CD spectra of the pepsin solutions in water with the pH values of 4, 6 and 10 had the same shape. The ellipticity of the minima of the curves slightly increased with increasing pH value. This was also observed for the far-UV CD spectra. Hence, there was no significant change of the

pepsin conformation between the pH values of 4, 6 and 10. The far-UV CD spectrum of the pepsin solution with a pH value of 2 was shifted towards shorter wavelengths, whereas the spectrum of pepsin in the citrate buffer solution (pH 4) was shifted towards longer wavelengths. The ellipticity of the minima of these spectra was higher compared to the ellipticity of the minima of the other spectra. This means that pepsin had a different secondary structure in these solutions. Whereas the near-UV CD spectrum of pepsin in the citrate buffer solution was comparable with the near-UV CD spectra of the other solutions, the spectrum of the pepsin solution of a pH value of 2 had a lower maximum. This means that pepsin had a slightly different tertiary structure at pH 2. Hence, it may be favorable to perform the rebinding in the same solution, which is used during the imprinting process.

The influence of the incubation time, exposure to ultrasound and UV light on the far- and near-UV CD spectrum of pepsin is shown in Figure 2.25.

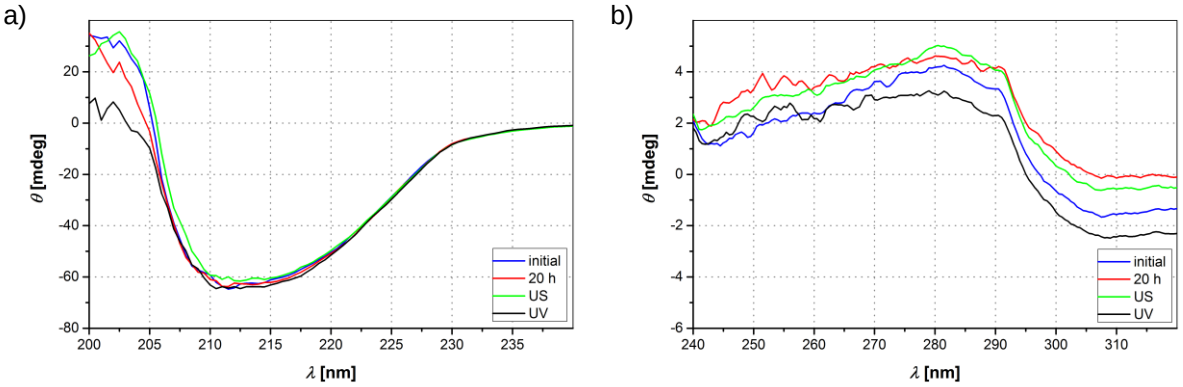

Figure 2.25 Far-UV (a) and near-UV (b) CD spectra of pepsin before (initial) and after 20 h of incubation, exposure to ultrasound (US) and UV light. All spectra represent the average of 5 measurements.

The far-UV CD spectra of pepsin before and after 20 h of incubation, exposure to ultrasound and UV light were comparable. This shows that these conditions did not cause a change of the secondary structure of pepsin. The near-UV spectrum of pepsin was only slightly affected by these conditions. This means that there is no significant change of the environment of the aromatic amino acid residues and disulfide bonds in the tertiary structure of pepsin. Hence, ultrasound may be used and UV light may be applied during 20 h. The same result was obtained after exposure of ultrasound to an RNase A solution, whereas the exposure of UV light caused a change of the RNase A conformation.[119]

The influence of the negatively charged sodium dodecyl sulfate (SDS), positively charged cetyltrimethylammonium bromide (CTAB) and non-ionic surfactant Lutensol AT 50 on the far- and near-UV CD spectrum of pepsin is shown in Figure 2.26. The amount of each surfactant was as high as required to prepare a miniemulsion polymerization.

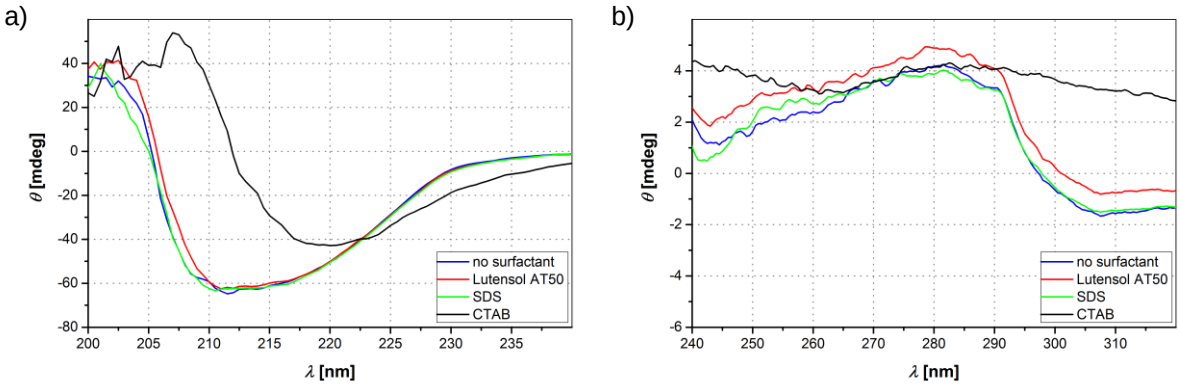

Figure 2.26 Far-UV (a) and near-UV (b) CD spectra of pepsin with and without the addition of sodium dodecyl sulfate (SDS), cetyltrimethylammonium bromide (CTAB) and Lutensol AT 50. All spectra represent the average of 5 measurements.

The addition of SDS and Lutensol AT 50 did not affect the conformation of pepsin, as the CD spectra of pepsin after the addition of SDS and Lutensol AT 50 were comparable with the CD spectra of the pure pepsin solution. Only a slight difference was observed between the near-UV CD spectrum of the pepsin solution with and without Lutensol AT 50. SDS did not interact with pepsin due to charge repulsion. Lutensol AT 50 had a low tendency to interact with pepsin, since it has no charge. This is comparable to other reports.[208] The addition of CTAB caused a strong shift of the minimum of the far-UV CD spectrum of pepsin towards longer wavelengths and higher ellipticity and a change of the near-UV CD spectrum. This indicates an interaction between pepsin and CTAB, since both have opposite charges and hydrophobic groups. This is similar to the results obtained with RNase A and SDS[120] and correlates with a study, which shows that CTAB adsorbs on pepsin at low CTAB concentrations and induces unfolding of pepsin at higher CTAB concentrations.[211] Hence, Lutensol AT 50 and SDS are suitable for the stabilization of the miniemulsion polymerization without significantly changing the conformation of pepsin.

2.6.2 Synthesis and imprinting strategy

The synthesis strategy for the preparation of pepsin surface imprinted polymer particles via miniemulsion polymerization is schematically shown in Figure 2.27. It was adapted from D. Vaihinger et al[105] and modified with regard of using pepsin as template molecule. The hydrophobic phase consists of the cross-linker, a functional monomer, an oil-soluble initiator and a hydrophobic agent. Pepsin is dissolved in the continuous water phase containing the surfactant. The two phases are mixed and a miniemulsion is prepared by the application of ultrasound. Pepsin is anticipated to interact with the functional monomer and thus to adsorb at the surface of the monomer droplets. The radical polymerization is carried out at room temperature after photochemical initiation to avoid structural changes of pepsin as a result of high temperatures (compare chapter 2.6.1). Small surface imprinted polymer particles shall be obtained with pepsin adsorbed on their surface.

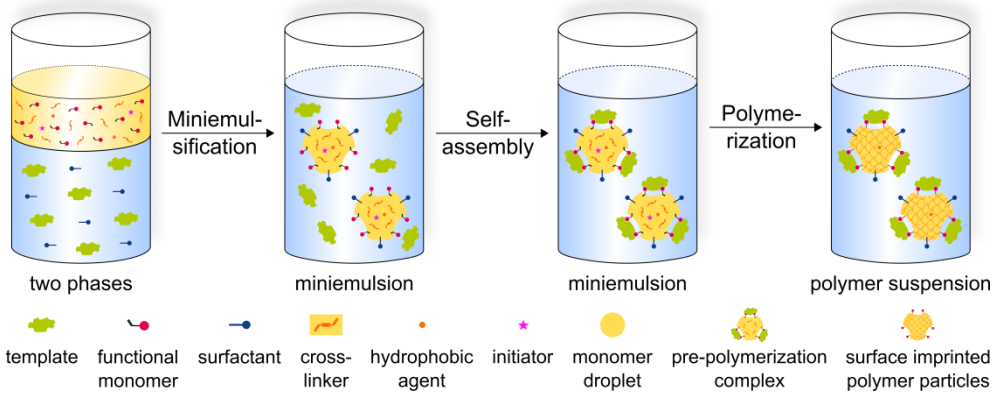

Figure 2.27 Scheme of the pepsin surface imprinting strategy via miniemulsion polymerization.

Water is used as continuous phase for the dissolution of pepsin. Buffer salts are not added to avoid interferences of the salts with the pre-polymerization complex. Hexadecane (HD) is used to prevent Ostwald ripening as typical hydrophobic agent[41,42]. The non-ionic surfactant Lutensol AT 50 is used to sterically stabilize the miniemulsion against coalescence[185], since it does not significantly change the conformation of pepsin (see chapter 2.6.1) and interfere with charged monomers. Different types of functional monomers are used and other parameters are varied to investigate their influence on the imprinting efficiency. These are explained in more detail in the following subchapters. Ethylene glycol dimethacrylate (EGDMA) is used as cross-linker, since it is widely used for the preparation of MIPs[35] and can be dispersed in water[105,119].

Figure 2.28 shows the chemical structures of all functional monomers and the cross-linker used for the imprinting of pepsin.

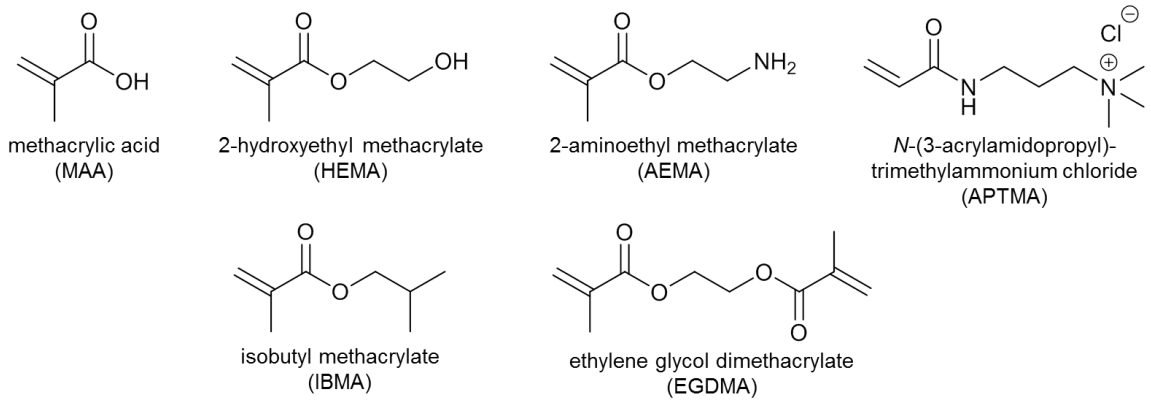

Figure 2.28 Chemical structures of the different types of functional monomers and the cross-linker for imprinting pepsin.

While isobutyl methacrylate (IBMA) is hydrophobic and methacrylic acid (MAA) and 2-hydroxyethyl methacrylate (HEMA) are little water-soluble and mix well with EGDMA, 2-aminoethyl methacrylate (AEMA) and *N*-(3-acrylamidopropyl)trimethylammonium chloride (APTMA) are water-soluble and have to be dissolved in the continuous water phase. An oil-soluble radical initiator is used to initiate the polymerization in the monomer droplets and thus to hinder the diffusion of little water-soluble monomers in the continuous water phase and to enable the copolymerization of a water-soluble monomer at the droplet surface after diffusion from the water phase to the droplet surface.[43–45]

The use of a water-soluble functional monomer can affect the way the pre-polymerization complex is formed. Whereas the pre-polymerization complex between pepsin and a not or little water-soluble functional monomer is most likely formed at the droplet surface, the pre-polymerization complex between pepsin and a water-soluble functional monomer is rather formed in the water phase (Figure 2.29). This complex may be adsorbed on the droplet surface, depending on whether there is an interaction between pepsin and the monomer droplet. This was investigated in experiments using surface tension measurements. The obtained results are described in the following chapter 2.6.3.

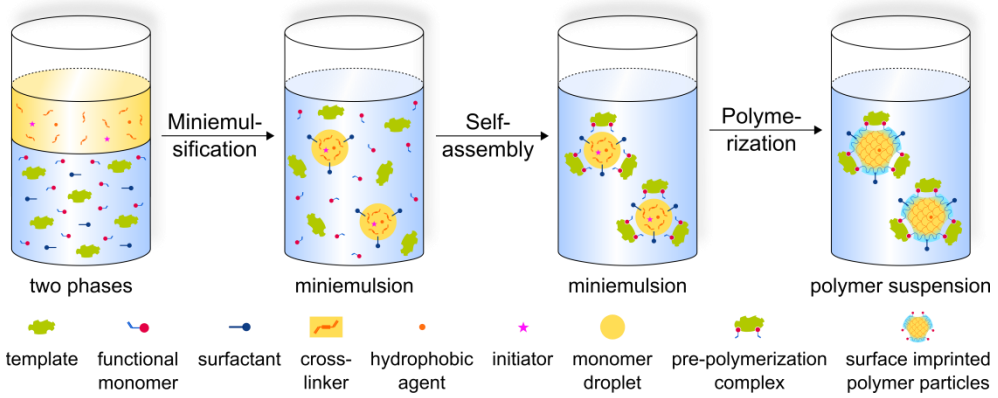

Figure 2.29 Scheme of the pepsin surface imprinting strategy with a water-soluble functional monomer via miniemulsion polymerization.

2.6.2.1 Different functional monomers

The monomers MAA, HEMA, AEMA and APTMA provide a variety of functional groups and may thus form different types of interactions with pepsin.[213] There is almost the same number of the protonated and deprotonated form of MAA (pK_a = 4.66[214]) in water (pH 5), which is used as incubation medium for rebinding pepsin. The protonated form may interact with hydroxyl and carboxyl groups of pepsin by hydrogen bonds, whereas the negatively charged deprotonated form of MAA may rather form repulsive ionic interactions with carboxylate groups of pepsin than attractive ionic interactions with basic amino acid residues of pepsin, since there are much more acidic than basic amino acid residues in pepsin. HEMA can interact with hydroxyl groups of leucine, isoleucine and valine residues of pepsin by hydrogen bonds. The equilibrium of AEMA (pK_a = 8.5[45]) in water (pH 5) is more shifted towards the protonated form, which can form attractive ionic interactions and a hydrogen bond with carboxylate groups of the acidic amino acid residues of pepsin. APTMA contains a positively charged quaternary ammonium group and 3 methyl groups and can thus interact with pepsin by ionic and hydrophobic interactions. All functional monomers can additionally form hydrogen bonds and hydrophobic interactions. A molar ratio between each functional monomer and the cross-linker of 1 : 4 is used, since this ratio is often used for molecular imprinting[35,105]. The molar ratio between the functional monomer and pepsin is around 860 : 1.

2.6.2.2 Different other parameters

After screening different functional monomers the influence of the double amount of pepsin template on the imprinting efficiency is investigated. The maximum amount of soluble pepsin (10 mg mL^{-1}) is therefore used during imprinting. Hence, the molar ratio between the functional monomer and pepsin is 430 : 1. After optimizing the pepsin template concentration the influence of the pH value on the imprinting efficiency is investigated. A citrate buffer solution with a pH value of 4 is used as continuous phase instead of pure water, since pepsin is stable[23] and adopts a native-like, but catalytically inactive conformation[215] there. A phosphate buffer solution with a pH value of 7 is used with regard to a selectivity study with other proteins and the application as scavenger material, since this is close to physiological conditions[6], where most of the proteins are stable, even if pepsin is less stable there[23]. Furthermore, the presence of the surfactant, a second functional monomer and the content of APTMA on the imprinting efficiency is investigated. A polymer is prepared in absence of the surfactant in order to offer more space for the adsorption of pepsin on the monomer droplet surface. IBMA (Figure 2.28) is used as second functional monomer in a molar ratio of 1 : 1 to APTMA. IBMA can be dispersed in the water phase together with EGDMA and thus improve the adsorption of pepsin on the droplet surface by hydrophobic interactions prior to the polymerization. A monomer with an isobutyl group is chosen, because pepsin has a high number of

amino acid residues with aliphatic C4 and C3 residues. Furthermore, the inhibitor pepstatin has several isobutyl groups, which contribute to the selective binding between pepsin and pepstatin[26] and are thought to be responsible for the inhibition of pepsin[8]. The amount of APTMA is decreased to one tenth of the prior amount, so that the total number of carboxyl groups of the pepsin molecules is equal to the number of quaternary ammonium groups of all APTMA molecules. The amount of EGDMA remains the same. The molar ratio between APTMA and EGDMA consequently is 1 : 40 and the maximum solid content decreases from 12 to 11 wt.-%. The molar ratio between APTMA and pepsin is 43 : 1.

2.6.3 Surface tension measurements

Surface and interfacial tension measurements were carried out with a du Noüy ring tensiometer. Solutions with and without pepsin were used in order to find out, whether pepsin is surface-active and adsorbs on the surface of droplets containing the cross-linker EGDMA or the hydrophobic monomer IBMA from a solution with or without the water-soluble functional monomer APTMA for surface imprinting via miniemulsion polymerization. The results are summarized in Table 2.1.

Table 2.1 Surface and interfacial tension (σ) between two different phases with (+) and without (-) pepsin. The numbers represent the average and standard deviation of at least 20 pull- and push-cycles.

pepsin	phase 1	phase 2	σ [mN m^{-1}]
-	water	air	72.4 ± 0.0
+			60.9 ± 0.2
-	water	EGDMA	14.1 ± 0.0
+			13.0 ± 0.1
-	water + APTMA	EGDMA	15.4 ± 0.0
+			12.1 ± 0.4
-	water	IBMA	22.2 ± 0.0
+			17.2 ± 0.2

The surface tension of water was reduced by 12 mN m^{-1} after the addition of pepsin, while it was reduced by 34 mN m^{-1} after the addition of the surfactant CTAB. This means that pepsin was only slightly surface-active. This is comparable to the results reported in the literature[211]. The interfacial tension between water and EGDMA was reduced by 1 mN m^{-1} after the addition of pepsin to the water phase, whereas this was reduced by 8 mN m^{-1} after the addition of the surfactant Lutensol AT 50. A slightly higher decrease of 3 mN m^{-1} was observed, when the positively charged monomer APTMA was added to the water phase. APTMA supported maybe to bring pepsin to the interface, as it is reported for CTAB[211], since the functional group of APTMA is structurally similar to the head group of CTAB. The interfacial tension between water and IBMA was decreased by 5 mN m^{-1} after the addition of pepsin to the water phase. This may be explained by a higher interaction between pepsin and the hydrophobic monomer or the fact that the initial interfacial tension between water and IBMA was higher than between water and EGDMA and could thus be reduced more. Hence, pepsin had a low tendency to adsorb on the interface between water and EGDMA or IBMA. The low decrease of the interfacial tension may be a result of the already low interfacial tension between water and EGDMA or IBMA. The addition of APTMA may support to bring pepsin to the interface for surface imprinting. These results suggest, but cannot clearly proof that pepsin and its pre-polymerization complex with a water-soluble functional monomer may adsorb on the droplet surface for surface imprinting.

2.6.4 Properties of the polymer particles after polymerization

The appearance and properties of the resulting polymer particles prepared by miniemulsion polymerization under different conditions were investigated. The conversion of the polymerizations was determined by gravimetric analysis. The average hydrodynamic particle diameter and the polydispersity index (PDI) were determined by dynamic light scattering (DLS). The zeta potential was determined by laser Doppler electrophoresis. The influence of the different conditions on these properties is discussed in the following.

2.6.4.1 Different functional monomers

Stable polymer suspensions without any coagulum were obtained after the polymerization with different functional monomers and in the presence and absence of pepsin (Figure 2.30).

Figure 2.30 Picture of an exemplary polymer suspension obtained by miniemulsion polymerization.

The conversion of the polymerization, the average hydrodynamic particle diameter and PDI depending on the type of functional monomer and presence of pepsin during the polymerization are summarized in Table 2.2. The conversion of the different polymerizations was around 90% and thus almost complete.[213] Hence, all different types of functional monomer were polymerized.

Table 2.2 Conversion (*X*), average hydrodynamic particle diameter (d_{DLS}) and polydispersity index (*PDI*) depending on the type of functional monomer.

Type of polymer		*X* [%]	d_{DLS} [nm]	*PDI* [-]
MIP 1	MAA	94	193 ± 1	0.18 ± 0.03
NIP 1		98	192 ± 4	0.15 ± 0.02
MIP 2	HEMA	89	205 ± 2	0.18 ± 0.03
NIP 2		88	195 ± 5	0.16 ± 0.01
MIP 3	AEMA	84	202 ± 2	0.15 ± 0.01
NIP 3		87	192 ± 8	0.14 ± 0.02
MIP 4	APTMA	85	209 ± 2	0.18 ± 0.02
NIP 4		87	214 ± 4	0.18 ± 0.02

Since the polymerization was started in the monomer droplets due to the use of an oil-soluble initiator, it is more likely that MAA and HEMA were copolymerized in the monomer droplets and that AEMA and APTMA were copolymerized on the surface of the droplets containing the cross-linker than in the water phase. Secondary nucleation followed by homo-polymerization of little or

water-soluble monomers in the aqueous phase was not obtained by similar polymerization systems.[45,105]

The polymer suspensions contained small polymer particles with an average hydrodynamic diameter of approximately 200 nm independent of the type of functional monomer and the presence of pepsin. This size is in the usual range for a miniemulsion polymerization[41]. The particle size distributions of the suspensions were rather broad indicated by the PDI values around 0.16. This was in accordance with transmission electron microscope images, which showed particles of differing diameters between 50 and 600 nm. This may be a result of the usage of a large amount of cross-linker, a non-ionic surfactant and an at least slightly water-soluble monomer. The here obtained particle properties are comparable with the ones obtained by D. Vaihinger et al[105].

2.6.4.2 Different other parameters

Stable polymer suspensions without any coagulum were obtained after the polymerization with the double amount of pepsin template, in the citrate buffer solution (CB) with a pH value of 4, in the phosphate buffer solution (PB) with a pH value of 7, with IBMA as second monomer and a lower APTMA content. The polymer suspension prepared in the PB solution and in the presence of pepsin was light red instead of white. After centrifugation it was clearly observed that the red color came from the solution and not from the polymer particles. The red color may come from unfolded pepsin, but this was not further investigated. The polymerization in absence of the surfactant yielded only in the presence of pepsin in a polymer suspension. A bulk polymer was obtained in the absence of pepsin (Figure 2.31).

Figure 2.31 Picture of MIP 7 (left) and NIP 7 (right) after the polymerization without surfactant.

This means that pepsin acted as surfactant and stabilized the miniemulsion. This observation incidentally shows that pepsin adsorbed on the EGDMA containing droplets prior to the polymerization and that a pre-polymerization complex between pepsin and APTMA may be formed at the droplet surface. The presence of APTMA may also have helped to bring pepsin to the surface, since its functional group is structurally similar to the head group of CTAB, which can bring pepsin to a surface after adsorbing to it and thus increasing the hydrophobicity of the obtained complex[211]. This supports the results described in chapter 2.6.3.

The conversion of the polymerization, average hydrodynamic particle diameter, PDI and zeta potential depending on the polymerization conditions are summarized in Table 2.3. The conversion of the different polymerizations was around 90%, thus almost complete and comparable with the conversions of the previous polymerizations (Table 2.2). This indicates that APTMA and IBMA were copolymerized with the cross-linker.

Table 2.3 Conversion (*X*), average hydrodynamic particle diameter (d_{DLS}), polydispersity index (*PDI*) and zeta potential (ζ) depending on the polymerization conditions.

Type of polymer		*X* [%]	d_{DLS} [nm]	*PDI* [-]	ζ [mV]
MIP 5	1 APTMA	90	707 ± 18	0.25 ± 0.01	56 ± 1
NIP 5		95	344 ± 4	0.19 ± 0.03	59 ± 1
MIP 6	CB, pH 4	93	445 ± 3	0.27 ± 0.01	50 ± 1
NIP 6		94	422 ± 2	0.26 ± 0.04	43 ± 0
MIP 7	PB, pH 7	87	2321± 242	0.50 ± 0.44	-12± 1
NIP 7		95	293 ± 3	0.21 ± 0.01	41 ± 1
MIP 8	w/o surf	95	4365± 292	0.41 ± 0.51	38 ± 1
MIP 9	0.5 IBMA	92	340 ± 5	0.32 ± 0.03	30 ± 0
NIP 9		97	260 ± 1	0.22 ± 0.01	46 ± 1
MIP 10	0.1 APTMA	101	241 ± 2	0.25 ± 0.01	-11± 0
NIP 10		97	239 ± 8	0.20 ± 0.02	25 ± 1

The average hydrodynamic diameters of most polymer particles were between 230 and 445 nm and thus slightly higher than the diameters of the previous polymer particles. The particles of MIP 5 with a diameter of approximately 700 nm were significantly larger than the particles of the corresponding NIP as well as of MIP 4 (Table 2.2), which was prepared in the same way, but with half the amount of pepsin. This indicates that the presence of more pepsin affected the polymerization reaction and the resulting particle diameter. However, the particles of NIP 5 were in average slightly larger than the particles of NIP 4 indicating that the average hydrodynamic particle diameter could not be perfectly reproduced. The average particle diameters of MIP 7 and 8 were very large ($d_{DLS} > 2$ µm). This may be a result of a complex formation in the case of MIP 7 and the lower stabilization of the miniemulsion by pepsin without surfactant in the case of MIP 8. Since NIP 8 was a bulk polymer, it was not further analyzed. The diameters of the other MIPs and NIPs were comparable, although they were also prepared in the presence of the double amount of pepsin. This can be attributed to the lower amount of APTMA resulting in fewer interactions with pepsin and the citrate buffer solution, in which pepsin is more stable. The PDI values of most polymer suspensions were between 0.19 and 0.32 indicating that their particle size distributions were slightly broader than of the previous polymer particles (Table 2.2). The PDI values of MIP 7 and 8 were higher ($PDI > 0.4$) due to the existence of larger particles.

The zeta potentials of most polymer particles were between 25 and 60 mV due to positively charged functional groups of APTMA units on the particle surfaces. MIP 7 had a negative zeta potential and was not further investigated due to all its differing properties. MIP 9 and MIP and NIP 10 had lower zeta potentials than the other polymer particles due to the lower content of APTMA in the monomer mixture. This was not valid for NIP 9, which had a higher zeta potential. The zeta potentials of MIP and NIP 5 were similar, while the zeta potential of MIP 6 was higher than of NIP 6. The zeta potentials of MIP 9 and 10 were significantly lower than of their corresponding NIPs. This may have resulted from negatively charged pepsin molecules adsorbed on their particle surfaces.

2.6.5 Washing of the polymer particles and extraction of pepsin

The polymer particles were washed by repeated centrifugation/resuspension cycles in order to remove residual monomer, cross-linker, the hydrophobic agent and surfactant and to extract pepsin. The smaller particles did not sediment during centrifugation and were therefore discarded with the supernatant. The extraction agent was added and removed to shift the adsorption equilibrium of pepsin between the polymer and the solution towards the solution. The type of extraction agent is described in the following subchapters. The removal was controlled by measuring absorbance spectra in the wavelength range from 200 to 360 nm between the different washing steps. The UV spectra of the MIPs showed higher absorbance values than the spectra of the NIPs due to the presence of pepsin. The washing procedure was carried out until the absorbance values between 180 and 360 nm were significantly reduced and no absorbance at 277 nm, where the second absorption maximum of pepsin was, was detected anymore. All components including pepsin absorbed UV light between 180 and 340 nm. Hence, their spectra overlaid and it was not possible to determine the exact amount of extracted pepsin. But the qualitative monitoring of the removal ensured that most of pepsin was extracted.

2.6.5.1 Different functional monomers

Water and ethanol were used as extraction agents for washing the polymer particles prepared with different functional monomers.

2.6.5.2 Different other parameters

Water was used as the only extraction agent for washing the polymer particles, since the use of a second extraction solvent was very time-consuming and water was sufficient.

2.6.5.3 Different extraction solutions

A half of the suspension of MIP and NIP 5, respectively, was washed with water and the other half with hydrochloric acid (HCl). Pepsin is positively charged in 0.1 M HCl (pH 1). It was anticipated that it is therefore repelled of the positively charged polymer. The addition of a high concentrated HCl can additionally result in an autocatalytic self-cleavage of pepsin.[216] A third of the MIP and NIP 10 suspension, respectively, was washed with water, another third with a concentrated sodium hydroxide solution (NaOH) and the last third with a 1 M sodium chloride (NaCl) solution. The addition of NaOH can denature pepsin.[24] Sodium chloride ions can weaken the ionic interactions between pepsin and the positively charged polymer and thus displace pepsin from the polymer. The extraction solutions were subsequently replaced by pure water for rebinding pepsin.

2.6.6 Properties of the polymer particles after extraction

The properties of the polymer particles were analyzed after the washing procedure again. The average hydrodynamic particle diameter and PDI were determined by DLS and the zeta potential by laser Doppler electrophoresis as previously. Additionally, the morphology and particle size distribution of the polymer particles were investigated with TEM (transmission electron microscope) and SEM (scanning electron microscope) images. Furthermore, the average particle diameter and particle size distribution were determined from TEM images by measuring the diameter of 1000 particles using the program ImageJ. The specific surface area of the polymer particles were determined by BET nitrogen analysis. The influence of the washing procedure on these properties and the differences in these properties between the different MIPs and NIPs are discussed in the following.

2.6.6.1 Different functional monomers

The average hydrodynamic diameters from DLS and average diameters from TEM images, PDIs, zeta potentials and specific surface areas of the polymer particles prepared from different functional monomers after the extraction are summarized in Table 2.4. The negative zeta potentials of MIP and NIP 1 and the positive zeta potentials of MIP and NIP 3 and 4 show that there were negatively and positively charged functional groups on the particle surfaces due to the polymerization of MAA, AEMA and APTMA.[213] However, there is no suitable explanation for the negative zeta potentials of MIP and NIP 2 prepared with HEMA.

Table 2.4 Average hydrodynamic diameters (d_{DLS}), average diameters (d_{TEM}), polydispersity indices (*PDI*), zeta potentials (ζ) and specific surface areas (A_s) of the polymer particles prepared from different functional monomers after extraction.

Type of polymer		d_{DLS} [nm]	d_{TEM} [nm]	*PDI* [-]	ζ [mV]	A_s [$m^2 g^{-1}$]
MIP 1	MAA	224 ± 5	159 ± 16	0.19 ± 0.03	-73 ± 2	37 ± 7
NIP 1		246 ± 9	156 ± 16	0.26 ± 0.05	-74 ± 1	26 ± 4
MIP 2	HEMA	269 ± 9	155 ± 16	0.21 ± 0.03	-32 ± 1	39 ± 3
NIP 2		273 ± 19	141 ± 14	0.19 ± 0.02	-35 ± 1	29 ± 7
MIP 3	AEMA	450 ± 23	235 ± 24	0.35 ± 0.06	29 ± 1	41 ± 2
NIP 3		429 ± 40	229 ± 23	0.29 ± 0.09	25 ± 1	42 ± 0
MIP 4	APTMA	464 ± 123	176 ± 18	0.34 ± 0.09	23 ± 1	34*
NIP 4		448 ± 113	202 ± 20	0.30 ± 0.09	12 ± 0	33*

* Only one value was determined due to lack of polymer.

The average hydrodynamic particle diameters of MIP and NIP 1 and 2 slightly increased to around 250 nm after the extraction process. The average diameters of the positively charged polymers MIP and NIP 3 and 4 increased to more than double ($d_{DLS} > 400$ nm).[213] The PDI values of all

polymers also increased and were between 0.19 and 0.35. Aggregation and loss of small particles during centrifugation and incomplete resuspension during the extraction process affected the particle size and size distribution. The particle sizes of MIP and NIP 1 and 2 were still quite similar and there was only a small difference in the particle size between MIP and NIP 3 and 4. This is illustrated in the graph of Figure 2.32 a). The green bars represent the MIPs and the orange bars represent the corresponding NIPs. This assignment of the bar colors is maintained for all following diagrams.

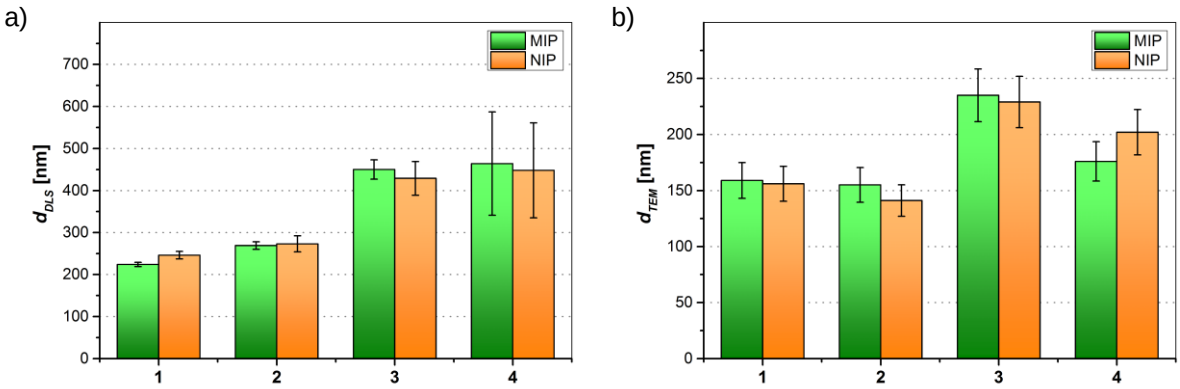

Figure 2.32 Average diameters (*d*) of the polymer particles prepared from different functional monomers obtained from DLS (a) and TEM (b) after extraction.

The graph of Figure 2.32 b) shows the average particle diameters from TEM images, which were between 140 and 235 nm. These followed a similar trend, except that the average particle diameter of MIP 4 was slightly smaller, and were generally smaller than the ones obtained by DLS. This is due to the fact that the average particle diameter is determined in suspension by DLS and in the dry state by TEM. The polymer particles are solvated and swollen in water and thus appear larger.[193] Several other reasons may therefore be that larger particles or aggregated particles scatter more light than smaller ones and thus have a higher contribution to the average hydrodynamic diameter[191], that the values from DLS contained errors, since the particle size distributions were not narrow and that it may be difficult to distinguish, if particles are aggregated on TEM images.

The TEM images in Figure 2.33 show round particles with diameters between approximately 50 and 600 nm. These properties are similar to those obtained by D. Vaihinger et al[105].

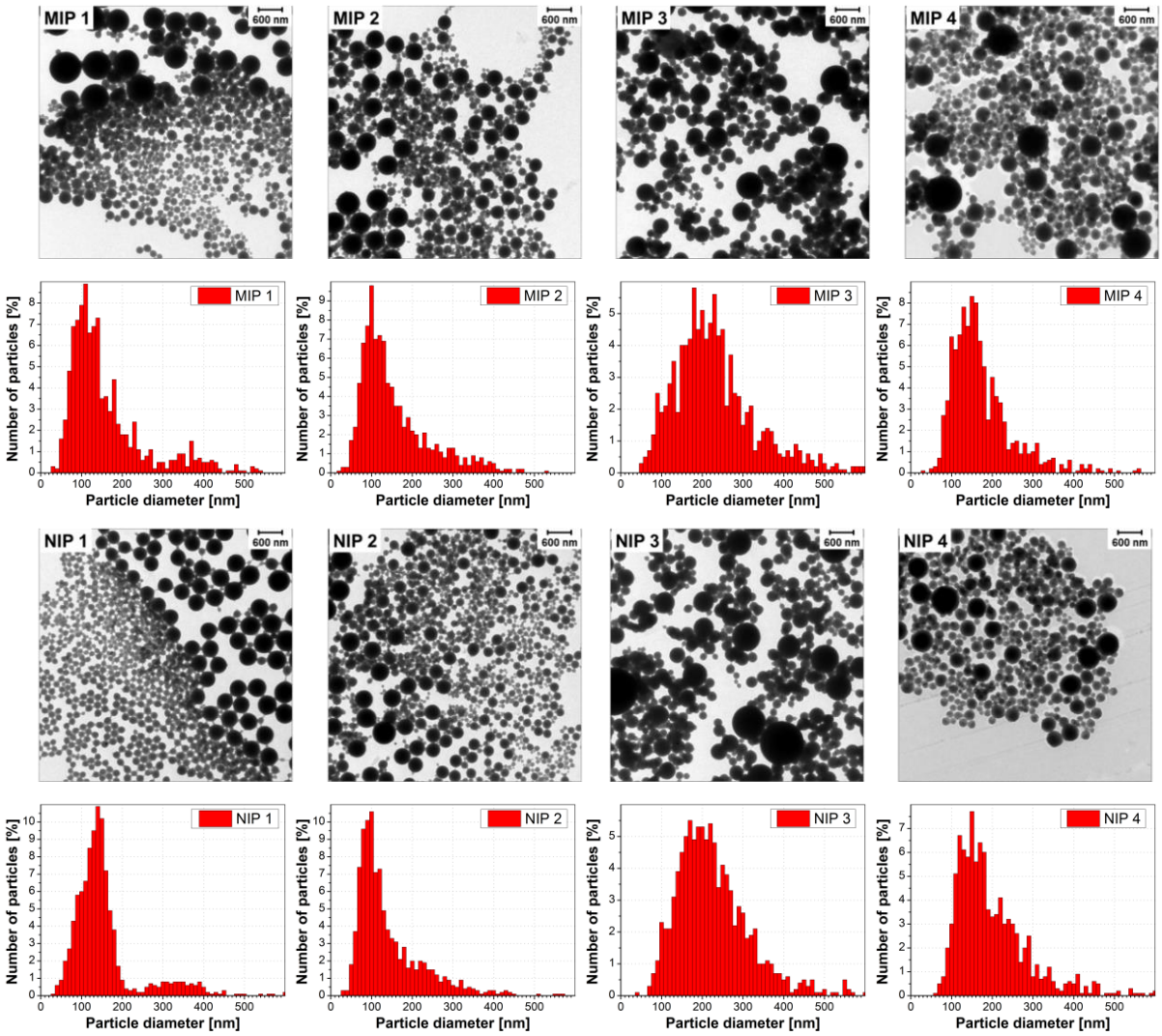

Figure 2.33 TEM images (magnification: 4000 x) and particle size distributions of the polymer particles prepared from different functional monomers after extraction.

For a better overview and comparison of the different particle size distributions the maximum of the x-axis (particle diameter) was 600 nm, even if there were sporadic particles larger than 600 nm. The corresponding particle size distributions were comparatively broad as already indicated by the PDI values and usually monomodal. Only MIP and NIP 1 had bimodal size distributions. A bimodal distribution was also obtained with a similar monomer system and Lutensol AT 50 by miniemulsion polymerization.[45] The distributions of the positively charged polymers were shifted towards larger sizes compared with the distributions of other polymers.

The SEM images in Figure 2.34 show that the polymer particles had a rough surface. The roughness of the surface was rather a result of the use of a large amount of cross-linker than of the imprinting process, since also the NIPs had a rough surface. The large amount of cross-linker most likely made the polymer chains less flexible and limited their rearrangement into a smooth spherical shape.

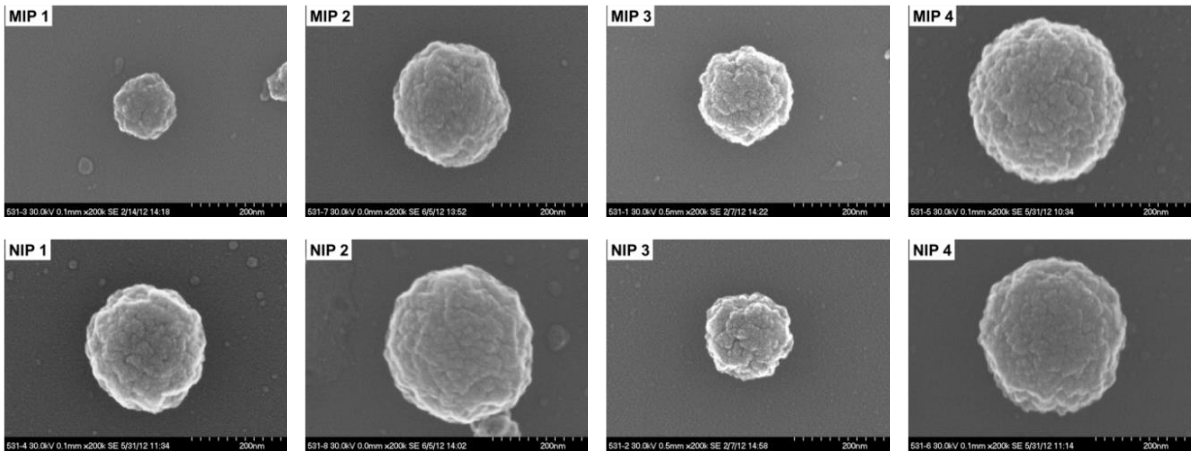

Figure 2.34 SEM images (magnification: 200000 x) of the polymer particles prepared from different functional monomers after extraction.

The curve progressions of the nitrogen adsorption isotherms of the polymer particles were comparable to the curve progression of a type 2 isotherm.[196] This and the SEM images suggest that the polymer particles were non-porous. The specific surface areas were between 26 and 42 $m^2 g^{-1}$ and are illustrated in Figure 2.35.

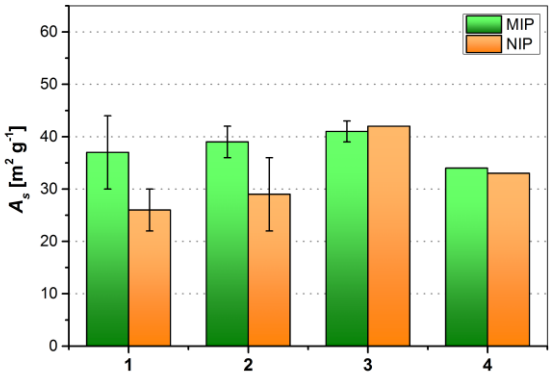

Figure 2.35 Specific surface areas (A_S) of the polymer particles prepared from different functional monomers obtained from BET nitrogen adsorption after extraction. The bars 1, 2 and 3 represent the average of two samples. The error bars show the spread. Bar 4 represents one sample due to lack of polymer.

The specific surface areas of MIP and NIP 1, 2 and 3 differ from the published values[213], since a second measurement was performed and taken into account. This could not be done with MIP and NIP 4 due to lack of polymer. All obtained specific surface areas are a bit smaller than the ones obtained by D. Vaihinger et al[105] due to the increase of the particle diameters after extraction. Whereas the specific surface areas of MIP and NIP 3 and 4 were comparable, the specific surface areas of MIP 1 and 2 were higher than those of their corresponding NIPs. This may be attributed to

the establishment of cavities on the surface of the MIPs as a result of the imprinting, because their particle diameters were similar. This has been reported a few times[105,119], but has not been clearly proven in literature so far. However, the spread and thus the uncertainty of the measurement were relatively high.

2.6.6.2 Different other parameters

The average hydrodynamic diameters and average diameters from TEM images, PDIs, zeta potentials and specific surface areas of the polymer particles prepared under different parameters after extraction are summarized in Table 2.5. The zeta potentials slightly changed after the extraction and were except for MIP and NIP 10 between 29 and 61 mV and thus in the same range as before extraction. The zeta potentials of MIP and NIP 10 were negative due to the low amount of APTMA in the monomer mixture. The zeta potentials of MIP and NIP 5 were higher than those obtained for MIP and NIP 4 due to the higher conversion. The increase of the zeta potentials of MIP 8 and 10 can be a hint for the extraction of pepsin. However, the zeta potential of NIP 6 also increased after extraction. There was no significant difference between the zeta potentials of the MIPs and NIPs except that NIP 9 had a higher zeta potential than MIP 9.

Table 2.5 Average hydrodynamic diameters (d_{DLS}), average diameters (d_{TEM}), polydispersity indices (*PDI*), zeta potentials (ζ) and specific surface areas (A_s) of the polymer particles prepared under different parameters after extraction.

Type of polymer		d_{DLS} [nm]	d_{TEM} [nm]	*PDI* [-]	ζ [mV]	A_s [$m^2 g^{-1}$]
MIP 5	1 APTMA	623 ± 27	192 ± 19	0.24 ± 0.16	43 ± 2	50 ± 12
NIP 5		466 ± 8	162 ± 16	0.22 ± 0.02	51 ± 2	43 ± 8
MIP 6	pH 4	413 ± 2	157 ± 16	0.22 ± 0.02	60 ± 1	30 ± 1
NIP 6		627 ± 16	175 ± 18	0.31 ± 0.06	61 ± 1	28 ± 2
MIP 8	w/o surf	713 ± 16	267 ± 27	0.36 ± 0.08	50 ± 1	36 ± 5
MIP 9	0.5 IBMA	257 ± 2	126 ± 13	0.25 ± 0.02	29 ± 0	33 ± 1
NIP 9		333 ± 2	131 ± 13	0.24 ± 0.01	45 ± 0	39 ± 0
MIP 10	0.1 APTMA	442 ± 52	184 ± 18	0.38 ± 0.16	-1 ± 0	38 ± 4
NIP 10		507 ± 18	189 ± 19	0.22 ± 0.01	-2 ± 0	39 ± 1

The average hydrodynamic particle diameters also changed and were between 250 and 720 nm after extraction. The average particle diameter of MIP 8 decreased from over 2000 nm to approximately 700 nm, but was still higher than the diameter of the other polymer particles. This decrease can be a result of the use of an ultrasonic bath, which may have resulted in the breakup of some aggregates, additionally to a shaker for the resuspension of the precipitate after centrifugation. The particle diameter of MIP 5 was larger than of NIP 5.[213] Vice versa, the particle diameter of MIP 6 was smaller than of MIP 6. The difference in the diameter between MIP and NIP 9 and 10 was small. This is illustrated in the graph of Figure 2.36 a). The PDI values of the polymer particles slightly changed and were between 0.22 and 0.38 after extraction indicating broader size distributions.

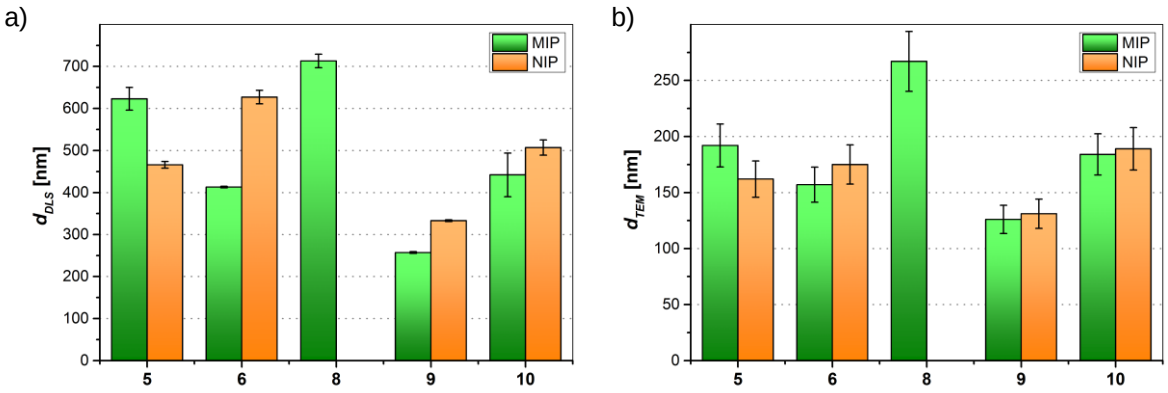

Figure 2.36 Average diameters (*d*) of the polymer particles prepared under different parameters obtained from DLS (a) and TEM (b) after extraction.

The graph of Figure 2.36 b) shows the average particle diameters from TEM images. These followed the same trend as the average diameters from DLS, but the difference between the MIPs and NIPs and the values were generally smaller. This is comparable with the results described in the previous chapter 2.6.6.1.

The TEM images in Figure 2.37 show that all polymer suspensions contained particles with a spherical shape and a relatively broad size distribution with diameters ranging from around 50 to 600 nm. This was comparable to the polymer suspensions described in the previous chapter 2.6.6.1.

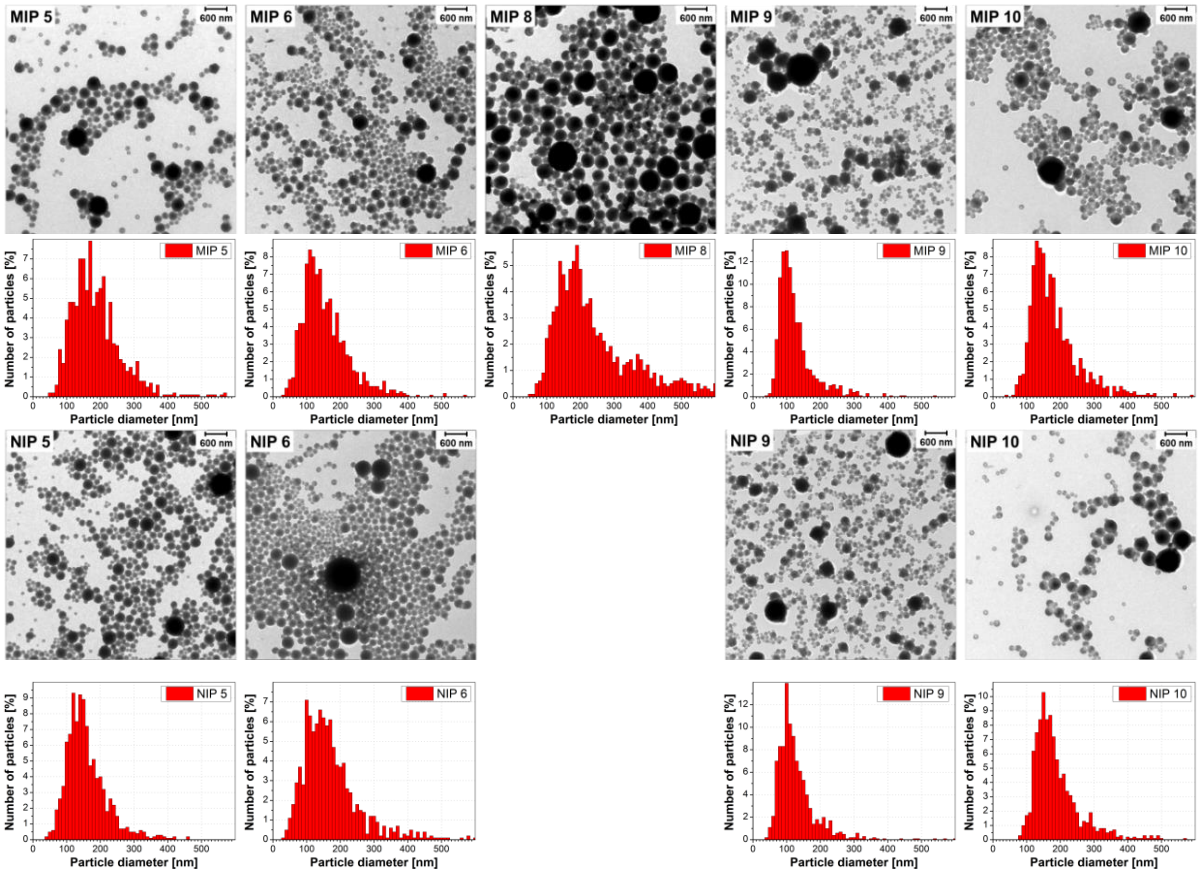

Figure 2.37 TEM images (magnification: 4000 x) and particle size distributions of the polymer particles prepared under different parameters after extraction.

The particle size distributions of MIP 5 and 6 were shifted towards larger diameters compared with their corresponding NIPs, whereas the particle size distributions of MIP and NIP 9 and 10 were comparable. The size distributions of NIP 6 and MIP and NIP 10 were shifted towards lower values. MIP 8 had a broader particle size distribution.

The TEM images recorded at a higher magnification in Figure 2.38 indicate that all polymer particles had a rough surface as the polymer particles described in chapter 2.6.6.1.

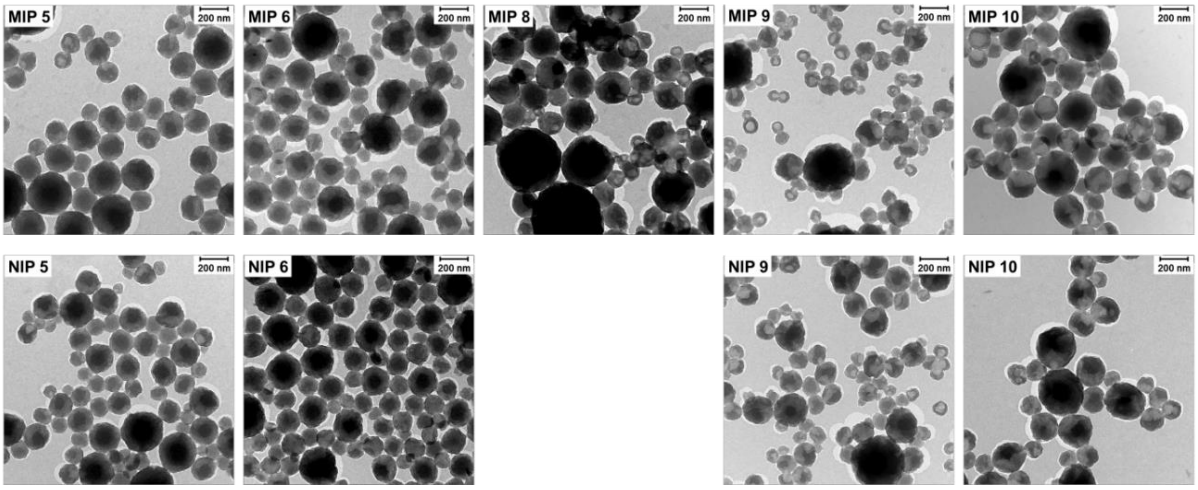

Figure 2.38 TEM images (magnification: 16000 x) of the polymer particles prepared under different parameters after extraction.

The nitrogen adsorption isotherms of the different polymer particles had the same curve progression as the isotherms of the polymer particles described in chapter 2.6.6.1. These were thus also rather non-porous. The specific surface areas were between 33 and 50 $m^2 g^{-1}$ (Figure 2.39) and thus slightly higher than the specific surface areas of the polymer particles in chapter 2.6.6.1.

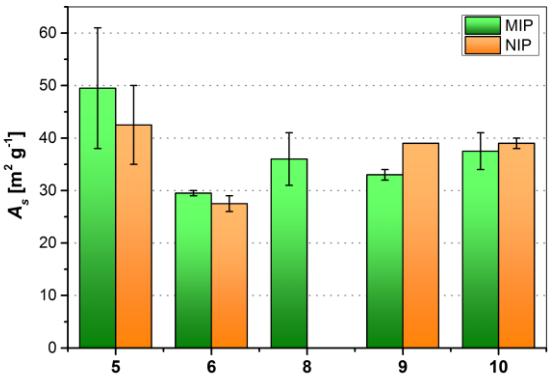

Figure 2.39 Specific surface areas (A_s) of the polymer particles prepared under different parameters obtained from BET nitrogen adsorption after extraction. All bars represent the average of two samples. The error bars show the spread.

Whereas the specific surface areas of MIP and NIP 6 and 10 were comparable, the specific surface area of MIP 9 was smaller than the specific surface area of NIP 9. In contrast to MIP and NIP 4, which had a similar specific surface area, the specific surface area of MIP 5 was higher than of NIP 5. This may be an indication of the creation of imprinted cavities, since the particle diameter of MIP 5 is also

larger than of NIP 5, what would result in a lower specific surface area. However, this can also be caused by a higher surface roughness and the uncertainty due to the relatively high spread.

2.6.6.3 Different extraction solutions

The average hydrodynamic diameters from DLS and average diameters from TEM images, PDIs, zeta potentials and specific surface areas of the particles of MIP and NIP 5 after extraction in water and HCl (MIP-NIP 11) and of MIP and NIP 10 after extraction in water, NaOH (MIP-NIP 12) and a NaCl solution (MIP-NIP 13) are summarized in Table 2.6. The zeta potentials of MIP and NIP 5 were higher after the extraction in HCl than in water. The zeta potentials of MIP and NIP 10 decreased to around -40 mV after washing with NaOH and became 11 mV after extraction with the NaCl solution. It seems that there were still hydroxide ions on the surface of MIP and NIP 12, although the suspensions were washed with water afterwards. The MIPs and corresponding NIPs had similar zeta potentials.

Table 2.6 Average hydrodynamic diameters (d_{DLS}), average diameters (d_{TEM}), polydispersity indices (*PDI*), zeta potentials (ζ) and specific surface areas (A_s) of the polymer particles washed with different extraction solutions.

Type of polymer		Extraction solution	d_{DLS} [nm]	d_{TEM} [nm]	*PDI* [-]	ζ [mV]	A_s [$m^2 g^{-1}$]
MIP 5	1 APTMA	H_2O	623 ± 27	192 ± 19	0.24 ± 0.16	43 ± 2	50 ± 12
NIP 5			466 ± 8	162 ± 16	0.22 ± 0.02	51 ± 2	43 ± 8
MIP 11		HCl	428 ± 9	138 ± 14	0.24 ± 0.02	53 ± 1	41 ± 4
NIP 11			383 ± 5	139 ± 14	0.26 ± 0.04	58 ± 1	43 ± 4
MIP 10	0.1 APTMA	H_2O	442 ± 52	184 ± 18	0.38 ± 0.16	-1 ± 0	38 ± 4
NIP 10			507 ± 18	189 ± 19	0.22 ± 0.01	-2 ± 0	39 ± 1
MIP 12		NaOH	260 ± 6	184 ± 18	0.24 ± 0.02	-43 ± 1	39 ± 2
NIP 12			258 ± 4	183 ± 18	0.19 ± 0.02	-41 ± 1	47 ± 7
MIP 13		NaCl	1305 ± 223	182 ± 18	0.24 ± 0.03	11 ± 0	37 ± 3
NIP 13			298 ± 9	165 ± 17	0.20 ± 0.02	11 ± 0	40 ± 8

The polymer particles of the same origin had different average hydrodynamic diameters after the extraction in different solutions, although the centrifugation and resuspension steps were the same. Hence, the compatibility between the polymer and the solution had an effect on the particle size. The average hydrodynamic diameters of all polymer particles except MIP 13 were between 250 and 625 nm after extraction. This was in the range of the polymer particles described in the previous chapters. MIP 13 had an average hydrodynamic particle diameter of over 1000 nm. The corresponding NIP had an average diameter of only approximately 300 nm, although these were treated in the same way during the extraction procedure. The NaCl solution seems to have caused particle aggregation with pepsin, which could have been unfolded due to the high salt content. MIP and NIP 12 had similar particle diameters and were smaller than the other polymer particles. The difference in the particle size between MIP and NIP 11 was smaller than between MIP and NIP 5.

This is illustrated in the graph of Figure 2.40 a). The PDI values of all polymer particles slightly changed after extraction and were between 0.20 and 0.38.

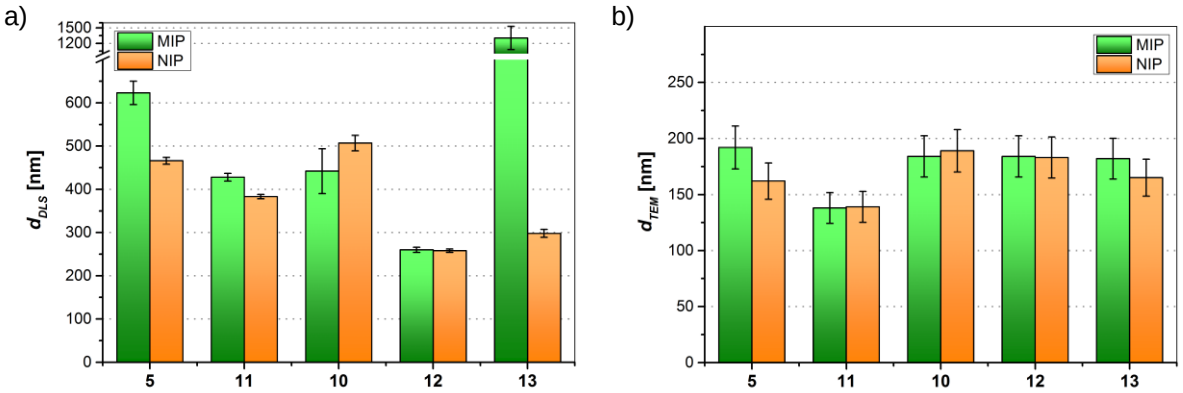

Figure 2.40 Average diameters (*d*) of the different polymer particles washed with different extraction solutions obtained from DLS (a) and TEM (b).

The graph of Figure 2.40 b) shows the average particle diameters from TEM images. These were between 130 and 195 nm and thus smaller than the diameters from DLS. In contrast to the previous results, the average particle diameters from TEM did not follow the same trend as the diameters from DLS here. The diameters of MIP 5 and 13 were larger than those of their corresponding NIPs, whereas the diameters of MIP and NIP 10, 11 and 12 were comparable. The diameter of MIP 13 was in the range of the other polymer particles in contrast to the results obtained by DLS.

The TEM images in Figure 2.41 show that all polymer suspensions contained particles with a spherical shape and a relatively broad size distribution with diameters ranging from around 50 to 600 nm. MIP 13 also contained larger particles, which probably caused the large particle diameter of MIP 13 revealed by DLS.

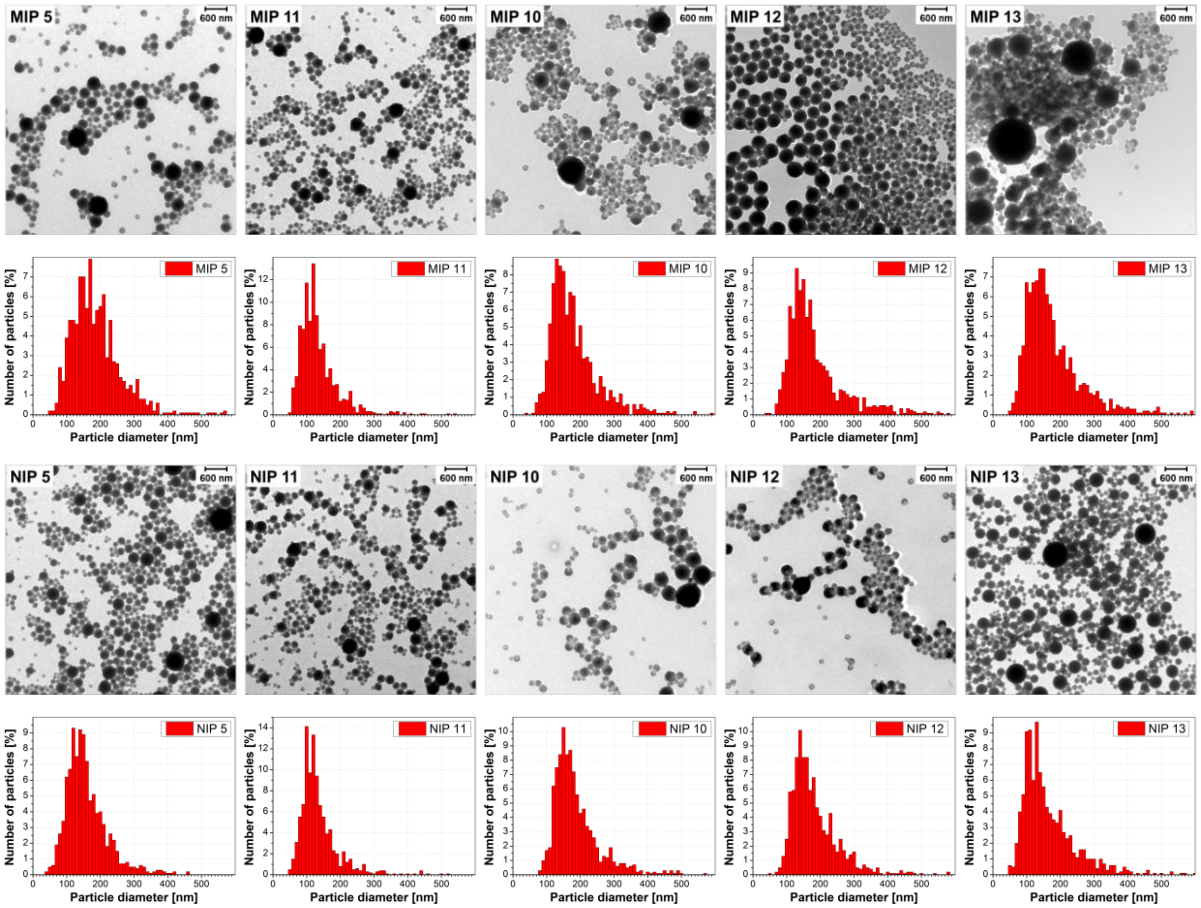

Figure 2.41 TEM images (magnification: 4000 x) and particle size distributions of the polymer particles washed with different extraction solutions.

The particle size distributions of the polymer particles were similar except that the size distributions of MIP and NIP 11 were shifted towards lower and the size distribution of MIP 13 was shifted towards higher values.

The TEM images recorded at a higher magnification in Figure 2.42 indicate that all polymer particles besides NIP 13, which inexplicably contained particles with a smooth surface, had a rough surface as the polymer particles described in chapter 2.6.6.1.

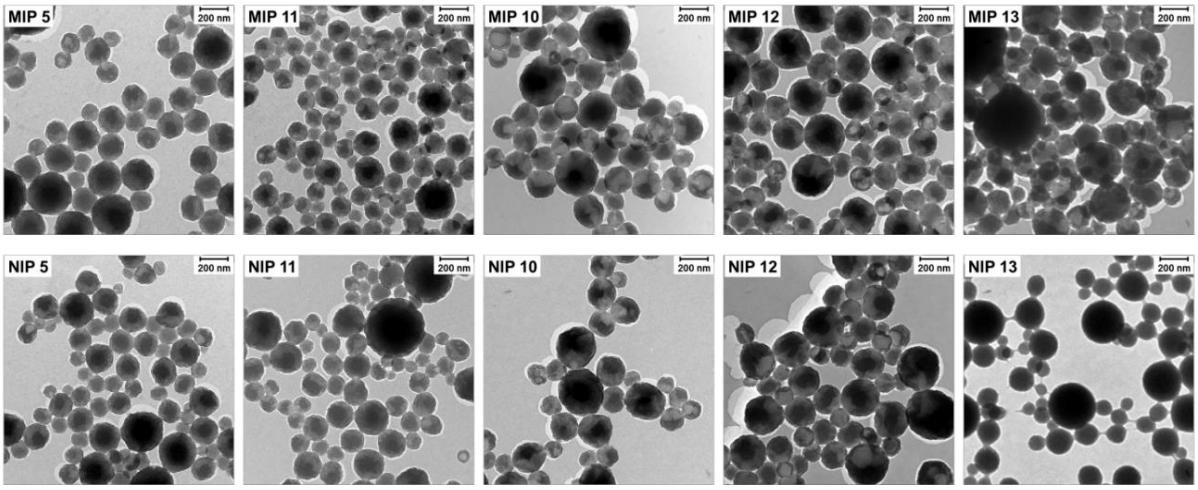

Figure 2.42 TEM images (magnification: 16000x) of the polymer particles washed with different extraction solutions.

The nitrogen adsorption isotherms of the polymer particles after extraction with different solutions had the same curve progression as after extraction in water. These were thus also rather non-porous. The specific surface areas were between 37 and 47 $m^2 g^{-1}$ and very similar (Figure 2.43).

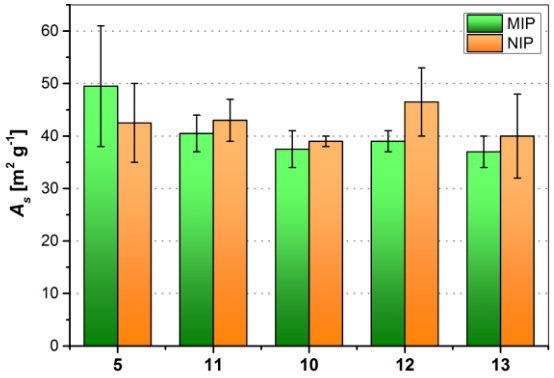

Figure 2.43 Specific surface areas (A_s) of the polymer particles washed with different extraction solutions obtained from BET nitrogen adsorption. All bars represent the average of two samples. The error bars show the spread.

Whereas MIP 5 had a larger specific surface area than NIP 5 and both, MIP and NIP 10, had comparable specific surface areas, the specific surface areas of the MIPs, which were washed with other solutions, were smaller than of their corresponding NIPs. Hence, no effect from imprinting was observed.

2.6.7 Comparison of the specific surface areas obtained from BET, DLS and TEM

For a good comparison of the results obtained from DLS, TEM and BET, the specific surface areas were calculated from the average diameters obtained from DLS and TEM under the approximation that the particles were smooth spheres and that the density of the particles was the same as the density of the cross-linker EGDMA. The obtained specific surface areas of the different polymers are shown in Figure 2.44.

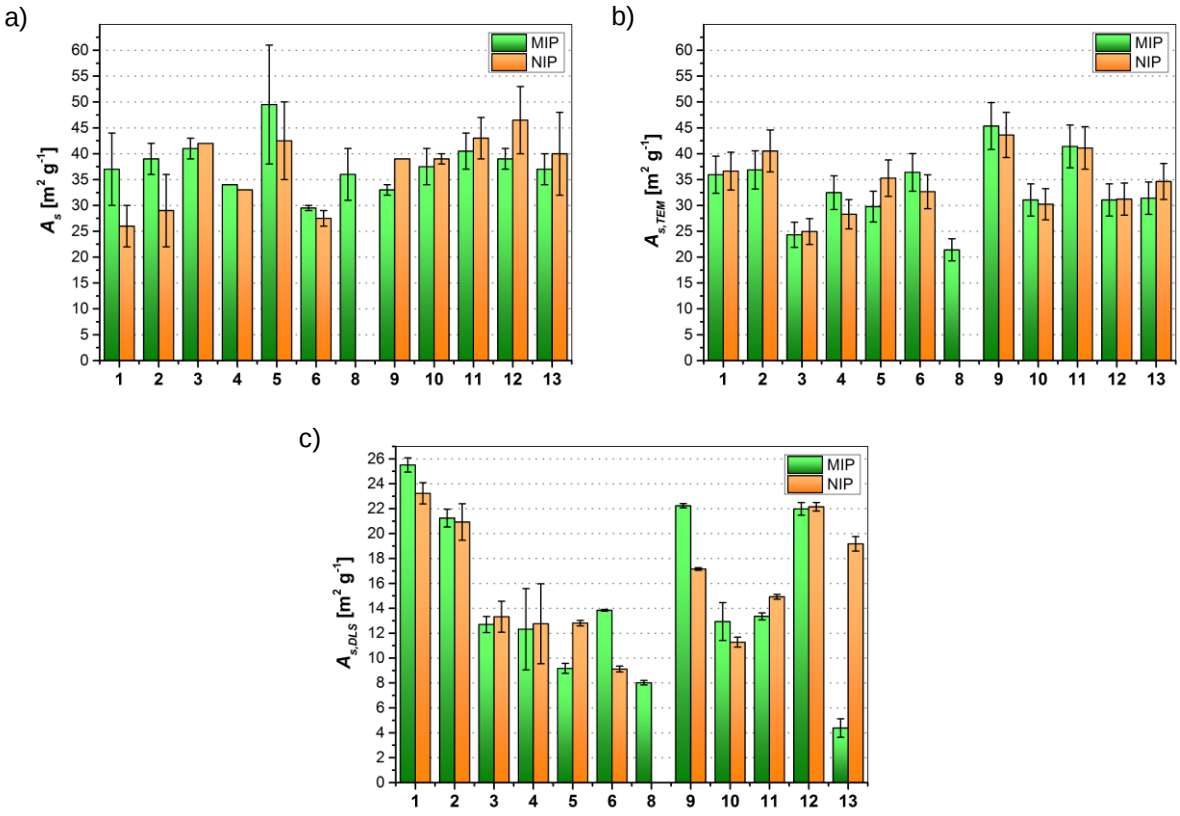

Figure 2.44 Specific surface areas (A_s) of all polymer particles obtained from BET (a), TEM (b) and DLS (c).

The specific surface areas obtained from BET and TEM were in the same order of magnitude, since the measurements are done with dried particles.[217] The DLS measurement is performed in a liquid, in which the particles are swollen and solvated and thus appear larger[193] and have a lower specific surface area. Other reasons were already described in chapter 2.6.6.1. The trend of the specific surface areas obtained from DLS was rather consistent with the trend obtained from TEM than from BET, since both methods are based on the particle size. However, there were differences in the specific surface area of the different polymer particles depending on the determination method. The influence of the surface area on the binding capacity is investigated in the following chapter 2.6.8.

2.6.8 Influence of the surface area on the binding capacity

Pepsin most likely adsorbed on the surface of the polymer particles instead of diffusing inside the particles due to the high cross-linking degree and the higher hydrophobicity of the particle inside. Since the obtained MIP and NIP particles have different diameters and thus different surface areas, it will raise the question, if there is an influence of the surface area on the binding capacity and thus also on the imprinting factor. This was investigated by an additional experiment, wherein NIP particles were used, which were prepared in the same way as NIP 5. These were centrifuged and the supernatant was separated from the precipitate. The precipitate was redispersed in water by shaking. This was done in order to obtain two polymer suspensions with particles of a different average size, but of the same chemical composition.

The TEM images and corresponding particle size distributions in Figure 2.45 show that the supernatant contained a higher fraction of smaller particles than the precipitate and that all particles were round and had a rough surface.

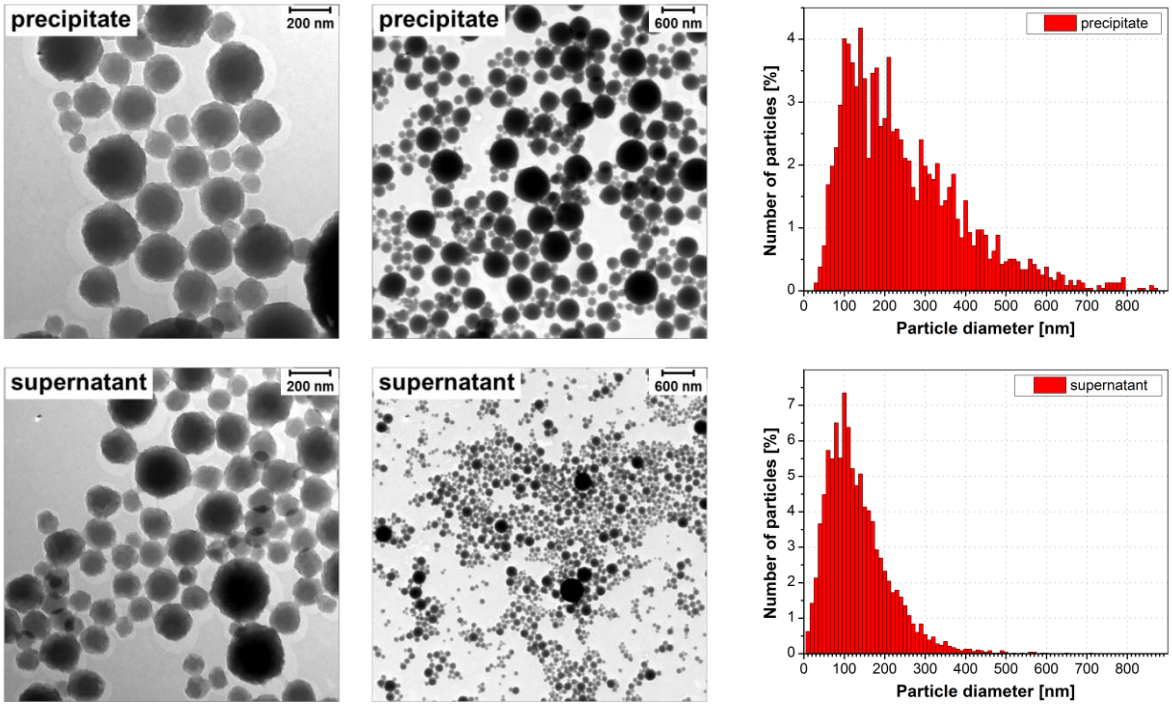

Figure 2.45 TEM images (magnifications: 16000 x (left) and 4000 x (right)) and particle size distributions of the polymer particles of the precipitate and supernatant.

The average hydrodynamic diameters and average diameters from TEM images, PDIs, zeta potentials and specific surface areas of the polymer particles of the supernatant and the precipitate are summarized in Table 2.7. The average diameters obtained from DLS and TEM images of the particles of the supernatant were around two times smaller than of the particles of the precipitate. The PDI of the polymer particles of the supernatant was also lower than of the polymer particles of the precipitate indicating a narrower particle size distribution, which is also visible in Figure 2.45.

The zeta potentials of the particles of both fractions are similar indicating that the particles of both fractions had around the same number of positively charged functional groups on the particle surface.

Table 2.7 Average hydrodynamic diameters (d_{DLS}), average diameters (d_{TEM}), polydispersity indices (*PDI*), zeta potentials (ζ) and specific surface areas (A_s) of the polymer particles of the precipitate and supernatant.

Type of polymer	d_{DLS} [nm]	d_{TEM} [nm]	*PDI* [-]	ζ [mV]	A_s [$m^2 g^{-1}$]
precipitate	606 ± 35	258 ± 26	0.38 ± 0.10	23 ± 1	30 ± 15
supernatant	263 ± 11	145 ± 15	0.18 ± 0.05	26 ± 2	46 ± 24

The specific surface areas of the particles of both fractions correlated with the particle sizes. The average diameter of the particles of the supernatant was two times smaller than of the particles of the precipitate and thus the specific surface area of the particles of the supernatant was two times larger than of the particles of the precipitate.

This correlation is clearly illustrated by the comparison of the specific surface areas of the particles of the supernatant and the precipitate obtained from DLS, TEM and BET determination in Figure 2.46. The specific surface areas were calculated from the average diameters obtained from DLS and TEM under the same approximation as described in chapter 2.6.7. The blue bars represent the fraction of the precipitate and the yellow bars the fraction of the supernatant. This will be maintained in the following graphs.

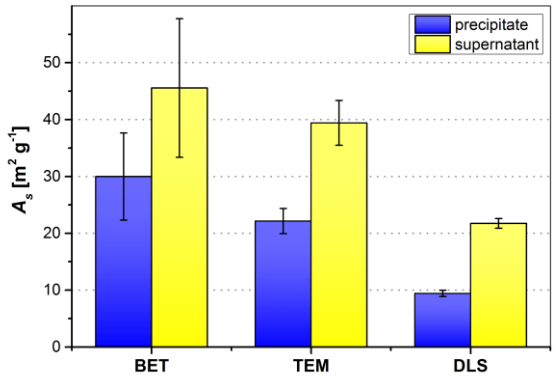

Figure 2.46 Specific surface areas (A_s) of the polymer particles of the precipitate and supernatant obtained from BET, TEM and DLS.

The specific surface area of the smaller polymer particles of the supernatant was around the double of the specific surface area of the larger polymer particles of the precipitate. This result was obtained with all three different methods of determination.

Batch rebinding experiments with a pepsin solution were performed to investigate the influence of the different specific surface areas on the pepsin binding capacity. The pepsin binding capacities of the two polymer particle fractions are shown in the graph of Figure 2.47. Approximately the double amount of pepsin was bound to the particles of the supernatant than to the particles of the

precipitate (Figure 2.47). Hence, the difference in the amount of bound pepsin came from the different specific surface areas as a result of the different particle sizes, since the two particle fractions had the same chemical composition and a similar zeta potential. This shows that the surface area affected the binding capacity and thus will also affect the imprinting factor, if the MIP and corresponding NIP particles have different specific surface areas.

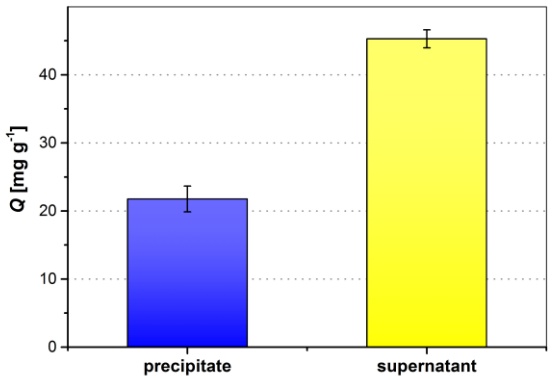

Figure 2.47 Pepsin binding capacities (*Q*) of the polymer particles of the precipitate and supernatant. All bars represent the average of two samples. The error bars show the spread.

The binding capacity was normalized by the surface area determined by BET, TEM and DLS to circumvent this effect and was plotted against the different methods used for the determination of the specific surface area in Figure 2.48.

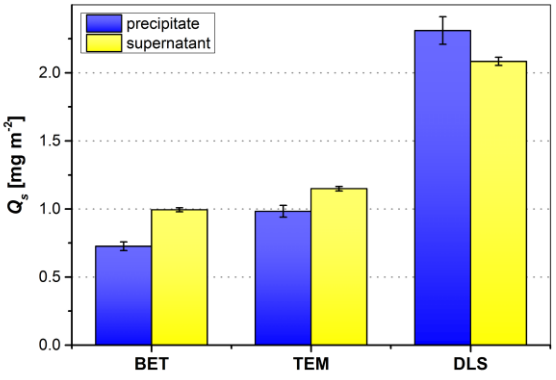

Figure 2.48 Pepsin binding capacities (Q_s) of the polymer particles of the precipitate and supernatant after normalization by the specific surface areas obtained from BET, TEM and DLS. All bars represent the average of two samples. The error bars show the spread.

The effect of the different surface areas of the smaller and larger particles on the pepsin binding capacity was largely reduced by the normalization of the binding capacity with the specific surface area, since the binding capacities of the smaller and larger particles were comparable afterwards. This result was obtained with all three determination methods. Slightly different values of the surface-normalized binding capacities were obtained due to slightly different surface areas obtained from the different methods.

2.6.9 Batch rebinding of pepsin

Batch rebinding experiments were performed to examine the pepsin binding capacity of the different MIP and NIP particles and the imprinting efficiency. The washed polymer particles were therefore incubated with a pepsin solution overnight. The same ratio between pepsin and the polymer was used as during imprinting. The polymer particles were removed by centrifugation and filtration. The concentration of pepsin in the remaining solution was determined by UV-Vis spectrophotometry. A control sample was prepared without pepsin in the same way to ensure that no pepsin leaches out of the polymer during the rebinding and to take the background signal into account. Binding capacities and imprinting factors were determined. Based upon the results in chapter 2.6.8 the obtained binding capacities were normalized by the specific surface areas in order to circumvent the influence of different surface areas resulting from different particle diameters on the binding capacity. The specific surface areas determined from the average hydrodynamic particle diameters obtained by DLS was used for the surface normalization of the binding capacity, since the DLS measurements were performed in polymer suspensions and thus under the same conditions as the rebinding experiments. The specific surface areas determined by BET nitrogen adsorption was considered less reliable, as aggregation of the polymer particles may occur during the drying process and nitrogen may be adsorbed in smaller cavities than pepsin, as nitrogen is much smaller. This normalization is maintained for all following diagrams in chapter 2, if nothing else is set. The binding capacities of the NIPs are analyzed in the first place in order to get an insight into the influence of different parameters on the pepsin binding capability. Then the binding capacities of the MIPs are compared with the binding capacities of their corresponding NIPs in order to investigate, whether there is increased pepsin binding as a result of the formation of selective binding sites during the imprinting referred to as imprinting effect. Furthermore, the different MIPs are compared with each other. Finally, the effect of different kinds of normalizations of the binding capacities on the imprinting factors is discussed and the pepsin binding capacity of an exemplary MIP is compared with the pepsin binding capacity of commercially available beads, which are used for the purification of pepsin.

2.6.9.1 Different functional monomers

The surface-normalized pepsin binding capacities of the MIP and NIP particles made of different functional monomers are shown in Figure 2.49.[213]

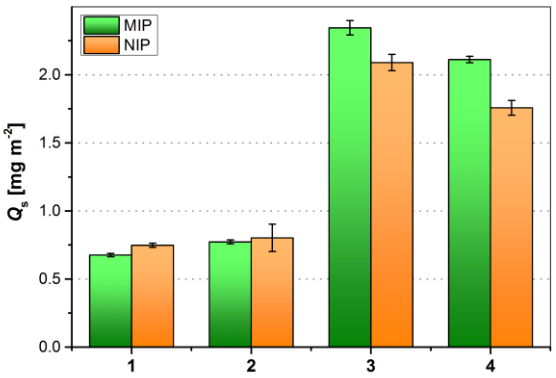

Figure 2.49 Surface-normalized pepsin binding capacities (Q_s) of the polymer particles prepared from different functional monomers. All bars represent the average of two samples. The error bars show the spread.

More pepsin was bound to NIP 3 and 4 having a positively charged surface than to NIP 1 and 2 with a negatively charged or neutral surface due to attractive ionic interactions between protonated amino groups of NIP 3 and quaternary ammonium groups of NIP 4 respectively and deprotonated carboxyl groups of the in pure water (pH 5) overall negatively charged pepsin.[213] A slightly higher amount of pepsin was bound to NIP 3. This may result from an additional hydrogen bond between the amino group and the carboxyl groups of pepsin and a higher charge density of the amino group in AEMA. The interactions supposed to be mainly hydrogen bonds between the carboxyl groups of NIP 1 and hydroxyl groups of NIP 2, respectively, and pepsin were less strong.

The binding capacities of MIP and NIP 1 and 2 were quite similar. This indicates that no imprinting effect was obtained with MAA and HEMA.[213] The interactions between pepsin and these functional monomers were probably too weak to form a stable pre-polymerization complex and thus no selective binding sites were obtained. This argues against the conclusion that the BET surface areas of the MIPs were higher than of the corresponding NIPs due to the formation of imprinted cavities on the MIPs in chapter 2.6.6.1. MIP 3 and 4 bound more pepsin than their corresponding NIPs very likely due to the formation of a stronger pre-polymerization complex based on ionic interactions. The difference between the binding capacities of MIP and NIP 4 ($IF = 1.2$) was larger than between MIP and NIP 3 ($IF = 1.1$), although more pepsin was bound to MIP 3. This may be explained by the ability of APTMA to interact with pepsin by additional hydrophobic interactions and that it contains an amide group instead of an ester group, which may be more compatible to pepsin. Hence, a higher imprinting effect was obtained by a combination of ionic and hydrophobic interactions instead of ionic interactions and hydrogen bonds, although hydrogen bonds are directional and thus more selective. Ionic and hydrophobic interactions are non-directional, but there are several protein

imprinted polymers that are based on cooperative multiple ionic interactions[143] or on a combination of ionic and hydrophobic interactions[104,124]. Another reason for the higher imprinting effect with APTMA may be that it is more suitable to bring pepsin to the monomer droplet surface for the formation of the pre-polymerization complex at the droplet surface and the preservation of the steric orientation of the functional groups of the monomer and of pepsin on the surface of the polymer particles. An argument that weakens the imprinting effect might be the difference between the zeta potentials of MIP 3 and 4 and their corresponding NIPs (see chapter 2.6.6.1). An imprinting factor of 1.2 is relatively low in comparison with imprinting factors obtained for other protein imprinted polymers, which are usually between 2 and 10 depending on the polymer and protein concentration.[105,116,119] Other parameters were investigated in order to optimize the imprinting factor and are described in the following subchapters.

2.6.9.2 Different other parameters

After the screening of different functional monomers the influence of the double amount of pepsin template, a citrate buffer solution with a pH value of 4, the absence of surfactant, the addition of a hydrophobic monomer IBMA and the reduction of the APTMA content on the pepsin binding capability and imprinting efficiency were investigated. The experimental protocol of the batch rebinding experiments was slightly changed compared with the protocol used for obtaining the binding capacities in the previous chapter 2.6.9.1. The polymer particles were used in suspension in order to bypass the drying before the rebinding experiment, which can cause aggregation of the particles, and to offer much easier handling. The double amount of pepsin was used for rebinding, since also the double amount was used for imprinting. The related surface-normalized pepsin binding capacities are shown in Figure 2.50.

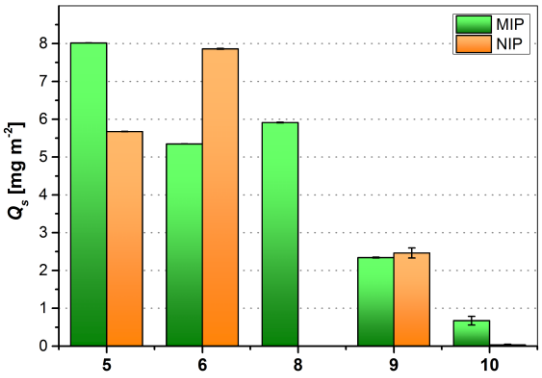

Figure 2.50 Surface-normalized pepsin binding capacities (Q_s) of the polymer particles prepared under different parameters. All bars represent the average of two samples. The error bars show the spread.

The binding capacity of NIP 5 was approximately 3 times higher than the binding capacity of NIP 4. This may be attributed to the use of the double amount of pepsin and suspended instead of dried polymer particles during the rebinding experiment and the higher zeta potential of NIP 5. More

pepsin was bound to NIP 6, which was prepared in a citrate buffer solution (pH 4). NIP 8 was not used for the batch rebinding experiments, because it was a bulk polymer. Less pepsin was bound to NIP 9 and hardly any pepsin was bound to NIP 10. This trend correlates with the zeta potentials and the amount of APTMA used for the polymerization. Half of the amount of APTMA was used for the preparation of NIP 9 and only a tenth was used for the preparation of NIP 10 compared with the amount of APTMA used for the preparation of NIP 5 and 6. The amount of bound pepsin decreased with decreasing zeta potential due to the decrease or disappearance of positively charged functional groups on the polymer surface. This shows that ionic interactions play an important role in binding pepsin. The very low binding capacity of NIP 10 also shows that there were almost no interactions between pepsin and polymerized EGDMA. This supports the theory that APTMA helps to adsorb pepsin at the droplet surface containing EGDMA. The increase of the hydrophobicity of NIP 9 did not result in an increase of the pepsin binding capacity. Ionic interactions between the polymer particles and pepsin are thus stronger than hydrophobic interactions, although these are weakened in water. Hydrophobic interactions do not have their maximum strength here, since the pH value is not equal to the isoelectric point of pepsin. The interactions between IBMA and pepsin are stronger than between EGDMA and pepsin, since more pepsin was bound to NIP 9 than to NIP 10.

The pepsin binding capacity of MIP 5 was higher than the binding capacity of NIP 5. This may be attributed to an imprinting effect. The zeta potential of MIP 5 was lower than of NIP 5. The imprinting factor increased from 1.2 to 1.4. Doubling the amount of pepsin template resulted in the creation of more imprinted binding sites. But still a high content of non-selective binding was obtained due to random copolymerization of excess functional monomer and non-directional interactions. No imprinting effect was obtained in the citrate buffer solution with a pH value of 4, maybe because the rebinding experiment was carried out in water for a better comparison with the other MIP-NIP pairs and the pepsin conformation in water was not recognized by MIP 6, since pepsin was imprinted in the citrate buffer solution, where it had another conformation (see chapter 2.6.1). The influence of the pH value of the incubation solution on the binding capacity is further investigated in chapter 2.6.12. The amount of pepsin bound to MIP 8 was lower than to MIP 5. It was expected that more imprinted binding sites were created due to more available space for pepsin on the droplet surface in the absence of the surfactant. However, some of the imprinted sites may have been lost due to aggregation of some particles. The addition of IBMA to the monomer droplets did not result in a higher pepsin binding capacity of MIP 9 compared with NIP 9. This may be explained by the additional hydrophobic interactions, which may have weakened the stability of the pre-polymerization complex, or by the significantly lower zeta potential of MIP 9 than of NIP 9. The reduction of the amount of APTMA resulted in an imprinting effect with an extraordinary high imprinting factor of 23.3 due to a better stoichiometry between the quaternary ammonium groups

of APTMA and the carboxyl groups of pepsin. Imprinting factors higher than 20 were also obtained for BSA surface imprinted submicron particles by Tan et al.[121] The binding capacity of MIP 10 was very low compared with the binding capacity of MIP 5 due to the low APTMA content in the monomer mixture.

2.6.9.3 Different extraction solutions

The influence of different extraction solutions on the pepsin binding capability and imprinting efficiency was investigated. MIP and NIP 5 were washed with pure water and HCl. MIP and NIP 10 were washed with pure water, NaOH and a NaCl solution. The related surface-normalized pepsin binding capacities are shown in Figure 2.51.

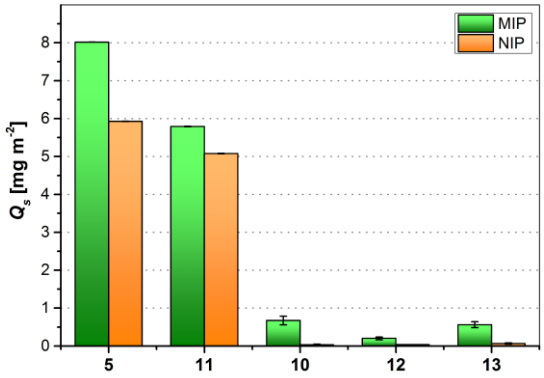

Figure 2.51 Surface-normalized pepsin binding capacities (Q_s) of the polymer particles washed with different extraction solutions. All bars represent the average of two samples. The error bars show the spread.

The binding capacity of NIP 5 slightly decreased after using HCl as extraction solution (NIP 11). The binding capacity of NIP 10 was not affected by the use of NaOH (NIP 12) and the NaCl solution (NIP 13) as extraction solution. There was no correlation between the different zeta potentials of the NIPs and the binding capacities.

There was no improvement of the imprinting effect and thus in the removal of pepsin by the use of HCl, NaOH and the NaCl solution. The extraction in HCl and NaOH might have been too harsh and resulted in a damage of some selective binding sites.[166] These results show that the extraction in pure water was absolutely sufficient and therefore is preferable.

2.6.9.4 Different normalizations of the binding capacities and imprinting factors

The graphs of Figure 2.52 a), b) and c) show the binding capacities of all polymer particles, which were normalized by the specific surface areas determined by DLS, TEM and BET determination, since different surface areas were obtained from the different methods. The graph of Figure 2.52 d) shows the content of bound pepsin to get an idea of how much of the initial pepsin could be bound to the polymer particles.

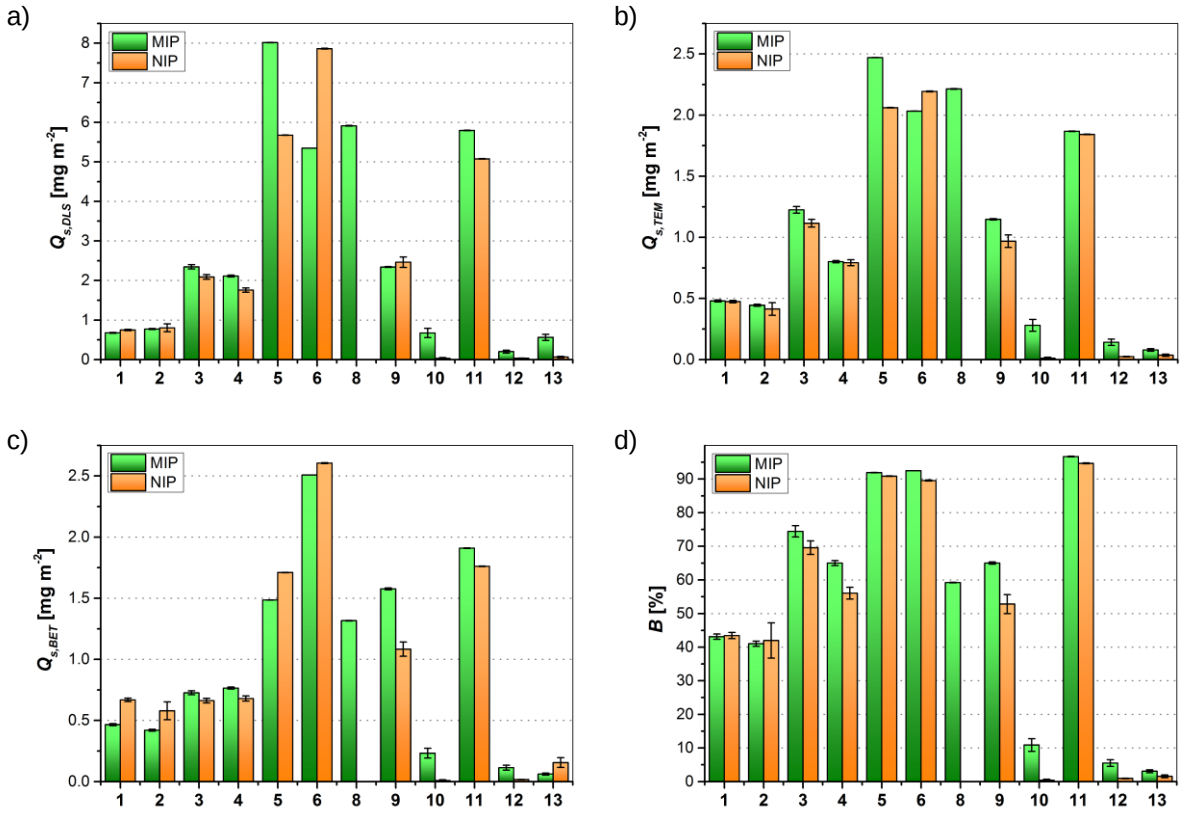

Figure 2.52 Pepsin binding capacities (Q_s) of all polymer particles normalized by the specific surface areas obtained from DLS (a), TEM (b) and BET (c) and the content of pepsin bound (B) to the different polymer particles (d). All bars represent the average of two samples. The error bars show the spread.

There was a general trend of the binding capacities of the different polymer particles, which was observed in all graphs. The pepsin binding capacity was mainly dependent on the type of functional monomer and the number of positive charges on the surface of the polymer particles. More than 90% of pepsin was bound to the polymers (5, 6 and 11), which were prepared with a high amount of APTMA. An imprinting effect can be attributed to different MIPs after different normalization of the binding capacity. For example, MIP 5 shows an imprinting effect after the normalization of the binding capacity by the surface area determined by DLS and TEM, but no imprinting effect after the normalization of the binding capacity by the BET surface area and by the mass of polymer. On the other hand, MIP 9 shows an imprinting effect after the normalization of the binding capacity by the surface area determined by TEM and BET and by the mass of polymer, but not after the normalization of the binding capacity by the surface area determined by DLS. All kinds of

normalizations resulted in an imprinting effect for MIP 3, 10 and 12. At least one kind of normalization resulted in an imprinting effect for all MIPs except for MIP 1 and 6. The dependence of the imprinting factor on the kind of normalization of the binding capacity is summarized in Table 2.8.

Table 2.8 Imprinting factor (*IF*) depending on the type of polymer and kind of normalization of the binding capacity. The numbers, which represent a positive imprinting effect (*IF* > 1), are marked in bold.

Type of polymer		Imprinting factor *IF*			
		DLS	TEM	BET	mass
MIP 1	MAA	0.9	1.0	0.7	1.0
MIP 2	HEMA	1.0	**1.1**	0.7	1.0
MIP 3	AEMA	**1.1**	**1.1**	**1.1**	**1.1**
MIP 4	APTMA	**1.2**	1.0	**1.1**	**1.2**
MIP 5	1 APTMA	**1.4**	**1.2**	0.9	1.0
MIP 6	pH 4	0.7	0.9	1.0	1.0
MIP 9	0.5 IBMA	1.0	**1.2**	**1.5**	**1.2**
MIP 10	0.1 APTMA	**23.2**	**25.9**	**27.7**	**26.6**
MIP 11	HCl*	**1.1**	1.0	**1.1**	1.0
MIP 12	NaOH*	**5.9**	**5.9**	**7.0**	**5.9**
MIP 13	NaCl*	**8.7**	**2.2**	0.4	**2.0**

* Extraction solution.

The imprinting factor was dependent on the kind of normalization of the binding capacity. The highest imprinting effect with an extraordinary high imprinting factor (*IF* > 20) was obtained with a low amount of APTMA, whereas the highest pepsin binding capacity was obtained with a high amount of APTMA. The extraction of MIP 10 in NaOH (MIP 12) and a NaCl solution (MIP 13) also resulted in high imprinting factors. But these were lower than the imprinting factor of MIP 10. An imprinting factor of 1.5 was obtained by using IBMA as second functional monomer after normalization of the binding capacity by the BET surface area. An imprinting factor of 1.4 was obtained by doubling the amount of template pepsin after normalization of the binding capacity by the surface area obtained from DLS. The other imprinting factors were between 1.1 and 1.2 and thus lower.

2.6.9.5 Comparison with pepstatin immobilized agarose beads

The binding capacity of MIP 5 was compared with the binding capacity of commercially available pepstatin immobilized agarose beads (PABs), which are used for the purification of cathepsin, pepsin and other proteases. MIP 5 was exemplarily used, since it showed an imprinting effect and had a high pepsin binding capacity. The same batch rebinding experiment as with MIP 5 was carried out with the suspension of the PABs, whose solid content was adjusted to the solid content of MIP 5, for a direct comparison. The content of pepsin bound to MIP 5 and the PABs is shown in Figure 2.53, since the surface area of the PABs was not determined.

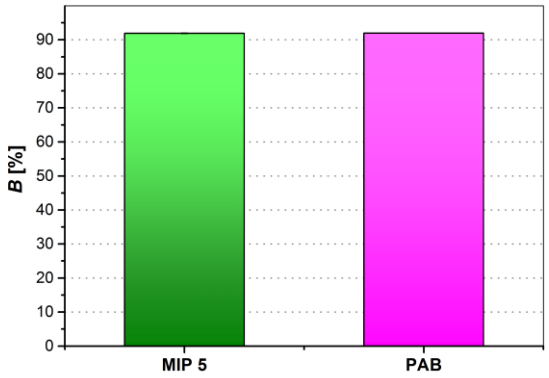

Figure 2.53 Content of pepsin bound (*B*) to MIP 5 and the PABs. All bars represent the average of two samples. The error bars show the spread.

MIP 5 bound the same amount of pepsin as the commercial PABs, although they have quite different properties in terms of particle size, porosity, chemical composition and type of interaction with pepsin. The particle size of MIP 5 is much lower than the size of the PABs, whose size is ranging between 45 and 165 µm. The PABs are porous, soft and not cross-linked in comparison with the non-porous highly cross-linked MIP particles. Whereas the binding between the PABs and pepsin is based on hydrogen bonds and van der Waals interactions[26], the binding between MIP 5 and pepsin is based on ionic and hydrophobic interactions.

2.6.10 Batch rebinding of different pepsin concentrations

A series of batch rebinding experiments was performed with pepsin solutions of different initial concentrations in order to investigate the binding properties of the MIPs and NIPs in further detail. The range of the pepsin concentrations was around the pepsin concentration used for the rebinding experiments in chapter 2.6.9. The ratio between pepsin and the polymer was thus lower, equal and higher than the ratio used during imprinting. The surface-normalized binding capacities were plotted versus the free pepsin concentration in the solution after the incubation. The Langmuir, Freundlich and Langmuir-Freundlich equations were fitted to the experimental data points by using the non-linear least-square analysis of the program OriginPro 9.0G for providing quantitative data about the binding affinity of the MIPs and NIPs. A better fit with a higher coefficient of determination was obtained with the Langmuir than with the Freundlich model for all MIPs and NIPs. Fitting the Langmuir-Freundlich equation resulted in an isotherm with a very similar curve progression as the Langmuir isotherm and a heterogeneity index of 1 for all MIPs and NIPs except for NIP 6. In the case of a heterogeneity index of 1 the Langmuir-Freundlich equation reduces to the Langmuir equation. Hence, the MIP and NIP particles had a homogeneous surface with one type of binding sites and bound a monolayer of pepsin. The heterogeneity index of NIP 6 was 0.75. This suggests that NIP 6 had different types of binding sites with different affinities for pepsin. However, the Langmuir model was also used for characterizing the binding behavior of NIP 6 for a better comparison with the other MIPs and NIPs. The binding isotherms are described in more detail in the following subchapter. The obtained maximum binding capacities and dissociation constants are compared and a modified Langmuir equation is introduced.

2.6.10.1 Binding isotherms

The binding isotherms of MIP and NIP 1 to 4 had a similar curve progression. There was no difference between the binding capacities of MIP and NIP 1 and 2 and a small difference between the binding capacities of MIP and NIP 3 across the entire concentration range. The highest difference in binding pepsin of different initial concentrations and thus the highest imprinting effect was obtained with MIP and NIP 4. The binding isotherms of MIP and NIP 4 therefore are exemplarily shown in Figure 2.54.[213] The green data points represent the MIP and the orange data points represent the corresponding NIP. This assignment of the bar colors is maintained for all following diagrams.

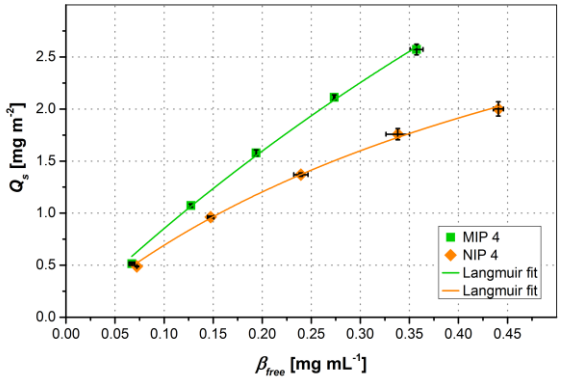

Figure 2.54 Surface-normalized pepsin binding capacities (Q_s) of MIP and NIP 4 depending on the free pepsin mass concentration (β_{free}). All data points represent the average of two samples. The error bars show the spread. The binding isotherms were fitted by using the Langmuir equation.

More pepsin was bound to MIP 4 than to the NIP 4 across the entire concentration range due to the imprinting. The difference in the binding capacity of pepsin between MIP and NIP 4 and thus the imprinting factor increased from 1.1 to 1.3 with increasing initial pepsin concentration. This indicates that non-selective binding to the MIP was more pronounced at lower concentrations. It was rather expected that the imprinting factor is higher at lower pepsin concentrations and decreases, when all selective binding sites of the MIP are occupied and non-selective binding to the MIP starts.[110] There are examples of decreasing[106,218], but also of constantly maintaining[151] and increasing[105,219] imprinting factors with increasing initial protein template concentration in the literature.

The binding isotherms of MIP and NIP 5 are shown in Figure 2.55.[220]

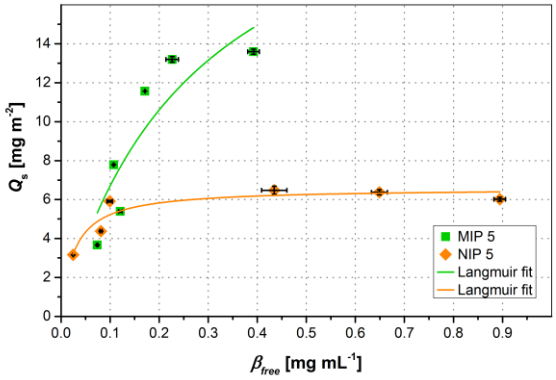

Figure 2.55 Surface-normalized pepsin binding capacities (Q_s) of MIP and NIP 5 depending on the free pepsin mass concentration (β_{free}). All data points represent the average of two samples. The error bars show the spread. The binding isotherms were fitted by using the Langmuir equation.

More pepsin was bound to MIP 5 than to NIP 5 across the entire concentration range due to the imprinting. The difference in the binding capacity between the MIP and NIP and thus the imprinting factor increased from 1.2 to 2.3 with increasing initial pepsin concentration. This is the same behavior as between MIP and NIP 4. The curve progression of the binding isotherms of MIP and NIP 5 indicates that there is a saturation of the binding sites due to the use of higher initial pepsin concentrations. The agreement of the Langmuir isotherms with the data points of NIP 5 and in particular of MIP 5 was lower than with the data points of MIP and NIP 4. A reason for this might be the higher uncertainty due to the smaller sample volume used here to reduce the amount of polymer.

The binding isotherms of MIP and NIP 6 were recorded in a citrate buffer solution with a pH value of 4 and are shown in Figure 2.56.

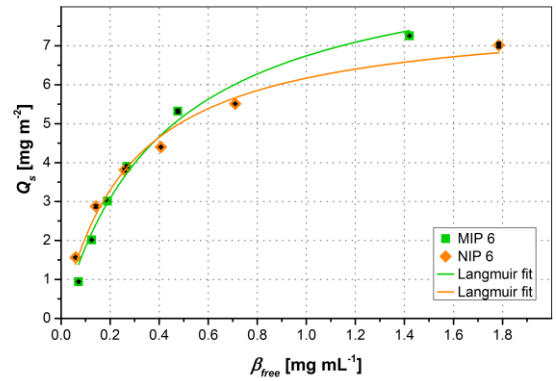

Figure 2.56 Surface-normalized pepsin binding capacities (Q_s) of MIP and NIP 6 depending on the free pepsin mass concentration (β_{free}). All data points represent the average of two samples. The error bars show the spread. The binding isotherms were fitted by using the Langmuir equation.

The binding capacities of MIP 6 were lower than of NIP 6 across the entire concentration range except at the highest pepsin concentration. Here slightly more pepsin was bound to the MIP. This does not show a clear effect from imprinting in the same solution, which was used during

imprinting. The difference between the binding capacities of the MIP and NIP turned with increasing initial pepsin concentration. This resembled the previous results, where the imprinting factor increased with increasing pepsin concentration. The curve progression of the Langmuir isotherms was in good agreement with the data points of the MIP and NIP. A saturation of the binding sites was not yet reached.

The binding isotherm of MIP 8 is shown in Figure 2.57.

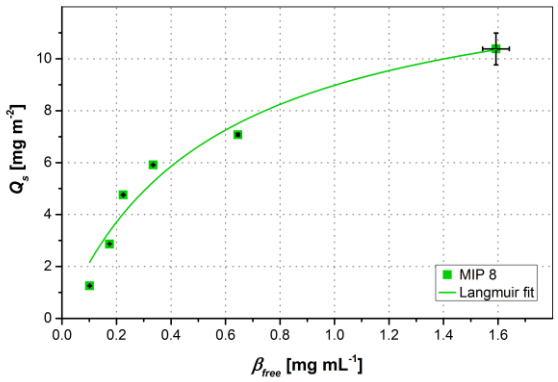

Figure 2.57 Surface-normalized pepsin binding capacities (Q_s) of MIP 8 depending on the free pepsin mass concentration (β_{free}). All data points represent the average of two samples. The error bars show the spread. The binding isotherms were fitted by using the Langmuir equation.

The curve progression of the binding isotherm of MIP 8 resembled the progression of the binding isotherm of MIP 6. The quality of the Langmuir fit was slightly lowered evident by the lower agreement between the Langmuir isotherm and the data points. There was an uncertainty concerning the data point of the highest free pepsin concentration visible by the relatively high error bars. However, there was hardly any difference between the fitted curves with and without this data point.

The binding isotherms of MIP and NIP 9 are shown in Figure 2.58.

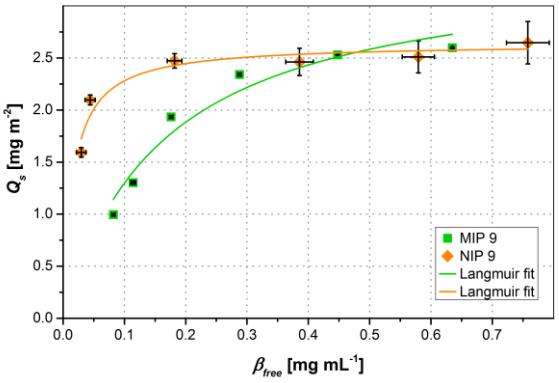

Figure 2.58 Surface-normalized pepsin binding capacities (Q_s) of MIP and NIP 9 depending on the free pepsin mass concentration (β_{free}). All data points represent the average of two samples. The error bars show the spread. The binding isotherms were fitted by using the Langmuir equation.

The binding capacities of MIP 9 were lower than of NIP 9 across the entire concentration range except at the second highest pepsin concentration, where slightly more pepsin was bound to the

MIP. This does not show a clear effect from imprinting. The difference between the binding capacities of the MIP and NIP also seems to turn with increasing initial pepsin concentrations as between MIP and NIP 6. The quality of the fits was sufficient. The curve progression of the binding isotherm of MIP 9 was similar to the progression of the binding isotherms of MIP 6 and 8, but different to the curve progression of binding isotherm of NIP 9. This had a higher initial slope and almost reached saturation similar to NIP 5.

2.6.10.2 Maximum binding capacities and dissociation constants

The maximum surface-normalized binding capacities and dissociation constants of the different MIPs and NIPs were determined with the Langmuir equation and are summarized together with the correlation coefficients of the fits in Table 2.9.

Table 2.9 Maximum surface-normalized pepsin binding capacities ($Q_{s,max}$), dissociation constants (K_d) and correlation coefficients (R^2) of the different polymer particles obtained after fitting the Langmuir equation to the data points of their binding isotherms. The numbers, which indicate a positive effect from imprinting, are marked in bold.

Type of polymer		$Q_{s,max}$ [mg m^{-2}]	K_d [µM]	R^2 [-]
MIP 4	APTMA	**12.8**	39.95	0.997
NIP 4		4.7	16.45	0.998
MIP 5	1 APTMA	**25.3**	7.95	0.759
NIP 5		6.6	0.75	0.847
MIP 6	pH 4	**9.6**	12.04	0.990
NIP 6		7.9	7.96	0.992
MIP 8	w/o surf	13.9	15.79	0.966
MIP 9	0.5 IBMA	**3.4**	4.71	0.978
NIP 9		2.6	0.45	0.988

The maximum pepsin binding capacities of all MIPs were between 3.4 and 25.3 mg m^{-2} and higher than of the corresponding NIPs thus showing that more binding sites were created through the imprinting process. The maximum pepsin binding capacities of MIP 4 and 5 were significantly higher than of the corresponding NIPs, whereas the difference between the maximum pepsin binding capacities of MIP 6 and 9 and their corresponding NIPs was low. The highest maximum pepsin binding capacity was obtained for MIP 5. The maximum binding capacity of MIP 4 was doubled by using the double amount of pepsin during the imprinting.

The dissociation constants of the MIPs were between 4.71 and 39.95 µM and did not follow the same trend as the maximum binding capacities. The lowest dissociation constant and thus highest binding affinity to pepsin had MIP 9 made with IBMA. A slightly higher dissociation constant had MIP 5, whereas the dissociation constant of MIP 4 was much higher. This confirms that the double amount of pepsin during the imprinting resulted in an enhancement of the pepsin binding properties of the MIP. The dissociation constants of MIP 6 and 8 were between the dissociation constants of

MIP 4 and 5. The dissociation constant (K_d = 4.71 µM) of MIP 9 is in a range, which is comparable with dissociation constants of other protein imprinted polymer particles. Dissociation constants of 7.9 µM[114], 3.63 µM[116] and 1.5 µM[106] were obtained with polymer particles imprinted with atrial natriuretic peptide, lysozyme and trypsin for example. The with poly-L-lysine pepsin imprinted film had a slightly lower dissociation constant (K_d = 1.37 µM[123]), whereas pepsin imprinted polyacrylamide based nanoparticles had a very low dissociation constant (K_d = 17 pM[124]). However, this constant was determined by a different analytical method. The dissociation constant of the natural antibody of pepsin, the anti-pepsin, was not found in the literature for comparison. The dissociation constant of a monoclonal antibody specific for renin, another aspartyl protease is 0.25 µM and thus only 19 times lower than the dissociation constant of MIP 9.[221] This means that the obtained binding affinity of MIP 9 to pepsin is quite good. However, the dissociation constants of all MIPs were higher than the dissociation constants of the corresponding NIPs. This indicates that the NIPs had a higher binding affinity to pepsin than the MIPs. This is surprisingly different to that was expected. The smallest difference in the dissociation constant between MIP and NIP was obtained with MIP 6 prepared in the citrate buffer solution followed by MIP 9 made with IBMA.

2.6.10.3 Modification of the Langmuir equation

A reason for the high dissociation constants of the MIPs in comparison with the dissociation constants of the NIPs may be that the progress of the MIP isotherms did not intersect the point of origin (chapter 2.6.10.1). This means that either some of the pepsin in the solution was adsorbed somewhere else or that the determined binding capacity was too low, since the signals of the calibration solutions or of the blank samples without pepsin were too low. These were treated in the same way as the samples, but could not be totally equal, because they did not contain polymer particles or pepsin. To circumvent this problem the data of the MIPs were fitted by a modified Langmuir equation to shift the hyperbolic function around the y-axis. The Langmuir equation was therefore expanded by the introduction of a new parameter resulting in equation (2-28).

$$Q = \frac{Q_{max} c}{K_d + c} + Q_y \qquad \textbf{(2-28)}$$

Q: binding capacity
Q_{max}: maximum binding capacity
c: equilibrium concentration
K_d: dissociation constant
Q_y: new parameter

The new fits (blue curves) are compared with the Langmuir fits (green curves) and the data points of the binding isotherms of MIP 5, 6, 8 and 9 in Figure 2.59.

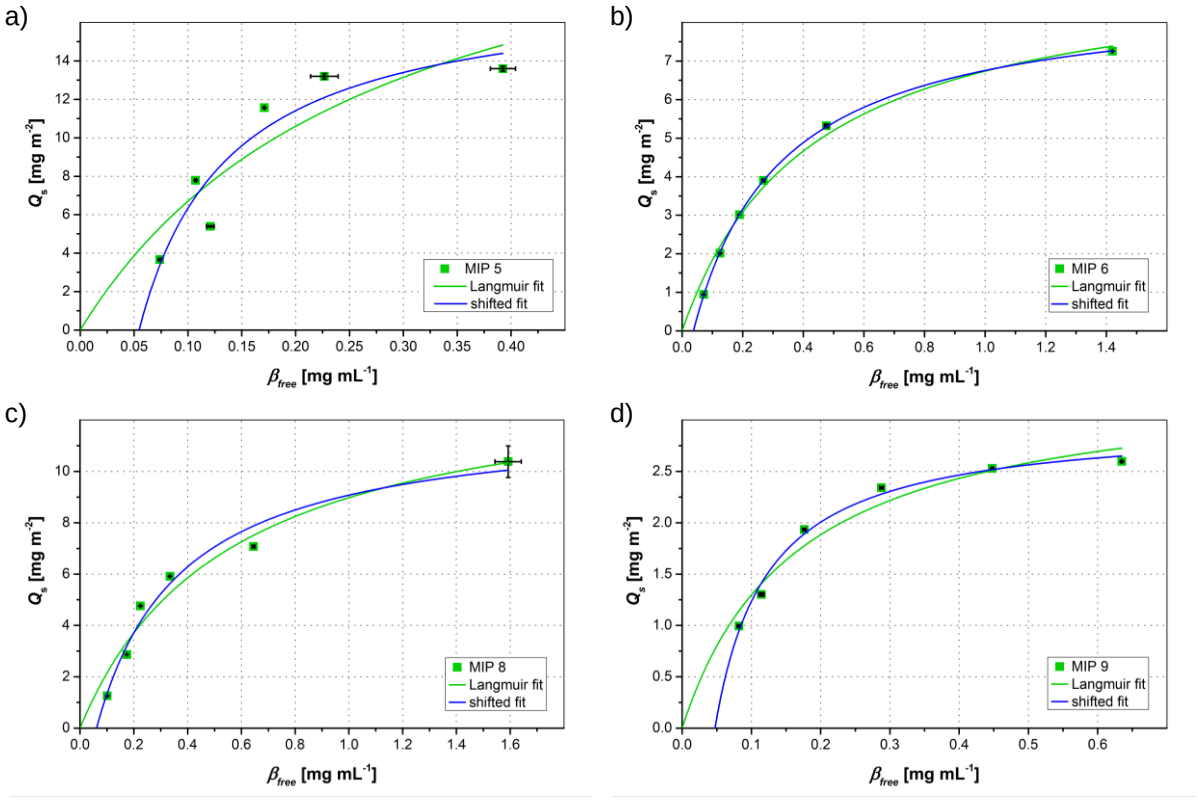

Figure 2.59 Surface-normalized pepsin binding capacities (Q_s) of MIP 5 (a), 6 (b), 8 (c) and 9 (d) depending on the free pepsin mass concentration (β_{free}). All data points represent the average of two samples. The error bars show the spread. The binding isotherms were fitted by using the usual (green) and shifted Langmuir equation (blue).

A higher curvature and a better match of the curves with the data points were obtained by shifting the fitted curves around the y-axis. Fits with a higher quality were obtained for all MIPs except for MIP 8 (compare R^2 in Table 2.10). This result was not obtained for the NIPs except for NIP 4. The maximum pepsin binding capacities and dissociation constants of the MIPs were determined with the modified Langmuir equation and are summarized in Table 2.10.

Table 2.10 Maximum surface-normalized pepsin binding capacities ($Q_{s,max}$), dissociation constants (K_d) and correlation coefficients (R^2) of the different MIPs obtained after fitting the modified Langmuir equation to the data points of their binding isotherms.

Type of polymer		$Q_{s,max}$ [mg m^{-2}]	K_d [µM]	R^2 [-]
MIP 4	APTMA	7.7	18.86	1.000
MIP 5	1 APTMA	15.9	0.81	0.803
MIP 6	pH 4	8.8	7.22	1.000
MIP 8	w/o surf	12.1	7.22	0.957
MIP 9	0.5 IBMA	3.0	0.78	0.983

The maximum surface-normalized pepsin binding capacities of all MIPs were between 3.0 and 15.9 mg m^{-2} and lower than the maximum binding capacities, which were determined with the Langmuir equation, but still higher than the maximum binding capacities of the NIPs determined with the Langmuir equation. The maximum binding capacities determined by the modified Langmuir equation followed the same trend as the ones determined with the Langmuir equation. The maximum binding capacity ($Q_{s,max}$ = 15.9 mg m^{-2}) of MIP 5 obtained with the modified Langmuir equation seems to be more realistic than the maximum binding capacity ($Q_{s,max}$ = 25.3 mg m^{-2}) obtained with the Langmuir equation when comparing with the data points. The higher curvature of the shifted fits resulted in lower dissociation constants. The dissociation constants were between 0.78 and 18.86 µM and followed the same trend as the dissociation constants determined with the Langmuir equation. The new dissociation constants of the MIPs were in the same range as the dissociation constants of the corresponding NIPs, but still slightly higher.

2.6.11 Batch rebinding of pepsin during different time intervals

A series of batch rebinding experiments was carried out during different time intervals ranging from 1 min to 20 h for studying the kinetic binding behavior of the MIPs and NIPs. The same initial pepsin concentration was used as for the rebinding experiments in chapter 2.6.9. The surface-normalized binding capacities were plotted versus the incubation time.

The surface-normalized binding capacities of MIP and NIP 5 depending on the incubation time are shown in the graph of Figure 2.60.[220] The binding capacities of the first hour are illustrated in the inset of the graph.

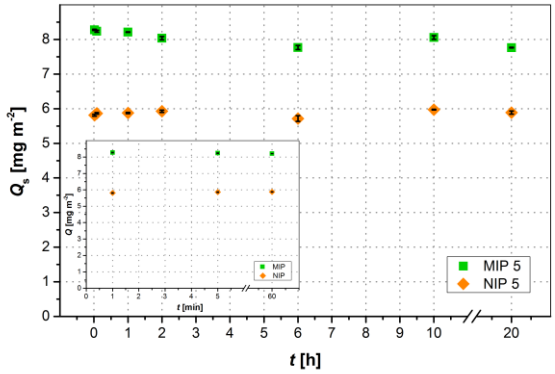

Figure 2.60 Surface-normalized pepsin binding capacities (Q_s) of MIP and NIP 5 depending on the incubation time (t). The inset illustrates the first hour. All data points represent the average of two samples. The error bars show the spread.

The maximum amount of pepsin was bound to MIP 5 after only 1 min of incubation and the amount of bound pepsin remained constant over 20 h. The binding equilibrium between pepsin and MIP 5 was thus obtained after only 1 min and the binding of pepsin to the MIP was exceptionally fast. These binding kinetics demonstrate that there was a high mass transfer rate of pepsin to the binding sites, which were located at the surface of the submicron polymer particles and thus readily accessible for the large protein molecules. The kinetic binding behavior of NIP 5 was comparably fast. The only difference of the binding behavior between MIP and NIP 5 was that significantly more pepsin was bound to the MIP. The obtained fast binding kinetics were comparable to the binding kinetics observed by G. Fu et al[116]. They reported that the binding equilibrium between lysozyme and surface imprinted core-shell submicron particles was reached within 5 min. Relative fast binding kinetics and a binding equilibrium after about 20 min were obtained by X. Shen et al[107]. In contrast, the binding equilibrium of other protein surface imprinted polymers was obtained only after around 60 min[100,150] or after up to several hours[122,143,151].

The surface-normalized binding capacities of MIP and NIP 6 were determined in a citrate buffer solution at a pH value of 4, which was also used during imprinting. Their dependence on the incubation time is illustrated in the graph of Figure 2.61. The binding capacities of the first 2 hours are illustrated in the inset of the graph.

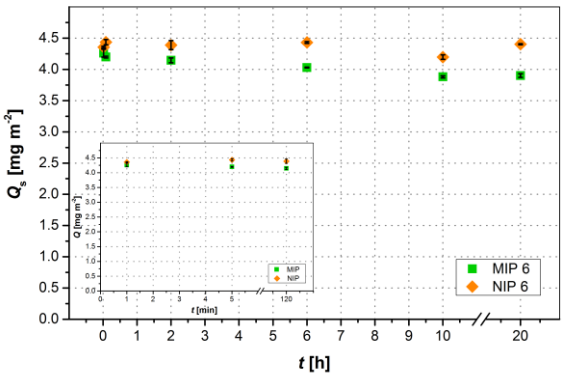

Figure 2.61 Surface-normalized pepsin binding capacities (Q_s) of MIP and NIP 6 depending on the incubation time (t). The inset illustrates the first 2 hours. All data points represent the average of two samples. The error bars show the spread.

The pepsin binding to MIP 6 was as fast as to MIP 5. The amount of bound pepsin remained almost constant over 20 h. The binding equilibrium between pepsin and the MIP was thus also obtained after only 1 min of incubation. This kinetic binding behavior demonstrates that there was a high mass transfer rate of pepsin to the binding sites of MIP 6, since they were also located at the surface of the polymer particles and thus readily accessible for pepsin. The same kinetic binding behavior was obtained for NIP 6. The use of the citrate buffer solution as incubation medium did not change the binding kinetics. Slightly more pepsin was bound to the NIP than to the MIP.

The surface-normalized binding capacities of MIP 8 depending on the incubation time are shown in the graph of Figure 2.62. The binding capacities of the first 2 hours are illustrated in the inset of the graph.

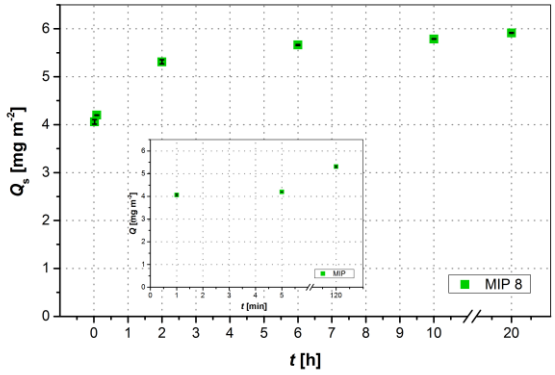

Figure 2.62 Surface-normalized pepsin binding capacities (Q_s) of MIP 8 depending on the incubation time (t). The inset illustrates the first 2 hours. All data points represent the average of two samples. The error bars show the spread.

The pepsin binding to MIP 8 was much slower than to MIP 5 and 6. The most amount of pepsin was bound only after around 6 h. The binding equilibrium was not reached after 20 h, as the pepsin binding capacities still slightly increased with increasing incubation time. These binding kinetics demonstrate that there was a lower mass transfer rate of pepsin to the binding sites of MIP 8. Possible reasons for this might be that there were more specific binding sites or that the imprinted cavities were deeper in the polymer. C. J. Tan et al reported of a MIP, which had slower binding kinetics than its corresponding NIP.[121] The binding equilibrium between BSA and the NIP was reached after around 2.5 h, whereas the binding equilibrium between BSA and the MIP was not yet reached after 23 h. They attributed this to the fact that the template protein needed more time to orientate itself to specifically fit into the imprinted cavity.

2.6.12 Batch rebinding of pepsin at different pH values

A series of batch rebinding experiments was performed at different pH values in order to investigate the influence of the pH value on the amount of bound pepsin. A citrate buffer solution was therefore used and adjusted to the pH values of 2 and 4. A phosphate buffer solution was used and adjusted to a pH value of 7. Binding capacities and imprinting factors were determined and compared with the binding capacity and imprinting factor obtained in pure water, which had a pH value of 5. The binding capacities of the NIPs are analyzed first in order to get an insight into the influence of the pH value on the pepsin binding capability. Then the binding capacities of the MIPs are compared with the binding capacities of their corresponding NIPs in order to find out, if there was increased pepsin binding as a result of the imprinting.

The surface-normalized binding capacities of MIP 6 were lower than of NIP 6 and thus no imprinting effect was observed at all pH values. A possible explanation for this is that the polymer particles may have another diameter due to a different swelling behavior in buffer solutions with different pH values, whereas the diameter used for the surface normalization was determined in pure water. Since the particle diameter was not determined in the different buffer solutions, the content of pepsin bound to MIP and NIP 6 at different pH values are shown in Figure 2.63.

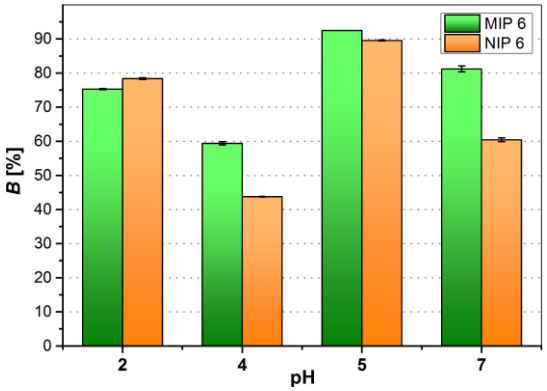

Figure 2.63 Content of pepsin bound (*B*) to MIP and NIP 6 at different pH values. All bars represent the average of two samples. The error bars show the spread.

A high amount of pepsin was bound to NIP 6 at the pH value of 2, which is minimally below the isoelectric point of pepsin (*pI* = 2.2-3.0). This means that pepsin was minimally positively charged, since pepsin contains only 4 basic amino acid residues[18]. The electrostatic repulsion between pepsin and the positively charged polymer particles was thus negligible and the high binding capacity of pepsin at pH 2 was a result of hydrophobic interactions between pepsin and the polymer. Less pepsin was bound at pH 4, at which pepsin has a negative net charge and could additionally interact with the polymer by ionic interactions. The pepsin binding capacity at pH 5 and 7 was higher than the pepsin binding capacity at pH 4, since pepsin has a higher negative net charge there and the number of ionic interactions between pepsin and the polymer particles increased. The highest

content of pepsin was bound to NIP 6 in pure water (pH 5). The binding capacity in water was probably higher than in the phosphate buffer solution (pH 7) due to the absence of buffer salts that may interfere with the ionic interactions.

More pepsin was bound to MIP 6 than to NIP 6 at the pH values of 4 and 7. This resulted in imprinting factors of 1.4 and 1.3. The imprinting effect in the citrate buffer solution with the pH value of 4 was obtained, since the imprinting was performed in the same solution. The pepsin conformation that existed during the polymerization was thus imprinted into the polymer and only this structure was selectively recognized by the MIP. Furthermore, the polymer had the same swelling behavior as during the imprinting, which can affect the steric position of the functional groups and thus the selective binding. An explanation for the imprinting effect at pH 7 might be that pepsin has a similar structure there. It has been reported that pepsin adopts a native-like, but catalytically inactive conformation between pH 4.0 and 6.5.[215]

The graph in Figure 2.64 shows the content of pepsin bound to MIP 8 at different pH values.

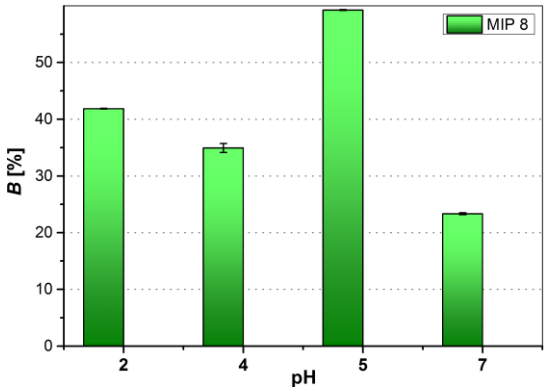

Figure 2.64 Content of pepsin bound (*B*) to MIP 8 at different pH values. All bars represent the average of two samples. The error bars show the spread.

The content of pepsin bound to MIP 8 at different pH values followed the same trend as the content of pepsin bound to MIP and NIP 6 except at pH 7. The content of bound pepsin at pH 7 was lower than the content of bound pepsin at the other pH values. The maximum amount of pepsin was bound to MIP 8 in water (pH 5) without any buffer salts.

2.6.13 Single batch rebinding of different proteins

Batch rebinding experiments were performed with different proteins in the same way as with pepsin in chapter 2.6.9 to examine the selectivity of the different polymer particles for pepsin. The same amount of substance of each protein as of pepsin was used. The surface-normalized binding capacities were divided by the molecular weight of the different proteins to compare the number of bound protein molecules. Selectivity factors were determined. Thermolysin (35 kDa, *pI* = 5), trypsin (24 kDa, *pI* = 11), lysozyme (14 kDa, *pI* = 11) and hemoglobin (65 kDa, *pI* = 7) were used as competitive proteins, since they have different molecular weights, isoelectric points and amino acid residue compositions. Thermolysin and trypsin are proteases as pepsin. Thermolysin has the same molecular weight as pepsin and an isoelectric point, which is not as low as the isoelectric point of pepsin, but relatively low compared with other proteins. The amount of bound pepsin (35 kDa, *pI* = 2.2-3.0) is compared with the amounts of bound competitive proteins. The binding capacities of the NIPs are analyzed first in order to get insight into the intrinsic selectivity of the different polymer particles. Then the selectivity of the MIPs is compared with the selectivity of their corresponding NIPs in order to find out, if there is increased selectivity as a result of the imprinting. Finally the MIPs are compared with one another and the selectivity factors are discussed.

2.6.13.1 Different other parameters

The surface-normalized binding capacities of MIP and NIP 5 for different proteins are compared in the graph of Figure 2.65.[213]

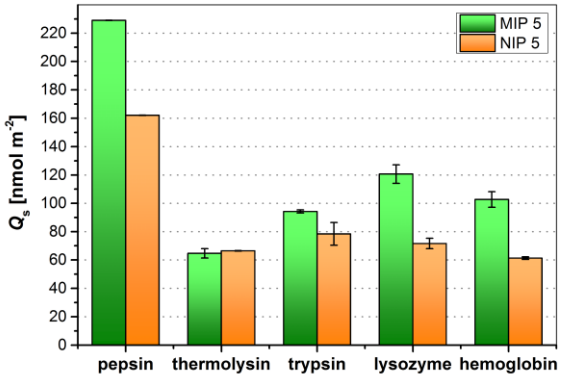

Figure 2.65 Surface-normalized binding capacities (Q_s) of MIP and NIP 5 for different proteins. All bars represent the average of two samples. The error bars show the spread.

At least two times more pepsin than the other proteins was bound to NIP 5. This shows that the polymer itself had a higher affinity to pepsin than for the other proteins and thus an intrinsic selectivity for pepsin. This can be explained by the different isoelectric points of the proteins coming from a different content of acidic and basic amino acid residues. This results in different net charges of the proteins depending on the pH value of the incubation medium. Pepsin is the only protein that

has a negative net charge in pure water with a pH value of 5 used as incubation medium. Thermolysin is neutral and trypsin, lysozyme and hemoglobin are positively charged here. Pepsin could thus form more ionic interactions with the positively charged polymer particles than the other proteins. These findings indicate that ionic interactions play an important role in binding pepsin. The different sizes of the proteins did not affect the binding capacity.

MIP 5 did not only bind more pepsin, but also more of all other proteins except of thermolysin than NIP 5 contrary to expectations. While the selectivity for pepsin against thermolysin was significantly and against trypsin slightly improved, the selectivity for pepsin against lysozyme and hemoglobin was not improved due to the imprinting.

The surface-normalized binding capacities of MIP and NIP 6 for different proteins are compared in the graph of Figure 2.66.

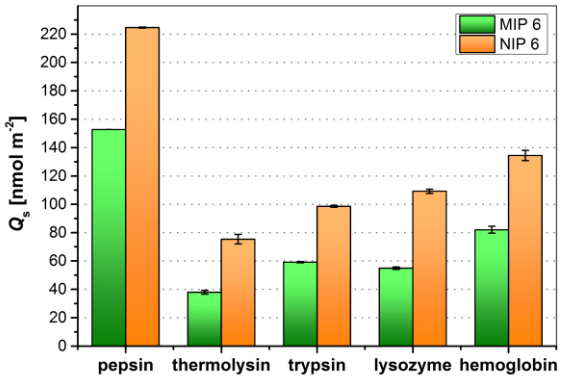

Figure 2.66 Surface-normalized binding capacities (Q_s) of MIP and NIP 6 for different proteins. All bars represent the average of two samples. The error bars show the spread.

Around 2 to 3 times more pepsin than the other proteins was bound to NIP 6 in pure water (pH 5). This shows that NIP 6 had an intrinsic selectivity for pepsin as NIP 5 due to the different isoelectric points of the different proteins and stronger ionic interactions with pepsin. There was no influence of the different sizes of the proteins on the binding capacity.

MIP 6 bound less of all proteins than NIP 6 and around 2 to 4 times more pepsin than the other proteins thus showing a higher selectivity for pepsin against all competitive proteins than NIP 6. The selectivity was thus improved due to the imprinting in a citrate buffer solution, even if the rebinding experiments were carried out in water and less pepsin was bound to the MIP than to the NIP.

The surface-normalized binding capacities of MIP 8 for different proteins are compared in the graph of Figure 2.67.

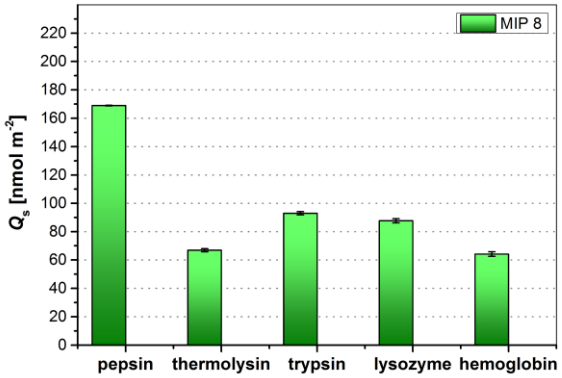

Figure 2.67 Surface-normalized binding capacities (Q_s) of MIP 8 for different proteins. All bars represent the average of two samples. The error bars show the spread.

MIP 8 bound around 2 times more pepsin than the other proteins. Certain selectivity for pepsin against the other proteins was thus obtained without the surfactant during the imprinting. The highest selectivity for pepsin was obtained against thermolysin and hemoglobin.

The surface-normalized binding capacities of MIP and NIP 9 for different proteins are compared in the graph of Figure 2.68.

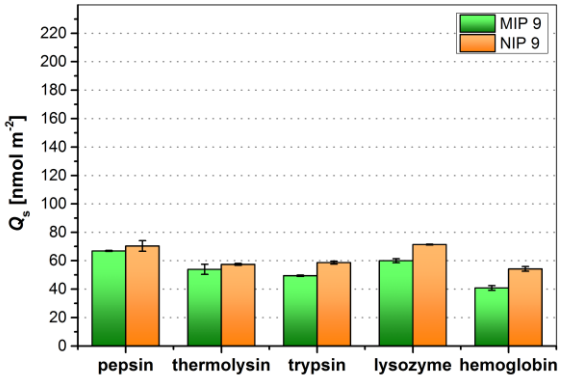

Figure 2.68 Surface-normalized binding capacities (Q_s) of MIP and NIP 9 for different proteins. All bars represent the average of two samples. The error bars show the spread.

Almost the same amount of each protein was bound to NIP 9. This shows that NIP 9 had no or a negligible selectivity for pepsin against the other proteins as a result of the lower number of positively charged functional groups in NIP 9 through the replacement of half the amount of APTMA by IBMA in the monomer mixture. The additional hydrophobic interactions with isobutyl groups of IBMA units seemed to be less effective in pepsin binding than ionic interactions, but did not affect the binding of the other proteins, as around the same amount of the other proteins was bound to NIP 9 as to NIP 5.

The binding capacities of MIP 9 for different proteins were quite comparable to the binding capacities of NIP 9. Minimally more pepsin than the other proteins was bound to the MIP. The selectivity of the MIP for pepsin was thus low. The use of an additional hydrophobic functional monomer did not increase the selectivity for pepsin, as the selectivity of MIP 9 was lower than the selectivity of MIP 5, 6 and 8.

The surface-normalized binding capacities of MIP and NIP 10 for different proteins are compared in the graph of Figure 2.69.

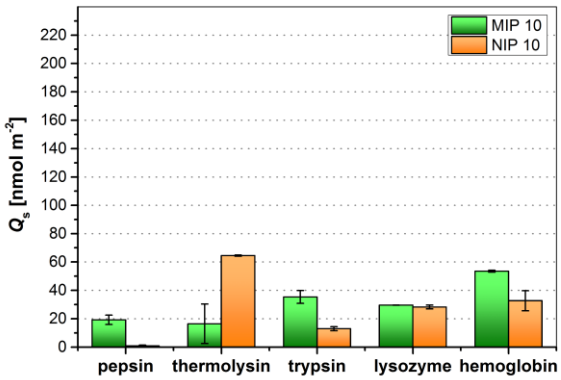

Figure 2.69 Surface-normalized binding capacities (Q_s) of MIP and NIP 10 for different proteins. All bars represent the average of two samples. The error bars show the spread.

A higher amount of the other proteins, in particular of thermolysin, than of pepsin was bound to NIP 10. No selectivity for pepsin against all other proteins was thus obtained due to the very low number of positively charged functional groups in the polymer. A lower amount of trypsin, lysozyme and hemoglobin was bound to NIP 10 than to NIP 5 and 9 due to fewer interactions of these proteins with the polymer made with mainly EGDMA.

The binding capacities of MIP 10 for different proteins were similarly low as the binding capacities of NIP 10. The MIP had a low selectivity for pepsin against thermolysin and no selectivity for pepsin against the other proteins as a result of the reduction of the amount of APTMA in the polymerization mixture, although this MIP showed a high imprinting effect.

2.6.13.2 Different extraction solutions

The surface-normalized binding capacities of MIP and NIP 11 for different proteins are compared in the graph of Figure 2.70.

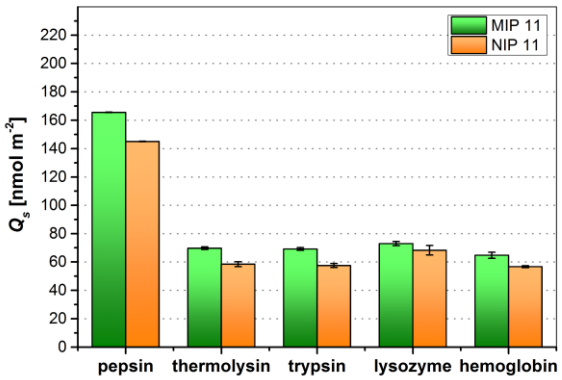

Figure 2.70 Surface-normalized binding capacities (Q_s) of MIP and NIP 11 for different proteins. All bars represent the average of two samples. The error bars show the spread.

At least 2 times more pepsin than the other proteins was bound to NIP 11. The binding capacities of NIP 11 were comparable with the binding capacities of NIP 5. This shows that NIP 11 also had an intrinsic selectivity for pepsin, which was not changed through washing the polymer particles in HCl. MIP 11 bound slightly more of all proteins than NIP 11. At least 2 times more pepsin than the other proteins was bound to MIP 11. This shows that the MIP also had selectivity for pepsin against the other proteins, but only an increased selectivity against lysozyme compared with NIP 11. The selectivity for pepsin against lysozyme and hemoglobin, but not against thermolysin and trypsin was increased compared with MIP 5 due to the extraction of pepsin in HCl.

The surface-normalized binding capacities of MIP and NIP 12 for different proteins are compared in the graph of Figure 2.71.

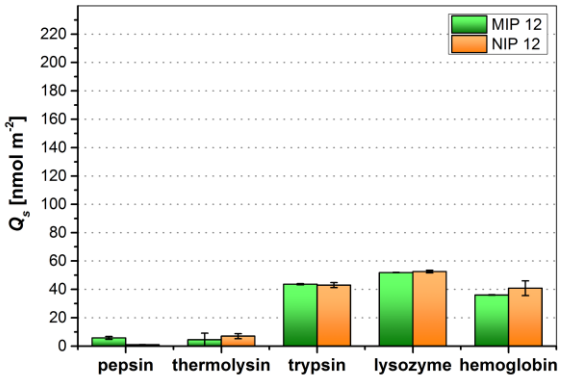

Figure 2.71 Surface-normalized binding capacities (Q_s) of MIP and NIP 12 for different proteins. All bars represent the average of two samples. The error bars show the spread.

A higher amount of the other proteins than of pepsin was bound to NIP 12. This shows that there was no selectivity for pepsin against all other proteins due to the very low number of positively charged functional groups in the polymer. This was the same result as obtained for NIP 10.

The binding capacities of MIP 12 for different proteins were as low as the binding capacities of NIP 12 and MIP 10. MIP 12 had a low selectivity for pepsin against thermolysin and no selectivity for pepsin against the other proteins as MIP 10. Hence, the extraction of pepsin with NaOH improved the selectivity of MIP 12 compared to NIP 12 and MIP 10 for pepsin against thermolysin.

The surface-normalized binding capacities of MIP and NIP 13 for different proteins are compared in the graph of Figure 2.72.

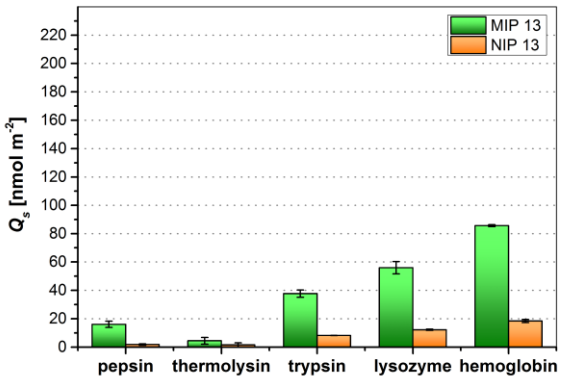

Figure 2.72 Surface-normalized binding capacities (Q_s) of MIP and NIP 13 for different proteins. All bars represent the average of two samples. The error bars show the spread.

A higher amount of the other proteins than of pepsin except of thermolysin was bound to NIP 13. This shows that there was a low selectivity for pepsin against thermolysin, but not against the other proteins due to the very low number of positively charged functional groups in the polymer. The low selectivity against thermolysin was not obtained for NIP 10 and 12 and may be a result of the washing in the sodium chloride solution.

The binding capacities of MIP 13 for different proteins were higher than of NIP 13. MIP 13 had a higher selectivity for pepsin against thermolysin than NIP 13 and MIP 10 and 12, but also no selectivity against the other proteins. Hence, the extraction of pepsin with the sodium chloride solution seems to have improved the selectivity for pepsin against thermolysin, but not against the other proteins.

2.6.13.3 Selectivity factors

The selectivity factors between pepsin and the different proteins of the different polymer particles are summarized in Table 2.11.

Table 2.11 Selectivity factor (*SF*) depending on the type of polymer and competitive protein. The numbers, which represent selectivity for pepsin (*SF* > 1), are marked in bold.

Type of polymer		Selectivity factor *SF*			
		thermolysin	trypsin	lysozyme	hemoglobin
MIP 5	1 APTMA	**3.5**	**2.4**	**1.9**	**2.2**
NIP 5		**2.4**	**2.1**	**2.3**	**2.6**
MIP 6	pH 4	**4.0**	**2.6**	**2.8**	**1.9**
NIP 6		**3.0**	**2.3**	**2.1**	**1.7**
MIP 8	w/o surf	**2.5**	**1.8**	**1.9**	**2.6**
MIP 9	0.5 IBMA	**1.2**	**1.4**	**1.1**	**1.6**
NIP 9		**1.2**	**1.2**	1.0	**1.3**
MIP 10	0.1 APTMA	**1.2**	0.5	0.6	0.4
NIP 10		0.0	0.1	0.0	0.0
MIP 11	HCl*	**2.4**	**2.4**	**2.3**	**2.6**
NIP 11		**2.5**	**2.5**	**2.1**	**2.6**
MIP 12	NaOH*	**1.3**	0.1	0.1	0.2
NIP 12		0.1	0.0	0.0	0.0
MIP 13	NaCl*	**3.6**	0.4	0.3	0.2
NIP 13		**1.2**	0.2	0.2	0.1

* Extraction solution.

MIP 5, 6, 8, 9 and 11 had selectivity factors above 1 meaning that they were selective for pepsin against all competitive proteins. The average selectivity factor of MIP 9 was lower than of MIP 5, 6, 8 and 11. MIP 10, 12 and 13 had only selectivity for pepsin against thermolysin. This suggests that the selectivity of MIP 5, 6, 8 and 11 was mainly based on ionic interactions. The highest selectivity factors between pepsin and thermolysin (*SF* = 4.0), trypsin (*SF* = 2.6) and lysozyme (*SF* = 2.8) and the highest average selectivity factor were obtained with MIP 6. The highest selectivity factor between pepsin and hemoglobin (*SF* = 2.6) was obtained with MIP 8 and MIP 11, but also with NIP 5 and 11. These selectivity factors are in the low to medium range compared with selectivity factors of other protein imprinted polymers, which are usually between 2 and 16[106,107,116,119].

Since most of the NIPs also showed selectivity for pepsin due to ionic interactions and different isoelectric points of the proteins, the selectivity factors of the MIPs were divided by the selectivity factors of the NIPs resulting in the relative selectivity factors, which are summarized in Table 2.12.

Table 2.12 Relative selectivity factor (*RSF*) depending on the type of polymer and competitive protein. The numbers, which represent a higher selectivity for pepsin of the MIP compared with the NIP (*RSF* > 1), are marked in bold.

Type of polymer		Relative selectivity factor *RSF*			
		thermolysin	trypsin	lysozyme	hemoglobin
5	1 APTMA	**1.5**	**1.2**	0.8	0.8
6	pH 4	**1.4**	**1.1**	**1.4**	**1.1**
9	0.5 IBMA	1.0	**1.1**	**1.1**	**1.3**
10	0.1 APTMA	**91.0**	**8.5**	**22.2**	**14.2**
11	HCl*	1.0	0.9	**1.1**	1.0
12	NaOH*	**9.3**	**5.8**	**6.0**	**6.7**
13	NaCl*	**3.0**	**1.9**	**1.9**	**1.9**

* Extraction agent.

The relative selectivity factors, which are higher than 1, are marked in bold. This stands for an increase of the selectivity factor due to the imprinting and was obtained with MIP 6, 10, 12 and 13 for pepsin against all proteins. This was obtained with MIP 9 against 3 proteins, with MIP 5 against 2 and with MIP 11 only against 1 protein. The highest increase of the selectivity factors of a MIP in comparison with the selectivity factors of its corresponding NIP was obtained with MIP 10, although only the selectivity factor of MIP 10 between pepsin and thermolysin was above 1. A similar result, but with lower relative selectivity factors was obtained with MIP 12 and 13. Since an increase of all selectivity factors due to the imprinting was also obtained with MIP 6 and all selectivity factors of MIP 6 were above 1, it was therefore considered that the highest improvement of the selectivity for pepsin against all proteins due to the imprinting was obtained with a high amount of APTMA in a citrate buffer solution.

2.6.14 Single batch rebinding of pepsin and α1-acid glycoprotein

Batch rebinding experiments were performed with pepsin and α1-acid glycoprotein in the same way as with pepsin in chapter 2.6.9 to further investigate the influence of the ionic interactions on the selectivity of the MIPs and NIPs for pepsin. The same amount of substance of α1-acid glycoprotein as of pepsin was used. The same normalization of the binding capacity as in chapter 2.6.13 was used and selectivity factors were determined. α1-Acid glycoprotein (41 kDa, *pI* = 2.7) is one of only few proteins, which has a very similar isoelectric point and molecular weight as pepsin, and was therefore used as an additional competitive protein. The amount of bound pepsin (35 kDa, *pI* = 2.2-3.0) is compared with the amount of bound α1-acid glycoprotein. The binding capacities of the NIPs are analyzed first in order to get insight into the intrinsic selectivity of the different polymer particles. Then the selectivity of the MIPs is compared with the selectivity of their corresponding NIPs in order to find out, if there is increased selectivity as a result of the imprinting. Finally the MIPs are compared with one another and the selectivity factors are discussed.

2.6.14.1 Binding capacities

The surface-normalized binding capacities of MIP and NIP 5 for pepsin and α1-acid glycoprotein are compared in the graph of Figure 2.73.[220]

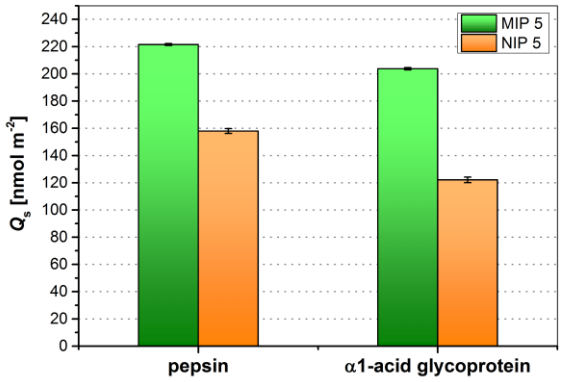

Figure 2.73 Surface-normalized binding capacities (Q_s) of MIP and NIP 5 for pepsin and α1-acid glycoprotein. All bars represent the average of two samples. The error bars show the spread.

More α1-acid glycoprotein than the other proteins of chapter 2.6.13 was bound to NIP 5, since this has a negative net charge in pure water (pH 5) used as incubation medium due to its lower isoelectric point and could thus interact with the positively charged polymer particles by ionic interactions as pepsin. This shows that there was a significant effect of ionic interactions and the isoelectric points of the proteins on the selectivity of the NIP, but still more pepsin than α1-acid glycoprotein was bound to the NIP.

A little less α1-acid glycoprotein than pepsin was bound to MIP 5. The selectivity of the MIP for pepsin against α1-acid glycoprotein was smaller than of NIP 5. Hence, the imprinting did not result

in a higher selectivity for pepsin against α1-acid glycoprotein, although more pepsin was bound to the MIP than to the NIP.

The surface-normalized binding capacities of MIP and NIP 6 for pepsin and α1-acid glycoprotein are compared in the graph of Figure 2.74.

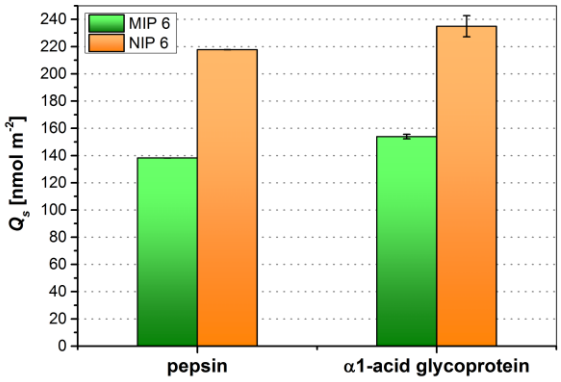

Figure 2.74 Surface-normalized binding capacities (Q_s) of MIP and NIP 6 for pepsin and α1-acid glycoprotein. All bars represent the average of two samples. The error bars show the spread.

More α1-acid glycoprotein was bound to NIP 6 than to NIP 5 and more α1-acid glycoprotein than pepsin and the other proteins of chapter 2.6.13 was bound to NIP 6. No selectivity for pepsin against α1-acid glycoprotein was thus obtained for NIP 6.

Also more α1-acid glycoprotein than pepsin was bound to MIP 6. No selectivity for pepsin against α1-acid glycoprotein was thus obtained in water through the imprinting in a citrate buffer solution.

The surface-normalized binding capacities of MIP and NIP 11 for pepsin and α1-acid glycoprotein are compared in the graph of Figure 2.75.

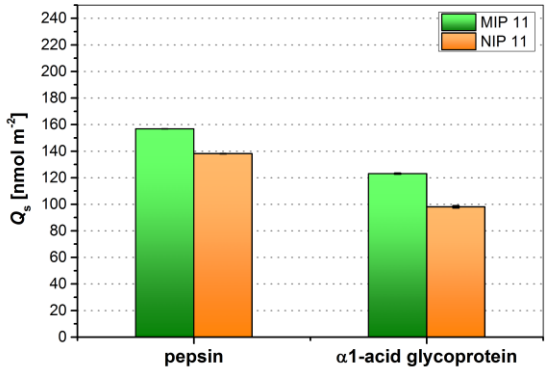

Figure 2.75 Surface-normalized binding capacities (Q_s) of MIP and NIP 11 for pepsin and α1-acid glycoprotein. All bars represent the average of two samples. The error bars show the spread.

More α1-acid glycoprotein than the other proteins of chapter 2.6.13 was bound to NIP 11, but less compared to NIP 5 and 6. Slightly more pepsin than α1-acid glycoprotein was bound to NIP 11 resulting in selectivity for pepsin against α1-acid glycoprotein as for NIP 5.

A little more pepsin than α1-acid glycoprotein was bound to MIP 11 resulting in a low selectivity for pepsin against α1-acid glycoprotein, which was lower than of the NIP. Hence, the imprinting did not

result in a higher selectivity for pepsin against α1-acid glycoprotein, although slightly more pepsin was bound to the MIP than to the NIP.

2.6.14.2 Selectivity factors

The selectivity factors between pepsin and α1-acid glycoprotein of the different polymer particles are summarized in Table 2.13.

Table 2.13 Selectivity factor (*SF*) between pepsin and α1-acid glycoprotein depending on the type of polymer. The numbers, which represent selectivity for pepsin (*SF* > 1), are marked in bold.

Type of polymer		Selectivity factor *SF*
		α1-acid glycoprotein
MIP 5	1 APTMA	**1.1**
NIP 5		**1.3**
MIP 6	pH 4	0.9
NIP 6		0.9
MIP 11	HCl*	**1.3**
NIP 11		**1.4**

* Extraction solution.

MIP 5 and 11 have selectivity factors above 1 meaning that they are selective for pepsin against α1-acid glycoprotein. But the selectivity factors of their corresponding NIPs are higher meaning that there is no improved selectivity due to the imprinting. Perhaps α1-acid glycoprotein has subdomains similar to pepsin and thus could also interact with the functional groups of the MIPs and fits into the imprinted cavities, since its molecular weight is similar. MIP and NIP 6 are not selective for pepsin against α1-acid glycoprotein. These results show that there was a big influence of ionic interactions and the isoelectric points of the proteins on the selectivity of the MIPs and NIPs.

2.6.15 Competitive batch rebinding of different proteins

Competitive batch rebinding experiments were performed with a mixture of different proteins to investigate the selectivity of the different polymer particles for pepsin in the presence of other proteins, which can compete for the binding sites of the polymer particles. The same amount of substance of each protein as of pepsin was used, while the same ratio between pepsin and the polymer was used as in the previous rebinding experiments. Pepsin was pre-incubated with the inhibitor pepstatin before the incubation with the polymer particles and the other proteins to quench their degradation by pepsin overnight. The polymer particles were removed from the solution by centrifugation after the incubation. The proteins remaining in the supernatant were separated by sodium dodecyl sulfate-polyacrylamide gel electrophoresis (SDS-PAGE) and stained with Coomassie blue, since their UV absorbance spectra overlaid and their quantification by UV-Vis spectrophotometry was therefore too complicated. The same experiments were performed with the proteins separately and a mixture of pepsin or the pepsin-pepstatin associate and the other proteins as reference samples. Control samples were prepared with the polymer particles, but without pepsin and the other proteins in the same way. The resulting gels did not show any pepsin bands. This ensured that there is no leaching out of pepsin from the polymer during the rebinding. The same batch rebinding experiments were carried out without pre-incubation of pepsin with pepstatin to provide additional information, if the polymer particles are able to inhibit the activity of pepsin through binding pepsin via the active site or affecting denaturation of pepsin.

Thermolysin has the same molecular weight as pepsin and could thus not be separated from pepsin by SDS-PAGE. The bands of lysozyme and hemoglobin overlaid and lysozyme formed a complex with pepsin. For these reasons, new competitive proteins were introduced. Bovine serum albumin (BSA, 66 kDa, $pI = 5$) and β-lactoglobulin (LG, 18 kDa, $pI = 5$) were used, since they have low isoelectric points, different amino acid residue compositions and different molecular weights, so that they can be separated from pepsin by SDS-PAGE. Another reason for using LG was that it is not degraded by pepsin[222]. The pattern of the reference lanes are discussed on the basis of the first SDS-PAGE gel with MIP and NIP 5. This is valid for the following gels, since they contain the same reference lanes with the same patterns. The competitive selectivity study with the inhibited pepsin is discussed first. The protein mixture after the incubation with the MIPs and NIPs are analyzed and compared with one another in order to find out, if there is increased pepsin binding and selectivity as a result of the imprinting. Then the inhibition study is discussed. Finally the content of proteins bound to the different MIPs and NIPs, which were determined by comparing the density of the sample bands with the density of the reference bands on the gels using the program ImageJ, are compared with one another and with the results of the previous rebinding experiments. The results of a competitive and an individual selectivity study analyzed by SDS-PAGE are compared in the last subchapter.

2.6.15.1 Different other parameters

An image of the SDS-PAGE gel of the competitive batch rebinding experiments with MIP and NIP 5 and the different proteins is shown in the graph of Figure 2.76.[220]

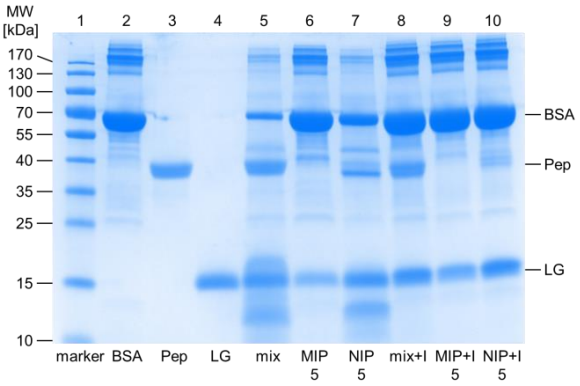

Figure 2.76 Image of the SDS-PAGE gel of the supernatants. Lane 1: molecular weight marker, lane 2: BSA, lane 3: pepsin (Pep), lane 4: LG, lane 5: protein mixture, lane 6 and 7: protein mixture after incubation with MIP and NIP 5, lane 8: protein mixture with pepstatin (+I), lane 9 and 10: protein mixture with pepstatin after incubation with MIP and NIP 5.

Lane 1 contained the protein molecular weight marker, while lane 2, 3 and 4 show the bands of neat BSA, pepsin and LG, respectively, and lane 5 shows the bands of these proteins in a mixture as references. The intensity of the BSA band in lane 5 was much lower than of the band of neat BSA in lane 2 due to the cleavage of BSA by pepsin during the incubation. The band of LG in lane 5 resembled the band of neat LG in lane 3 except that it was convoluted with bands of BSA fragments. This means that LG was evidently not degraded by pepsin as reported[222]. Lane 8 shows the protein mixture after the pre-incubation of pepsin with pepstatin as further reference. The band of each protein was comparable to the band of the respective neat protein. This thus confirms that the pepsin activity was effectively inhibited by the addition of pepstatin and that the band of each protein was not affected due to the presence of the other proteins and the inhibitor in the same solution.

The lanes 9 and 10 show the protein mixture after the pre-incubation of pepsin with pepstatin and the incubation with MIP and NIP 5, respectively. NIP 5 apparently bound more than half the amount of pepsin and no LG and BSA, since less than half the amount of pepsin and the entire amount of LG and BSA were still in the supernatant. This shows that the NIP had an intrinsic selectivity for pepsin against BSA and LG. BSA and LG have a higher isoelectric point than pepsin and are thus neutral in water (pH 5), whereas pepsin has a negative net charge and thus was subject to attractive ionic interactions. The entire amount of pepsin and a little less than half the amount of LG were absent in the protein mixture and thus apparently bound to MIP 5, whereas the entire amount of BSA was still in the solution. No improvement of the selectivity was thus obtained due to the imprinting.

The lanes 6 and 7 show the protein mixture without pre-incubation of pepsin with pepstatin after the incubation with MIP and NIP 5, respectively. The patterns of the lanes 6 and 9 were comparable

thus indicating that the pepsin activity was inhibited by binding to the MIP and thus blocking the access of the substrate to the catalytic site. The bands of pepsin in the lanes 6 and 9 were comparable thus indicating that pepstatin did not influence the binding efficiency between pepsin and the MIP. The intensity of the BSA band in lane 7 was smaller than of the band of neat BSA in lane 2, but larger than of the BSA band in the protein mixture in lane 5. This shows that the pepsin remaining in solution, which was not bound to the NIP, was able to degrade BSA, whereas the bound pepsin was inhibited.

An image of the SDS-PAGE gel of the competitive batch rebinding experiments with MIP and NIP 6 and the different proteins is shown in the graph of Figure 2.77.

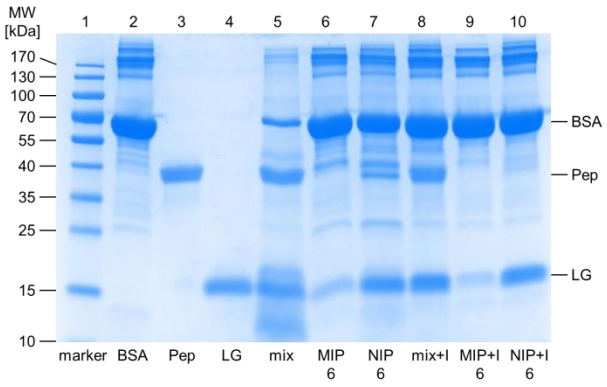

Figure 2.77 Image of the SDS-PAGE gel of the supernatants. Lane 1: molecular weight marker, lane 2: BSA, lane 3: pepsin (Pep), lane 4: LG, lane 5: protein mixture, lane 6 and 7: protein mixture after incubation with MIP and NIP 6, lane 8: protein mixture with pepstatin (+I), lane 9 and 10: protein mixture with pepstatin after incubation with MIP and NIP 6.

The patterns of the lanes 9 and 10 show that the entire content of pepsin was bound to MIP 6 and slightly less pepsin was bound to NIP 6. BSA was neither bound to the MIP nor to the NIP. Much more LG was bound to MIP 6 than to NIP 6. Hence, selectivity against BSA was obtained with the MIP and the NIP and a lower selectivity against LG was obtained with MIP 6 than with NIP 6, maybe since the selectivity study was carried out in water and not in a citrate buffer solution as the imprinting.

The patterns of the lanes 6 and 9 were comparable thus indicating that the pepsin activity was inhibited by binding to MIP 6. The intensity of the BSA band in lane 7 of the gel of NIP 6 was higher than of the same band of the gel of NIP 5, since more pepsin was bound to NIP 6. This clarifies that only the pepsin remaining in solution was able to degrade BSA, whereas the bound pepsin was inhibited by binding to the NIP.

An image of the SDS-PAGE gel of the competitive batch rebinding experiments with MIP 8 and the different proteins is shown in the graph of Figure 2.78.

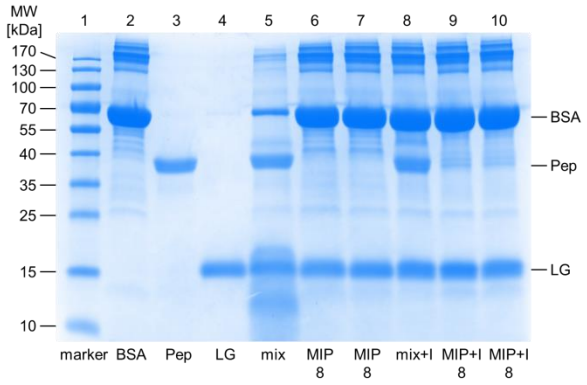

Figure 2.78 Image of the SDS-PAGE gel of the supernatants. Lane 1: molecular weight marker, lane 2: BSA, lane 3: pepsin (Pep), lane 4: LG, lane 5: protein mixture, lane 6 and 7: protein mixture after incubation with MIP 8, lane 8: protein mixture with pepstatin (+I), lane 9 and 10: protein mixture with pepstatin after incubation with MIP 8.

The pattern of lane 9 shows that a high amount of pepsin and no LG and BSA were bound to MIP 8. This resulted in a high selectivity against LG and BSA. This result was reproduced in lane 10 and may come from successful imprinting without the surfactant. The patterns of the lanes 6 and 9 were slightly different. It seems that more pepsin was bound to the MIP without pepstatin here.

An image of the SDS-PAGE gel of the competitive batch rebinding experiments with MIP and NIP 9 and the different proteins is shown in the graph of Figure 2.79.[159]

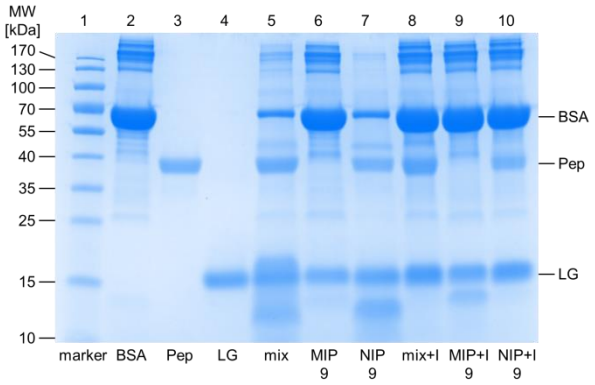

Figure 2.79 Image of the SDS-PAGE gel of the supernatants. Lane 1: molecular weight marker, lane 2: BSA, lane 3: pepsin (Pep), lane 4: LG, lane 5: protein mixture, lane 6 and 7: protein mixture after incubation with MIP and NIP 9, lane 8: protein mixture with pepstatin (+I), lane 9 and 10: protein mixture with pepstatin after incubation with MIP and NIP 9.

The patterns of the lanes 9 and 10 show that the entire amount of pepsin was bound to MIP 9, but only a low amount of pepsin was bound to NIP 9. No BSA was bound to the MIP and NIP. Slightly more LG was bound to the MIP than to the NIP. This resulted in an improvement of the selectivity against both proteins due to the imprinting. The patterns of the lanes 6 and 9 were comparable thus indicating that the pepsin activity was inhibited by binding to the MIP. The intensity of the BSA band in lane 7 was low, since only a low amount of pepsin was bound to NIP 6.

An image of the SDS-PAGE gel of the competitive batch rebinding experiments with MIP and NIP 10 and the different proteins is shown in the graph of Figure 2.80.

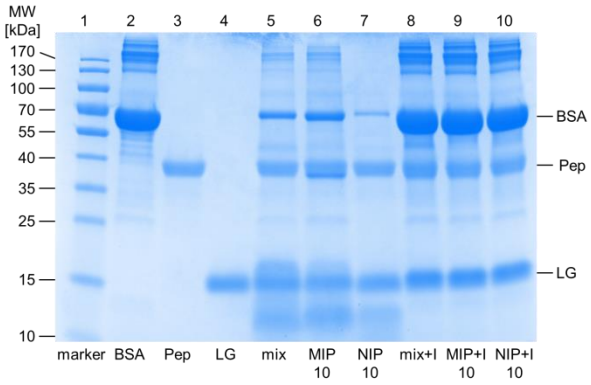

Figure 2.80 Image of the SDS-PAGE gel of the supernatants. Lane 1: molecular weight marker, lane 2: BSA, lane 3: pepsin (Pep), lane 4: LG, lane 5: protein mixture, lane 6 and 7: protein mixture after incubation with MIP and NIP 10, lane 8: protein mixture with pepstatin (+I), lane 9 and 10: protein mixture with pepstatin after incubation with MIP and NIP 10.

The patterns of the lanes 9 and 10 show that almost the entire amounts of all proteins were still in the solution and thus apparently not bound to MIP and NIP 10. This may be explained by the low amount of APTMA units in the polymer and that the proteins did not interact with EGDMA units. Hence, neither pepsin binding nor any selectivity was obtained. The intensity of the BSA bands in the lanes 6 and 7 was low, since almost no pepsin was bound to the MIP and NIP. This shows that the inhibition of the pepsin activity by the polymer came from a binding event.

2.6.15.2 Different extraction solutions

An image of the SDS-PAGE gel of the competitive batch rebinding experiments with MIP and NIP 11 and the different proteins is shown in the graph of Figure 2.81.

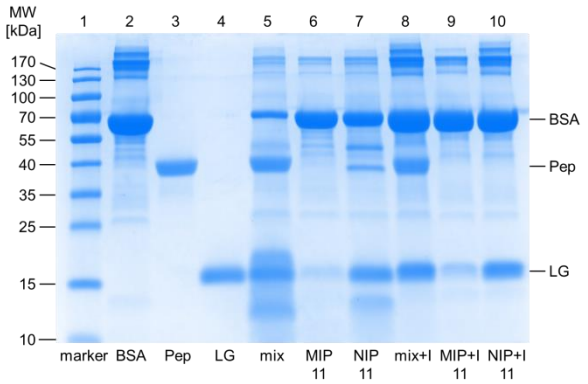

Figure 2.81 Image of the SDS-PAGE gel of the supernatants. Lane 1: molecular weight marker, lane 2: BSA, lane 3: pepsin (Pep), lane 4: LG, lane 5: protein mixture, lane 6 and 7: protein mixture after incubation with MIP and NIP 11, lane 8: protein mixture with pepstatin (+I), lane 9 and 10: protein mixture with pepstatin after incubation with MIP and NIP 11.

The patterns of the lanes 9 and 10 show that in each case the entire amount of pepsin was bound to MIP and NIP 11. BSA was neither bound to the MIP nor to the NIP. Much more LG was bound to MIP than to NIP 11. The selectivity for pepsin against LG and BSA was thus not improved due to the

extraction in HCl. The intensity of the BSA bands in the lanes 6 and 7 was slightly lower than of the BSA bands in the lanes 9 and 10. It seems as if slightly less pepsin was bound without the inhibitor.
An image of the SDS-PAGE gel of the competitive batch rebinding experiments with MIP and NIP 12 and the different proteins is shown in the graph of Figure 2.82.

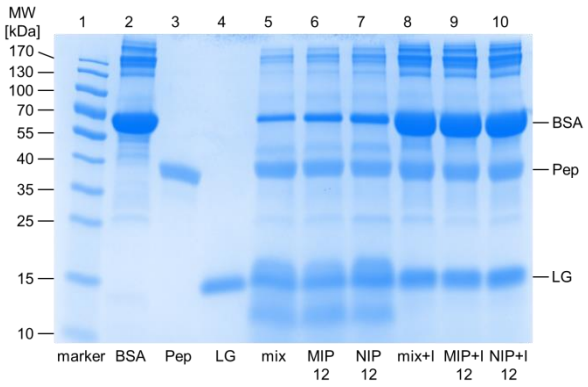

Figure 2.82 Image of the SDS-PAGE gel of the supernatants. Lane 1: molecular weight marker, lane 2: BSA, lane 3: pepsin (Pep), lane 4: LG, lane 5: protein mixture, lane 6 and 7: protein mixture after incubation with MIP and NIP 12, lane 8: protein mixture with pepstatin (+I), lane 9 and 10: protein mixture with pepstatin after incubation with MIP and NIP 12.

The patterns of the lanes 9 and 10 show that almost the entire amounts of all proteins were still in the solution and thus apparently not bound to MIP and NIP 12. This means that the selectivity was not improved due to the extraction in sodium hydroxide. The intensity of the BSA bands in the lanes 6 and 7 was low, since almost no pepsin was bound to the MIP and NIP.
An image of the SDS-PAGE gel of the competitive batch rebinding experiments with MIP and NIP 13 and the different proteins is shown in the graph of Figure 2.83.

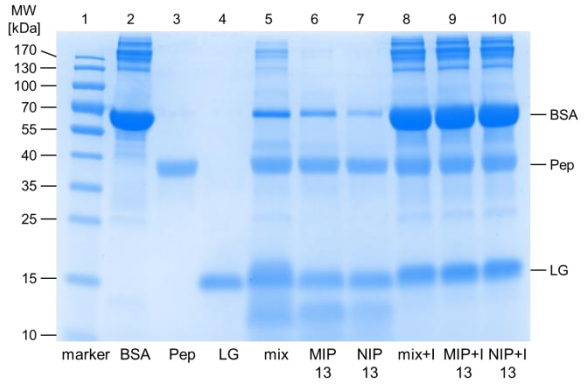

Figure 2.83 Image of the SDS-PAGE gel of the supernatants. Lane 1: molecular weight marker, lane 2: BSA, lane 3: pepsin (Pep), lane 4: LG, lane 5: protein mixture, lane 6 and 7: protein mixture after incubation with MIP and NIP 13, lane 8: protein mixture with pepstatin (+I), lane 9 and 10: protein mixture with pepstatin after incubation with MIP and NIP 13.

The patterns of the lanes 9 and 10 show that almost the entire amounts of all proteins were still in the solution and thus apparently not bound to MIP and NIP 13. This means that the selectivity was not improved due to the extraction in a sodium chloride solution. The intensity of the BSA band in the lanes 6 and 7 was low, since no pepsin was bound to the MIP and NIP.

2.6.15.3 Content of bound proteins

The content of proteins bound to the different polymer particles from the protein mixture are summarized in Table 2.14. The negative numbers come from the inaccuracy of the rough densitometric determination.

Table 2.14 Content of bound protein (*B*) dependent on the type of polymer and protein. A general error of 10% of bound protein was assumed.

Type of polymer		*B* [%]		
		pepsin	BSA	LG
MIP 5	1 APTMA	100	1	44
NIP 5		60	-8	5
MIP 6	pH 4	100	-7	88
NIP 6		96	-10	11
MIP 8	w/o surf	82	-2	-1
MIP 9	0.5 IBMA	100	6	34
NIP 9		22	2	22
MIP 10	0.1 APTMA	1	-1	6
NIP 10		1	1	26
MIP 11	HCl*	100	1	83
NIP 11		100	-4	14
MIP 12	NaOH*	8	-3	12
NIP 12		9	-6	16
MIP 13	NaCl*	-1	4	-8
NIP 13		-2	1	4

* Extraction solution.

The entire or almost entire content of pepsin was bound to MIP 5, 6 and 11 and NIP 6 and 11 due to the high number of APTMA units in the polymers. These results were comparable with the results of the rebinding experiments with the pure pepsin solution described in chapter 2.6.9.4. Less pepsin was bound to NIP 5 than to MIP 5 from the protein mixture. Less pepsin was bound to NIP 5 from the protein mixture than from the pure pepsin solution. A higher imprinting effect was thus obtained by this study. The entire content of pepsin was also bound to MIP 9. This was more than was bound to MIP 9 from the pure pepsin solution. The replacement of half the amount of APTMA by IBMA did not result in a decrease of the pepsin binding capacity or the presence of the other proteins improved the pepsin binding here. In contrast to the MIP less pepsin was bound to NIP 9 from the protein mixture than from the pure pepsin solution. A more pronounced imprinting effect was thus obtained by this study. Most of pepsin thus a higher content of pepsin was bound to MIP 8 from the protein mixture than from the pepsin solution. Little to no pepsin was bound to MIP and NIP 10, 12 and 13 due to the low number of APTMA units in the polymers. This result was comparable with the result obtained after single pepsin rebinding except that less pepsin was bound to the MIPs and that there was thus no effect from imprinting anymore.

Little to no BSA was bound to all MIPs and NIPs meaning that all MIPs and NIPs except MIP and NIP 10 and 13 showed selectivity for pepsin against BSA. This may be explained by the higher isoelectric point of BSA, which is neutral in pure water (pH 5) and thus did not interact with the polymers by ionic interactions, as the negatively charged pepsin did. More thermolysin than BSA was bound to the MIPs and NIPs after single batch rebinding, although it has the same isoelectric point as BSA. This may be explained by the fact that the binding sites of the polymers were already occupied by pepsin (and LG) during this study, in which the proteins had to compete for the binding sites of the polymers, and by the different amino acid residue compositions of thermolysin and BSA. The highest selectivity for pepsin against BSA was obtained with MIP 5, 6, 9 and 11 and NIP 11 followed by MIP 8 and NIP 6. These MIPs except MIP 11 had a higher selectivity compared with their corresponding NIPs, since they bound more pepsin. The highest improvement of the selectivity due to the imprinting was obtained with MIP 5 and thus a high amount of APTMA.

More LG than BSA was bound to most of the MIPs and NIPs, although it has the same isoelectric point as BSA. Hence, the isoelectric point did not affect protein binding here, rather the protein size and amino acid composition. Most of LG was bound to MIP 6 and 11. Less than half the content of LG was bound to MIP 5, 9 and 12 and NIP 6, 9, 10, 11 and 12. Less than 10% of LG was bound to MIP 10 and NIP 5 and 13. No LG was bound to MIP 8 and 13. This resulted in a low selectivity of MIP 6 and 11 for pepsin against LG and in a higher selectivity of MIP 5 and 9 and NIP 6 and 11. A still higher selectivity was obtained with NIP 5 and the highest selectivity was obtained with MIP 8, which bound most of pepsin and no LG. Hence, a high selectivity for pepsin against competitive proteins in the same mixture was obtained in the absence of the surfactant enabling more space for pepsin at the surface of the monomer droplets.

MIP 9 was the only MIP, which had a higher selectivity for pepsin against BSA and LG than the corresponding NIP. The replacement of half the amount of APTMA with IBMA resulted in an increase of the selectivity for pepsin against competitive proteins in the same mixture due to the imprinting.

2.6.15.4 Direct comparison of competitive with single batch rebinding of different proteins

Single batch rebinding experiments were performed with pepsin, BSA and LG in the same way as the competitive rebinding experiments except that each protein was therefore separately incubated with MIP and NIP 9, respectively. The pre-incubation of pepsin with pepstatin was therefore not necessary. The images of the SDS-PAGE gel of the individual and competitive selectivity studies with MIP and NIP 9 and the different proteins are shown in the graphs of Figure 2.84 a) and b).[159]

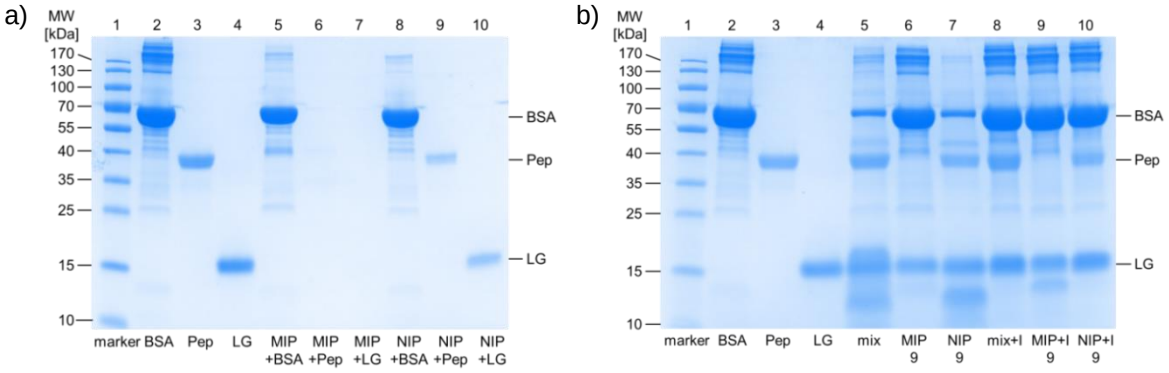

Figure 2.84 Image of the SDS-PAGE gel of the supernatants after single batch rebinding (a). Lane 1: molecular weight marker, lane 2: BSA, lane 3: pepsin (Pep), lane 4: LG, lane 5, 6 and 7: BSA, pepsin (Pep) and LG, respectively, after incubation with MIP 9, lane 8, 9 and 10: BSA, pepsin (Pep) and LG, respectively, after separate incubation with NIP 9. Image of the SDS-PAGE gel of the supernatants after competitive batch rebinding with MIP and NIP 9 (b).

The lane 1 contained the protein molecular weight marker, while the lanes 2, 3 and 4 show the bands of neat BSA, pepsin and LG, respectively. The lanes 5, 6 and 7 show the remaining BSA, pepsin and LG in the supernatant after incubation with MIP 9. It is evident that the MIP apparently bound little BSA, but the entire pepsin and LG. This observation differs from the results obtained from the competitive rebinding (chapter 2.6.15.1), in which MIP 9 bound the entire amount of pepsin, but no BSA and a low amount of LG. These findings indicate that the competition of the proteins for the binding sites of the MIP resulted in a reduction of the binding of the other proteins, since the binding sites of the MIP were already occupied through the bound pepsin. The lanes 8, 9 and 10 show the remaining BSA, pepsin and LG in the supernatant after incubation with NIP 9. The NIP bound more pepsin, BSA and LG after single than after competitive rebinding. Apparently, the competition of the proteins in the mixture resulted in reduced total binding to the NIP. Hence, these results show that individual selectivity studies provide different results than competitive selectivity studies.[159] However, less pepsin was bound to MIP 9 and more pepsin was bound to NIP 9 after the single rebinding experiments analyzed by UV-Vis spectrophotometry in chapter 2.6.13.2 than after the single rebinding experiments analyzed by SDS-PAGE. The results obtained by SDS-PAGE may be better and thus show a more pronounced imprinting effect, since no filtration was necessary and that there was no interfering background coming from the polymer particles and no influence of the structure of the proteins on the results, what can occur during the measurements with UV-Vis spectrophotometry.

2.7 Conclusion and outlook

Stable polymer suspensions were obtained with different hydrophobic and hydrophilic functional monomers, a high content of cross-linker and in presence of pepsin under a high conversion by the miniemulsion polymerization. The average hydrodynamic diameter of most polymer particles was between 200 and 400 nm and the particle size distribution was rather broad. The qualitative monitoring of the pepsin extraction by measuring UV absorbance spectra of the extraction solutions showed that most of pepsin was removed. The average hydrodynamic diameter was between 200 and 700 nm after the extraction procedure. TEM images showed that all polymer suspensions contained particles with a spherical shape, rough surface and a relatively broad size distribution with diameters ranging from around 50 to 600 nm primarily due to the high content of cross-linker. The specific surface area determined by BET analysis was between 26 and 50 $m^2 g^{-1}$ as a result of the small particle size. There were differences in these properties between some MIPs and their corresponding NIPs, but a clear effect, which could be assigned to a result of the imprinting such as an increase of the specific surface area due to the establishment of imprinted cavities on the surface of the MIPs, was not obtained.

The influence of different parameters such as the type and amount of functional monomer, the pepsin template amount, the pH value, the presence of the surfactant and the type of extraction solution on the pepsin binding capacity and affinity, the binding behavior, selectivity and the imprinting efficiency of the resulting polymer particles was investigated by batch rebinding experiments. Pepsin and different other proteins were therefore incubated with the MIP and NIP particles. UV-Vis spectrophotometry was used for the analysis of the protein concentration remaining in the solution after the removal of the polymer particles and bound protein by centrifugation and filtration. A strategy for a competitive selectivity study with pepsin, BSA and LG was developed. The SDS-PAGE was used to separate the proteins remaining in the supernatant after the incubation with the polymer particles and removal of the polymer particles and bound protein. The separated proteins were subsequently stained with Coomassie blue for their analysis. The pepsin activity was inhibited with pepstatin prior to the incubation with BSA, LG and the polymer particles to avoid the proteolytic degradation of the other proteins. Hence, the disappearance of the protein bands on the gels could be assigned to the binding to the polymers instead of to the degradation of the proteins. An individual selectivity study, which was performed in the same way as the competitive selectivity study except that each protein was therefore separately incubated with the polymer particles, showed that a different binding selectivity was obtained from the protein mixture, in which different proteins had to compete for the binding sites of the polymer particles, than from the pure protein solutions. An inhibition study was performed under the same conditions

as the competitive selectivity study, but without the pre-incubation of pepsin with pepstatin to provide information, whether the polymer particles are able to inhibit the activity of pepsin.

The results of the batch rebinding experiments showed that the highest influence on the pepsin binding capacity and selectivity was obtained by the type and amount of functional monomer and thus the type and number of interactions between the polymer particles and pepsin. Higher pepsin binding capacities were obtained with the positively charged functional monomers AEMA and APTMA than with the neutral and negatively charged HEMA and MAA due to the formation of ionic interactions with the in water (pH 5) overall negatively charged pepsin instead of hydrogen bonds. The binding capacity increased with the content of APTMA in the monomer mixture due to an increase of ionic interactions. As a result almost the whole amount of pepsin could be bound to these polymers. This result was comparable with the amount of pepsin bound to commercially available beads for pepsin purification. The polymer particles made with a high amount of APTMA selectively bound pepsin due to ionic interactions. The other proteins had higher isoelectric points than pepsin and were thus neutral or negatively charged in pure water (pH 5) and could not interact with the polymer particles by attractive ionic interactions. The size of the proteins did not play a role. An individual selectivity study with α1-acid glycoprotein, which has a similar low isoelectric point as pepsin, emphasized that there was a big influence of ionic interactions and thus of the isoelectric point of the proteins on the selectivity. The replacement of half the amount of APTMA through the hydrophobic monomer IBMA resulted in a decrease of the pepsin binding capacity and the selectivity. This shows that ionic interactions between pepsin and the polymer were stronger than hydrophobic interactions here. The reduction of the APTMA content resulted in a lower pepsin binding capacity, while no pepsin was bound to this polymer from a protein mixture. Batch rebinding experiments in water (pH 5) and in different buffer solutions with pH values of 2, 4 and 7 showed that the highest amount of pepsin was bound in pure water due to the absence of buffer salts and a high negative net charge of pepsin resulting in a high number of ionic interactions with the positively charged polymers. The inhibition study showed that the pepsin activity was inhibited through binding pepsin to the polymer particles thus blocking the access of the substrate to the active site of pepsin. The pepsin remaining in solution was able to degrade BSA, but not LG.

The imprinting efficiency was investigated by comparing the pepsin binding capacity and selectivity of the MIPs with those of the corresponding NIPs by means of imprinting and relative selectivity factors. The pepsin binding capacity and selectivity of the MIPs were not significantly improved compared with their corresponding NIPs by using hydrochloric acid, sodium hydroxide or a sodium chloride solution instead of pure water as extraction agent. The result of the screening of different functional monomers carried out that the highest imprinting factor ($IF = 1.2$) was obtained with APTMA due to a combination of ionic and hydrophobic interactions. These interactions are non-

directional, but are not unusual for protein imprinted polymers[104,124]. The imprinting factor (*IF* = 1.4) was slightly increased by using the double amount of pepsin template during imprinting. Similar imprinting factors were obtained with the polymers prepared in a citrate buffer solution (pH 4) and with IBMA as second functional monomer. The highest imprinting factor (*IF* = 23.2), but also the lowest binding capacity was obtained with MIP 10 and thus a low amount of APTMA. An imprinting factor for MIP 8, which was prepared without a surfactant, could not be determined, since the NIP was a bulk polymer. All polymers showed an improved selectivity for pepsin against 2 to 4 of different other proteins used in the individual selectivity study. The highest relative selectivity factors were obtained with MIP 10, although this MIP was only selective for pepsin against 1 of these proteins. MIP 5 showed selectivity for pepsin against α1-acid glycoprotein, but no improved selectivity compared with NIP 5. MIP 6 did not show any selectivity for pepsin against α1-acid glycoprotein. MIP 5 and 6 showed selectivity for pepsin against BSA and LG in the competitive selectivity study, but only a higher improved selectivity for pepsin against BSA, but not against LG compared with their corresponding NIPs. This may be explained for MIP 6 by the fact that the selectivity studies were performed in water and not in a citrate buffer solution, wherein the imprinting was performed and an imprinting factor of 1.4 was obtained. A selectivity study with MIP 6 in a citrate buffer solution is required to finally proof the imprinting effect. MIP 10 did not bind any pepsin from the protein mixture. An imprinting effect could thus not be proven through the competitive selectivity study. MIP 9 showed an increased selectivity for pepsin against BSA and LG in the competitive selectivity study and increased pepsin binding in an individual selectivity study analyzed by SDS-PAGE compared with NIP 9. These results indicate that there was an effect from the imprinting. IBMA was added as second functional monomer to improve the adsorption of pepsin on the droplet surface by hydrophobic interactions for the formation of the pre-polymerization complex with APTMA and IBMA at the droplet surface prior to the polymerization. Further experiments are necessary to proof this result, since a rebinding experiment with pepsin analyzed by UV-Vis-spectrophotometry showed a slightly different result. MIP 8 showed the highest selectivity for pepsin against BSA and LG in the competitive selectivity study, since it bound most of pepsin and no BSA and no LG. This indicates that the imprinting was successful in the absence of the surfactant, which enabled more space for the adsorption of pepsin at the monomer droplets. But this could not be fully proven due to the absence of a suitable NIP.

Binding isotherms of the MIPs and NIPs 4 and 5 showed that the imprinting factors increased with increasing pepsin concentration. This indicates that non-selective binding to the MIP was more pronounced at lower concentrations, what was contrary to the expectations. The progression of the binding isotherms of the MIPs and NIPs 4, 5, 6 and 9 and of MIP 8 resembled the progression of a Langmuir isotherm. This suggests that the polymer particles had a homogeneous surface with equal

adsorption sites and could bind a monolayer of pepsin. The maximum binding capacities of the MIPs were between 3.4 and 25.3 mg m^{-2} and significantly higher than of the NIPs, thereby indicating that the MIPs had significantly more binding sites. The dissociation constants of the MIPs were between 4.71 and 39.95 µM and thus in a range, which is comparable with dissociation constants of other protein imprinted polymer particles. However, the dissociation constants of the NIPs were lower and thus the NIPs had a higher affinity to pepsin. This may be explained by difficulties concerning the evaluation of the data of the MIPs or indicates that the imprinting did not result in a higher affinity. The binding kinetics of the MIPs and NIPs 5 and 6 demonstrated that the binding equilibrium with pepsin was obtained after only 1 min. The binding of pepsin to the MIPs and NIPs was exceptionally fast due to a high mass transfer rate of pepsin to the binding sites, which were located at the surface of the submicron polymer particles and thus readily accessible for the large biomolecule. The pepsin binding to MIP 8 was much slower. Most of pepsin was bound after around 6 h and the binding equilibrium was not yet reached after 20 h. This binding kinetic may be a result of the formation of more selective interactions, which are slower, or was obtained, since the imprinted cavities were deeper in the polymer and more time was necessary to reach them.

In conclusion, submicron polymer particles were prepared in presence and absence of pepsin as template molecule by miniemulsion polymerization. These showed a high pepsin binding capacity, a high affinity and selectivity for pepsin, enabled fast pepsin binding and the inhibition of the pepsin activity. The pepsin binding capacity and selectivity could be improved due to the imprinting. The most promising results from imprinting were obtained with APTMA as functional monomer and IBMA as second functional monomer and without a surfactant. A further improvement of the imprinting could be a combination of these parameters. Different batch rebinding experiments and analysis methods were used to evaluate the imprinting efficiency. This was challenging, since the MIPs and NIPs had rather broad particle size distributions, different surface areas and partly different zeta potentials indicating different surface charges. The exceptional low isoelectric point of pepsin made it difficult to compare the selectivity of the polymer particles for pepsin against other proteins.

There are still experiments, which can be done in future to facilitate the evaluation of the imprinting efficiency and to completely proof the imprinting effect. The miniemulsion polymerization can be prepared with less cross-linker, another surfactant such as SDS or under different sonication conditions to obtain polymer particles with a narrower size distribution. The polymers can be further characterized by IR- and NMR-spectroscopy in order to obtain more information on the composition of the copolymers. Surface titrations can be performed to investigate the number of charged groups on the surface of the polymer particles. A washing step for the removal of non-selectively bound pepsin can be included into the pepsin rebinding experiments to exclude the contribution of non-

selective binding. The development of an HPLC method e. g. with a size exclusion chromatography column for the separation of pepsin from other components such as residual monomer after the extraction and from other proteins after a competitive rebinding experiment would be helpful for the investigation of the amount of extracted pepsin and to enable a faster analysis of the rebinding experiments and a better quantification of the protein content in the solution after competitive rebinding experiments. An additional evaluation method of the imprinting efficiency would be the study of the cross-reactivity. A miniemulsion polymerization therefore has to be prepared in the presence of another protein. The comparison of the pepsin binding capacity of the so-prepared polymer particles with the MIPs will show, if the presence of any protein is responsible for the differing properties between the MIPs and NIPs or if these are a result of the imprinting of pepsin. This is helpful, since the existence of a template molecule during the polymerization can affect the amount and distribution of the functional groups and thus change some properties of the resulting polymer such as the specific surface area and the surface charge. A competitive selectivity study with α1-acid glycoprotein should finally proof the imprinting effect. Furthermore, it was assumed that the missing amount of pepsin in the solution after a rebinding experiment was bound to the polymer. The bound pepsin may be qualitatively identified by IR- or Raman-spectroscopy or by staining with Ninhydrin or Coomassie blue or semi-quantitatively be verified by SDS-PAGE after the elution from the polymer particles with an elution buffer. This should ensure that pepsin was bound to the polymer particles and is not missing in the solution due to aggregation or precipitation. Another method to analyze the bound protein could be the incubation study in microtiter wells represented in chapter 3. Finally, the reproducibility should be investigated.

Different parameters were investigated in this thesis, but there are still many other parameters, which can be varied, to improve the imprinting. Other different functional monomers and a different ratio between functional monomer and cross-linker can still be used for further imprinting experiments. Another possibility would be the use of the cationic surfmer (11-acryloyloxyundecyl)-dimethylethylammonium bromide, which serves as monomer and surfactant at the same time and can form a pre-polymerization complex with pepsin at the droplet surface. CTAB can also be used to improve the adsorption of pepsin at the droplet surface, but also affects the structure of pepsin. CTAB could maybe improve the extraction of pepsin, too. Another imprinting strategy would be a core-shell approach including the immobilization of pepsin on the surface of core particles prior to the imprinting. The inverse miniemulsion polymerization would be an alternative polymerization method, in which pepsin and APTMA or different other acrylamides can be dispersed in a hydrophobic phase such as cyclohexane.

Finally this imprinting approach provides a fundamental step towards the development of a protease scavenger material and protease assay and may be transferred to other proteases such as trypsin and thermolysin in future.

3. Designed polymer nanoparticles with high affinity to pepsin

3.1 Motivation and scope

The design of polymer nanoparticles (NPs) with high affinity and selectivity for a specific target protein by controlling their chemical composition[223] provides a complementary approach to the imprinting approach without the need of a template molecule and a time-consuming and elaborative extraction process. This approach has the same aim of preparing cheaper and more stable synthetic substitutes of natural antibodies, which may be applied in separations, biosensors, diagnostics, drug delivery, disease therapy and as antidotes for toxins and viruses. The small size of the NPs enables a high binding capacity for the adsorption of proteins on their surface due to the inverse proportionality of the surface area per volume to the size. NPs are therefore advantageous for the use in immunosorbent assays[224,225] and sensors[226] or may be injected into the blood stream for therapeutic applications[227]. A precipitation polymerization with a low monomer concentration and a small amount of surfactant enables a straightforward preparation of polymer NPs[104,223], which are compatible to peptides and proteins[228], from water-soluble monomers such as different acrylamides and a water-soluble cross-linker in water.

In this part of the thesis, a synthesis strategy using rational design and precipitation polymerization is reported for the preparation of lightly cross-linked NPs with high affinity to pepsin. The type and ratio of the functional monomers are therefore tailored to the amino acid residue composition of pepsin and varied resulting in different NPs, a NP library. The binding affinities of the different NPs for pepsin are evaluated by two different incubation studies. One incubation study is done in solution using UV-Vis spectrophotometry for the determination of the remaining pepsin concentration and an EnzChek® protease assay kit for the determination of the remaining pepsin activity in solution. Another incubation study is developed in order to enable a faster screening of the NP affinity to pepsin. This is done in wells of a 96-well plate after the immobilization of the NPs on the surface of the wells by physical adsorption. The amount of the bound and free pepsin is determined separately by pepsin activity measurements using the EnzChek® protease assay kit and a fluorescence microplate reader. Furthermore, it is investigated, if the association or contact of pepsin with the NPs results in an inhibition of the activity of pepsin. A similar incubation study is therefore performed, except that here the activity of the bound and free pepsin is determined with the protease assay kit at once.

3.2 Principle of designing polymer nanoparticles for protein binding

The high affinity of an antibody for its antigen is achieved through a sum of multiple weak interactions like ionic, hydrophobic interactions and hydrogen bonds.[229,230] These interactions are mimicked by the use of a combination of monomers with different functional groups such as acrylic acid, *N*-(*tert*-butyl)acrylamide and *N*-hydroxyethyl acrylamide that can interact with the amino acid side chains of the proteins by ionic, hydrophobic interactions and hydrogen bonds resulting in multiple weak interactions between the obtained NPs and the target protein.[231] By selecting the type and ratio of the functional monomers according to the chemical composition of the surface of the target protein and optimization of this selection, NPs with a high intrinsic affinity and selectivity for the target protein are obtained. The functional monomers are randomly distributed in the polymer during free radical polymerization.[223] A low degree of cross-linking is used to give the polymer chains considerable flexibility.[232] The chain flexibility allows the functional groups to orientate towards the complementary functional groups on the protein resulting in a high number of interactions between the NPs and the protein surface.

3.3 Precipitation polymerization

The precipitation polymerization is initiated in a solution of monomer, cross-linker and an initiator forming soluble oligomers. After a critical point the growing polymers precipitate and phase-separate from the continuous medium.[233] These further grow to a certain size by the addition of monomers and oligomers from the solution. Aggregation of the precipitated polymer particles is usually prevented by their rigid, cross-linked surfaces[234] and sometimes additionally by gentle shaking. Spherical, monodisperse polymer particles[235] are obtained in a size range of 0.1-10 µm[236] dependent on the type and amount of solvent, cross-linker,[237] initiator[234] and other conditions as shaking[238] and the temperature[66]. Usually a high content of cross-linker is used and no polymeric stabilizer is required.[234,236] The precipitation polymerization protocol can be modified for the preparation of lightly cross-linked polymer particles also referred to as micro- and nanogels. For this purpose water-soluble monomers such as different acrylamides and a low amount of a water-soluble cross-linker are copolymerized in water. These components are more compatible to peptides[104,114] and proteins[106]. Polymer particles in the size range between 20 and 110 nm can be obtained by using a low monomer concentration and introducing a small amount of surfactant.[223,231,232,239,240]

3.4 State of the art

The strategy of designing polymer NPs for the selective capture of a biomacromolecular target was developed by the research group of K. J. Shea. The first example target was the toxic peptide melittin.[227,231] The highest affinity, binding capacity and neutralization capability was obtained with a monomer mixture containing 40 mol-% of *N*-(*tert*-butyl)acrylamide (TBAm), 5 mol-% of acrylic acid (AAc), 53 mol-% of *N*-isopropylacrylamide (NIPAm) and 2 mol-% of *N,N'*-methylenebisacrylamide (BIS).[241] This enabled efficient capture of melittin by the resulting NPs due to ionic and hydrophobic interactions and was explained with the analysis of the amino acid residue sequence of melittin, which contains 26 amino acid residues including 6 positively charged and a high proportion of hydrophobic amino acid residues. A further optimization of the monomer combination by increasing the feed ratio of AAc to 40 mol-% resulted in a further increase of the binding affinity, capacity and neutralization capability.[231] The combination of this strategy with the imprinting approach resulted in an enhancement of the average binding affinity.[104,227] The optimized NPs were able to neutralize the toxin in vitro[241] and in vivo[231,242].

This strategy was successfully applied to other protein targets. Lysozyme was selectively captured by using the same monomer composition used for capturing melittin and thus through a combination of ionic and hydrophobic interactions.[239] NPs that bind with high affinity to the Fc fragment of immunoglobulin G (IgG) were obtained from a monomer mixture composed of 20 mol-% of AAc, 40 mol-% of TBAm, 38 mol% of NIPAm and 2 mol-% of BIS.[232] The different positively charged functional monomers *N*-(3-methacrylamidopropyl)guanidinium chloride (GUA), *N*-(3-aminopropyl)-methacrylamide hydrochloride (APM) and *N*-(3-acrylamidopropyl)trimethylammonium chloride (APTMA) were used to obtain NPs with high affinity to fibrinogen, because fibrinogen has a high number of carboxylate groups on its surface.[240] NPs were prepared with 5, 10 or 20 mol-% of the positively charged monomers, 40 mol-% of TBAm, since fibrinogen is relatively hydrophobic, 2 mol-% of BIS and 53, 48 or 38 mol-% of NIPAm. Their affinity to fibrinogen was screened using UV-Vis spectrophotometry and quartz crystal microbalance measurements. The highest affinity was achieved by the incorporation of GUA in the NPs. GUA contains a guanidinium group, which is also present in the positively charged amino acid arginine and can form two hydrogen bonds and ionic interactions[243]. The selectivity of the NPs for fibrinogen was explained by the combination of ionic and hydrophobic interactions and hydrogen bonds.

3.5 Fluorescence

Fluorescence is the spontaneous emission of light immediately after absorption of electromagnetic radiation by a substance.[204] The absorbed radiation is usually in the UV region, while the emitted radiation is in the visible region. Fluorescent substances are small polyaromatic or heterocyclic organic molecules[204] or proteins[187] and can be covalently bound to biomacromolecules in order to label them for further applications in fluorescence detection, spectroscopy and imaging[206].

Fluorescence is the result of a three-stage process, which is illustrated by a simplified electronic-state diagram in Figure 3.1. The absorption of electromagnetic radiation causes the excitation of valence electrons in a fluorophore from the electronic ground state to one of the vibrational states in an excited electronic singlet state of higher energy.[244] A non-radiative transition (internal conversion) from a higher to a lower excited electronic singlet state and from a higher to the lowest vibrational level of the excited electronic state (vibrational relaxation) follows due to collisions with surrounding molecules. The molecule subsequently drops down to one of the vibrational levels of the electronic ground state by emitting a photon, which is called fluorescence.

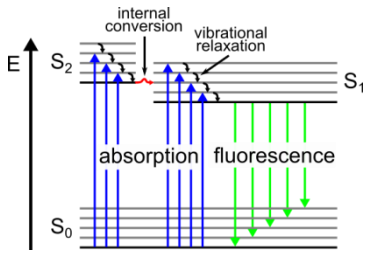

Figure 3.1 Scheme of a simplified electronic-state diagram explaining fluorescence.

The emitted light has a lower energy and thus a longer wavelength than the absorbed radiation due to the energy dissipation during the excited-state lifetime.[204] This difference is called Stokes shift and is fundamental for the sensitivity of fluorescence techniques, because it allows the direct detection of the emitted light in contrast to UV-Vis absorption measurements.[244]

The excitation and emission spectra are characteristic for each substance and analyzed by fluorescence spectroscopy. The emitted light intensity is proportional to the absorbed light intensity and the concentration of the fluorophore in dilute solutions as described by equation (3-1).[204]

$$I_F = 2.3 Q_F I_E \varepsilon_\lambda d c \qquad \textbf{(3-1)}$$

I_F: intensity of fluorescence radiation
Q_F: fluorescence quantum yield
I_E: intensity of excitation radiation
ε_λ: molar decadic extinction coefficient
d: optical path length
c: concentration of the substance

The fluorescence quantum yield describes the ratio between the number of emitted and absorbed

photons and is lower than 1, if excited molecules return to the ground state by other processes such as quenching, fluorescence resonance energy transfer or intersystem crossing.[244]

The fluorescence is measured with a fluorescence spectrometer or a fluorimeter (Figure 3.2).

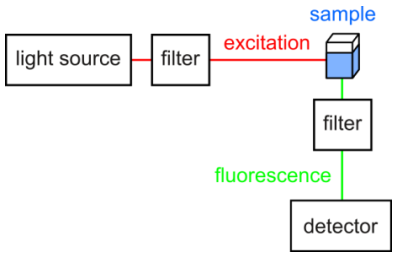

Figure 3.2 Scheme of a fluorimeter.

The light from an excitation source is passed through a filter or monochromator first and then strikes a cuvette containing the sample.[187] The sample is excited by absorbing the incident light and re-emits fluorescence light in all directions. A part of the fluorescent light is detected at an angle of 90° to the incident light beam in order to avoid interferences with the transmitted light after passing through a second filter or monochromator. A fluorescence microplate reader can detect the fluorescence intensity of several samples placed in wells of a microtiter plate at the same time.[204]

3.6 EnzChek® protease assay kit

EnzChek® protease assay kits are fast, simple and direct fluorescence-based assays for the sensitive detection of the activity of different proteases. The kits contain casein derivatives, which are heavily labeled with a pH-insensitive, green-fluorescent BODIPY FL® or red-fluorescent BODIPY TR-X® dye.[245] The high fluorophore labeling density of the casein derivatives results in an almost total intramolecular self-quenching, which is the quenching of one fluorophore by another in the same molecule. After the cleavage of the casein substrate by a protease, fluorescent peptides are released and the self-quenching is relieved (Figure 3.3).

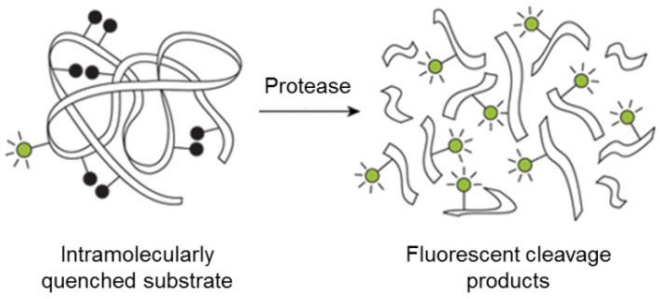

Figure 3.3 Principle of the EnzChek® protease assay kit.[245]

The fluorescence intensity is proportional to the protease activity.[245] The maximum excitation/emission wavelengths of the green- and red-fluorescent peptides are approximately 505/513 nm and 589/617 nm.

3.7 Experimental

3.7.1 Chemicals

N-isopropylacrylamide (NIPAm), *N*-(3-acrylamidopropyl)trimethylammonium chloride (APTMA, 75 wt.-% in water), *N*-(2-hydroxyethyl)acrylamide (HEAm), *N,N'*-methylenebisacrylamide (BIS) and pepsin pepsin from porcine gastric mucosa (lyophilized powder, 3200-4500 U mg^{-1} protein) were from Sigma-Aldrich. Acrylic acid (AAc), sodium dodecyl sulfate (SDS), cetyltrimethylammonium bromide (CTAB) and azobisisobutyronitrile (AIBN) were from Aldrich Chemical Company. *N*-(*tert*-butyl)acrylamide (TBAm) was from Acros Organics and citric acid was from Fisher Chemicals. *N*-(3-aminopropyl)methacrylamide hydrochloride (APM) and *N*-(3-methacrylamidopropyl)guanidinium chloride (GUA)[240] were synthesized by the Shea research group. NIPAm was recrystallized from hexane and AAc was distilled under reduced pressure before use. Other chemicals were used as received. Water was distilled and then purified using a Barnstead Nanopure Diamond™ system (from Thermo Scientific).

3.7.2 Synthesis of the nanoparticles

Positively, negatively charged and neutral nanoparticles (NPs) were synthesized with different functional monomers and monomer compositions, which are summarized in Table 3.1, by precipitation polymerization as follows.

Table 3.1 The monomer feed ratios for the synthesis of the different nanoparticles (NPs).

Type of NP		Monomer feed ratio [mol-%]							
		GUA	APM	APTMA	HEAm	AAc	TBAm	NIPAm	BIS
1	GUA 5	5	-	-	-	-	40	53	2
2	GUA 10	10	-	-	-	-	40	48	2
3	GUA 20	20	-	-	-	-	40	38	2
4	APM 5	-	5	-	-	-	40	53	2
5	APM 10	-	10	-	-	-	40	48	2
6	APM 20	-	20	-	-	-	40	38	2
7	APTMA 5	-	-	5	-	-	40	53	2
8	APTMA 10	-	-	10	-	-	40	48	2
9	APTMA 20	-	-	20	-	-	40	38	2
10	TBAm 0	-	-	-	-	-	0	98	2
11	TBAm 20	-	-	-	-	-	20	78	2
12	TBAm 40	-	-	-	-	-	40	58	2
13	HEAm 10	-	-	-	10	-	40	48	2
14	HEAm 20	-	-	-	20	-	40	38	2
15	HEAm APM	-	20	-	20	-	40	18	2
16	AAc 20	-	-	-	-	20	40	38	2

APM, APTMA, GUA, HEAm, AAc or a mixture of HEAm and APM (X mol-%), NIPAm (98-X-Y mol-%), BIS (2 mol-%) and the surfactant were dissolved in water (50 mL). CTAB (20 mg) was used for the synthesis of positively charged NPs and SDS (10 mg) for the synthesis of negatively charged and neutral NPs. TBAm (Y mol-%) was dissolved in 1 mL of ethanol and GUA in dimethyl sulfoxide (50 mg mL^{-1}) before the addition to the solution. The total monomer concentration was 6.5 mM. The resulting solutions were filtered through a standard grade filter paper (from Whatman) and purged with nitrogen for 30 min. After the addition of AIBN (30 mg in 500 µL of acetone) the polymerization was carried out at 60-65 °C for 3 h under nitrogen atmosphere. The obtained polymer solutions were purified by dialysis (12-14 kDa molecular weight cut-off (MWCO), regenerated cellulose, fisherbrand™ from Thermo Scientific) against excess amount of water (4 changes per day) for 4 days.

3.7.3 Characterization of the nanoparticles

3.7.3.1 Dynamic light scattering

The hydrodynamic diameter of the NPs was determined in aqueous solution used as received at 25 °C by dynamic light scattering (DLS) with a Zetasizer Nano ZS (from Malvern Instruments Ltd). The laser wavelength was 633 nm and the scattering angle 173°. The z-average was used as average hydrodynamic diameter. All measurements were done twice and the results averaged.

3.7.3.2 Zeta potential measurements

The electrophoretic mobility of the NPs was determined in aqueous solution used as received at 25 °C by laser Doppler electrophoresis with a Zetasizer Nano ZS (from Malvern Instruments Ltd). The zeta potential was calculated by using the Smoluchowski equation. All measurements were done twice and the results averaged.

3.7.3.3 Determination of NP concentration and conversion

The concentration of the NPs in solution was determined by gravimetric analysis before and after lyophilization. An aliquot of the NP solution was weighted after lyophilization and divided by its volume before lyophilization. The weight of the whole NPs was calculated and divided by the initial weight of the monomers for the determination of the conversion. The dilution obtained after dialysis was corrected.

3.7.4 Incubation study in solution

A pepsin stock solution (1000 µg mL^{-1}) was prepared by dissolving pepsin in a citric buffer solution (20 mM, pH 5). All the NP solutions were diluted in water to a concentration of 100 µg mL^{-1}. 250 µL of the pepsin stock solution (1000 µg mL^{-1}, pH 5) and 250 µL of each NP solution (100 µg mL^{-1}) were mixed and incubated under shaking at room temperature (RT) for 30 min. A NP control sample was prepared in the same way, but without pepsin. A pepsin reference sample was prepared in the same way, but without the NPs. Additionally to the pepsin reference sample the pepsin stock solution was diluted to concentrations of 800, 500, 400, 200 and 100 µg mL^{-1}. The diluted pepsin solutions were treated in the same way as the other samples. The NPs including the bound pepsin were removed through centrifugal filters (100 kDa MWCO, modified PES, Nanosep from Pall) by centrifugation at 3000 rpm for 5 min. All experiments were performed in triplicates.

The absorbance spectra of all samples were measured 3 times with a UV-Vis spectrophotometer (Nanodrop 2000C from Thermo Scientific). The absorbance at 277 nm was averaged and plotted against the pepsin concentration. The content of bound pepsin was determined according to the following equation (3-2). The average and standard deviation of the 3 samples were calculated.

$$B = \left[1 - \left(\frac{A_{277}(fil) - A_{277}(NP)}{A_{277}(pep)}\right)\right] 100 \qquad \textbf{(3-2)}$$

B: content of bound
A_{277}: absorbance at 277 nm
fil: filtrate
NP: NP solution
pep: pepsin solution

The activity of pepsin in the filtrates was determined as follows. A stock solution of the protease assay (EnzChek® from Life Technology) was prepared by diluting the content of one vial (2 mg of the BODIPY FL® dye-labeled casein derivative) in 200 µL of a phosphate buffer solution (35 mM, pH 7.3) as described in the protocol of Life Technology[245]. A working solution of the protease assay (10 µg mL^{-1}) was prepared by diluting the whole stock solution in 19.8 mL of a 10 mM hydrochloric acid (HCl). 20 µL of each filtrate of the respective 3 samples were diluted in 1.44 mL of a citric buffer solution (10 mM, pH 5). 4 times 50 µL of each diluted filtrate were pipetted in the wells of a Nunc-Immuno™ MicroWell™ 96-well plate (PolySorp, PS, flat-bottom, pinch bar, 400 µL from Nunc). Then 50 µL of a 120 mM HCl were added to adjust the pH value to 2. 100 µL of the working solution were loaded into the wells. After the incubation under shaking at RT for 1 h the fluorescence intensity at 530 nm was measured with a fluorescence microplate reader (Spectra max Gemini XPS from Molecular Devices) after an excitation at 485 nm. 6 readings per well were carried out and averaged. The average and standard deviation of the 4 samples were calculated.

3.7.5 Incubation study in microtiter wells

Two stock solutions of the protease assay (EnzChek® from Life Technology) were prepared as described in the previous chapter 3.7.4. A working solution of the protease assay (5 µg mL^{-1}) was prepared by diluting a complete stock solution in 39.8 mL of a 10 mM HCl. A second working solution of the protease assay (10 µg mL^{-1}) was prepared by diluting the whole second stock solution in 19.8 mL of a 120 mM HCl. 4 times 200 µL of each NP solution (100 µg mL^{-1}) were loaded into the wells of a 96-well plate (PolySorp, PS, flat-bottom, pinch bar, 400 µL from Nunc) and incubated under shaking at RT for 1 h to immobilize the NPs on the wells. After the removal of the supernatants 200 µL of a pepsin solution (5 µg mL^{-1}) in citric buffer (10 mM, pH 5) were loaded into the wells. A pepsin control sample was prepared in the same way, but without the immobilization of the NPs before the addition of the pepsin solution. A control sample of a pure NP solution was prepared in the same way, but without the addition of pepsin. After the incubation under shaking at RT for 30 min 100 µL of the supernatants were pipetted into the wells of a second 96-well plate (PolySorp, PS, flat-bottom, pinch bar, 400 µL from Nunc). The residual supernatants were removed and each well was washed with 200 µL of the citric buffer solution (10 mM, pH 5) once. 200 µL of the first working solution (5 µg mL^{-1}, in 10 mM HCl) were loaded into the wells of the first 96-well plate. 100 µL of the second working solution (10 µg mL^{-1}, in 120 mM HCl) were loaded into the wells of the second well plate. A higher concentration of HCl in the second working solution was used to adjust the pH value of the supernatants from 5 to 2. 4 times 100 µL of a pepsin solution (10 µg mL^{-1}) in a citric buffer solution (10 mM, pH 5) were loaded into the wells of a third 96-well plate (PolySorp, PS, flat-bottom, pinch bar, 400 µL from Nunc) for the preparation of a pepsin reference sample. Then 100 µL of the second working solution (10 µg mL^{-1}, in 120 mM HCl) were added. All mixtures were incubated under shaking at RT for 1 h. The fluorescence intensity at 530 nm was measured with a fluorescence microplate reader (Spectra max Gemini XPS from Molecular Devices) after an excitation at 485 nm. 6 readings per well were carried out and averaged. The average and standard deviation of the 4 samples were calculated.

3.7.6 Inhibition study in microtiter wells

A stock solution of the protease assay (EnzChek® from Life Technology) was prepared as described in the previous chapter 3.7.4. A working solution of the protease assay (10 µg mL^{-1}) was prepared by diluting the whole stock solution in 19.8 mL of a citric buffer solution (10 mM, pH 5). The NPs were immobilized on the wells of a microtiter plate as described in the previous chapter 3.7.5. 100 µL of a pepsin solution (10 µg mL^{-1}) in a citric buffer solution (10 mM, pH 5) were loaded into the wells. After the incubation under shaking at RT for 30 min 100 µL of the working solution (10 µg mL^{-1}) were pipetted into the wells. A NP control sample was prepared in the same way, but without the addition of pepsin. A pepsin control sample was prepared in the same way, but without the immobilization of the NPs before the addition of the pepsin solution. The mixtures were incubated under shaking at RT for 1 h. The fluorescence intensity at 530 nm was measured with a fluorescence microplate reader (Infinite 200 pro from Tecan) after an excitation at 485 nm. 6 readings per well were carried out and averaged. The average and standard deviation of the 4 samples were calculated.

3.7.7 Incubation study with different pepsin concentrations

Pepsin (4000 mg mL^{-1}) was dissolved in a citric buffer solution (20 mM, pH 5). The pepsin solution was diluted in the citric buffer solution (20 mM, pH 5) to the concentrations of 3000, 2500, 2000, 1500, 1000 and 500 µg mL^{-1}. The NP solution prepared with 20 mol-% of APTMA was diluted in water to a concentration of 100 µg mL^{-1}. 250 µL of each pepsin solution (4000-500 µg mL^{-1}, pH 5) and 250 µL of the APTMA 20 NP solution (100 µg mL^{-1}) were mixed and incubated under shaking at RT for 30 min. A NP control sample was prepared in the same way, but without pepsin. For calibration the pepsin solution (1000 µg mL^{-1}, pH 5) was diluted in the citric buffer solution (20 mM, pH 5) to concentrations of 800, 600, 500, 400, 200 and 100 µg mL^{-1}. 250 µL of each pepsin solution were mixed with 250 µL of pure water and treated in the same way as the other samples. After the incubation the NPs including the bound pepsin were removed through centrifugal filters (100 kDa MWCO, modified PES, Nanosep from Pall) by centrifugation at 3000 rpm for 5 min. The absorbance at 277 nm of the filtrates was determined 3 times by a UV-Vis spectrophotometer (Nanodrop 2000C from Thermo Scientific) and averaged. All experiments were performed in triplicates.

The binding capacity of pepsin was determined according to the following equation (3-3).

$$Q = \frac{(\beta_{in} - \beta_{free})V}{m_p} = \frac{m_b}{m_p} \quad \textbf{(3-3)}$$

Q: binding capacity
β_{in}: initial pepsin mass concentration
β_{free}: free pepsin mass concentration
V: volume of solution
m_p: mass of polymer particles
m_b: mass of bound pepsin

The free pepsin concentration was obtained from the pepsin calibration function after subtracting the absorbance of the NP control sample from the absorbance of the filtrates. The average and standard deviation of the 3 samples were calculated.

3.7.8 Incubation study during different time intervals

Pepsin (1000 µg mL^{-1}) was dissolved in a citric buffer solution (20 mM, pH 5). The NP solution synthesized with 20 mol-% of APTMA was diluted in water to a concentration of 100 µg mL^{-1}. 250 µL of the pepsin solution (1000 µg mL^{-1}, pH 5) and 250 µL of the APTMA 20 NP solution (100 µg mL^{-1}) were mixed and incubated under shaking at RT for 1, 5, 15, 30, 60 and 90 min. A NP control sample was prepared in the same way, but without pepsin. The further protocol is the same as described in the previous chapter 3.7.7.

3.7.9 Comparison with MIP 5 and pepstatin immobilized agarose beads

The suspensions of MIP 5 and of pepstatin immobilized agarose beads (PAB) were diluted in water to a concentration of 100 µg mL^{-1}. The same experiment, which was carried out with the NPs in the first part of chapter 3.7.4, was carried out with the diluted MIP 5 and PAB suspensions. Centrifugal filters of a MWCO of 300 kDa (modified PES, Nanosep from Pall) were therefore used. The time of centrifugation was 15 min. All experiments were performed in duplicates. The average and spread of the two samples were calculated.

3.8 Results and discussion

3.8.1 Analysis of the amino acid residue composition of pepsin

The content of acidic, basic, polar neutral and hydrophobic amino acid residues in pepsin was calculated from the amino acid residue composition of pepsin[18] and is summarized in Table 3.2. The content of the different classes of amino acid residues on the surface of pepsin was obtained by a rough estimation by analyzing the three-dimensional structure of pepsin[22]. There is a higher probability that the polymer particles interact with the amino acid residue side chains on the surface of pepsin because of the higher accessibility.

Table 3.2 Content of different classes of amino acid residues in pepsin and on its surface.

Class of amino acid residues	Content in pepsin	Content on surface
Acidic	13%	~ 20%
Basic	1%	~ 1%
Polar neutral	46%	~ 20%
Hydrophobic	40%	~ 59%

The results show that pepsin contains substantially more acidic than basic amino acid residues, particularly on its surface. The content of polar neutral and hydrophobic amino acid residues is similar in the whole protein, but there are more hydrophobic amino acid residues on the surface. This is illustrated in the image of Figure 3.4.

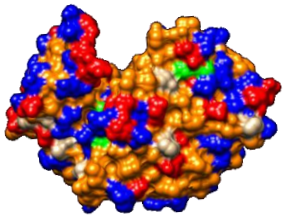

Figure 3.4 Image of the surface of pepsin obtained from crystal structure data[22] using the program UCSF Chimera 1.8. Acidic amino acid residues are highlighted in red, basic in green, polar neutral in blue and hydrophobic in orange.

The high content of serine, tyrosine and threonine residues containing a hydroxyl group (26%) and of leucine, isoleucine and valine residues (23%) in pepsin, which have an aliphatic C4 and C3 residue, are noticeable. This is illustrated in Figure 3.5.

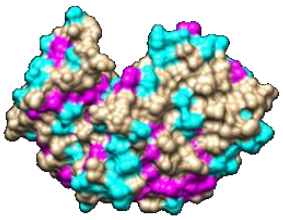

Figure 3.5 Image of the surface of pepsin obtained from crystal structure data[22] using the program UCSF Chimera 1.8. Amino acid residues with a hydroxyl groups are highlighted in cyan and with a C4 and C3 residue in magenta.

3.8.2 Selection of the nanoparticle library

Based on the knowledge of the amino acid residue composition of pepsin (chapter 3.8.1) the type and ratio of the functional monomers (Figure 3.6) for the NP synthesis were selected.

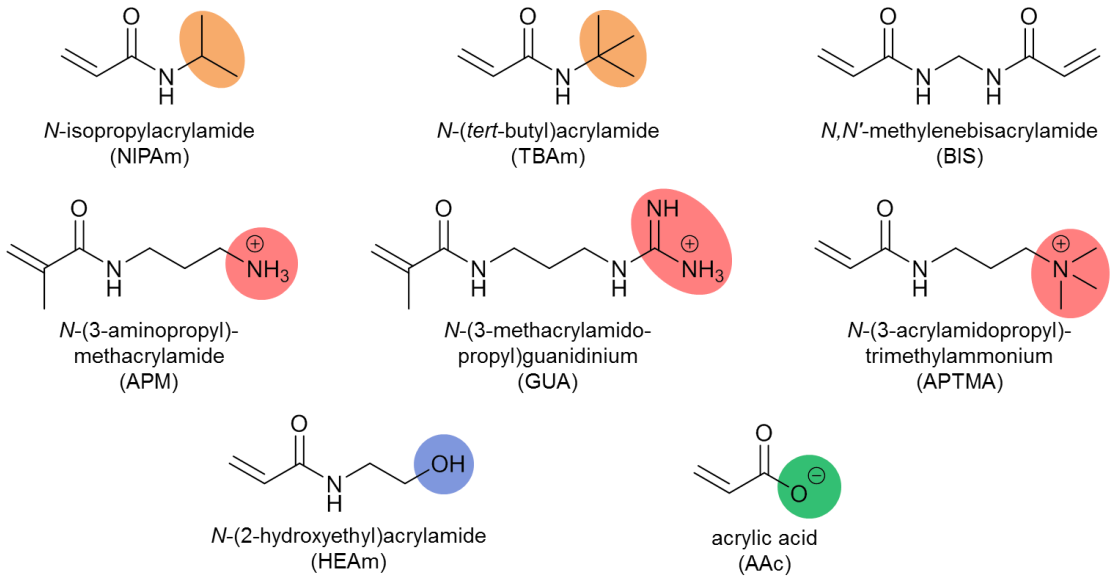

Figure 3.6 Chemical structures of the different types of functional monomers and the cross-linker used for the synthesis of the polymer nanoparticles (NPs).

N-Isopropylacrylamide (NIPAm) was used as backbone monomer for the synthesis of all NPs and can form hydrogen bonds with the amide group like the other acrylamides and additional hydrophobic interactions with the isopropyl group. *N*-(*tert*-Butyl)acrylamide (TBAm) was used to increase the hydrophobicity of the NPs. The feed ratio of TBAm for the preparation of the NPs was 40 mol-% due to the fact that pepsin contains 40% of hydrophobic amino acid residues including a high number of amino acid residues with an aliphatic C4 and C3 residue and that this ratio was successful in binding various proteins[223,231,232,239,240]. NPs with a lower TBAm ratio (20 mol-%) and no TBAm were also synthesized to investigate the influence of TBAm on the affinity of the NPs to pepsin. The lack of TBAm was compensated by increasing the NIPAm content.

Different basic and positively charged monomers were selected due to the high number of acidic amino acid residues in pepsin. The content of these monomers was adjusted to the content of these amino acid residues in pepsin (13%) and on its surface (~ 20%) and varied between 5, 10 and 20% (Table 3.1 in chapter 3.7.2). The basic monomers *N*-(3-aminopropyl)methacrylamide (APM) and *N*-(3-methacrylamidopropyl)guanidinium chloride (GUA) are mainly positively charged in a buffer solution of a pH value of 5, since the equilibrium of APM and GUA is on the side of the protonated form due to their high pK_a values. A buffer solution of a pH value of 5 is used for the incubation studies. *N*-(3-Acrylamidopropyl)trimethylammonium chloride (APTMA) contains a positively charged quaternary ammonium group. All of them are thus collectively referred to as positively charged monomers. Pepsin has a negative net charge at these pH values due to its low isoelectric point[20].

APM contains a primary amine group and can thus form one ionic interaction and one hydrogen bond with the carboxyl groups of the acidic amino acid residues in pepsin. GUA has a guanidinium group and can thus form one ionic interaction and two hydrogen bonds with the carboxyl groups of pepsin.[243] APM has the same functional group like lysine and GUA has the same functional group like arginine. APTMA can form ionic and hydrophobic interactions with pepsin.

Under the binding conditions mainly negatively charged NPs are prepared with 20 mol-% of acrylic acid (AAc). These shall serve as negative control for the binding studies. Low binding of pepsin is expected due to electrostatic repulsion of the negative charges of the carboxylate groups of AAc and pepsin. The functional monomer *N*-(2-hydroxyethyl)acrylamide (HEAm) with a hydroxyl group (10 and 20 mol-%) was introduced for the formation of additional hydrogen bonds due to the high amount of amino acid residues with hydroxyl groups in pepsin (26%). NPs were prepared from a combination of the positively charged monomer APM (20 mol-%) and HEAm (20 mol-%) to find out, if additional hydrogen bonds in combination with ionic and hydrophobic increase the affinity to pepsin.

3.8.3 Properties of the nanoparticles

The NPs were prepared by precipitation polymerization using a low total monomer concentration and a small amount of surfactant. The positively charged surfactant cetyltrimethylammonium bromide (CTAB) was used for the synthesis of positively charged NPs and the negatively charged surfactant sodium dodecyl sulfate (SDS) was used for the preparation of negatively charged and neutral NPs in order to avoid aggregation of the NPs. After the polymerization the NPs were purified by dialysis to remove the surfactant, unreacted monomer and oligomers. The average hydrodynamic particle diameter, polydispersity index (PDI), zeta potential, concentration and conversion of the NPs were determined by dynamic light scattering (DLS), laser Doppler electrophoresis and gravimetric analysis after dialysis and are summarized in Table 3.3.

Table 3.3 Properties of the synthesized NPs including average hydrodynamic particle diameter (d_{DLS}), polydispersity index (*PDI*), zeta potential (ζ), NP concentration (c) and conversion (X) determined after dialysis.

	Type of NP	d_{DLS} [nm]	*PDI* [-]	ζ [mV]	c [µg mL^{-1}]	X [%]
1	GUA 5	86	0.29	40	350	44
2	GUA 10	164	0.44	43	240	30
3	GUA 20	108	0.21	43	220	26
4	APM 5	114	0.26	54	320	40
5	APM 10	100	0.28	51	975*	128*
6	APM 20	130	0.17	54	215	27
7	APTMA 5	124	0.22	35	285	36
8	APTMA 10	132	0.15	42	260	33
9	APTMA 20	183	0.28	45	225	27
10	TBAm 0	131	0.19	-18	440	60
11	TBAm 20	159	0.09	-23	455	64
12	TBAm 40	93	0.20	-27	415	57
13	HEAm 10	131	0.19	-18	490	65
14	HEAm 20	159	0.09	-23	455	64
15	HEAm APM	126	0.15	38	110	14
16	AAc 20	140	0.11	-29	200	30

* Values are too high maybe due to incomplete lyophilization.

The average hydrodynamic diameters of all NPs were between 90 and 180 nm. According to the IUPAC definition[246] not all of them were NPs, but are further called like this for simplicity. The obtained size range is larger compared with the results of the previous work from the Shea group[231,232,239,240]. This can come from the use of another average diameter from the DLS measurement. The obtained particles were smaller than the polymer particles prepared by miniemulsion polymerization (chapter 2.6.4). The diameters and PDI values did not follow a clear trend with regard to the type and ratio of the functional monomers. The PDI values were between 0.1 and 0.4 indicating that the particle size distributions were between narrow and broad. The

particle size distributions were monomodal. The obtained PDI values of the NPs are comparable to the PDI values obtained by miniemulsion polymerization (chapter 2.6.4).

The zeta potentials of the NPs prepared with different positively charged monomers were between 35 and 51 mV due to the incorporation of the positively charged monomers. These values were similar to the zeta potentials of the MIP and NIP particles obtained in the previous chapter 2.6.3. The zeta potential of the NPs increased with increasing feed ratio of APTMA. This trend was not that clear for the NPs prepared with APM and GUA. The highest zeta potentials were obtained with APM. This could indicate that more APM was incorporated in the polymer network. This matched the results of the analysis of the NP composition by proton nuclear magnetic resonance (^{1}H-NMR) spectroscopy[240]. The NPs prepared with AAc had a negative zeta potential of -29 mV due to the negatively charged carboxylate groups. The zeta potentials of the NPs prepared with neutral monomers were negative maybe due to remaining surfactant.

The concentration of most NPs was between 200 and 450 µg mL^{-1} and the conversion between 30 and 60%. The conversion of the NPs was lower than of the MIP and NIP particles in chapter 2.6.4. It is noticeable that the NPs prepared with positively and negatively charged monomers had a lower conversion than the other ones. This indicates that fewer charged monomers than neutral monomers were incorporated in the polymer network. This matches the results of the analysis of the NP composition by ^{1}H-NMR spectroscopy and elemental analysis[240]. These show that the actual molar ratios of the positively charged monomers in the NPs are lower than in the feed ratios. The conversion decreased with increasing monomer feed ratio of the positively charged monomers. This may be due to electrostatic repulsion between the positively charged monomers in solution and the reacted monomer units in the polymer. The concentration and conversion of the NPs prepared with 10 mol-% of APM was too high, maybe because not the entire water could be removed during the lyophilization. The concentration and conversion of the NPs prepared with both, 20 mol-% of HEAm and 20 mol-% of APM, were lower than the concentration and conversion of the NPs prepared either with 20 mol-% of HEAm or 20 mol-% of APM.

3.8.4 Incubation study in solution

The capability of the different NPs to bind pepsin was evaluated by batch binding experiments in solution according to the procedure illustrated in Figure 3.7. A pepsin solution in citric buffer of pH 5 was incubated with the same volume of the different NP solutions. A pH value of 5 was chosen, because pepsin and various other proteins are stable at this pH value in regard to a selectivity study and the application as protease scavenger material.

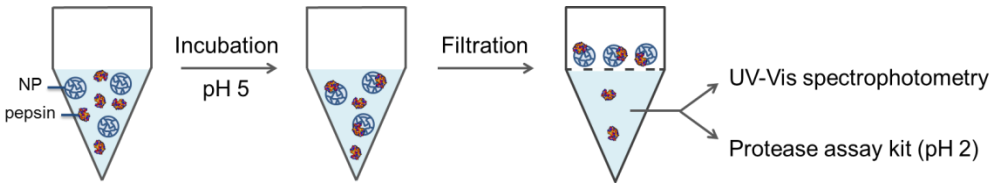

Figure 3.7 Procedure of the incubation study in solution.

After the removal of the NPs with the bound pepsin by centrifugal filtration the absorbance of remaining pepsin in the filtrate was determined by UV-Vis spectrophotometry and the remaining pepsin activity was determined by using an EnzChek® protease assay kit at a pH value of 2 and a fluorescence microplate reader. A NP control sample (negative control) was prepared in the same way, but without pepsin. A pepsin reference sample (positive control) and samples containing different pepsin concentrations were prepared in the same way, but without the NPs.

The absorbance at 277 nm of the filtrates after the incubation of pepsin and the different NPs, of the pepsin reference and the NP control sample is shown in Figure 3.8.

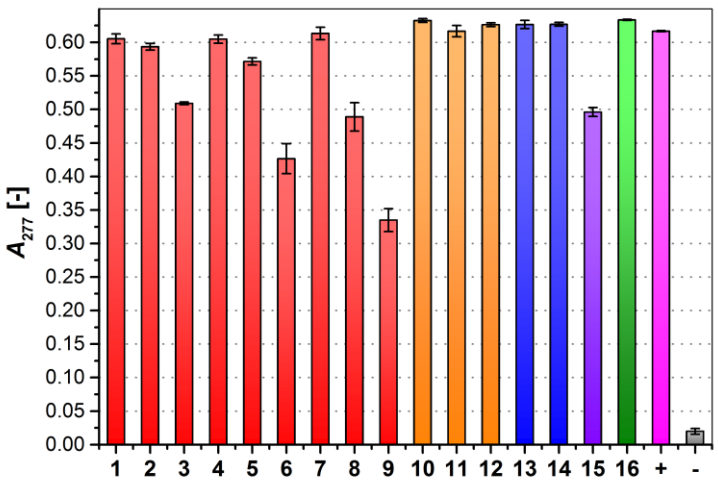

Figure 3.8 Absorbance at 277 nm (A_{277}) of the filtrates after the incubation of pepsin and the different NPs (1-16), of the pepsin reference (+) and the NP control sample (-). All bars represent the average of three samples. The error bars show the standard deviation.

The bars of the different NPs are shown in different colors dependent on their physicochemical properties (red: positively charged, orange: hydrophobic, blue: hydrophilic, violet: positively charged and hydrophilic and green: negatively charged). The pink bar represents the pepsin reference

sample and the grey bar represents the NP control sample. The colors are maintained in all following graphs of this chapter. The absorbance of the NP control sample was low confirming that at least most of the NPs that can scatter UV light were removed by centrifugal filtration. It is assumed that the missing amount of pepsin in the filtrate was bound to the NPs. The content of bound pepsin was determined as described in chapter 3.7.4 after confirming that there was a linear relationship between the absorbance and different pepsin concentrations in the measuring range. The content of bound pepsin is shown in Figure 3.9.

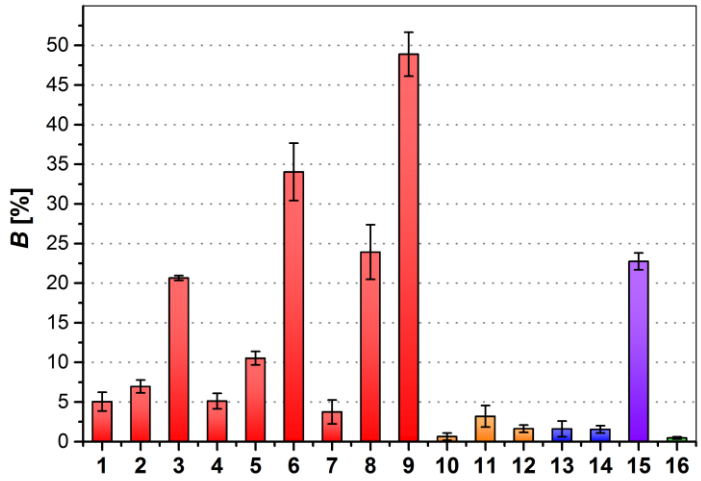

Figure 3.9 Content of pepsin bound (*B*) to the different NPs (1-16). All bars represent the average of three samples. The error bars show the standard deviation.

More pepsin was bound to the positively charged NPs than to the neutral and negatively charged NPs due to ionic interactions between the overall negatively charged pepsin and the positively charged NPs at pH 5. The higher the feed ratio of the positively charged monomers was the more pepsin was bound due to an increase of ionic interactions. By the way this conversely indicates that a higher feed ratio of the positively charged monomers led to a higher incorporation of these in the polymer NPs. This matched the results obtained from the analysis of the NP composition[240], which show that an increasing feed ratio resulted in a higher ratio of the positively charged monomers in the NPs. This is comparable to the results obtained with the MIPs and NIPs in chapter 2.6.9.

The content of bound pepsin was dependent on the type of positively charged monomer used for the NP synthesis. The highest amount of pepsin was bound to the NPs prepared with 20 mol-% of APTMA, even if its particle size was highest meaning that its surface area was lowest. This was also the most suitable monomer for the imprinting of pepsin in chapter 2.6.9.1. Less pepsin was bound to the NPs prepared with 20 mol-% of APM and the lowest amount of pepsin was bound to the NPs prepared with 20 mol-% of GUA. The difference between APTMA and both, APM and GUA, is that it contains three additional methyl groups, which seem to improve the affinity to pepsin due to the formation of additional hydrophobic interactions. The amine group in APM has the highest local

positive charge density and the positive charge in APM is not sterically hindered as in GUA. This may be the reason, why pepsin had a higher affinity to APM compared to GUA containing NPs. The obtained trend in the affinity of pepsin to the NPs prepared with the three different types of positively charged monomers was in contrast to the obtained trend in the affinity of fibrinogen to comparable NPs[240]. Y. Yonamine et al explained the higher affinity of fibrinogen to GUA than to APM and APTMA containing NPs with the formation of additional hydrogen bonds between the positively charged functional groups and fibrinogen. GUA can form two additional, APM one and APTMA no additional hydrogen bond. The hydrogen bonds did not seem to play an important role for the interaction with pepsin. It is somewhat surprising that pepsin had the highest affinity to APTMA containing NP, since APTMA is the only monomer with a functional group, which differs from the functional groups of natural positively charged amino acids.

As expected almost no pepsin was bound to the negatively charged NPs due to charge repulsion. Hardly any pepsin was bound to the hydrophobic NPs, although pepsin has a high amount of hydrophobic amino acid residues on the surface and proteins usually adsorb on hydrophobic surfaces.[30] The ratio of TBAm in the feed ratio for the preparation of the hydrophobic NPs had no effect on the pepsin binding capability. The incorporation of the monomer HEAm for the formation of additional hydrogen bonds did not increase the amount of bound pepsin. It seems that hydrophobic interactions and hydrogen bonds were too weak to bind pepsin in a citric buffer solution (pH 5). The replacement of 20 mol-% of NIPAm by HEAm in the monomer mixture, which also contained APM and TBAm, resulted in a decrease of the content of bound pepsin.

This shows that a combination of hydrophobic interactions and ionic interactions resulted in a higher affinity of the NPs to pepsin than a combination of hydrogen bonds and ionic interactions. This result is comparable with the results obtained for the NPs, which had a high affinity to fibrinogen[240], melittin[231,241], lysozyme[239] and IgG[232] due to a combination of ionic and hydrophobic interactions. The obtained order of the most suitable functional groups for binding pepsin to the NPs was slightly different from the obtained order for binding pepsin to the MIP and NIP particles (chapter 2.6.9). Slightly more pepsin was bound to the MIP and NIP particles prepared with AEMA having the same functional group as APM and to the polymer particles prepared with MAA having the same functional group as AAc. However, ionic interactions played an important role in binding pepsin to both types of polymer particles.

In summary, the highest affinity of the NPs to pepsin was achieved by the addition of 20 mol-% of APTMA to the monomer mixture of TBAm (40 mol-%), NIPAm (38 mol-%) and BIS (2 mol-%) due to mainly ionic and hydrophobic interactions besides hydrogen bonds between the NPs and pepsin.

For the determination of the remaining pepsin activity in the filtrates the filtrates were diluted and the pH value was adjusted to 2, at which pepsin has its maximum activity[23], for the enzymatic reaction with the casein derivative of the Enzchek® protease assay kit. The results of a pre-experiment showed that pepsin had 71% of its maximum activity after back titration of the pH value of the solution from 5 to 2 under comparable conditions. This is a sufficient activity for the determination of the pepsin activity in the filtrates. The fluorescence intensity at 530 nm released from the peptides of the casein derivative, which was cleaved by remaining pepsin in the filtrates after the incubation of pepsin with the different NPs, by the pepsin reference and the NP control sample, is shown in Figure 3.10.

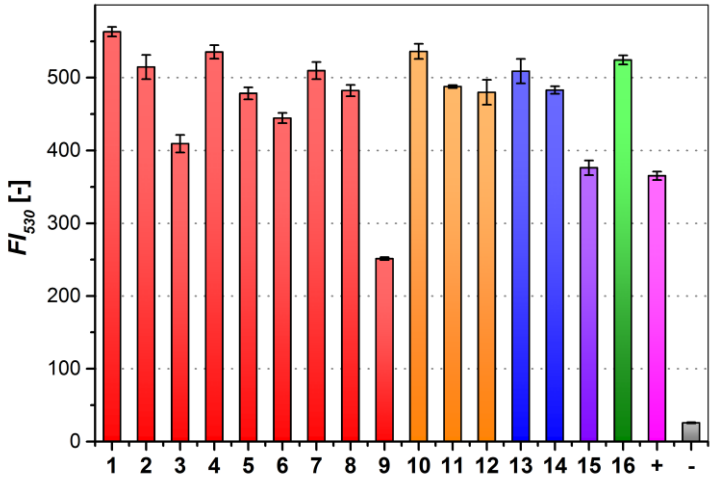

Figure 3.10 Fluorescence intensity at 530 nm (FI_{530}) released from the peptides of the casein derivative, which was cleaved by remaining pepsin in the filtrates after the incubation of pepsin with the different NPs (1-16), by the pepsin reference (+) and the NP control sample (-). All bars represent the average of 4 samples. The error bars show the standard deviation.

The fluorescent intensity of the NP control sample was low, as expected. The fluorescent intensity of the pepsin reference sample was lower than the fluorescent intensity of most of the other samples instead of being higher. This was not consistent with the absorbance of the pepsin reference sample (Figure 3.8) and was most likely caused by a pipetting error during the dilution. The preparation of this sample has thus to be repeated. Since the fluorescence intensity is proportional to the pepsin activity,[245] which was verified by a pre-experiment, it is assumed that the higher the fluorescence intensity was the higher was the concentration of remaining, active pepsin in the filtrate. The signals in Figure 3.10 followed the same trend as the signals in Figure 3.8 with only one exception that the order of signal 3 and 6 is the other way round. This shows that both analysis methods are comparable and that the remaining pepsin in the filtrate was still active after being titrated from pH 5 to 2 and staying in the same solution as the NPs. From this it follows that the pepsin activity measurements can also be used to analyze the binding experiments.

3.8.5 Incubation study in microtiter wells

Another method for the evaluation of the affinity of the NPs to pepsin was developed in order to enable a faster screening without a filtration step and the direct measurement of the content of bound pepsin. A scheme of the new incubation study in microtiter wells is shown in Figure 3.11. The NPs were therefore immobilized on wells of a 96-well plate by physical adsorption before the incubation with pepsin in a citric buffer solution of a pH value 5. A hydrophobic well plate was used, because all NPs contained the monomers TBAm and NIPAm having a hydrophobic group. After the incubation a part of the supernatants was pipetted into wells of another 96-well plate to measure the activity of free pepsin in the solutions. The remaining part of the supernatants was removed from the first 96-well plate and the NPs were washed with a citric buffer solution (pH 5) to remove non- or unspecifically bound pepsin.

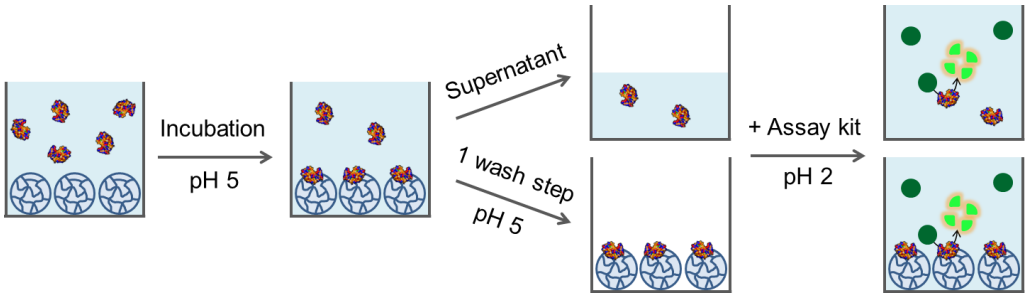

Figure 3.11 Procedure of the incubation study in microtiter plates.

Protease assay working solutions containing hydrochloric acid (HCl) were added to the first and second 96-well plate containing the bound and free pepsin. The concentration of HCl was adjusted so that the final pH value of the mixture of pepsin and the protease assay solution was 2. A higher concentration of HCl in the protease assay solution for the supernatants was necessary to adjust their pH value from 5 to 2. After the enzymatic reaction the fluorescence intensity was measured with a fluorescence microplate reader. A NP control sample (negative control) was prepared in the same way as the samples, but without the addition of pepsin. A pepsin control sample (positive control) was prepared in the same way, but without the prior immobilization of the NPs on the wells. As pepsin reference sample a pepsin solution in citric buffer of pH 5 was added to another well plate and mixed with the protease assay solution containing an equivalent HCl concentration in order to titrate the pH value from 5 to 2.

The fluorescence intensity at 530 nm released from the peptides of the casein derivative, which was cleaved by the pepsin bound to the different immobilized NPs, by the pepsin and NP control sample and the pepsin reference sample, which is represented by the black bar, is shown in Figure 3.12.

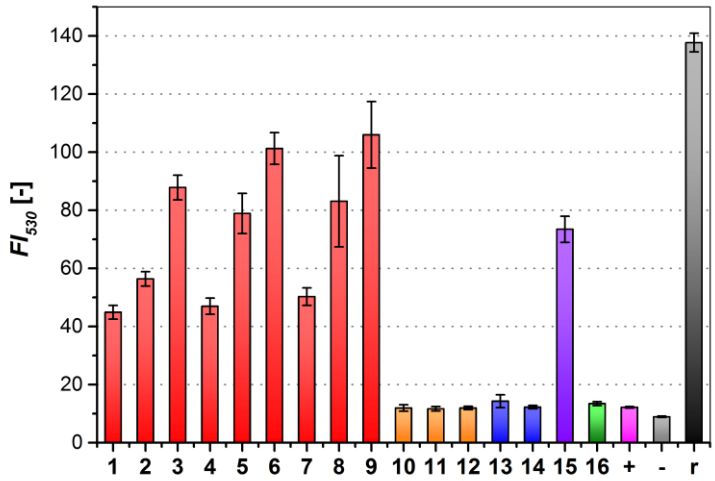

Figure 3.12 Fluorescence intensity at 530 nm (FI_{530}) released from the peptides of the casein derivative, which was cleaved by the pepsin bound to the different immobilized NPs (1-16), by the pepsin (+) and NP control sample (-) and pepsin reference sample (r). All bars represent the average of 4 samples. The error bars show the standard deviation.

The fluorescence intensity of the pepsin reference sample was lower than the fluorescence intensity of the pepsin reference sample of the previous chapter 3.8.4, since the procedure of the back titration of the pH value from 5 to 2 was slightly different. The fluorescence intensity coming from active pepsin bound to the positively charged NPs was significantly higher than the fluorescence intensity coming from the pepsin control sample. This may show that more pepsin was bound to the positively charged NPs than to the well and a blocking agent was not necessary, unless the binding to the hydrophobic well resulted in an inhibition of the pepsin activity. The use of a blocking agent was waived, because most blocking agents are proteins such as bovine serum albumin and can be cleaved by pepsin.

The fluorescence intensity coming from active pepsin bound to the positively charged NPs was higher than the fluorescence intensity coming from active pepsin bound to the hydrophobic, hydrophilic and negatively charged NPs. The fluorescence intensity increased with increasing feed ratio of the positively charged monomers. The highest fluorescence intensity was obtained after binding pepsin to the NPs synthesized with 20 mol-% of APTMA. The fluorescence intensity of the pepsin bound to these NPs was only slightly lower than the fluorescence intensity of the pepsin reference sample. The obtained trend of the fluorescence intensity was similar to the trend of the content of bound pepsin obtained by the incubation study in solution. Only the difference between the signal coming from pepsin bound to the NPs prepared with 5 mol-% of the positively charged monomers and the signal coming from pepsin bound to the hydrophilic and hydrophobic NPs was higher in this study. This shows that the bound pepsin was still active and not inhibited through the

adsorption on the NPs and that the fluorescence intensity was thus proportional to the content of bound pepsin. This conversely means that a sufficient number of all NPs were immobilized on the wells. There are two possible reasons for the activity of pepsin. The interactions between pepsin and the NPs were either weakened by the change of the pH value from 5 to 2 and pepsin went back into the solution or the catalytic site of pepsin was still accessible for the substrate while being bound to the NPs. The first explanation applies especially to the positively charged NPs, since pepsin is overall neutral at a pH value of 2, what may cancel the ionic interactions.

The graph in Figure 3.13 shows the fluorescence intensity at 530 nm released from the peptides of the casein derivative, which was cleaved by the free pepsin in the supernatants above the different immobilized NPs, by the pepsin control and reference sample.

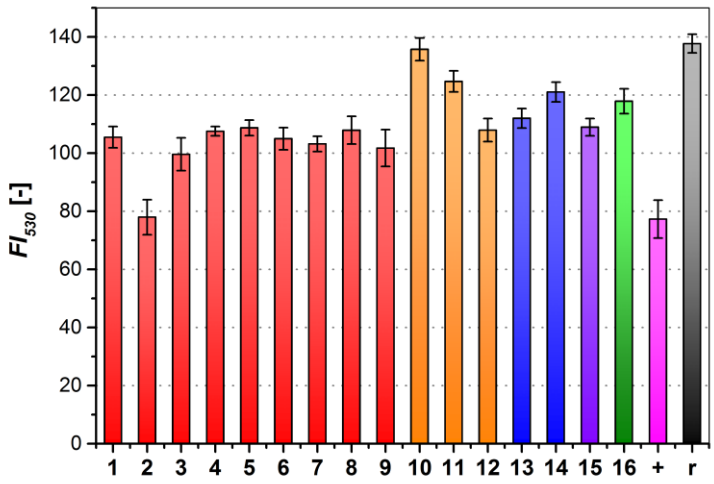

Figure 3.13 Fluorescence intensity at 530 nm (FI_{530}) released from the peptides of the casein derivative, which was cleaved by the free pepsin in the supernatant above the different immobilized NPs (1-16), by the pepsin control (+) and reference sample (r). All bars represent the average of 4 samples. The error bars show the standard deviation.

The fluorescence intensities obtained from the different supernatants were quite similar. This means that there was almost the same amount of active, free pepsin in the solution independent on the composition of the NPs. A slightly lower content of active, free pepsin was in the supernatants above the positively charged NPs than in the supernatants above the neutral and negatively charged NPs. There was no difference in the amount of active, free pepsin in the supernatants above the NPs prepared with different ratios of the positively charged monomers except above the NPs prepared with 10 mol-% of GUA. A comparable low content of free, active pepsin was in the solution after incubation of pepsin with the wells without NPs (pepsin control sample).

These results were not consistent with the results obtained by the incubation study in solution (Figure 3.10 of chapter 3.8.4). The obtained trend of the content of free, active pepsin in the supernatant was also not complementary to the trend obtained by the measurement of the bound, active pepsin in Figure 3.12.

For a better overview of the results of the whole study the fluorescence intensity at 530 nm released from the peptides of the casein derivative, which was cleaved by the free pepsin in the supernatant and the pepsin bound to the different NPs, by the free and bound pepsin in the pepsin control sample and by the pepsin reference sample, is summarized in the graph of Figure 3.14.

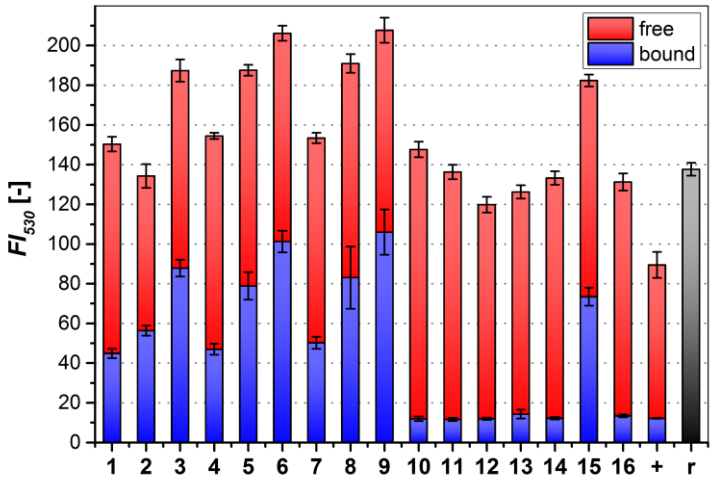

Figure 3.14 Fluorescence intensity at 530 nm (FI_{530}) released from the peptides of the casein derivative, which was cleaved by the free pepsin in the supernatant (red) and the pepsin bound (blue) to the different NPs (1-16) and of the pepsin control sample (+) and by the pepsin reference sample (r). All bars represent the average of 4 samples. The error bars show the standard deviation.

The total fluorescence intensity released from the peptides of the casein derivative, which was cleaved by the free and bound pepsin after the incubation with the neutral and negatively charged NPs and the NPs prepared with a low ratio of the positively charged monomers, was comparable with the fluorescence intensity obtained by the pepsin reference sample. This means that no pepsin was removed during the washing step and pepsin had a comparable activity. The total fluorescence intensity obtained by the free and bound pepsin after incubation with the well was lower than the fluorescence intensity obtained by the pepsin reference sample. Either non- and unspecifically bound pepsin was removed during the washing step or a part of pepsin was deactivated after the adsorption to the hydrophobic well.

The total fluorescence intensity obtained by the free and bound pepsin after the incubation with the NPs prepared with a high ratio of the positively charged monomers was higher than the fluorescence intensity obtained by the pepsin reference sample. Maybe the presence of positively charged NPs resulted in an activation of pepsin. It may also be that the fluorescence intensity of the pepsin reference sample was too low due to a higher salt concentration by the use of the citric buffer and a higher HCl concentration. In comparison, a lower HCl concentration and no citric buffer solution was used for the experiments with the bound pepsin. These conditions may have resulted in a higher activity of pepsin. Another possibility is that some pepsin molecules were deactivated after contact with the wells without immobilized NPs. This effect could be more pronounced, when

there were more pepsin molecules in the supernatants. This was the case in the supernatants above the hydrophobic, hydrophilic NPs and the NPs prepared with a low content of positively charged monomers.

In conclusion, the fast screening of the different NPs for their affinity to pepsin bound to different NPs is possible, since the obtained results were comparable to the results of the binding study in solution. The determination of the free pepsin in the supernatants requires further investigations and optimization.

3.8.6 Inhibition study in microtiter wells

The incubation study in the previous chapter 3.8.5 was modified for the investigation, whether the binding of pepsin to the NPs inhibits the activity of pepsin. The inhibition of the pepsin activity may occur, when the catalytic center of pepsin is bound to the NPs and thus inaccessible for the substrate or when the binding to the NPs results in a conformational change and thus a denaturation of pepsin. The NPs were therefore immobilized on wells of a 96-well plate by physical adsorption before the incubation with the pepsin solution in citric buffer of pH value 5. After the incubation a protease assay working solution in a citric buffer (pH 5) was added. The supernatant was not removed as in chapter 3.8.5, so that there was free as well as bound pepsin in the wells. The pH value was kept constant at 5 to avoid any changes of the interactions between pepsin and the NPs. The results of a pre-experiment showed that pepsin had 8% of its maximum activity under comparable conditions. After the enzymatic reaction the fluorescence intensity was measured (Figure 3.15).

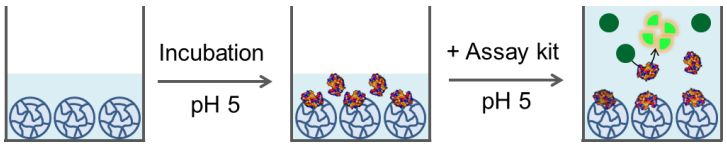

Figure 3.15 Procedure of the inhibition study in microtiter wells.

A NP control sample (negative control) was prepared in the same way, but without the addition of pepsin. A pepsin control sample (positive control) was prepared in the same way, but without the immobilization of the NPs.

The fluorescence intensity at 530 nm released from the peptides of the casein derivative, which was cleaved by the pepsin incubated with the different immobilized NPs, by the pepsin and NP control sample, is shown in Figure 3.16.

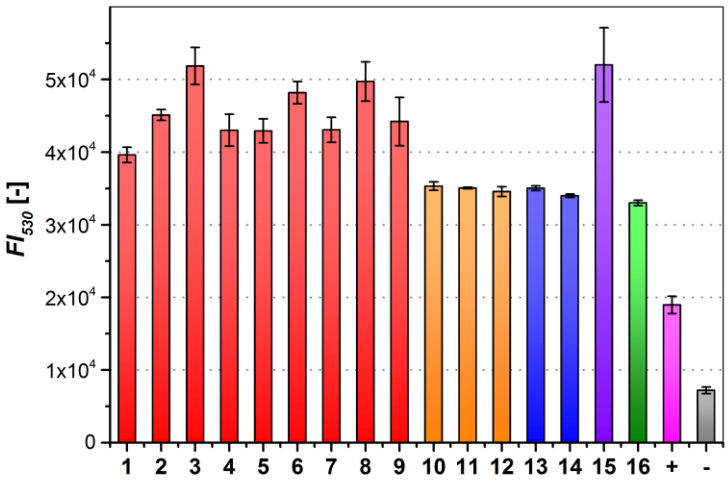

Figure 3.16 Fluorescence intensity at 530 nm (FI_{530}) released from the peptides of the casein derivative, which was cleaved by the pepsin incubated with the different immobilized NPs (1-16), by the pepsin (+) and NP control sample (-). All bars represent the average of 4 samples. The error bars show the standard deviation.

The obtained fluorescence intensity was generally higher than the fluorescence intensity of the chapters 3.8.4 and 3.8.5, because another fluorescence reader with a different setting was used. The fluorescence intensity of the pepsin control sample was lower than the fluorescence intensity of the other samples. This means that the activity of pepsin was partially inhibited after the adsorption on the hydrophobic well as presumed in the previous chapter 3.8.5. The fluorescence intensity obtained after incubation of pepsin with the neutral and negatively charged NPs was lower than the fluorescence intensity obtained after incubation of pepsin with the positively charged NPs. This shows that more pepsin was inhibited by the neutral and negatively charged NPs, although the previous results (chapter 3.8.4 and 3.8.5) showed that almost no pepsin was bound to the neutral and negatively charged NPs. The fluorescence intensity increased with increasing feed ratio of the positively charged monomers with the exception of the NPs synthesized with 20 mol-% of APTMA and 10 mol-% of APM. The obtained trend was not as expected. It was rather expected that there was less active pepsin the more pepsin was bound to the NPs. It is unlikely that the lower activity of pepsin, which was incubated with the neutral NPs, resulted from an inhibition of pepsin after the adsorption on free space on the wells, since more hydrophobic than positively NPs should be immobilized on the wells due to the hydrophobic surface of the wells. The trend of the fluorescence intensity obtained by this incubation study was similar to the one shown in Figure 3.14. It looks like as if the pepsin activity was activated by the presence of the positively charged NPs. Another reason might be that the contact of pepsin with the more hydrophobic and neutral NPs resulted in a change of the pepsin conformation and thus in a partial denaturation.

In conclusion, the binding of pepsin to the NPs did not result in an inhibition of its activity. This is in contrast to the result obtained with the MIPs and NIPs in chapter 2 by another inhibition study using SDS-PAGE. This may come from the different composition of the NPs or a different binding mechanism.

3.8.7 Incubation study with different pepsin concentrations

Batch binding experiments in solution were carried out with the NPs 9 prepared with 20 mol-% of APTMA, since these showed the highest affinity to pepsin, and different initial concentrations of pepsin (4000-500 µg mL^{-1}) in order to investigate the binding behavior in further detail. The amount of bound pepsin per amount of NP is plotted against the free pepsin concentration in the filtrates in Figure 3.17.

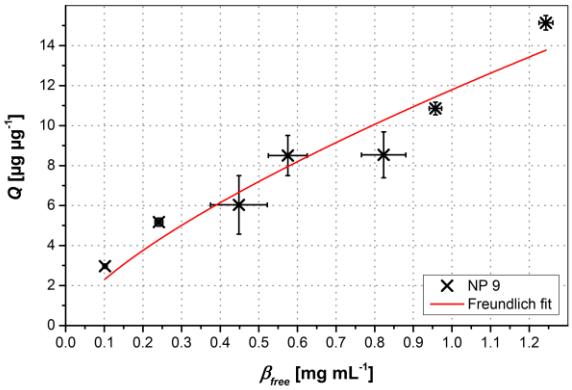

Figure 3.17 Binding isotherm of the NPs 9. All data points represent the average of three samples. The error bars show the standard deviation. The red curve was obtained by fitting the Freundlich equation to the experimental data points.

The amount of bound pepsin increased with increasing free pepsin concentration. The progression of the data points suggests that there was no saturation of the NPs with pepsin at higher pepsin concentrations. The Freundlich, Langmuir and Langmuir-Freundlich equations were fitted to the experimental data points by using a non-linear least-square analysis of the program OriginPro 9.0G. The best fit with the smallest correlation coefficient (R^2 = 0.912) was obtained with the Freundlich equation (red curve in Figure 3.17). The Langmuir equation was fitted to the binding isotherms of similar nanoparticles[231]. A better fit was obtained with the Langmuir equation to the binding isotherms of the MIP and NIP particles (chapter 2.6.10). The obtained heterogeneity index was 0.72 and the Freundlich constant 11.79 µg $µg^{-1}$. This suggests that the NPs had a rather heterogeneous surface with different adsorption sites, which may come from the random distribution of the monomer units in the NPs, and could bind several layers of pepsin. However, the agreement of the curve with the experimental data points was moderate and there was an uncertainty due to the relatively high standard deviation of the middle data points.

3.8.8 Incubation study during different time intervals

Batch binding experiments in solution were carried out with the NPs 9 prepared with 20 mol-% of APTMA, since these showed the highest affinity to pepsin, during different time intervals (1-90 min) in order to investigate the kinetic binding behavior. The amount of bound pepsin per amount of NP is plotted against the incubation time in Figure 3.18.

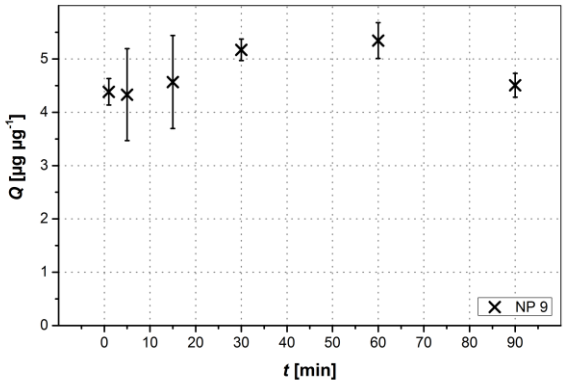

Figure 3.18 Binding kinetic of the NPs 9. All data points represent the average of three samples. The error bars show the standard deviation.

The progression of the data points shows that the adsorption of pepsin to the NPs was very fast due to the good availability of the binding sites for pepsin, since most of the binding sites were probably at the surface due to the small size, and due to the flexibility of the lowly cross-linked polymer particles. The binding equilibrium seems to be already reached after 1 minute, when considering the uncertainty of the data. Hence, an incubation time of 30 min used during the binding experiments was sufficient. This was comparable to the result obtained with MIP and NIP 5 and 6 (chapter 2.6.11).

3.8.9 Comparison with a MIP and pepstatin immobilized agarose beads

Batch binding experiments in solution were carried out with MIP 5 and commercially available pepstatin immobilized agarose beads (PABs) under the same conditions as with the NPs in chapter 3.8.4 for a direct comparison. MIP 5 is one of the MIPs, which showed the highest content of bound pepsin in chapter 2.6.9.2. The content of pepsin bound to MIP 5 and to the PABs is compared to the content of pepsin bound to the NPs 7, 8 and 9 prepared from 5, 10 and 20 mol-% of APTMA in Figure 3.19.

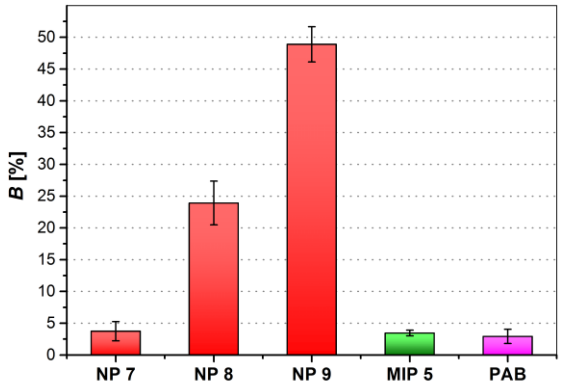

Figure 3.19 Content of pepsin bound (*B*) to the NPs 7, 8 and 9, to MIP 5 and the PABs. All bars represent the average of two (MIP 5, PABs) or three samples (NPs). The error bars show the spread (MIP 5, PABs) or standard deviation (NPs).

Significantly more pepsin was bound to the positively charged NPs 8 and 9 than to MIP 5. The content of pepsin bound to MIP 5 was comparable to the content of pepsin bound to the NPs 7 prepared from 5 mol-% of APTMA, although 20 mol-% of the same monomer were used for the synthesis of MIP 5. The NPs 8 and 9 and MIP 5 had similar zeta potentials and the conversion of the NPs was lower than of MIP 5. This arguments against that the higher pepsin binding was a result of a higher incorporation of APTMA in the polymer network of the NPs. The higher content of bound pepsin may be explained with the larger particle size of MIP 5 resulting in a lower surface area. Other reasons may be a better accessibility of the functional groups of the monomer units for pepsin due to the higher flexibility of the lowly cross-linked NPs and that acrylamide based micro- and nanogels may be more compatible to proteins[228] than rigid and highly cross-linked particles as MIP 5. The formation of additional hydrophobic interactions between the NPs 8 and 9 and pepsin coming from the copolymerization of TBAm may have further enhanced the pepsin binding capability.

Significantly more pepsin was also bound to the positively charged NPs 8 and 9 than to the PABs. This may be explained by the fact that the binding between the PABs and pepsin is based on hydrogen bonds and van der Waals interactions[26], which are weaker in an aqueous environment than ionic and hydrophobic interactions. The inhibition of pepsin by pepstatin is less effective at pH values higher than 4.[29] Probably the binding of pepsin to the PABs was also less effective at a pH value of 5, which was used during these binding experiments. Another reason may be the smaller

size of the NPs and the better accessibility of the functional groups on the polymer surface for pepsin, whereas most of the immobilized pepstatin residues are in the pores of the PABs.

A general lower content of pepsin was bound to MIP 5 and the PABs compared to the results of chapter 2.6.9, since a lower amount of polymer and pepsin and a buffer solution instead of pure water were used during these binding experiments.

3.9 Conclusion and outlook

Monodisperse NPs with an average hydrodynamic diameter of 90-180 nm were synthesized by precipitation polymerization. Acrylamides with different functional groups were used and their ratios were varied in order to find the NPs with the highest affinity to pepsin. The different NPs were evaluated for their affinity to pepsin by two different incubation studies. One was a conventional incubation study in solution. UV-Vis spectrophotometry and an Enzchek® protease assay kit were thereby used for the analysis of the remaining concentration and activity of pepsin in the solution after removal of the NPs with the bound pepsin by centrifugal filtration. Another incubation study in microtiter wells was established. The NPs were immobilized on a 96-well plate before the incubation with the pepsin solution. The content of active, bound pepsin and free pepsin in the supernatants were separately determined by pepsin activity measurements using the protease assay kit and a fluorescence reader. The results in terms of bound pepsin were in agreement with the incubation study in solution. The plate-supported assay can thus be used in future with the advantage that it enables a fast screening of the different NPs for their affinity to pepsin and the direct detection of the bound pepsin. The results from the study of the supernatants were not as expected and thus require further investigations. The inhibition capability of the pepsin activity through the NPs was investigated by an inhibition study, which was similar to the incubation study in microtiter wells. The only difference was that here the activity of the bound and free pepsin was determined at once.

The results of the incubation studies showed that the highest content of pepsin was bound to the NPs with a quaternary ammonium, primary amino and guanidinium group additionally to *tert*-butyl and isopropyl groups. All of them were positively charged under the binding conditions (pH 5) and could interact with pepsin, which has a negative net charge at pH 5, by mainly ionic and hydrophobic interactions. The increase in the feed ratio of the positively charged monomers resulted in an increase of the affinity of the NPs to pepsin due to the high content of carboxyl groups of acidic amino acid residues on the surface of pepsin. This was comparable to the results obtained with the polymer particles described in chapter 2. The highest affinity to pepsin showed the NPs synthesized from 20 mol-% of APTMA, 40 mol-% of TBAm, 38 mol-% of NIPAm and 2 mol-% of BIS. APTMA was thus the most suitable positively charged monomer for binding pepsin. APTMA has a permanent positive charge and contains 3 methyl groups for additional hydrophobic interactions and was also the most suitable monomer for imprinting pepsin in chapter 2. The copolymerization of a new acrylamide with a hydroxyl group for the formation of additional hydrogen bonds did not increase the affinity of the NPs to pepsin. The influence of the contribution of hydrophobic interactions on the affinity of the NPs to pepsin was investigated by varying the content of TBAm in the NPs. Due to the absence of a positively charged monomer the affinity to pepsin was low regardless of the content of TBAm.

The inhibition study showed that a higher pepsin activity was inhibited by the presence of neutral NPs, although these showed a lower affinity to pepsin than the positively charged NPs. Maybe pepsin was partially denatured after the contact with the neutral NPs or activated by the presence of the positively charged NPs. The adsorption of pepsin to a well resulted in a partial inhibition of the pepsin activity, too. For this reason the use of a suitable blocking agent could possibly improve the quality of the plate-supported incubation studies. The result that pepsin was still active after binding to the positively charged NPs is in contrast to the result obtained with the MIPs and NIPs in chapter 2 by another inhibition study using SDS-PAGE. This may come from the different composition of the NPs and a different binding mechanism. Such an inhibition study can be performed with the NPs to obtain more information about their inhibition capability and for a better comparison with the MIPs.

The curve progression of a recorded binding isotherm resembled the progression of a Freundlich isotherm without a saturation of the binding sites. This suggests that the NPs had a rather heterogeneous surface with different adsorption sites, which may come from the random distribution of the monomer units in the NPs, and could bind several layers of pepsin. This was in contrast to the results obtained in chapter 2, in which the binding isotherms resembled the progression of a Langmuir isotherm suggesting that the particles had a homogeneous surface with equal adsorption sites and could only adsorb a monolayer of pepsin. The dependence of the amount of bound pepsin on the incubation time showed that the binding equilibrium was already reached after 1 minute. The adsorption of pepsin to the NPs was very fast due to the good availability of the binding sites for pepsin due to the small size and flexibility of the lowly cross-linked NPs. This fast binding kinetic was comparable to the binding kinetic of some polymer particles of chapter 2.

The direct comparison of the pepsin binding capability of the NPs with an exemplary MIP and commercially available beads for pepsin purification showed that significantly more pepsin was bound to the NPs. This may be a result of the smaller size of the NPs, the better accessibility of the functional groups on the polymer particles for pepsin, the combination of ionic and hydrophobic interactions and that acrylamide based micro- and nanogels may be more compatible to proteins.

A further improvement of the affinity of the NPs to pepsin may be obtained by further increasing the feed ratio of APTMA, by varying the content of TBAm in a monomer mixture also containing APTMA or by combining this strategy with the imprinting approach. After this, the selectivity of the NPs for pepsin should be analyzed. This can be done with a competitive selectivity study with different proteins such as β-lactoglobulin and α1-acid glycoprotein using SDS-PAGE in the same way as the competitive selectivity study described in chapter 2.

Finally this approach provides a complementary approach to the imprinting approach and thus additional fundamental steps towards the development of a protease scavenger material and assay and may be transferred to other proteases such as trypsin or thermolysin in future.

4. References

[1] G. Walsh, *Biopharmaceuticals: Biochemistry and Biotechnology*, J. Wiley, Chichester, West Sussex, England; Hoboken, NJ, **2003**.

[2] "https://www.gesundheitsindustrie-bw.de/de/fachbeitrag/aktuell/rasterfahndung-nach-wirkstoff-killern/," **2009**.

[3] W. Wang, M. Singh, in *Biotechnol. Drug Prod. Dev. Strateg.*, John Wiley & Sons, Hoboken, USA, **2013**, pp. 203–233.

[4] S. Eppler, T. Schröder, J. Friedle, S. Michl, W. Dangel, B. Mizaikoff, *Biosens. Bioelectron.* **2012**, *35*, 27–32.

[5] A. Poma, A. P. F. Turner, S. A. Piletsky, *Trends Biotechnol.* **2010**, *28*, 629–637.

[6] D. Nelson, M. Cox, *Lehninger Biochemie*, Springer-Verlag, Berlin Heidelberg, Deutschland, **2009**.

[7] M. B. Rao, A. M. Tanksale, M. S. Ghatge, V. V. Deshpande, *Microbiol. Mol. Biol. Rev.* **1998**, *62*, 597–635.

[8] J. Marciniszyn, J. Hartsuck, J. Tang, *J. Biol. Chem.* **1976**, *251*, 7088–7094.

[9] L. H. Pearl, *FEBS Lett.* **1987**, *214*, 8–12.

[10] D. R. Davies, *Annu. Rev. Biophys. Biophys. Chem.* **1990**, *19*, 189–215.

[11] J. H. Northrop, *J. Gen. Physiol.* **1930**, *13*, 739–766.

[12] T. Kageyama, K. Takahashi, *Biochem. Biophys. Res. Commun.* **1982**, *107*, 1117–1122.

[13] M. N. G. James, A. R. Sielecki, *Nature* **1986**, *319*, 33–38.

[14] J. S. Fruton, *Q. Rev. Biol.* **2002**, *77*, 127–147.

[15] J. S. Fruton, S. Fujii, M. H. Knappenberger, *Biochemistry (Mosc.)* **1961**, *47*, 759–761.

[16] T. Uchino, *J. Biochem. (Tokyo)* **1940**, *31*, 323–330.

[17] Worthington Biochemical Corporation, "www.worthington-biochem.com/pm/default.html," **2015**.

[18] J. Tang, P. Sepulveda, J. Marciniszyn, K. C. S. Chen, W. Y. Huang, N. Tao, D. Liu, J. P. Lanier, *Proc. Natl. Acad. Sci.* **1973**, *70*, 3437–3439.

[19] P. Sepulveda, J. Marciniszyn, D. Liu, J. Tang, *J. Biol. Chem.* **1975**, *250*, 5082–5088.

[20] M. Jonsson, *Acta Chim. Scand.* **1972**, *26*, 3435–3440.

[21] A. R. Sielecki, A. A. Fedorov, A. Boodhoo, N. S. Andreeva, M. N. James, *J. Mol. Biol.* **1990**, *214*, 143–170.

[22] C. Abad-Zapatero, T. J. Rydel, J. Erickson, *Proteins Struct. Funct. Bioinforma.* **1990**, *8*, 62–81.

[23] D. W. Piper, B. H. Fenton, *Gut* **1965**, *6*, 506–508.

[24] H. Edelhoch, *J. Am. Chem. Soc.* **1957**, *79*, 6100–6109.

[25] Y. O. Kamatari, *Protein Sci.* **2003**, *12*, 717–724.

[26] M. Fujinaga, M. M. Chernaia, S. C. Mosimann, M. N. James, N. I. Tarasova, *Protein Sci.* **1995**, *4*, 960–972.

[27] D. H. Rich, E. T. Sun, *Biochem. Pharmacol.* **1980**, *29*, 2205–2212.

[28] S. Kunimoto, Aoyagi, R. Nishizawa, T. Komai, T. Takeuchi, H. Umezawa, *J. Antibiot. (Tokyo)* **1974**, *17*, 413–418.

[29] N. B. Roberts, W. H. Taylor, *J. Enzyme Inhib. Med. Chem.* **2003**, *18*, 209–217.

[30] J.-H. Kim, J.-Y. Yoon, *Encycl. Surf. Colloid Sci.* **2002**, *1*, 4373–4381.

[31] L. Ye, K. Mosbach, *Chem. Mater.* **2008**, *20*, 859–868.

[32] K. Haupt, K. Mosbach, *Trends Biotechnol.* **1998**, *16*, 468–475.

[33] B. Sellergren, *Trends Anal. Chem.* **1997**, *16*, 310–320.

[34] K. Mosbach, K. Haupt, *J. Mol. Recognit.* **1998**, *11*, 62–68.

[35] M. Yan, O. Ramström, *Molecularly Imprinted Materials: Science and Technology*, Marcel Dekker, New York, USA, **2005**.

[36] F. Meier, B. Mizaikoff, in *Artif. Recept. Chem. Sens. Eds V M Mirsky K Yatsimirsky*, Wiley-VCH Verlag GmbH & Co. KGaA, Weinheim, Germany, **2010**, pp. 391–437.

[37] N. W. Turner, C. W. Jeans, K. R. Brain, C. J. Allender, V. Hlady, D. W. Britt, *Biotechnol. Prog.* **2006**, *22*, 1474–1489.
[38] Y. Ge, A. P. F. Turner, *Trends Biotechnol.* **2008**, *26*, 218–224.
[39] X. Ding, P. A. Heiden, *Macromol. Mater. Eng.* **2014**, *299*, 268–282.
[40] C. J. Tan, Y. W. Tong, *Anal. Bioanal. Chem.* **2007**, *389*, 369–376.
[41] K. Landfester, *Macromol. Rapid Commun.* **2001**, *22*, 896–936.
[42] F. J. Schork, Y. Luo, W. Smulders, J. P. Russum, A. Butté, K. Fontenot, in *Polym. Part.* (Ed.: M. Okubo), Springer Berlin Heidelberg, Berlin, Heidelberg, **2005**, pp. 129–255.
[43] M. Willert, K. Landfester, *Macromol. Chem. Phys.* **2002**, *203*, 825–836.
[44] I.-M. Grabs, G. Schmidt-Naake, *Macromol. Symp.* **2009**, *275-276*, 133–141.
[45] A. Musyanovych, R. Rossmanith, C. Tontsch, K. Landfester, *Langmuir* **2007**, *23*, 5367–5376.
[46] M. V. Polyakov, *Zhurnal Fizieskoj Khimii* **1931**, *2*, 799–805.
[47] F. H. Dickey, *Proc. Natl. Acad. Sci. U. S. A.* **1949**, *35*, 227.
[48] L. Pauling, *J. Am. Chem. Soc.* **1940**, *62*, 2643–2657.
[49] G. Wulff, A. Sarhan, *Angew Chem Intern. Ed.* **1972**, *11*, 341.
[50] T. Takagishi, I. M. Klotz, *Biopolymers* **1972**, *11*, 483–491.
[51] G. Wulff, W. Vesper, R. Grobe-Einsler, A. Sarhan, *Makromol. Chem.* **1977**, *178*, 2799–2816.
[52] G. Wulff, *Pure ApplChem* **1982**, *54*, 2093–2102.
[53] R. Arshady, K. Mosbach, *Makromol. Chem.* **1981**, *182*, 687–692.
[54] B. Sellergren, B. Ekberg, K. Mosbach, *J. Chromatogr. A* **1985**, *347*, 1–10.
[55] B. Sellergren, L. Andersson, *J. Org. Chem.* **1990**, *55*, 3381–3383.
[56] G. Vlatakis, L. I. Andersson, R. Müller, K. Mosbach, *Nature* **1993**, *361*, 645–647.
[57] C. Alexander, H. S. Andersson, L. I. Andersson, R. J. Ansell, N. Kirsch, I. A. Nicholls, J. O'Mahony, M. J. Whitcombe, *J. Mol. Recognit.* **2006**, *19*, 106–180.
[58] J. L. Bowen, P. Manesiotis, C. J. Allender, *Mol. Imprinting* **2013**, *1*, 35–40.
[59] N. Pérez-Moral, A. G. Mayes, *Anal. Chim. Acta* **2004**, *504*, 15–21.
[60] X. Shen, L. Ye, *Macromolecules* **2011**, *44*, 5631–5637.
[61] N. Pérez, M. J. Whitcombe, E. N. Vulfson, *J. Appl. Polym. Sci.* **2000**, *77*, 1851–1859.
[62] N. Pérez, M. J. Whitcombe, E. N. Vulfson, *Macromolecules* **2001**, *34*, 830–836.
[63] L. Ye, R. Weiss, K. Mosbach, *Macromolecules* **2000**, *33*, 8239–8245.
[64] S. R. Carter, S. Rimmer, *Adv. Funct. Mater.* **2004**, *14*, 553–561.
[65] S. Wei, M. Jakusch, B. Mizaikoff, *Anal. Chim. Acta* **2006**, *578*, 50–58.
[66] L. Ye, P. A. Cormack, K. Mosbach, *Anal. Commun.* **1999**, *36*, 35–38.
[67] G. Wulff, *Angew. Chem. Int. Ed. Engl.* **1995**, *34*, 1812–1832.
[68] L. Ye, K. Mosbach, *J. Incl. Phenom. Macrocycl. Chem.* **2001**, *41*, 107–113.
[69] O. Ramström, R. J. Ansell, *Chirality* **1998**, *10*, 195–209.
[70] T. Takeuchi, J. Matsui, *Acta Polym.* **1996**, *47*, 471–480.
[71] L. Fischer, R. Mueller, B. Ekberg, K. Mosbach, *J. Am. Chem. Soc.* **1991**, *113*, 9358–9360.
[72] R. J. Ansell, K. Mosbach, *J. Chromatogr. A* **1997**, *787*, 55–66.
[73] M. Kempe, K. Mosbach, *J. Chromatogr. A* **1995**, *694*, 3–13.
[74] V. T. Remcho, Z. J. Tan, *Anal. Chem.* **1999**, *71*, 248A–255A.
[75] I. A. Nicholls, L. I. Andersson, K. Mosbach, B. Ekberg, *Trends Biotechnol.* **1995**, *13*, 47–51.
[76] B. Sellergren, *Anal. Chem.* **1994**, *66*, 1578–1582.
[77] A. Molinelli, R. Weiss, B. Mizaikoff, *J. Agric. Food Chem.* **2002**, *50*, 1804–1808.
[78] D. Stevenson, *Trends Anal. Chem.* **1999**, *18*, 154–158.
[79] L. I. Andersson, *J. Chromatogr. B. Biomed. Sci. App.* **2000**, *739*, 163–173.
[80] S. A. Piletsky, E. V. Piletska, A. Bossi, K. Karim, P. Lowe, A. P. Turner, *Biosens. Bioelectron.* **2001**, *16*, 701–707.
[81] R. Ansell, *J. Chromatogr. B* **2004**, *804*, 151–165.
[82] K. Haupt, *Chem. Commun.* **2003**, 171–178.
[83] D. Kriz, K. Mosbach, *Anal. Chim. Acta* **1995**, *300*, 71–75.
[84] A. Yarman, F. Scheller, *Sensors* **2014**, *14*, 7647–7654.

[85] K. Haupt, K. Mosbach, *Chem. Rev.* **2000**, *100*, 2495–2504.
[86] D. Carboni, K. Flavin, A. Servant, V. Gouverneur, M. Resmini, *Chem. - Eur. J.* **2008**, *14*, 7059 – 7065.
[87] G. Wulff, B.-O. Chong, U. Kolb, *Angew. Chem. Int. Ed.* **2006**, *45*, 2955–2958.
[88] M. A. Markowitz, P. R. Kust, G. Deng, P. E. Schoen, J. S. Dordick, D. S. Clark, B. P. Gaber, *Langmuir* **2000**, *16*, 1759–1765.
[89] G. Wulff, *Chem. Rev.* **2002**, *102*, 1–28.
[90] G. Cirillo, O. I. Parisi, M. Curcio, F. Puoci, F. Iemma, U. G. Spizzirri, N. Picci, *J. Pharm. Pharmacol.* **2010**, *62*, 577–582.
[91] M. Curcio, G. Cirillo, O. I. Parisi, F. Iemma, N. Picci, F. Puoci, *J. Funct. Biomater.* **2012**, *3*, 269–282.
[92] C. Alvarez-Lorenzo, A. Concheiro, *J. Chromatogr. B* **2004**, *804*, 231–245.
[93] B. Sellergren, C. Allender, *Adv. Drug Deliv. Rev.* **2005**, *57*, 1733–1741.
[94] S. A. Piletsky, S. Alcock, A. P. Turner, *Trends Biotechnol.* **2001**, *19*, 9–12.
[95] K. Haupt, *Anal. Chem.* **2003**, *75*, 377A–383A.
[96] A. Molinelli, J. O'Mahony, K. Nolan, M. R. Smyth, M. Jakusch, B. Mizaikoff, *Anal. Chem.* **2005**, *77*, 5196–5204.
[97] I. Chianella, M. Lotierzo, S. A. Piletsky, I. E. Tothill, B. Chen, K. Karim, A. P. F. Turner, *Anal. Chem.* **2002**, *74*, 1288–1293.
[98] S. Wei, M. Jakusch, B. Mizaikoff, *Anal. Bioanal. Chem.* **2007**, *389*, 423–431.
[99] I. A. Nicholls, H. S. Andersson, K. Golker, H. Henschel, B. C. G. Karlsson, G. D. Olsson, A. M. Rosengren, S. Shoravi, S. Suriyanarayanan, J. G. Wiklander, et al., *Anal. Bioanal. Chem.* **2011**, *400*, 1771–1786.
[100] Y. Lu, C.-L. Yan, S.-Y. Gao, *Appl. Surf. Sci.* **2009**, *255*, 6061–6066.
[101] I. A. Nicholls, J. P. Rosengren, *Bioseparation* **2001**, *10*, 301–305.
[102] G. Dvorakova, R. Haschick, K. Chiad, M. Klapper, K. Müllen, A. Biffis, *Macromol. Rapid Commun.* **2010**, *31*, 2035–2040.
[103] K. Flavin, M. Resmini, *Anal. Bioanal. Chem.* **2009**, *393*, 437–444.
[104] Y. Hoshino, T. Kodama, Y. Okahata, K. J. Shea, *J. Am. Chem. Soc.* **2008**, *130*, 15242–15243.
[105] D. Vaihinger, K. Landfester, I. Kräuter, H. Brunner, G. E. Tovar, *Macromol. Chem. Phys.* **2002**, *203*, 1965–1973.
[106] A. Cutivet, C. Schembri, J. Kovensky, K. Haupt, *J. Am. Chem. Soc.* **2009**, *131*, 14699–14702.
[107] X. Shen, T. Zhou, L. Ye, *Chem. Commun.* **2012**, *48*, 8198.
[108] D. E. Hansen, *Biomaterials* **2007**, *28*, 4178–4191.
[109] M. Glad, O. Norrlöw, B. Sellergren, N. Siegbahn, K. Mosbach, *J. Chromatogr.* **1985**, *347*, 11–23.
[110] E. Verheyen, J. P. Schillemans, M. van Wijk, M.-A. Demeniex, W. E. Hennink, C. F. van Nostrum, *Biomaterials* **2011**, *32*, 3008–3020.
[111] D. S. Janiak, P. Kofinas, *Anal. Bioanal. Chem.* **2007**, *389*, 399–404.
[112] A. Bossi, F. Bonini, A. P. F. Turner, S. A. Piletsky, *Biosens. Bioelectron.* **2007**, *22*, 1131–1137.
[113] J.-L. Liao, Y. Wang, S. Hjertén, *Chromatographia* **1996**, *42*, 259–262.
[114] C. Wang, M. Howell, P. Raulji, Y. Davis, S. Mohapatra, *Adv. Funct. Mater.* **2011**, *21*, 4423–4429.
[115] Y. Lu, C.-L. Yan, X.-J. Wang, G.-K. Wang, *Appl. Surf. Sci.* **2009**, *256*, 1341–1346.
[116] G. Fu, H. He, Z. Chai, H. Chen, J. Kong, Y. Wang, Y. Jiang, *Anal. Chem.* **2011**, *83*, 1431–1436.
[117] Z. Zeng, Y. Hoshino, A. Rodriguez, H. Yoo, K. J. Shea, *ACS Nano* **2010**, *4*, 199–204.
[118] M. E. Corman, C. Armutçu, L. Uzun, R. Say, A. Denizli, *Proc. Int. Conf. Nanomater. Appl. Prop.* **2012**, *1*, 1–2.
[119] C. J. Tan, Y. W. Tong, *Langmuir* **2007**, *23*, 2722–2730.
[120] C. J. Tan, S. Wangrangsimakul, R. Bai, Y. W. Tong, *Chem. Mater.* **2008**, *20*, 118–127.
[121] C. J. Tan, H. G. Chua, K. H. Ker, Y. W. Tong, *Anal. Chem.* **2008**, *80*, 683–692.
[122] N. Sankarakumar, Y. W. Tong, *RSC Adv.* **2013**, *3*, 1519–1527.

[123] M. Tatemichi, M. Sakamoto, M. Mizuhata, S. Deki, T. Takeuchi, *J. Am. Chem. Soc.* **2007**, *129*, 10906–10910.
[124] A. Poma, A. Guerreiro, S. Caygill, E. Moczko, S. Piletsky, *RSC Adv* **2014**, *4*, 4203–4206.
[125] J. Kuriyan, B. Konforti, D. Wemmer, in *Mol. Life Phys. Chem. Princ.*, Garland Science, New York, USA, **2013**, pp. 531–580.
[126] B. Sellergren, M. Lepistoe, K. Mosbach, *J. Am. Chem. Soc.* **1988**, *110*, 5853–5860.
[127] H. S. Andersson, A.-C. Koch-Schmidt, S. Ohlson, *J. Mol. Recognit.* **1996**, *9*, 675–682.
[128] H. S. Andersson, I. A. Nicholls, *Bioorganic Chem.* **1997**, *25*, 203–211.
[129] R. J. Umpleby II, M. Bode, K. D. Shimizu, *The Analyst* **2000**, *125*, 1261–1265.
[130] G. Wulff, H.-G. Poll, M. Minárik, *J. Liq. Chromatogr.* **1986**, *9*, 385–405.
[131] M. J. Whitcombe, M. E. Rotriguez, P. Villar, E. N. Vulfson, *J. Am. Chem. Soc.* **1995**, *117*, 7105–7111.
[132] M. Kempe, *Anal. Chem.* **1996**, *68*, 1948–1953.
[133] S. Wei, A. Molinelli, B. Mizaikoff, *Biosens. Bioelectron.* **2006**, *21*, 1943–1951.
[134] J. Matsui, M. Okada, M. Tsuruoka, T. Takeuchi, *Anal Commun* **1997**, *34*, 85–87.
[135] H. Kempe, M. Kempe, *Macromol. Rapid Commun.* **2004**, *25*, 315–320.
[136] J. Haginaka, H. Takehira, K. Hosoya, N. Tanaka, *J. Chromatogr. A* **1999**, *849*, 331–339.
[137] C.-H. Lu, W.-H. Zhou, B. Han, H.-H. Yang, X. Chen, X.-R. Wang, *Anal. Chem.* **2007**, *79*, 5457–5461.
[138] M. Pourfarzib, M. Shekarchi, H. Rastegar, B. Akbari-Adergani, A. Mehramizi, R. Dinarvand, *J. Chromatogr. B* **2015**, *974*, 1–8.
[139] P. Curcio, C. Zandanel, A. Wagner, C. Mioskowski, R. Baati, *Macromol. Biosci.* **2009**, *9*, 596–604.
[140] A. A. Vaidya, B. S. Lele, M. G. Kulkarni, R. A. Mashelkar, *J. Appl. Polym. Sci.* **2001**, *81*, 1075–1083.
[141] D. L. Venton, E. Gudipati, *Biochim. Biophys. Acta* **1995**, *1250*, 117–125.
[142] D. M. Hawkins, D. Stevenson, S. M. Reddy, *Anal. Chim. Acta* **2005**, *542*, 61–65.
[143] X. Pang, G. Cheng, S. Lu, E. Tang, *Anal. Bioanal. Chem.* **2006**, *384*, 225–230.
[144] P. Çakir, A. Cutivet, M. Resmini, B. T. S. Bui, K. Haupt, *Adv. Mater.* **2013**, *25*, 1048–1051.
[145] H. Nishino, C.-S. Huang, K. J. Shea, *Angew. Chem. Int. Ed.* **2006**, *45*, 2392–2396.
[146] T. Shiomi, M. Matsui, F. Mizukami, K. Sakaguchi, *Biomaterials* **2005**, *26*, 5564–5571.
[147] S. Ambrosini, S. Beyazit, K. Haupt, B. Tse Sum Bui, *Chem. Commun.* **2013**, *49*, 6746–6748.
[148] A. Ramanaviciene, A. Ramanavicius, *Biosens. Bioelectron.* **2004**, *20*, 1076–1082.
[149] M. Kempe, M. Glad, K. Mosbach, *J. Mol. Recognit.* **1995**, *8*, 35–39.
[150] C.-L. Yan, Y. Lu, S.-Y. Gao, *J. Polym. Sci. Part Polym. Chem.* **2007**, *45*, 1911–1919.
[151] L. Qin, X.-W. He, X. Yuan, W.-Y. Li, Y.-K. Zhang, *Anal. Bioanal. Chem.* **2011**, *399*, 3375–3385.
[152] A. Bossi, S. A. Piletsky, E. V. Piletska, P. G. Righetti, A. P. F. Turner, *Anal. Chem.* **2001**, *73*, 5281–5286.
[153] H. Shi, W.-B. Tsai, M. D. Garrison, S. Ferrari, B. D. Ratner, *Nature* **1999**, *398*, 593–597.
[154] Z. Zhang, Y. Long, L. Nie, S. Yao, *Biosens. Bioelectron.* **2006**, *21*, 1244–1251.
[155] M. Burow, N. Minoura, *Biochem. Biophys. Res. Commun.* **1996**, *227*, 419–422.
[156] N. Pérez-Moral, A. G. Mayes, *Bioseparation* **2001**, *10*, 287–299.
[157] M. M. Titirici, B. Sellergren, *Anal. Bioanal. Chem.* **2004**, *378*, 1913–1921.
[158] J. Liu, Q. Deng, D. Tao, K. Yang, L. Zhang, Z. Liang, Y. Zhang, *Sci. Rep.* **2014**, *4*, 1–6.
[159] B. Pluhar, B. Mizaikoff, *Macromol. Biosci.* **2015**, *15*, 1507–1511.
[160] A. Rachkov, N. Minoura, *Biochim. Biophys. Acta BBA-Protein Struct. Mol. Enzymol.* **2001**, *1544*, 255–266.
[161] D. Dechtrirat, K. J. Jetzschmann, W. F. M. Stöcklein, F. W. Scheller, N. Gajovic-Eichelmann, *Adv. Funct. Mater.* **2012**, *22*, 5231–5237.
[162] G. Vasapollo, R. D. Sole, L. Mergola, M. R. Lazzoi, A. Scardino, S. Scorrano, G. Mele, *Int. J. Mol. Sci.* **2011**, *12*, 5908–5945.
[163] D. J. O'Shannessy, B. Ekberg, K. Mosbach, *Anal. Biochem.* **1989**, *177*, 144–149.

[164] E. V. Piletska, A. R. Guerreiro, M. J. Whitcombe, S. A. Piletsky, *Macromolecules* **2009**, *42*, 4921–4928.
[165] S. A. Piletsky, E. V. Piletska, K. Karim, K. W. Freebairn, C. H. Legge, A. P. F. Turner, *Macromolecules* **2002**, *35*, 7499–7504.
[166] R. Lorenzo, A. Carro, C. Alvarez-Lorenzo, A. Concheiro, *Int. J. Mol. Sci.* **2011**, *12*, 4327–4347.
[167] B. Sellergren, *Makromol. Chem.* **1989**, *190*, 2703–2711.
[168] A. Rosengren, B. Karlsson, I. Nicholls, *Int. J. Mol. Sci.* **2013**, *14*, 1207–1217.
[169] L. A. Tom, N. A. Schneck, C. Walter, *J. Chromatogr. B* **2012**, *909*, 61–64.
[170] C. Yu, K. Mosbach, *J. Chromatogr. A* **2000**, *888*, 63–72.
[171] B. Sellergren, K. J. Shea, *J. Chromatogr.* **1993**, *635*, 31–49.
[172] D. Spivak, M. A. Gilmore, K. J. Shea, *J. Am. Chem. Soc.* **1997**, *119*, 4388–4393.
[173] F. L. Dickert, M. Tortschanoff, W. E. Bulst, G. Fischerauer, *Anal. Chem.* **1999**, *71*, 4559–4563.
[174] S. Boonpangrak, M. J. Whitcombe, V. Prachayasittikul, K. Mosbach, L. Ye, *Biosens. Bioelectron.* **2006**, *22*, 349–354.
[175] D. Spivak, *Adv. Drug Deliv. Rev.* **2005**, *57*, 1779–1794.
[176] Z.-L. Shen, X.-L. Zhu, J. Yang, J.-B. Cai, Q.-D. Su, *J. Chin. Chem. Soc.* **2008**, *55*, 587–593.
[177] O. K. Castell, D. A. Barrow, A. R. Kamarudin, C. J. Allender, *J. Mol. Recognit.* **2011**, *24*, 1115–1122.
[178] I. Langmuir, *J. Am. Chem. Soc.* **1918**, *40*, 1361–1403.
[179] G. Freundlich, *Z. Für Phys. Chem.* **1907**, *57*, 385–470.
[180] R. J. Umpleby, S. C. Baxter, M. Bode, J. K. Berch, R. N. Shah, K. D. Shimizu, *Anal. Chim. Acta* **2001**, *435*, 35–42.
[181] J. A. García-Calzón, M. E. Díaz-García, *Sens. Actuators B Chem.* **2007**, *123*, 1180–1194.
[182] R. Umpleby, S. Baxter, A. Rampey, G. Rushton, Y. Chen, K. Shimizu, *J. Chromatogr. B* **2004**, *804*, 141–149.
[183] R. J. Umpleby, S. C. Baxter, Y. Chen, R. N. Shah, K. D. Shimizu, *Anal. Chem.* **2001**, *73*, 4584–4591.
[184] G. Alberti, V. Amendola, M. Pesavento, R. Biesuz, *Coord. Chem. Rev.* **2012**, *256*, 28–45.
[185] K. Landfester, N. Bechthold, F. Tiarks, M. Antonietti, *Macromolecules* **1999**, *32*, 2679–2683.
[186] K. Landfester, M. Willert, M. Antonietti, *Macromolecules* **2000**, *33*, 2370–2376.
[187] F. Lottspeich, J. W. Engels, in *Bioanalytik*, Springer, Berlin Heidelberg, Germany, **2012**, pp. 151–200.
[188] S. M. Kelly, T. J. Jess, N. C. Price, *Biochim. Biophys. Acta BBA - Proteins Proteomics* **2005**, *1751*, 119–139.
[189] D. H. Correcirc, C. H. Ramos, *Afr. J. Biochem. Res.* **2009**, *3*, 164–173.
[190] H.-D. Dörfler, in *Grenzflächen- Kolloidchem.*, VCH Weihnheim, Weinheim, Germany, **1994**, pp. 13–42.
[191] *Zetasizer Nano Series User Manual*, Malvern Instruments Ltd, Worcestershire, United Kingdom, **2004**.
[192] W. Schärtl, *Light Scattering from Polymer Solutions and Nanoparticle Dispersions*, Springer Berlin Heidelberg, Heidelberg, Germany, **2007**.
[193] A. R. Barron, *Physical Methods in Chemistry and Nano Science*, **2014**.
[194] H.-D. Dörfler, in *Grenzflächen- Kolloidchem.*, VCH Weihnheim, Weinheim, Germany, **1994**, pp. 112–155.
[195] K. Sing, *Colloids Surf. Physicochem. Eng. Asp.* **2001**, *187*, 3–9.
[196] S. Brunauer, L. S. Deming, W. E. Deming, E. Teller, *J. Am. Chem. Soc.* **1940**, *62*, 1723–1732.
[197] S. Brunauer, P. H. Emmett, E. Teller, *J. Am. Chem. Soc.* **1938**, *60*, 309–319.
[198] K. S. W. Sing, D. H. Everett, R. A. W. Haul, L. Moscou, R. A. Pierotti, J. Rouquerol, T. Siemieniewska, *Pure Appl Chem* **1985**, *57*, 603–619.
[199] S. Brunauer, P. H. Emmett, *J. Am. Chem. Soc.* **1937**, *59*, 2682–2689.
[200] P. H. Emmett, S. Brunauer, *J. Am. Chem. Soc.* **1937**, *59*, 1553–1564.
[201] H.-D. Dörfler, in *Grenzflächen- Kolloidchem.*, VCH Weihnheim, Weinheim, Germany, **1994**, pp. 510–527.

[202] P. J. Goodhew, J. Humphreys, R. Beanland, *Electron Microscopy and Analysis*, Taylor & Francis, London, United Kingdom, **2001**.
[203] G. H. Michler, *Electron Microscopy of Polymers*, Springer Berlin Heidelberg, Heidelberg, Germany, **2008**.
[204] K. Cammann, in *Instrumentelle Anal. Chem. Verfahr. Anwendungen Qual.*, Spektrum Akademischer Verlag GmbH, Heidelberg, Germany, **2001**, pp. 1–81.
[205] T. Owen, *Fundamentals of Modern UV-Visible Spectroscopy: Primer*, Agilent Technologies, Germany, **2000**.
[206] F. Lottspeich, J. W. Engels, in *Bioanalytik*, Springer, Berlin Heidelberg, Germany, **2012**, pp. 201–228.
[207] U. K. Laemmli, *Nature* **1970**, *227*, 680–685.
[208] D. Otzen, *Biochim. Biophys. Acta BBA - Proteins Proteomics* **2011**, *1814*, 562–591.
[209] L. Whitmore, B. A. Wallace, *Biopolymers* **2008**, *89*, 392–400.
[210] K. Gekko, R. Yonehara, Y. Sakurada, K. Matsuo, *J. Electron Spectrosc. Relat. Phenom.* **2005**, *144-147*, 295–297.
[211] T. Chakraborty, I. Chakraborty, S. P. Moulik, S. Ghosh, *J. Phys. Chem. B* **2007**, *111*, 2736–2746.
[212] S. R. Tello-Solís, B. Romero-García, *Int. J. Biol. Macromol.* **2001**, *28*, 129–133.
[213] B. Pluhar, U. Ziener, B. Mizaikoff, *J. Mater. Chem. B* **2013**, *1*, 5489–5495.
[214] E. L. Ibarra-Montaño, N. Rodríguez-Laguna, A. Sánchez-Hernández, A. Rojas-Hernández, *J. Appl. Solut. Chem. Model.* **2015**, *4*, 7–18.
[215] L. A. Campos, J. Sancho, *FEBS Lett.* **2003**, *538*, 89–95.
[216] H. Determann, D. Jaworek, R. Kotitschke, A. Walch, *Z. Für Physiol. Chem.* **1969**, *350*, 379–388.
[217] D.-H. Lee, G. Cho, H. M. Lim, D. S. Kim, C. Kim, S.-H. Lee, *J. Ceram. Process. Res.* **2013**, *14*, 274–278.
[218] Q.-Q. Gai, F. Qu, Z.-J. Liu, R.-J. Dai, Y.-K. Zhang, *J. Chromatogr. A* **2010**, *1217*, 5035–5042.
[219] F. Bonini, S. Piletsky, A. P. F. Turner, A. Speghini, A. Bossi, *Biosens. Bioelectron.* **2007**, *22*, 2322–2328.
[220] B. Pluhar, U. Ziener, B. Mizaikoff, *J Mater Chem B* **2015**, *3*, 6248–6254.
[221] W. M. Zuo, R. E. Pratt, C. H. Heusser, J. P. Bews, M. M. de Gasparo, V. J. Dzau, *Hypertension* **1992**, *19*, 249–254.
[222] N. Kitabatake, Y.-I. Kinekawa, *J. Agric. Food Chem.* **1998**, *46*, 4917–4923.
[223] Y. Hoshino, T. Urakami, T. Kodama, H. Koide, N. Oku, Y. Okahata, K. J. Shea, *Small* **2009**, *5*, 1562–1568.
[224] J. Henry, A. Anand, M. Chowdhury, G. Coté, R. Moreira, T. Good, *Anal. Biochem.* **2004**, *334*, 1–8.
[225] J. Ashby, Y. Duan, E. Ligans, M. Tamsi, W. Zhong, *Anal. Chem.* **2015**, *87*, 2213–2219.
[226] C.-C. You, O. R. Miranda, B. Gider, P. S. Ghosh, I.-B. Kim, B. Erdogan, S. A. Krovi, U. H. F. Bunz, V. M. Rotello, *Nat. Nanotechnol.* **2007**, *2*, 318–323.
[227] Y. Hoshino, K. J. Shea, *J. Mater. Chem.* **2011**, *21*, 3517–3521.
[228] T.-H. Yang, *Recent Pat. Mater. Sci.* **2008**, *1*, 29–40.
[229] C. J. van Oss, *Macromol. Immunol.* **1995**, *32*, 199–211.
[230] C. J. van Oss, *J. Chromatogr.* **1986**, *376*, 111–119.
[231] Y. Hoshino, H. Koide, K. Furuya, W. W. Haberaecker, S.-H. Lee, T. Kodama, H. Kanazawa, N. Oku, K. J. Shea, *Proc. Natl. Acad. Sci.* **2012**, *109*, 33–38.
[232] S.-H. Lee, Y. Hoshino, A. Randall, Z. Zeng, P. Baldi, R. Doong, K. J. Shea, *J. Am. Chem. Soc.* **2012**, *134*, 15765–15772.
[233] D. Zhang, X. Yang, in *Encycl. Polym. Nanomater.* (Eds.: S. Kobayashi, K. Müllen), Springer Berlin Heidelberg, Berlin, Heidelberg, **2014**, pp. 1–10.
[234] K. Li, H. D. Stöver, *J. Polym. Sci. Part Polym. Chem.* **1993**, *31*, 3257–3263.
[235] J. Wang, P. A. G. Cormack, D. C. Sherrington, E. Khoshdel, *Pure Appl. Chem.* **2007**, *79*, 1505–1519.
[236] M. T. Gokmen, F. E. Du Prez, *Prog. Polym. Sci.* **2012**, *37*, 365–405.
[237] B. Sellergren, *J. Chromatogr. A* **1994**, *673*, 133–141.

[238] K. Yoshimatsu, K. Reimhult, A. Krozer, K. Mosbach, K. Sode, L. Ye, *Anal. Chim. Acta* **2007**, *584*, 112–121.
[239] K. Yoshimatsu, B. K. Lesel, Y. Yonamine, J. M. Beierle, Y. Hoshino, K. J. Shea, *Angew. Chem. Int. Ed.* **2012**, *51*, 2405–2408.
[240] Y. Yonamine, K. Yoshimatsu, S.-H. Lee, Y. Hoshino, Y. Okahata, K. J. Shea, *ACS Appl. Mater. Interfaces* **2013**, *5*, 374–379.
[241] Y. Hoshino, T. Urakami, T. Kodama, H. Koide, N. Oku, Y. Okahata, K. J. Shea, *Small* **2009**, *5*, 1562–1568.
[242] Y. Hoshino, H. Koide, T. Urakami, H. Kanazawa, T. Kodama, N. Oku, K. J. Shea, *J. Am. Chem. Soc.* **2010**, *132*, 6644–6645.
[243] F. P. Schmidtchen, M. Berger, *Chem. Rev.* **1997**, *97*, 1609–1646.
[244] *Molecular Probes™ Handbook - A Guide to Fluorescent Probes and Labeling Technologies*, Invitrogen, **2010**.
[245] *EnzChek® Protease Assay Kits*, Assay Molecular Probes - Invitrogen Detection Technologies, **2004**.
[246] S. Slomkowski, J. V. Alemán, R. G. Gilbert, M. Hess, K. Horie, R. G. Jones, P. Kubisa, I. Meisel, W. Mormann, S. Penczek, et al., *Pure Appl. Chem.* **2011**, *83*, 2229–2259.

VI. List of figures

VII. List of tables

VIII. Acknowledgments

Firstly, I would like to thank Prof. Dr. Boris Mizaikoff for giving me the great opportunity to work on this very interesting and challenging topic at the Institute of Analytical and Bioanalytical Chemistry. I would also like to thank him for all his motivation and support during the last years.

Then I would like to thank Apl. Prof. Dr. Ulrich Ziener for the great cooperation and friendly acceptance of the second opinion. Furthermore, I would like to thank him for supporting me with the miniemulsion polymerization and many other scientific issues.

I would like to express my gratitude to Prof. Dr. Kenneth J. Shea for the great support and time during my research stay in his research group at the UCI in California.

My warm thanks go to all members of the IABC for the great working atmosphere, the good team spirit, the technical and moral support and for all the nice moments outside of work. Especially, I would like to thank Florian Meier, Roland Schindl, Cornelia Weber, Nadine Feichtmeier, Jessica Huber, Stefan Eppler, Stefan Zink, Tanja Sandner, Katharina Wörle, Andreas Wilk, Hasan Basan and the whole MIP team for the expert and personal conversations. Furthermore, I would like to thank Sandra Gienger for her technical support at the institute.

I would like to thank my bachelor students Aline Marian and Johannes Habermehl for their interest in my topic and their motivated dedication.

Other thanks go to all members of the Institute of Organic Chemistry III for the good cooperation. Especially, I would like to thank Anika Schrade and Berend Eggers for their helpfulness and their kind reception into their lab. I would also like to thank Christian Zwerger for the friendly support with the SDS-PAGE.

Furthermore, I would like to thank all members of the Shea Research Group at the UCI for the pleasant and supportive working atmosphere. My special thanks go to Michelle Shih-Hui Lee for her great support in the scientific treatment of new subjects and other organizational things and the great cooperation.

I would like to thank Cornelia Egger of the Institute of Inorganic Chemistry II for the numerous BET measurements, Dr. Günther Götz of the Institute of Organic Chemistry II for the introduction to the CD spectropolarimeter and Dr. Carola Hoffmann-Richter of the Institute of Organic Chemistry III for the introduction to the du Noüy ring tensiometer. Then I would like to thank Eberhard Schmid and all other members of the Institute of Electron Microscopy for the sample preparation and assistance with the electron microscopy.

Furthermore, I would like to thank our partners of the company Labor Dr. Merk & Kollegen GmbH and Atoll GmbH for the kind and interesting cooperation within the protease scavenger project.

Financial support by the Bundesministerium für Bildung und Forschung (BMBF) within the project PROTSCAV (#0315511) is greatly acknowledged as well as the financial funding of my research stay in the Shea group at the UCI in California by the Fulbright Commission.

Last but not least, I would like to warmly thank Christian Blasczyk, my family and all my friends for their great support, motivation and the very good time together.

Thank you all for your contribution to this thesis!

IX. Curriculum vitae

The curriculum vitae was removed for reasons of data protection.

Der Lebenslauf wurde aus Gründen des Datenschutzes entfernt.

X. Eidesstattliche Erklärung

Hiermit erkläre ich, dass ich die vorliegende Dissertation selbständig angefertigt und keine anderen als die in der Arbeit aufgeführten Quellen und Hilfsmittel verwendet habe.

Ulm, den 15.07.2016 _____
(Bettina Pluhar)